

Evolution of the Giant Southern North Sea Shelf-Prism: Testing sequence stratigraphic concepts and the global sea level curve with full-three dimensional control

A thesis submitted to the University of Manchester for the degree
of Doctor of
Philosophy in the Faculty of Engineering and Physical Sciences

2015

Rachel Harding

School of Earth, Atmospheric and Environmental Sciences

TABLE OF CONTENTS

<i>Title Page</i>	1
<i>Table of Contents</i>	2
<i>List of Figures</i>	6
<i>List of Tables</i>	9
<i>Abstract</i>	10
<i>Declaration</i>	11
<i>Copyright Statement</i>	12
<i>Preface</i>	13
<i>Acknowledgements</i>	15
 TABLE OF CONTENTS	 2
CHAPTER 1 INTRODUCTION.....	17
1.1 PROJECT RATIONALE.....	17
1.2 AIMS	23
1.3 THESIS SYNOPSIS.....	23
1.4 REFERENCES.....	26
CHAPTER 2 METHODOLOGY.....	31
2.1 DATASET	33
2.1.1 Chronostratigraphy.....	35
2.2 SEISMIC INTERPRETATION APPROACH.....	45
2.2.1 Imaging Techniques	45
2.2.2 Limitations	48
2.3 REFERENCES.....	51
CHAPTER 3: REGIONAL EVOLUTION OF A SHELF-PRISM IN THE LATE CENOZOIC: EUSTACY, SEDIMENT SUPPLY AND SUBSIDENCE IN THE SOUTHERN NORTH SEA.....	55
3.0 ABSTRACT	55
3.1 INTRODUCTION	56
3.1.1 Geological Setting.....	58

3.1.2 Chronostratigraphic Framework	63
3.1.3 Clinoform Terminology	66
3.2 DATA AND METHODOLOGY	68
3.2.1 Data	68
3.2.2 Methodology.....	68
3.3 STRATIGRAPHIC FRAMEWORK.....	70
3.3.1 Key to Unit Descriptions.....	77
3.3.2 Seismic Architecture	77
3.3.3 Seismic Facies	78
3.3.2 Unit Descriptions.....	81
3.4 BASIN INFILL AND DEPOSITIONAL MODEL	123
3.4.1 Basin Infill.....	123
3.4.2 Depositional Model.....	128
3.5 DISCUSSION	130
3.5.1 Eustatic Control.....	130
3.5.2 Sequence Variability	131
3.5.3 Subsidence and Tectonics.....	131
3.5.4 Sediment Input and Shelf Geomorphology	132
3.6 CONCLUSIONS.....	133
3.7 REFERENCES	134
CHAPTER 4: DEEP WATER SEDIMENTARY SYSTEMS LINKED TO SHELF EDGE	
TRAJECTORY AND GLOBAL SEA LEVEL.....	144
4.0 ABSTRACT	144
4.1 INTRODUCTION	145
4.1.1 Geological Setting.....	147
4.1.2 Chronostratigraphic Framework	148
4.2 DATASET AND METHODOLOGY	152
4.3 SEISMIC STRATIGRAPHIC FRAMEWORK.....	153
4.4 DEEP WATER SEDIMENTATION	158
4.4.1 Single Feeder Systems.....	158
4.4.2 Single Feeder System Clinoform Architectures.....	165
4.4.3 Multiple Line Source Systems.....	167
4.4.4 Multiple Line Source Clinoform Architectures.....	176

4.5 DISCUSSION	177
4.5.1 Deep Water Sedimentation and Glacial-Interglacial Cycles.....	177
4.5.2 Deep Water Sedimentation Model.....	179
4.5.3 Role of Eustacy and Controlling Factors	181
4.5.4 Sequence Stratigraphic Context.....	184
4.5.5 Implications and Limitations	186
4.6 CONCLUSIONS.....	188
4.7 REFERENCES	189
CHAPTER 5: CAN ENIGMATIC INTRA SLOPE CLINOFORMS PROVIDE AN INDEPENDENT CALIBRATION OF EARLY PLEISTOCENE EUSTATIC CHANGES?.....	197
5.0 ABSTRACT	197
5.1 INTRODUCTION	198
5.1.1 Geological Setting.....	198
5.1.2 Chronostratigraphic Framework	200
5.2. DATASET AND METHODOLOGY	203
5.3 SEISMIC STRATIGRAPHIC FRAMEWORK.....	204
5.4 DESCRIPTION OF INTRA SLOPE CLINOFORMS	213
5.4.1 Seismic Reflection Character	213
5.4.2 Well Log Character	217
5.4.3 Relationship to the Shelf Edge	219
5.4.4 Sequence Position	219
5.5 DEPOSITIONAL ENVIRONMENT	220
5.6 INTRA SLOPE CLINOFORM DISTRIBUTION	222
5.7 DISCUSSION	223
5.7.1 Intra Slope Clinoform Genesis	223
5.7.2 Comparisons to Global Events.....	226
5.7.3 Implications for Sequence Stratigraphy	227
5.8 CONCLUSIONS.....	230
5.9 REFERENCES	231
CHAPTER 6: SECOND AUTHOR PAPERS	237
6.1 EVIDENCE FOR REPEATED LOW LATITUDE MARINE TERMINATING ICE SHEETS IN A 41 KYR EARLY QUATERNARY WORLD	237
6.1.1 First Paragraph.....	237

6.1.2 Main Text	238
6.1.3 Methods	246
6.1.4 References	247
6.2 THE EARLY QUATERNARY OF THE NORTH SEA BASIN	250
6.2.1 Introduction.....	251
6.2.3 Data and Methods.....	253
6.2.4 Chronostratigraphic Calibration of the Base Quaternary	258
6.2.5 The Quaternary North Sea Basin	260
6.2.6 Discussion	269
6.2.7 Implications	272
6.2.8 Conclusions	273
CHAPTER 7: SYNTHESIS AND CONCLUSIONS	282
7.1. SUMMARY OF RESULTS AND CONCLUSIONS	282
7.1.1 Regional Evolution of a Shelf-Prism in the Late Cenozoic: Eustacy, Sediment Supply and Subsidence in the Southern North Sea.....	282
7.1.2 Deep Water Sedimentary Systems Linked to Shelf Edge Trajectory and Global Sea Level.....	284
7.1.3 Can Enigmatic Intra Slope Clinoforms Provide an Independent Calibration of Early Pleistocene Eustatic Changes?	287
7.2 FUTURE WORK.....	288
7.3 REFERENCES	291
APPENDIX A.....	294

Word Count 75,210

LIST OF FIGURES

CHAPTER 1 - INTRODUCTION

Figure 1.1 Regional setting and dataset map.....	19
Figure 1.2 Exxon Mobile “Slug Model”	20
Figure 1.3 Basin floor deposition scenarios.....	21
Figure 1.4 Stratal stacking patterns.....	22
Figure 1.5 Clinoform classification decision tree.....	22

CHAPTER 2 – METHODOLOGY

Figure 2.1 Mega scale dataset methodology.....	33
Figure 2.2 Comparison of polarity and phase of sections of the MegaSurvey	35
Figure 2.3 Complimenting datasets provided by TNO	36
Figure 2.4 Focus on A15 Block	38
Figure 2.5 Seismic scheme comparison.....	39
Figure 2.6 Correlation between A15-03 and CNS MegaSurvey	40
Figure 2.7 Well correlation along strike basinwards of the shelf edge.....	41
Figure 2.8 Location of strike well correlation from A15-03 to F11 and the area of the SNS MegaSurvey	42
Figure 2.9 Synthetic seismogram for A15-03 and F11-02.....	43
Figure 2.10 Gamma ray logs for Wells F11-02 and F11-01.....	45
Figure 2.11 Seismic interpretation and imaging techniques.....	48
Figure 2.12 Comparison of clinoforms from seismic data to outcrop.....	50
Figure 2.13 Hierarchies of channel geobodies.	51

CHAPTER 3 – REGIONAL EVOLUTION OF A SHELF-PRISM IN THE LATE CENOZOIC: EUSTACY, SEDIMENT SUPPLY AND SUBSIDENCE IN THE SOUTHERN NORTH SEA

Figure 3.1 Regional setting and dataset map.....	59
Figure 3.2 Structural Domains within southern North Sea.....	61
Figure 3.3 Regional cross section through the southern North Sea.....	63
Figure 3.4 Chronostratigraphic framework.....	65
Figure 3.5 Clinoform nomenclature.....	67

Figure 3.6 Seismic cross sections.....	71, 72, 74, 75
Figure 3.7 Well log correlation.....	76, 77
Figure 3.8 Seismic architectures.....	80
Figure 3.9 Seismic facies.....	81
Figure 3.10 Unit thickness maps with seismic architecture distribution.....	84, 85
Figure 3.11 Unit thickness maps with seismic facies distributions.....	86, 87
Figure 3.12 Structure maps.....	88
Figure 3.13 <i>Mio 2</i> example of SA1 Intra Slope Clinoforms.....	92
Figure 3.14 <i>Top Mio 3</i> surface.....	96
Figure 3.15 <i>Plio 1</i> SF2 Intra Shelf Clinoform example.....	100
Figure 3.16 Cross section through lobate geometry of <i>Plio 1</i>	101
Figure 3.17 Gamma ray logs for Wells F11-02 and F11-01.....	108
Figure 3.18 Well correlation along strike basinwards of the shelf edge.....	109
Figure 3.19 Iceberg scours.....	110
Figure 3.20 Large scale river channel systems during <i>Pleisto 5</i>	123
Figure 3.21 Depositional models.....	129

CHAPTER 4 - DEEP WATER SEDIMENTARY SYSTEMS LINKED TO SHELF EDGE TRAJECTORY AND GLOBAL SEA LEVEL

Figure 4.1 Regional setting and dataset map.....	148
Figure 4.2 Chronostratigraphic framework.....	151
Figure 4.3 Submarine channel map.....	156
Figure 4.4 Seismic architectures and clinoform types.....	158
Figure 4.5 Single Feeder System seismic cross section examples.....	164
Figure 4.6 Single feeder system 3D examples.....	165
Figure 4.7 Single feeder system shelf edge trajectories.....	167
Figure 4.8 Multiple line source examples: <i>Plio 1D</i> gullies.....	168
Figure 4.9 Multiple line source 3D example: <i>Pleisto 1A</i> channel levee complex.....	171
Figure 4.10 Seismic cross sections through <i>Pleisto 1A</i> channel levee.....	173

Figure 4.11 Multiple line source example <i>Pleisto 1H</i> sinuous canyons.....	175
Figure 4.12 Seismic cross sections through <i>Pleisto 1</i>	176
Figure 4.13 Submarine channel link to global sea level curve.....	182

CHAPTER 5 - CAN ENIGMATIC INTRA SLOPE CLINOFORMS PROVIDE AN INDEPENDENT CALIBRATION OF EARLY PLEISTOCENE EUSTATIC CHANGES?

Figure 5.1 Regional setting and dataset map.....	200
Figure 5.2 Chronostratigraphic framework.....	202
Figure 5.3 Clinoform terminology.....	206
Figure 5.4 Intra Slope Clinoform seismic cross sections.....	207, 208, 209, 210
Figure 5.5 Distribution of Intra Slope Clinoforms.....	211
Figure 5.6 Planform examples of Intra Slope Clinoforms.....	215, 216
Figure 5.7 Well log correlations.....	219
Figure 5.8 Sequence stratigraphic models.....	230

CHAPTER 6 – SECOND AUTHOR PAPERS

Figure 6.1.1 Map of the North Sea and data coverage.....	240
Figure 6.1.2 Late Cenozoic datasets.....	241
Figure 6.1.3 Clinoform geometry.....	242
Figure 6.1.4 Iceberg scour distribution.....	244
Figure 6.2.1 Location map and datasets.....	254
Figure 6.2.2 Seismic section and line interpretation.....	257
Figure 6.2.3 Depth Conversion.....	258
Figure 6.2.4 TWT structure map of the 2.58 Ma surface.....	262
Figure 6.2.5 Depth converted 2.58 Ma surface.....	263
Figure 6.2.6 Simplified sections used in backstripping process.....	264
Figure 6.2.7 Simplified line transects used in back-stripping process.....	264
Figure 6.2.8 Sub-crop interpretation.....	266
Figure 6.2.9 Simplified map of the base-Quaternary subcrop.....	267
Figure 6.2.10 Thickness maps of Quaternary strata.....	269

Figure 6.2.11 Earliest Quaternary geomorphology.....	270
Figure 6.2.12 Reconstructed palaeo-environmental map based on results of this study.....	273

LIST OF TABLES

CHAPTER 4 - DEEP WATER SEDIMENTARY SYSTEMS LINKED TO SHELF EDGE TRAJECTORY AND GLOBAL SEA LEVEL

Table 4.1 Description of Single Feeder Systems.....	161
Table 4.2 Description of Multiple Line Source submarine systems.....	162,163

CHAPTER 6 – SECOND AUTHOR PAPERS

Table 6.2.1 Chronostratigraphic Correlation.....	259
---	-----

Evolution of the Giant Southern North Sea Shelf-Prism: Testing sequence stratigraphic concepts and the global sea level curve with full-three dimensional control

Rachel Harding

A thesis submitted to the University of Manchester for the degree of Doctor of Philosophy in the Faculty of Engineering and Physical Sciences, September 2015

This thesis investigates the utility of sequence stratigraphy on a regional scale and the control of eustasy on basin infill in unprecedented detail. To achieve this, the thesis utilises a wealth of data, including a continuous 3D seismic MegaSurvey dataset covering 55,000 sq. km, combined with state of the art seismic interpretation software to interpret the basin infill of the Late Cenozoic southern North Sea. The prograding shelf-prism clinoforms of the Late Cenozoic are calibrated to high density borehole penetrations, high resolution chronostratigraphy and climate proxies. The chronostratigraphic control enables a correlation of geomorphology, seismic architectures and seismic facies with full 3D control to the global sea level curve, which enables an evaluation of the impact of eustatic change on sequence development.

The control of eustasy and the limitations of sequence stratigraphy are highlighted by:

- 1) Investigating the regional expression of chronostratigraphically calibrated seismic units, which are linked to the global sea level curve. This was carried out by mapping across the region, the dominance of oblique or sigmoidal clinoform types and seismic features such as iceberg scours, terrestrial channels and submarine fans in order to evaluate the lateral variation of depositional systems and accommodation.
- 2) Investigating sediment partitioning basinwards of the shelf edge and how deposition basinwards can be predicted via observations of seismic facies and architecture. This was achieved by focusing on specific seismic architectures of forced regressive slope clinoforms and deep water sedimentary systems and the link updip to the shelf within the highly constrained chronostratigraphic framework.

The thesis results suggest that sequence stratigraphic models do not represent lateral variation well or integrate other allocyclic forcings on sequence development. A holistic and observation based approach to understanding basin infill and recognising the importance of sediment supply, pre-existing geomorphology, process type of the feeder system, differential subsidence, as well as eustasy, is imperative.

DECLARATION

No portion of the work referred to in the thesis has been submitted in support of an application for another degree or qualification of this or any other university or other institute of learning.

COPYRIGHT STATEMENT

- i. The author of this thesis (including any appendices and/or schedules to this thesis) owns certain copyright or related rights in it (the “Copyright”) and s/he has given The University of Manchester certain rights to use such Copyright, including for administrative purposes.
- ii. Copies of this thesis, either in full or in extracts and whether in hard or electronic copy, may be made **only** in accordance with the Copyright, Designs and Patents Act 1988 (as amended) and regulations issued under it or, where appropriate, in accordance with licensing agreements which the University has from time to time. This page must form part of any such copies made.
- iii. The ownership of certain Copyright, patents, designs, trade marks and other intellectual property (the “Intellectual Property”) and any reproductions of copyright works in the thesis, for example graphs and tables (“Reproductions”), which may be described in this thesis, may not be owned by the author and may be owned by third parties. Such Intellectual Property and Reproductions cannot and must not be made available for use without the prior written permission of the owner(s) of the relevant Intellectual Property and/or Reproductions.
- iv. Further information on the conditions under which disclosure, publication and commercialisation of this thesis, the Copyright and any Intellectual Property and/or Reproductions described in it may take place is available in the University IP Policy (see <http://documents.manchester.ac.uk/DocuInfo.aspx?DocID=487>), in any relevant Thesis restriction declarations deposited in the University Library, The University Library’s regulations (see <http://www.manchester.ac.uk/library/aboutus/regulations>) and in The University’s policy on Presentation of Theses

PREFACE

This thesis represents the conclusion of a PhD study carried out at the School of Earth, Atmospheric and Environmental Sciences, University of Manchester, UK under the main supervision of Dr. Mads Huuse (Reader in Geophysics at the University of Manchester) and Professor Rob Gawthorpe (Professor in Earth Science, University of Bergen). The study was initiated in July 2011 and submitted in September 2015.

The PhD project is entitled “Evolution of the Giant Southern North Sea Shelf-Prism: Testing sequence stratigraphic concepts and the global sea-level curve with full-three dimensional control”. The study was initiated with the objective of interpreting the well dated Late Cenozoic clinoforms in the southern North Sea, using high resolution chronostratigraphic control to understand the evolution of the shelf/slope/basin system in the North Sea over an incredibly interesting time in the earth’s history. The initial idea also was to use this case study to understand what seismic geometries and basin infill could tell us about the relative sea level changes (base level) and in turn how this could be related to the global sea level curve. The overarching theme, which would be relevant not just to North Sea, was to test sequence stratigraphic concepts and how well the methodology could be applied at a basin scale, with full 3D control.

The project first started in July 2011 with 2D seismic data and individual 3D seismic surveys supplied by TNO (Netherlands Geological Survey). Continuous 3D seismic data over the southern North Sea in the form of the PGS Southern and Central North Sea MegaSurvey increased the power of the study in 2012 as now continuous interpretation could be carried out across the basin without mismatch problems between surveys. This increased the likeliness that the same reflection was being traced. It also allowed us to compare the different structural domains as the Central North Sea MegaSurvey area showed much greater subsidence than in the Southern North Sea MegaSurvey.

Publications by author

Harding, R & Huuse, M (2015), Salt on the move: Multi stage evolution of salt diapirs in the Netherlands North Sea. *Marine and Petroleum Geology*. **61**. 39-55.

Published abstracts not included in thesis

Harding, R, Newton, A, Huuse, M & Gawthorpe, R (2015), *Early Quaternary geomorphology of the southern North Sea: results from high resolution 3D MegaSurvey seismic analysis*. Quaternary Research Association Annual Discussion Meeting, Edinburgh, January 2015.

Newton, A, **Harding, R**, Lamb, R., Huuse, M (2015), *Early Quaternary environments in the North and Norwegian Seas*. Quaternary Research Association Annual Discussion Meeting, Edinburgh, January 2015.

Harding, R, Huuse, M & Gawthorpe, R (2014), *Testing sequence stratigraphy on a mega scale: Lateral variation in key stratal surfaces from 3D seismic analysis of the Late Cenozoic southern North Sea*. William Smith Meeting, Geological Society London, September 2014.

Harding, R, Huuse, M & Gawthorpe, R (2014), *Controls of shelf evolution on a mega scale: 3D seismic analysis of the Late Cenozoic southern North Sea*. 19th International Sedimentological Congress, Geneva, Switzerland, August 2014.

Harding, R, Huuse, M & Gawthorpe, R (2014), *Testing sequence stratigraphy on a mega scale: Lateral variation of key stratal surfaces from 3D seismic analysis of the Late Cenozoic southern North Sea*. 19th International Sedimentological Congress, Geneva, Switzerland, August 2014.

Harding, R & Huuse, M (2013), *3D seismic characteristics of the Late Cenozoic southern North Sea clinoforms*, International Association of Sedimentologists (IAS) annual meeting, Manchester, September 2013.

Harding, R & Huuse, M (2013), *Regional 3D seismic analysis of the Late Cenozoic southern North Sea delta*. American Association of Petroleum Geologists Annual Conference and Exhibition, Pittsburgh, USA, May 2013.

Harding, R & Huuse, M (2012), *Late Cenozoic southern North Sea basin: testing sequence stratigraphy concepts and the global sea level curve with full-three dimensional control*. William Smith Meeting, Geological Society London, September 2012.

Harding, R & Huuse, M (2011), *Mega scale seismic interpretation of the Neogene southern North Sea delta*. BSRG Imperial College London, December 2011.

Harding, R & Huuse, M (2011), *Seismic interpretation of the Neogene southern North Sea delta* Miocene Workshop GEUS, Copenhagen, October 2011.

ACKNOWLEDGMENTS

I would like to thank firstly my supervisors Mads Huuse and Rob Gawthorpe for continual and unwavering encouragement, enthusiasm and patience throughout the PhD.

I thank the Natural Environmental Research Council (NERC) for funding the majority of the project and TNO (Netherlands Geological Survey) for a CASE contribution. Johan ten Veen, Geert De Bruin and Timme Donders were particularly supportive during the project with data and discussion and I look forward to continual collaboration with them. PGS are thanked for both providing the MegaSurvey data and supporting the projects with their knowledge, in particular Richard Lamb, Steve Morse and Stefano Patruno. Chris King, independent biostratigraphy consultant, who sadly passed away this year, is greatly thanked for his input with biostratigraphy data of the North Sea.

I would like to thank Emma Finch and Kofi Owusu for technical support during the PhD. Schlumberger for Petrel, FFA for Geoteric and Eliis for Paleoscan seismic interpretation software.

I have made great friends within the department during my time in SEAES who were able to make everyday fun and also provided a good sounding board for ideas at times, in particular in the basins lab, Georgina, Tobi, Tom, Rachel L and Andrew and from the department, Rhodri, Billy, Brian, Ash, Harriet, Will, Richard Newport and my housemate for two years Richard McAllister. I thank my friends out of the department, and best friends Jane and Lucy Chard, I would also like to thank Rick for pragmatic advice and bags of patience during thesis writing!

Rachel Harding
School of Earth, Atmospheric and Environmental Sciences,
University of Manchester
Williamson Building,
Oxford Road
Manchester, M13 9LP

CHAPTER 1

INTRODUCTION

CHAPTER 1 INTRODUCTION

This thesis investigates the development of a prograding clinoform wedge in the southern North Sea (sNS) during the Late Cenozoic using largely indirect geophysical imaging data; 3D seismic reflection and borehole data such as gamma ray and sonic logs. The development of the clinoforms and depositional systems such as incised valleys, slope fans and basin floor fans can be put in time context by the high resolution chronostratigraphic control and linked to the global sea level curve which creates a powerful tool to investigate many sequence stratigraphic concepts.

1.1 PROJECT RATIONALE

There are two overarching motivations for carrying out this study. The first relates to the case study of interpreting Late Cenozoic clinoforms in the southern North Sea using high resolution chronostratigraphic control to understand the evolution of the shelf-prism depositional system in the North Sea over an incredibly interesting time in the earth's history, the descent into icehouse conditions. Little is known of the depositional environments of the North Sea during the earliest Quaternary and this dataset covers an expanded section of the Gelasian (2.58 Ma to 1.78 Ma) which corresponds to the earliest large scale glaciations to affect the sNS (Gibbard et al., 1991; Zagwijn, 1992; Kuhlmann et al., 2004; Noorbergen et al., 2015).

Prior studies of the Late Cenozoic have either focused on individual 3D seismic surveys in one area of the sNS (Kuhlmann and Wong, 2008; Benvenuti et al., 2012; Stuart and Huuse, 2012), or are regional in scale but use 2D seismic surveys (Cameron et al., 1987; Sorensen, 1998; Overeem et al., 2001; Anell et al., 2012; Thöle et al., 2014). The stratigraphy of the Late Cenozoic Netherlands North Sea is constrained by high resolution chronostratigraphic, lithological, quantitative palynological and geochemical data from core; and palaeomagnetic logs for wells *A15-03* and *A15-04* in the north Netherlands North Sea (Kuhlmann et al., 2006ab; ten Veen et al., 2013) (Fig. 1.1). Biostratigraphy and benthic stable isotope analysis in the Noordwijk borehole, onshore Netherlands, has also been carried out (Meijer et al., 2006; Noorbergen et al., 2015) (Fig. 1.1).

Linking local climate and sea level change events from palynology and geochemical studies from the Netherlands North Sea and onshore Netherlands to the Marine Isotope Stages (MIS) of the global oxygen isotope curve (Lisiecki and Raymo, 2005) suggests a complex relationship between glacioeustasy and the sedimentary record in the SNS (Meijer et al., 2006; Kuhlmann et al., 2006ab; Noorbergen et al., 2015 Donders et al., in prep).

This chronostratigraphic framework had yet to be extended across the SNS basin and utilised to understand in detail the regional basin infill in relation to the global sea level curve. The resolution in the earliest Gelasian (2.58 Ma to 2.43 Ma) combined with a high sediment supply allowed individual glacial–interglacial cycles to be matched to sediment packages. The application of this is to understand not only the evolution of the depositional environments during the descent to icehouse conditions but also to investigate fundamental geological principles. For an in-depth geological setting and previous work on the case study see Chapter 3).

Interest in the Late Cenozoic, especially in the Netherlands North Sea, has increased in the last 15 years due to the exploration of a shallow gas play. The first shallow gas field (Block A12) is in production by Chevron and a second field in Block F02 is now being developed by Petrocanada/Dana (ten Veen et al., 2011). Kuhlman and Wong (2008) related the occurrence of gas related bright spots with specific units and palaeoenvironments of the shelf-prism, hence the importance of understanding the extent and characteristics regionally of the units. Recent hydrocarbon discovery LilleJohn in the Miocene Ustira formation in the Danish Sector of the North Sea is associated with a basin floor sands play (Trampe et al., 2013).

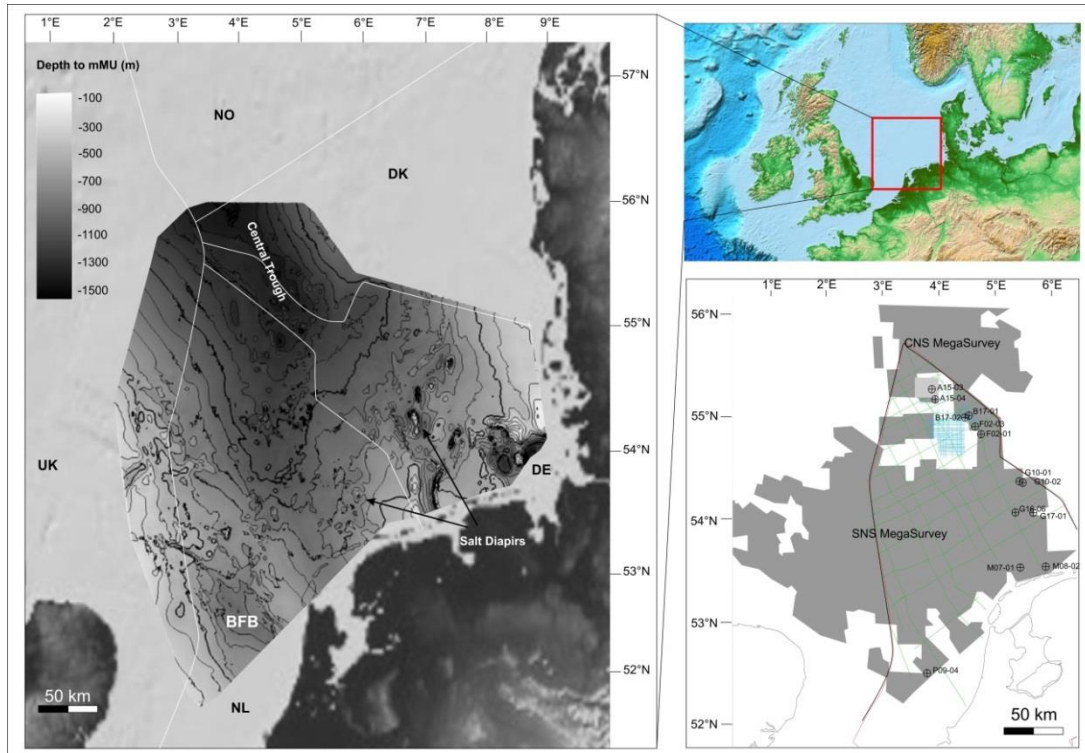


Figure 1.1 Regional setting and dataset map. Left: Mid Miocene Unconformity (mMU) depth structure map. Map is the result of seismic interpretation from this study, (UK, NL and DK sectors) combined with the German mMU structure map from Geopotenzial Deutsch Nordsee project (www.gpdn.de). Key areas of accommodation creation marked, Central Trough and BFB (Broad Fourteens Basin). NL Netherlands; DE Germany; DK Denmark; NO Norway. Top Right: GEBCO bathymetry for North Sea showing location of dataset within the contemporary setting. Bottom right: Dataset map. Grey areas represent 3D seismic coverage. 2D seismic lines and key boreholes used the lithological determination also shown.

The second overarching motivation for the project was to map seismic geometries and basin infill of the regionally correlatable sediment packages, on the scale of 100's km and link them to specific periods within the global sea level curve. This was carried out to determine the influence eustasy has on the depositional architecture and how well sequence stratigraphy methodology can be applied at basin scale, with full 3D control, to predict reservoir quality sands.

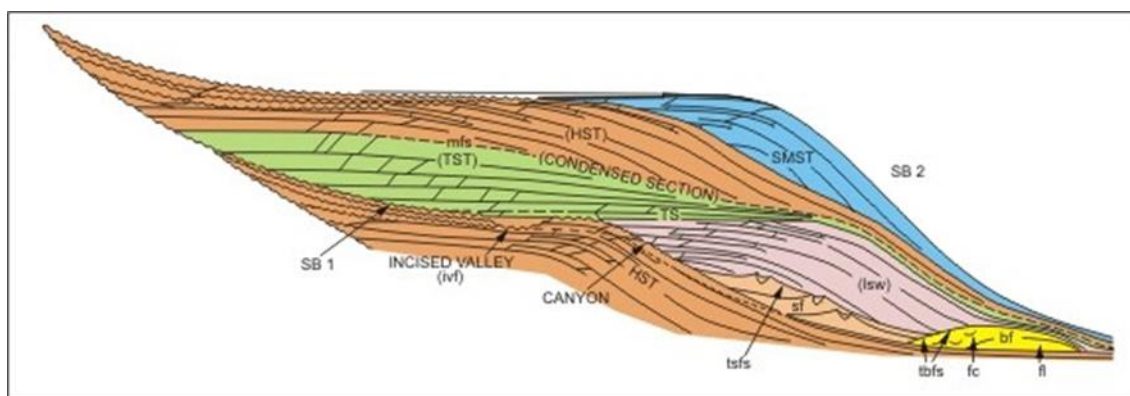


Figure 1.2 Exxon Mobil “Slug Model”. Illustrating traditional systems tracts from Vail (1987)

Original sequence stratigraphic methodology was developed using 2D seismic lines and poorer seismic data than is available today. The original methodology was based on the idea that global sequences can be correlated, as eustasy was identified as the main control on the sequence of seismic architectures and this can be used in the prediction of key elements of the hydrocarbon play (Vail et al., 1977; Haq, 1988; Posamentier and Vail, 1988). The identification of eustasy as the main control on sequence development is apparent in the sequence stratigraphic nomenclature which impressed sea level terms on sequence architectures (e.g. “Lowstand” or “Highstand”).

Modifications of the original sequence stratigraphic methodology have been large in number over the years with the attempts to standardise the methodology and terminology within the last ten years (Catuneanu et al., 2009). During the 1990’s 3D seismic data and higher resolution datasets became available and many studies recognised lateral variability in seismic architectures regionally. This led to publications questioning the governance of eustasy over sequence development and the ability to globally correlate sequences, recognising sediment supply, underlying geomorphology and tectonics as key factors which can override the eustatic sea level signal and create lateral variation (Posamentier and Allen, 1993; Gawthorpe et al., 1994; Martinsen and Helland-Hansen, 1995).

Studies on the prediction of basin floor fans and the partitioning of reservoir quality sands across a basin also highlighted a flaw in the original sequence stratigraphic methodology. Early sequence stratigraphic models placed the sediment transfer basinwards of the shelf edge within lowstands of global sea level and within the Lowstand Systems Tract (LST), comprising the basin floor fan, slope fan and prograding

wedge (Vail et al., 1977; Posamentier and Vail, 1988) (Fig. 1.2). Fall in relative sea level below the shelf edge enables river systems to reach the shelf edge and directly supply coarser-grained sediment into deep water settings (Johannessen and Steel, 2005). Many modern submarine fans, such as the Indus, Amazon, Mississippi and Bengal, have become inactive during the Holocene highstand of sea level as sediment is stored on the shelf (Leeder, 2009). However, transfer of sediment to the basin floor occurs during the Highstand Systems Tract (HST) in ancient and modern systems with high sediment supply, narrow shelf width and tectonic uplift identified as key factors which can override eustatic sea level (Kolla and Perlmutter, 1993; Gawthorpe et al., 1994; Burgess and Hovius, 1998; Carvajal and Steel, 2006; Covault et al., 2007; Henriksen et al., 2011). In supply driven systems the coastline can reach the shelf edge regardless of the relative sea level condition (Porebski and Steel, 2006).

If the coastline is entrenched at the shelf edge during LST conditions this does not necessarily translate to significant sand volumes transferred to the basin floor (Dixon et al., 2012b). Delta process regime influences whether sediment is transferred past the shelf edge. River-dominated deltas are shown to transfer sediment regardless of base level, and wave-dominated and tidal-dominated deltas are less likely to have associated basin floor deposition even in LST conditions (Dixon et al., 2012ab; Jones et al., 2015) (Fig. 1.3).

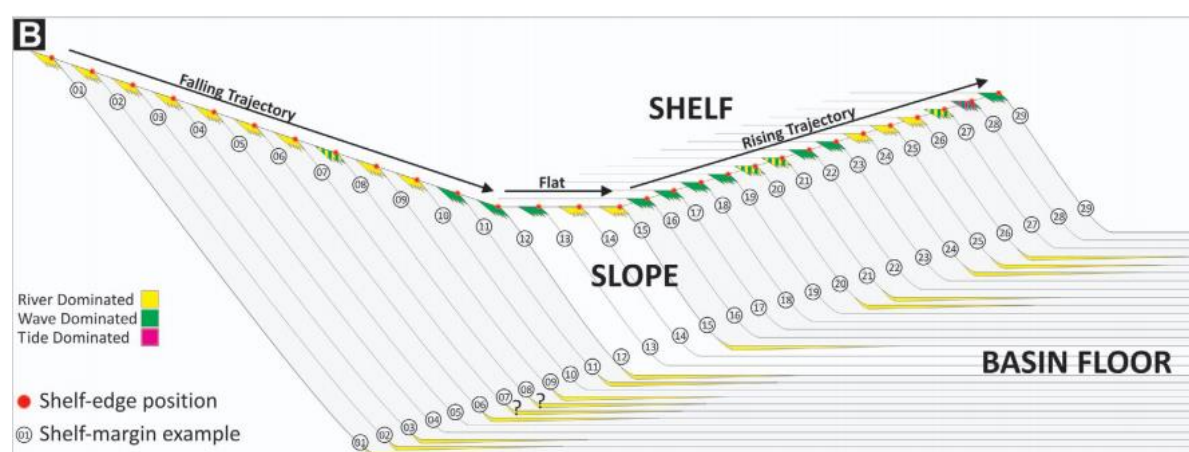


Figure 1.3 Basin floor deposition scenarios Schematic representation of clinoformal successions with varying deltaic styles (including mixed-influence systems), shelf-edge trajectories (flat, rising, or falling) and deep-water depositional systems. From Dixon et al., (2012a).

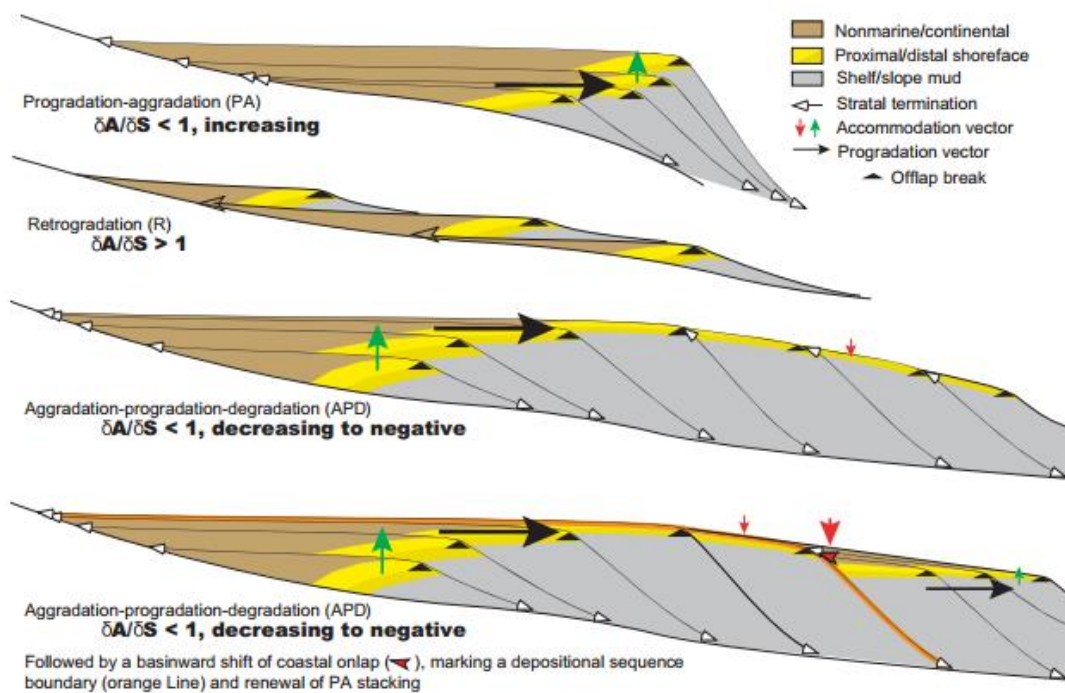


Figure 1.4 Stratigraphic stacking patterns. From Neal and Abreu, (2009)

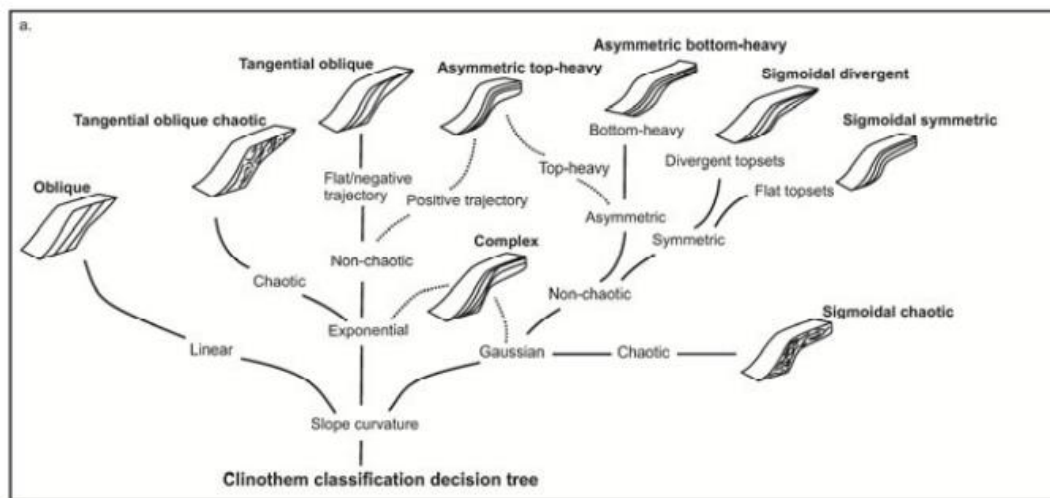


Figure 1.5 Clinoform classification decision tree. From Anell and Midtkandal (2015)

The identification that eustasy was not the only control on sequence development led to more observation based approaches of Helland-Hansen and Hampson, (2009); Neal and Abreu, (2009) and Miller et al., (2013). These approaches utilise clinoform geometries, clinoform stacking patterns and trajectories (Fig. 1.4). This approach does not press upon the physical controls on sequence formation on observations unlike traditional sequence stratigraphic terms such as “highstand” and “lowstand” which suggestive sea level as the dominant control (Helland-Hansen and Hampson, 2009).

The most recent studies on clinoform architectures and the ability to predict where specific elements of the depositional system recognise the complexity of lateral variation of sequences which comes with higher resolution seismic data and greater coverage (Ryan et al., 2009; Anell and Midtkandal, 2015; Fongngern et al., 2015; Patruno et al., 2015;) (Fig. 1.5). These studies focus on quantitative measurements of clinoform architectures to understand accommodation and sediment partitioning and build on the observational based seismic stratigraphic techniques of Helland-Hansen and Hampson (2009) and Neal and Abreu (2009).

1.2 AIMS

The broad aims of this study are to:

- 1) Develop a regional chronostratigraphic framework for the Late Cenozoic section of the southern North Sea using seismic and well correlation.
- 2) Utilise “Mega Scale” continuous 3D seismic data to investigate the geomorphology and depositional environment model of the SNS basin for an important period of time in climate history, the descent into icehouse conditions.
- 3) Use the chronostratigraphic framework to link the southern North Sea stratigraphy to the Marine Isotope Curve in order to assess the control of eustasy on the formation of stratigraphic architectures and investigate other controlling forces on stratigraphic architecture and sequence development.
- 4) Investigate the utility of sequence stratigraphic concepts and methodologies to predict sediment dispersal basinwards of the shelf edge in full spatial-temporal detail.

1.3 THESIS SYNOPSIS

The thesis is divided into seven chapters. **Chapter 1** acts as an introduction to the rationale of the project and the current state of literature. **Chapter 2** details the methodology used to analyse and interpret the data available for the study. Original

research is presented in **Chapters 3, 4 and 5**. A detailed geological setting and relevant literature reviews form part of the original research chapters.

Chapter 3 Regional evolution of a shelf-prism in the Late Cenozoic: Eustacy, sediment supply and subsidence in the southern North Sea focuses on the regional interpretation and the seismic stratigraphy of the case study during the Late Cenozoic. The chapter is the unabbreviated version of a paper which, when published will not contain the detailed/extensive unit descriptions present in *Chapter 3*. The challenge of this study and particularly this chapter is that we have a large amount of information, a huge study area and a time period which we want to understand in detail. The lateral variation of the units over such a large area means that we wanted to describe them in great detail in order to back up the interpretations and conclusions of this paper and in the thesis as a whole, as we feel that many papers do not include sufficiently detailed descriptions. In the paper only one full unit description will be given and the rest will be given as supplementary information available online. This paper aims to unravel the controlling factors on the evolution of a large shelf-prism on the scale of a basin at the resolution of 10's kya eustatic cycles and to take a step towards better visualisation of the lateral variation of sequences within a basin, whilst still having to conform to the 2D constraints of a paper based project. The paper will look to be submitted to *Basin Research*. The chapter does not just present a case study but invokes global implications in the rate of progradation seen in clastic systems and the importance of regional studies in the understanding the amount of lateral variation and the translation of the eustatic signal in the sedimentary record.

Chapter 4 Deep water sedimentary systems linked to shelf edge trajectory and global sea level is a long version of a post PhD paper targeting the journal *Geology*. However, the study became a more detailed study and therefore is still debating which journal the paper should be aimed at. This paper builds on the detailed unit description of *Chapter 3* and focuses on using the chronostratigraphic framework to investigate submarine channel systems and associated basin floor deposition. The rationale of the paper is to provide a link up dip to the shelf edge trajectory and the conditions on the shelf at the time of each event and hitherto establish where the depositional systems fit within the sequence stratigraphic framework.

Chapter 5 Can enigmatic Intra Slope Clinoforms provide an independent calibration of early Pleistocene eustatic changes? Builds on the results of the previous two chapters focusing on one depositional architecture type, the Intra Slope Clinoforms, which are sand prone wedges present basinwards of the shelf edge cyclically through the Cenozoic of the southern North Sea. The depositional relevance and position within the sequence stratigraphic framework is the main focus.

Chapter 6 presents two second author papers which have built upon the work of this thesis, and utilised the seismic reflection interpretation and the chronostratigraphic framework created during this PhD.

Chapter 6.1 Evidence for repeated low latitude marine-terminating ice sheets in a 41 kyr Early Quaternary world, authored with Andrew Newton (first author), Rachel Lamb, Dr Mads Huuse and Dr Simon Brocklehurst all of the University of Manchester was the product of interpretation of reflections where iceberg scouring events were identified and correlated across the SNS (by myself) and CNS (Rachel Lamb) and combining this with Andrew Newton's knowledge of glaciology to create a paper that reflects the importance of basin scale mapping of iceberg scouring events to understanding the magnitude of glaciations in the earliest Quaternary. This paper has been written as a Letter for *Nature* Journal, and this format has been kept for this thesis. The contribution of the author to this paper is the identification and interpretation of seismic reflections within the PGS SNS MegaSurvey and a small part of the PGS CNS MegaSurvey, where iceberg scours were identified; chronostratigraphic correlation of the surfaces, positions of shelf edge, and depositional environmental information and interpretation. The author has continued to have input in the editing process of the manuscript.

Chapter 6.2 The Early Quaternary of the North Sea Basin, authored with Rachel Lamb, Dr. Mads Huuse, Margaret Stewart of BGS, Edinburgh and Simon Brocklehurst. This paper presents a new interpretation of the base Quaternary North Sea basin, interpreted using SNS and CNS MegaSurveys. This includes a new correlation for the base Quaternary in the central North Sea (cNS) and insight into the infill and paleo-water depths throughout the time period 2.58-1.1 Ma. The contribution of the author to this paper was the chronostratigraphic ties from the SNS to the cNS dataset area, the

base Quaternary interpretation and structure map for the SNS area (combined with Rachel Lamb's cNS base Quaternary map for the paper) and data and interpretation about the SNS or "southern clinoform" as it is termed in the paper and manuscript editing. This paper was submitted to Quaternary Science Reviews in October 2015.

Chapter 7 focuses on synthesising the results and discussions of the previous chapters and discussing their contribution to the literature, the implications of the study and also talking about the limitations of the project. Looking to the future, further research questions are presented which have arisen during the PhD project.

Additionally the author published a paper "Salt on the move: Multistage evolution of salt diapirs in the Netherlands North Sea". This paper is a result of data interpreted during a Masters project but was largely written as a paper and further interpretation was carried out during the PhD. This paper was published in March 2015 in *Marine and Petroleum Geology*.

1.4 REFERENCES

- Anell, I., Midtkandal, I., 2015. The quantifiable clinothem – types, shapes and geometric relationships in the Plio-Pleistocene Giant Foresets Formation, Taranaki Basin, New Zealand. Basin Research.
- Anell, I., Thybo, H., Rasmussen, E., 2012. A synthesis of Cenozoic sedimentation in the North Sea. Basin Research 24, 154–179.
- Benvenuti, a, Kombrink, H., Ten Veen, J.H., Munsterman, D.K., Bardi, F., Benvenuti, M., 2012. Late Cenozoic shelf delta development and Mass Transport Deposits in the Dutch offshore area – results of 3D seismic interpretation. Netherlands Journal of Geosciences 91, 591–608.
- Burgess, P.M., Hovius, N., 1998. Rates of delta progradation during highstands: consequences for timing of deposition in deep-marine systems. Journal of the Geological Society 155, 217–222.
- Cameron, T.D.J., Stoker, M.S., Long, D., 1987. The history of Quaternary sedimentation in the UK sector of the North Sea Basin. Journal of the Geological Society 144, 43–58.
- Carvajal, C.R., Steel, R.J., 2006. Thick turbidite successions from supply-dominated shelves during sea-level highstand. Geology 34, 665–668.
- Catuneanu, O., Abreu, V., Bhattacharya, J.P., Blum, M.D., Dalrymple, R.W., Eriksson, P.G., Fielding, C.R., Fisher, W.L., Galloway, W.E., Gibling, M.R., Giles, K. A., Holbrook, J.M.,

- Jordan, R., Kendall, C.G.S.C., Macurda, B., Martinsen, O.J., Miall, A. D., Neal, J.E., Nummedal, D., Pomar, L., Posamentier, H.W., Pratt, B.R., Sarg, J.F., Shanley, K.W., Steel, R.J., Strasser, A., Tucker, M.E., Winker, C., 2009. Towards the standardization of sequence stratigraphy. *Earth-Science Reviews* 92, 1–33.
- Covault, J. A., Normark, W.R., Romans, B.W., Graham, S. A., 2007. Highstand fans in the California borderland: The overlooked deep-water depositional systems. *Geology* 35, 783–786.
- Dixon, J.F., Steel, R.J., Olariu, C., 2012. Shelf-edge delta regime as a predictor of deep-water deposition. *Journal of Sedimentary Research* 82, 681–687.
- Donders, T., Verreussel, R., van Helmond, N., Munsterman, D., Ten Veen, J., Speijer, R., Weijers, J., Sangiorgi, F., Reichart, G-J., Damsté, J-S., Lourens, L., Kuhlmann, G., Brinkhuis, H. Early Pleistocene glaciations exhibit predominant Northern Hemisphere forcing. In Prep.
- Fongngern, R., Olariu, C., Steel, R.J., Krézsek, C., 2015. Clinoform growth in a Miocene, Para-Tethyan deep lake basin: Thin topsets, irregular foresets, and thick bottomsets. *Basin Research*.
- Gawthorpe, R.L., Fraser, A.J., Collier, R.E.L., 1994. Sequence stratigraphy in active extensional basins: implications for the interpretation of ancient basin-fills. *Marine and Petroleum Geology* 11, 642–658.
- Gibbard, P.L., West, R.G., Zagwijn, W.H., Balson, P.S., Burger, A.W., Funnell, B.M., Jeffery, D.H., de Jong, J., van Kolfschoten, T., Lister, A.M., Meijer, T., Norton, P.E.P., Preece, R.C., Rose, J., Stuart, A.J., Whiteman, C.A., Zalasiewicz, J.A., 1991. Early and early Middle Pleistocene correlations in the southern North Sea basin. *Quaternary International* 10, 23–52.
- Haq, B.U., 1988. Mesozoic and Cenozoic chronostratigraphy and cycles of sea-level change. *SEPM Special Publication* 42, 71-108.
- Helland-Hansen, W., Hampson, G.J., 2009. Trajectory analysis: concepts and applications. *Basin Research* 21, 454–483.
- Henriksen, S., Helland-Hansen, W., Bullimore, S., 2011. Relationships between shelf-edge trajectories and sediment dispersal along depositional dip and strike: A different approach to sequence stratigraphy. *Basin Research* 23, 3–21.
- Johannessen, E.P., Steel, R.J., 2005. Shelf-margin clinoforms and prediction of deepwater sands. *Basin Research* 17, 521–550.
- Jones, G.E.D., Hodgson, D.M., Flint, S.S., 2015. Lateral variability in clinoform trajectory, process regime, and sediment dispersal patterns beyond the shelf-edge rollover in exhumed basin margin-scale clinoforms. *Basin Research*, 27 (6), 657-680.

- Kolla, V., Perlmutter, M.A., 1993. Timing of turbidite sedimentation on the Mississippi Fan. *AAPG Bulletin* 77, 1129–1141.
- Kuhlmann, G., Wong, T.E., 2008. Pliocene paleoenvironment evolution as interpreted from 3D-seismic data in the southern North Sea, Dutch offshore sector. *Marine and Petroleum Geology* 25, 173–189.
- Kuhlmann, G., de Boer, P.L., Pedersen, R.B., Wong, T.E., 2004. Provenance of Pliocene sediments and paleoenvironmental changes in the southern North Sea region using Samarium-Neodymium (Sm/Nd) provenance ages and clay mineralogy. *Sedimentary Geology* 171, 205–226.
- Leeder, M.R., 2009. *Sedimentology and sedimentary basins: from turbulence to tectonics*. John Wiley & Sons.
- Lisiecki, L.E., Raymo, M.E., 2005. A Pliocene-Pleistocene stack of 57 globally distributed benthic $\delta^{18}O$ records. *Paleoceanography* 20, 1–17.
- Martinsen, O.J., Helland-Hansen, W., 1995. Strike variability of clastic depositional systems: does it matter for sequence-stratigraphic analysis? *Geology* 23, 439–442.
- Meijer, T., Cleveringa, P., Munsterman, D.K., Verreussel, R.M.C.H., 2006. The Early Pleistocene Praetigian and Ludhamian pollen stages in the North Sea Basin and their relationship to the marine isotope record. *Journal of Quaternary Science* 21, 307–310.
- Miller, K.G., Mountain, G.S., Browning, J. V., Katz, M.E., Monteverde, D., Sugarman, P.J., Ando, H., Bassetti, M. a., Bjerrum, C.J., Hodgson, D., Hesselbo, S., Karakaya, S., Proust, J.N., Rabineau, M., 2013. Testing sequence stratigraphic models by drilling Miocene foresets on the New Jersey shallow shelf. *Geosphere* 9, 1236–1256.
- Neal, J., Abreu, V., 2009. Sequence stratigraphy hierarchy and the accommodation succession method. *Geology* 37, 779–782.
- Noorbergen, L.J., Lourens, L.J., Munsterman, D.K., Verreussel, R.M.C.H., 2015. Stable isotope stratigraphy of the early Quaternary of borehole Noordwijk, southern North Sea. *Quaternary International* 386, 148–157.
- Overeem, I., Weltje, G.J., Bishop-Kay, C., Kroonenberg, S.B., 2001. The Late Cenozoic Eridanos delta system in the Southern North Sea Basin: a climate signal in sediment supply? *Basin Research* 13, 293–312.
- Patrino, S., Hampson, G.J., Jackson, C.A.-L., 2015. Quantitative characterisation of deltaic and subaqueous clinoforms. *Earth-Science Reviews* 142, 79–119.
- Porebski, S.J., Steel, R.J., 2006. Deltas and Sea-Level Change. *Journal of Sedimentary Research* 76, 390–403.

- Posamentier, H.W., Allen, G.P., 1993. Variability of the sequence stratigraphic model: effects of local basin factors. *Sedimentary Geology* 86, 91–109.
- Posamentier, H.W., Vail, P.R., 1988. Eustatic controls on clastic deposition II — Sequence and systems tract models. *SEPM Special Publication* 42, 125-154.
- Ryan, M.C., Helland-Hansen, W., Johannessen, E.P., Steel, R.J., 2009. Erosional vs. accretionary shelf margins: The influence of margin type on deepwater sedimentation: An example from the Porcupine Basin, offshore western Ireland. *Basin Research* 21, 676–703.
- Sorensen, K., 1998. The salt pillow to diapir transition; evidence from unroofing unconformities in the Norwegian-Danish Basin. *Petroleum Geoscience* 4, 193–202.
- Stuart, J.Y., Huuse, M., 2012. 3D seismic geomorphology of a large Plio-Pleistocene delta – “Bright spots” and contourites in the Southern North Sea. *Marine and Petroleum Geology* 38, 143–157.
- Thöle, H., Gaedicke, C., Kuhlmann, G., Reinhardt, L., 2014. Late Cenozoic sedimentary evolution of the German North Sea? A seismic stratigraphic approach. *Newsletters on Stratigraphy* 47, 299–329.
- Trampe, A.F., Lutz, R., Franke, D., Thöle, H., Arfai, J., 2013. Shallow gas in Cenozoic sediments of the Southern North Sea, in: *EGU General Assembly Conference Abstracts*. p. 1835.
- Vail, P.R., Mitchum, R.M., Thompson, S., 1977. Seismic stratigraphy and global changes of sea level, Part IV: Global cycles of relative changes of sea level. In: *Stratigraphic interpretations of seismic data*. American Association of Petroleum Geologists 26, 83–97.
- Vail, P.R., Seismic Stratigraphy Interpretation Using Sequence Stratigraphy Part I : Seismic Stratigraphy Interpretation Procedure. *AAPG Studies in Geology* 27 (1), 1-10.
- Zagwijn, W.H., 1992. The beginning of the Ice Age in Europe and its major subdivisions. *Quaternary Science Reviews* 11, 583-591.

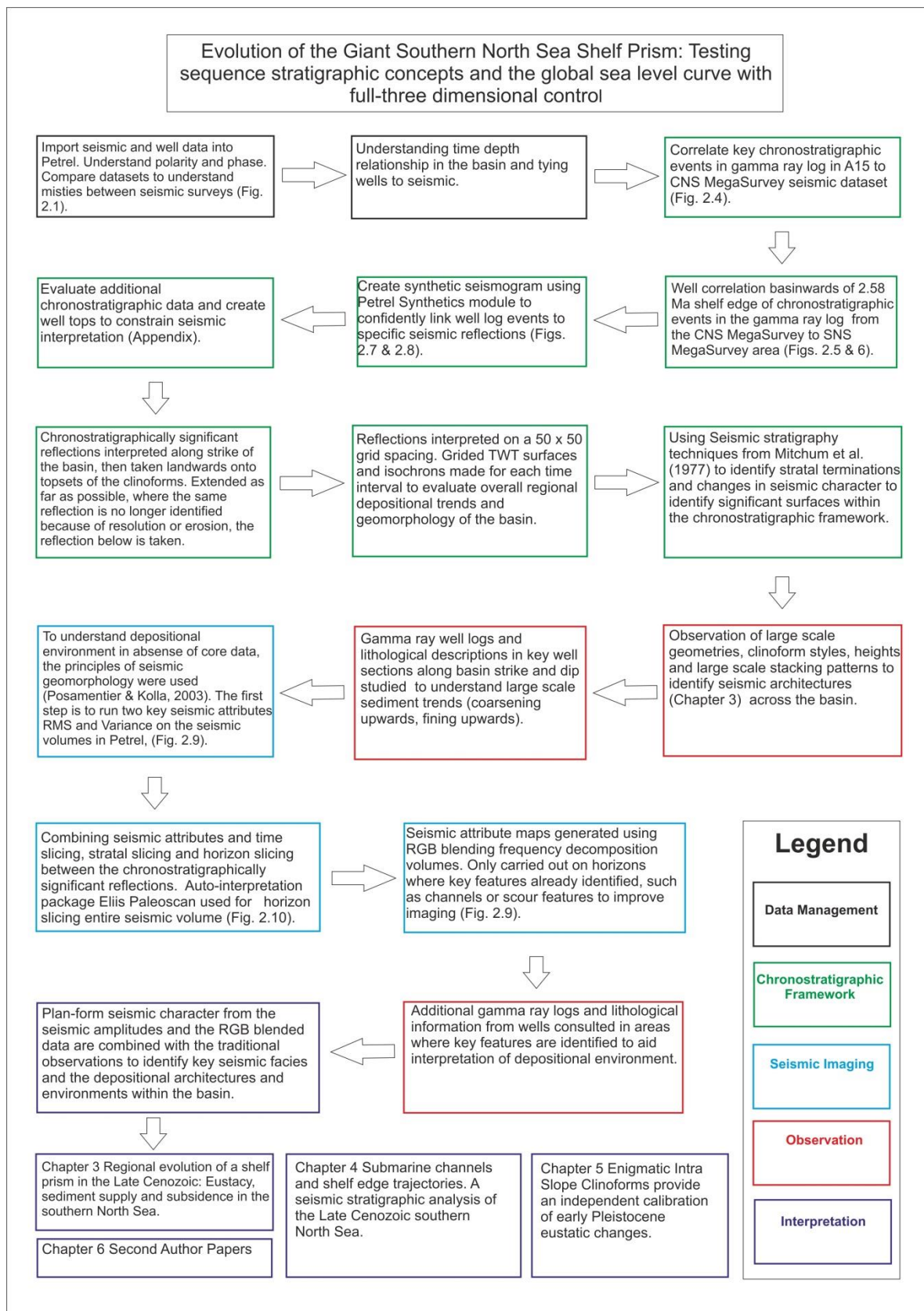
CHAPTER 2

DATASET AND METHODOLOGY

CHAPTER 2 METHODOLOGY

This chapter aims to set out the processes undertaken during the PhD to make the most of the large amount of data available for the project. “MegaSurvey” and large datasets are increasingly used in academia and industry and therefore key software and techniques are required to “process” the amount of geological variability within a large dataset. The approach to interpreting a large seismic dataset and seismic analysis techniques are described. The chapter also focuses on the chronostratigraphic control of the Late Cenozoic, an important component of the project and the basis for the link between the seismic interpretation and the global sea level curve.

Figure 2.1 Mega Scale Dataset Methodology (following page).



2.1 DATASET

The dataset comprises 3D continuous seismic PGS (Petroleum Geo-Services) SNS MegaSurvey, covering 40,000 km² of the NL and UK sectors of the SNS, and part of the PGS CNS MegaSurvey covering ~15,000 km² of the NL, DK and DE sectors (Fig. 1.1). The bin spacing is 50 m x 50 m, sampling rate 4 ms TWT with a maximum vertical resolution of 10-15 m and a dominant frequency of 40Hz in the top 1500 m. The SNS data is largely normal polarity (zero phase) and a hard kick represents positive (peak) reflection. The CNS is largely in reverse polarity (minimum phase 90 degrees) and a hard kick represents a negative (trough) reflection (Fig. 2.2). The MegaSurveys consist of individual seismic surveys stitched together to create the continuous dataset. Individual seismic datasets within the continuous MegaSurvey dataset retained original polarity differences as operators wished to maintain well ties and therefore there are inconsistencies of polarity. The CNS MegaSurvey is not internally consistent in terms of the wavelet character. For example in the eastern Netherlands North Sea section of the MegaSurvey shows a different character from the Dutch sector of the CNS MegaSurvey (Fig. 2.1). This has been taken into account during interpretation and subsequent analysis (discussed further in section 2.2.2).

The MegaSurvey data is complimented by individual 3D and 2D seismic surveys from TNO-DINO (Fig. 2.1). The 3D surveys are 12.5 x 12.5 bin spacing, with a similar vertical resolution to the MegaSurveys, and the 2D surveys are of variable vintage. The most important of the individual 3D seismic datasets is the A15 seismic dataset (Z3WIN2000A seismic survey) located within the very north of the Netherlands North Sea which allows correlation from A15-03 and A15-04 wells to the MegaSurvey area.

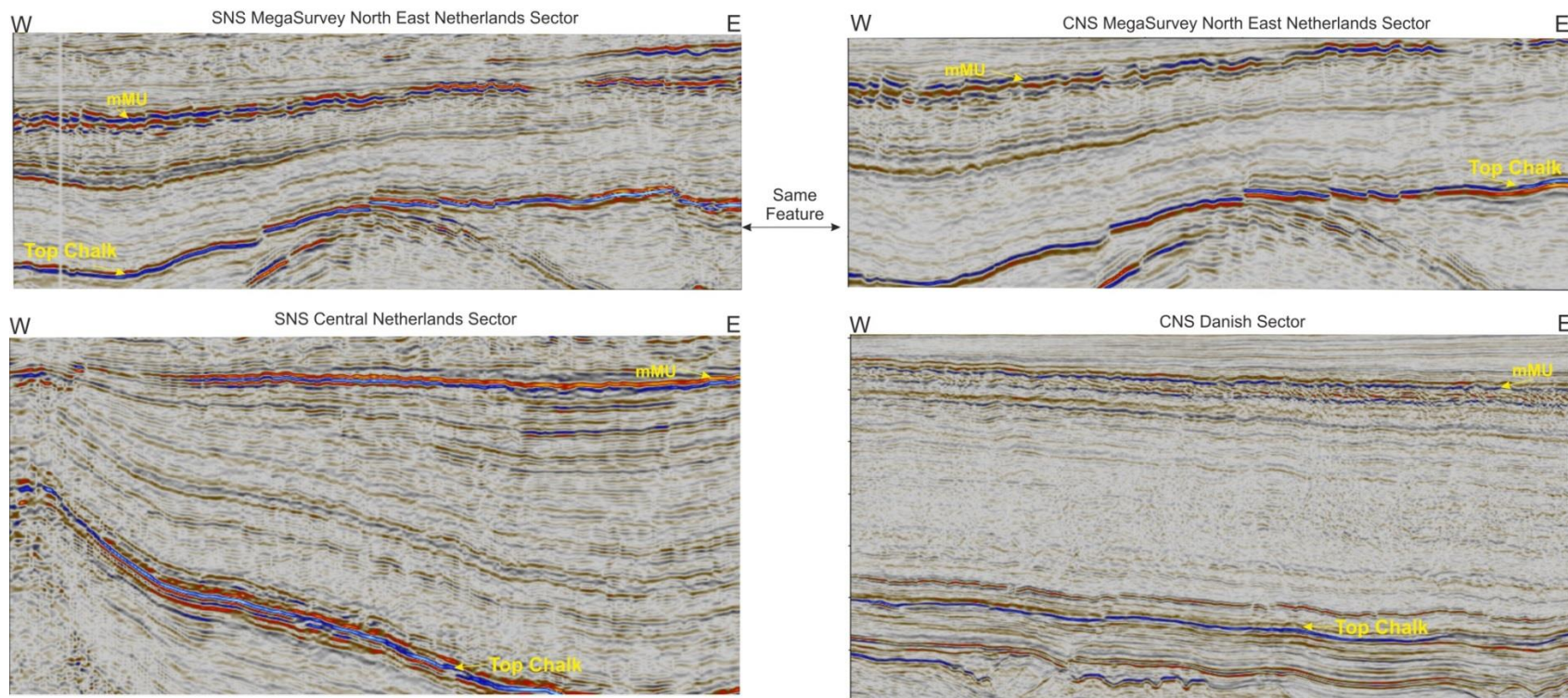


Figure 2.2. Comparison of polarity and phase of sections of the MegaSurvey. Using the Top Chalk and the mMU (mid Miocene Unconformity) for comparison **Top left**, zero phase, SEG convention where an increase in acoustic impedance is represented by a positive peak (red-blue) as shown by the mMU and the Top Chalk; **top right**, same feature as top left, but this is part of the CNS MegaSurvey in zero phase and where an increase in acoustic impedance is represented by a negative trough (blue-red). Likely the same original seismic survey but the polarity has been changed to fit the rest of the MegaSurvey. **bottom left**, SNS MegaSurvey further to the south to show the variation in the character of key surfaces across the MegaSurvey area. **bottom right**, In the Danish sector of the North Sea, the CNS MegaSurvey is in minimum phase rather than in zero phase and this leads to a red-blue-red peak-trough-peak configuration.

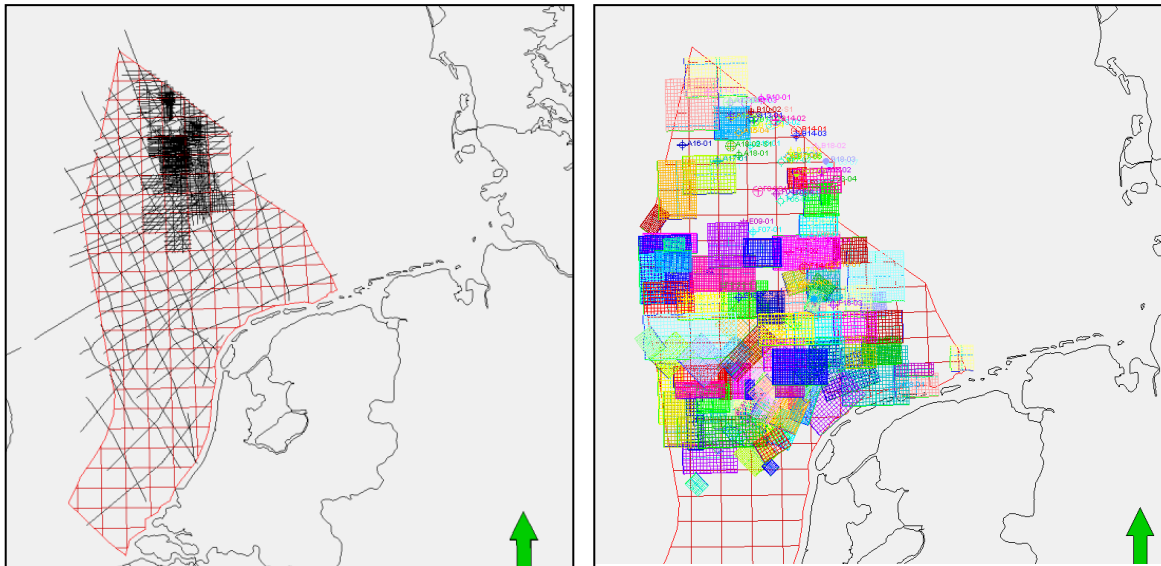


Figure 2.3 Complimenting datasets provided by TNO. left 2D seismic dataset. right individual 3D seismic surveys.

For the first year of the project, prior to gaining the PGS MegaSurvey data the individual 2D and 3D surveys were used to attempt to create a chronostratigraphic framework. Misties of reflections between the individual seismic surveys meant it was very important to understand the character of the reflection being picked, either a downlap surface or an onlap surface. The benefit of the MegaSurveys was that it reduced the amount of misties across the region, however as mentioned above they are not perfect and caution should still be heeded when picking reflections.

The complement of the two datasets means that we can have a more accurate way of correlation across the basin due to the continuous regional scale data, but can also ‘zoom in’ to look at individual elements in closer detail.

2.1.1 Chronostratigraphy

Well data consists of petrophysical well logs, including gamma ray and sonic log. Cuttings descriptions from commercial well reports are also available and utilised. Over 100 boreholes were utilised for which meter scale resolution was possible (Fig. 2.4). High resolution chronostratigraphic, lithological, quantitative palynological and geochemical data from core plus palaeomagnetic logs for wells *A15-03* and *A15-04* in the north of the NL sector (Kuhlmann et al., 2006ab; ten Veen et al., 2011) are utilised

in the expansion of the chronostratigraphic framework from the north of the Netherlands North Sea across the basin. The geomagnetic polarity data available for well A15-03 was tied to the global standard by using tops and bottoms of calibrated dinoflagellate cyst events (Kuhlmann et al., 2006a). Magnetostratigraphy from well B16-01 was also utilised by Kuhlmann et al. (2006), highlighted in Fig. 2.3.

Additional chronostratigraphic information is gained from seismic correlation to Late Cenozoic studies in the Danish sector (Rasmussen et al., 2005; Møller et al., 2009), German Sector (Köthe, 2012; Thöle et al., 2014) in the SE Netherlands sector wells *G10-01*, *G10-02*, *G16-06* and *M07-01* (Benvenuti et al., 2012) and to the UK central North Sea Josephine well (Chapter 6.2). Biostratigraphy derived dates for the Top and Base Gelasian (2.58 & 1.8 Ma) in wells G17-01, M08-02, P09-02 and P09-04 plus an additional Intra Zanclean date at 4.2 Ma in well B17-01, B17-02, F02-01, F02-03 are used to constrain the chronostratigraphic correlation (Chris King *pers comms*, 2013, See Appendix A).

The first aim of the project was to correlate across the dataset the chronostratigraphic framework via seismic interpretation and well log correlation. There were several well log events and associated reflections identified in seismic block A15 Z3WIN2000A (Fig. 2.3) that were dated and could be interpreted across the dataset. Thirteen log units were identified in Kuhlmann et al., (2006ab) in well A15-03 and A15-04 and correlated to seismic block A15 in Kuhlmann and Wong, (2008) (Fig. 2.5). The well to seismic tie across the AB blocks was improved by TNO in the following years including linking key well log responses to the global sea level curve using climate proxies and chronostratigraphic control (ten Veen et al., 2011). The first part of this project focused on interpreting the thirteen log units across from the A15 wells and linking the surrounding seismic to the PGS CNS MegaSurvey, as the CNS MegaSurvey itself does not cover the area of the key wells (Figs. 2.4 & 2.6). Fig. 2.6 shows the early interpretations of the project and the correlation across from the A15-03 well to the MegaSurvey data.

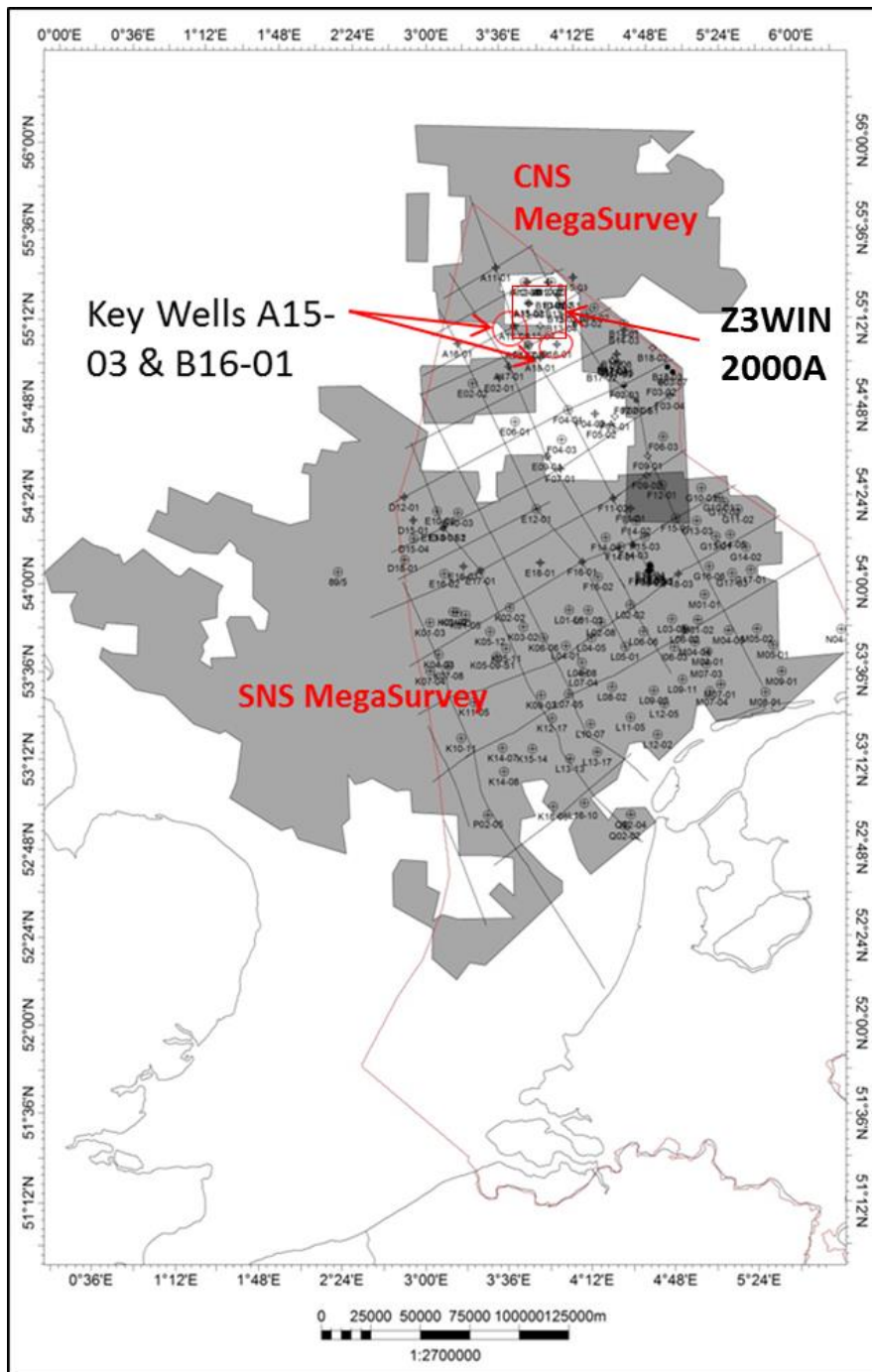


Figure 2.4 Focuses on A15 Block. Dataset map, grey blocks represent MegaSurvey data coverage. Red square represents outline of the Z3WIN2000A 3D seismic survey (A15 3D) which covers the area of the A15-03, A15-04 and B16-01 wells which are the most important chronostratigraphic wells. The MegaSurvey data does not intersect these wells and therefore a correlation was done via the A15 3D seismic to the CNS MegaSurvey.

Age (Ma)	Stages		Magneto-stratigraphy	Seismic Units (This Study)	Newton et al. (Chapter 6)	Sorensen et al. (1997)	Kuhlmann et al. (2004, 2006ab, 2008)	Rasmussen et al. (2005)	Thöle et al. (2014)	Key Surfaces (This Study)
1.78 Ma	Calabrian			1.78 Ma						Top Pleisto 5
Pleistocene	Gelasian (Expanded Section)	Olduvai		Pleisto 5	SU5	Composite Sequence IX	SU12-13	J	—	Top Pleisto 4
				1.94 Ma						
				Pleisto 4	SU4	IX	SU9-11	J	—	
		Reunion?		2.15 Ma						Top Pleisto 3
		Matuyama		Pleisto 3	SU3	VIII	SU7-8	J	—	
				2.35 Ma						Top Pleisto 2
Pliocene	Zanclean			Pleisto 2	SU2	VIII	SU6	J	—	Top Pleisto 1
				2.43 Ma						
		X Event		Pleisto 1	SU1	VI-VII	SU5	I	—	
				2.58 Ma						Top Plio 1
		Gauss		Plio 1	—	IV-V	SU3-4	G-I	SU7	
				4.2 Ma						Top Mio 3
5.33 Ma	Messinian			Mio 3	—	Within IV	Upper SU2	Lower G	SU5-6	
7.2 Ma	Tortonian			Mio 2	—	Early IV	Lower SU2	Upper F	SU3-4	Top Mio 2
11.6 Ma	Serravalian			Mio 1	—	I-III	SU1	E-F	SU1-3	Top Mio 1
13 Ma										

Figure. 2.5 Seismic scheme comparison. Comparison of seismic units interpreted in this study and other seismic studies of the same strata.

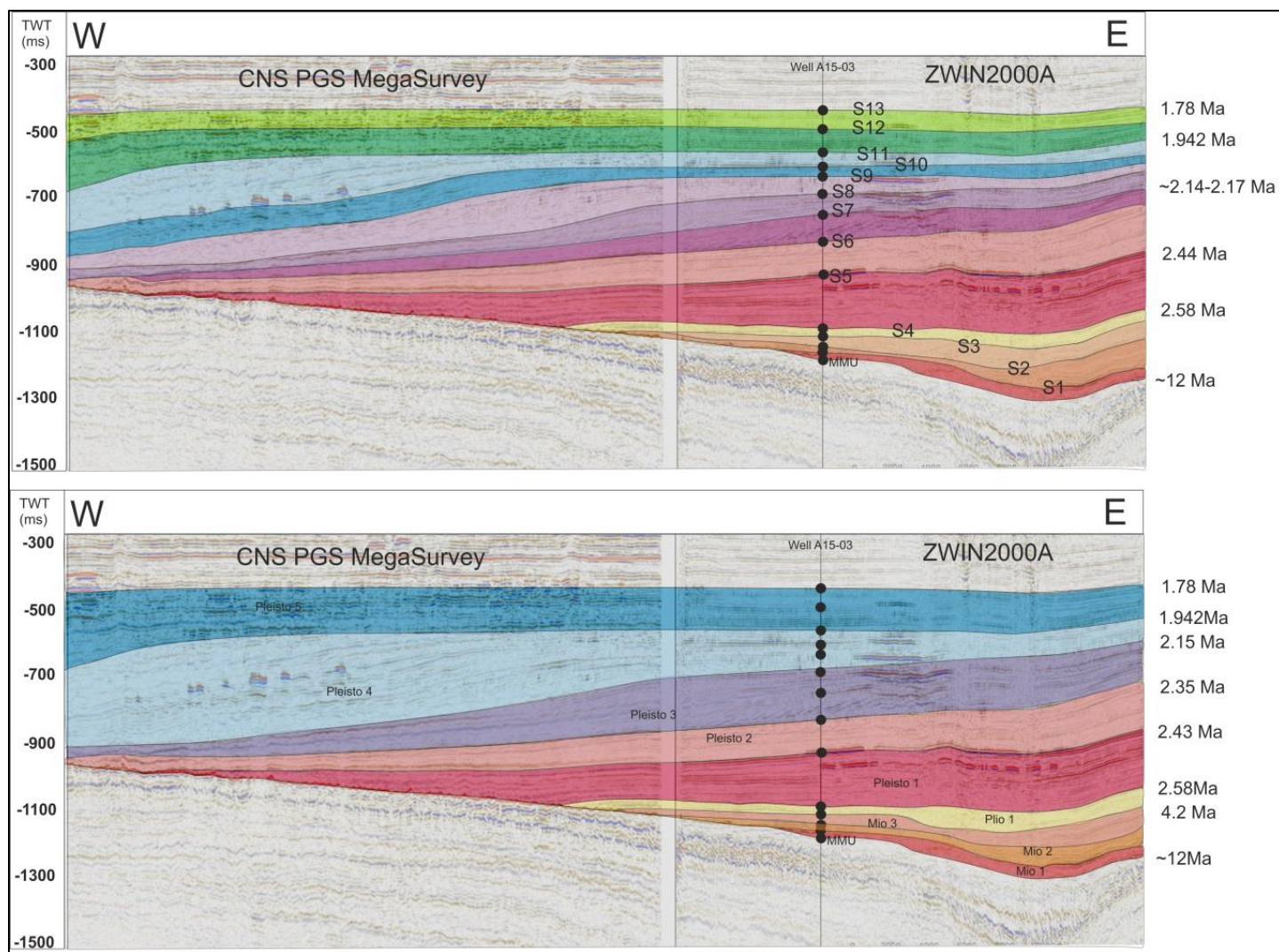


Figure. 2.6 Correlation between A15-03 and CNS MegaSurvey. Based on seismic units from Kuhlmann and Wong, (2008).

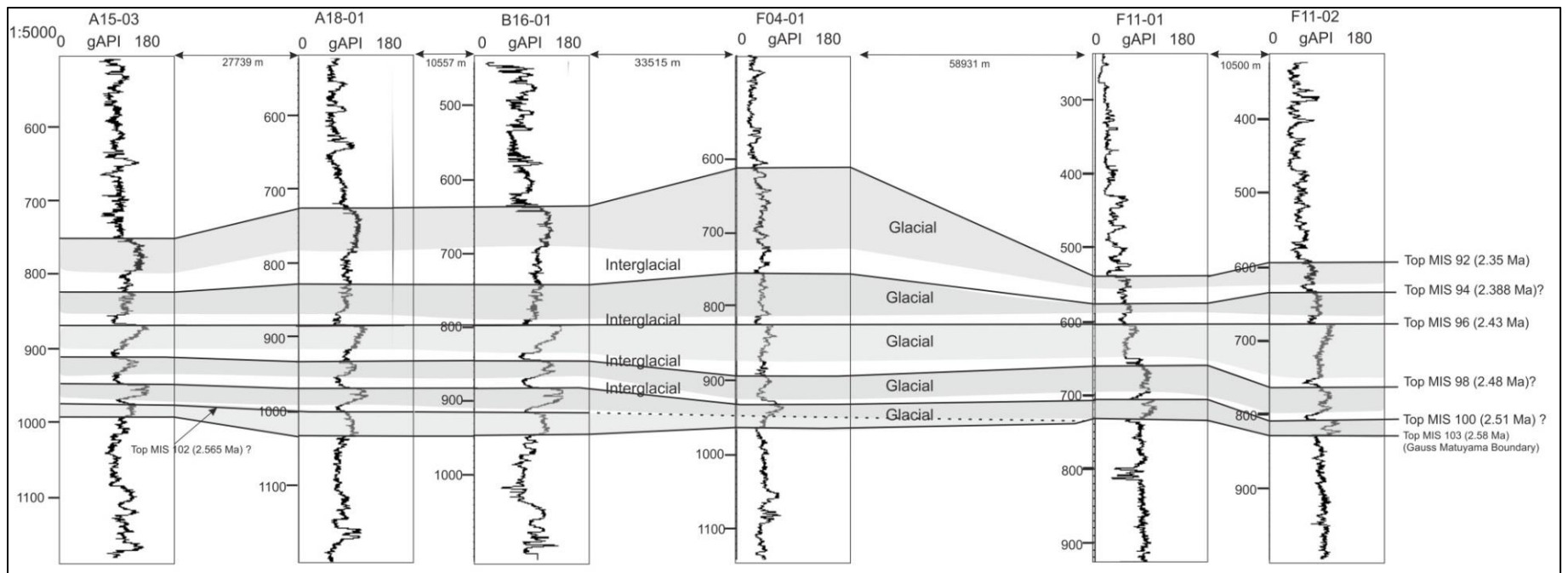


Figure. 2.7 Well correlation along strike basinwards of the shelf edge. Linking A15-03 and SNS MegaSurvey area. Locations of the wells are shown in Fig. 2.8.

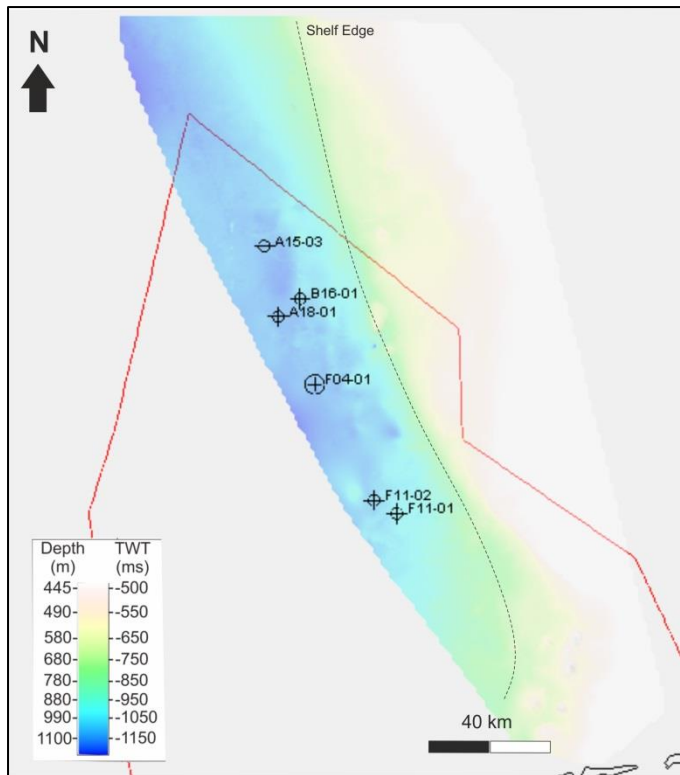


Figure 2.8 Location of strike well correlation from A15-03 to F11 and the area of the SNS MegaSurvey. The background is the Top base Quaternary maps 2.58 Ma. *Top Plio 1* seismic unit. This is displayed to show that the easiest way to correlate the chronostratigraphic framework to the south of the dataset was to concentrate on an area with a similar evolution and depositional environment, moving along strike basinwards of the base Quaternary shelf edge, then taking the correlation up dip and landwards.

When interpreting the 13 units it was found that some were only significant in the area of the north Netherlands North Sea, and that there were more significant reflections in the Danish sector and the southern Netherlands North Sea. This led to a modification of the chronostratigraphic framework to nine units, to reflect the main units across the entire study area. In most cases it is the tops which are chronostratigraphically significant (Fig. 2.4). A change in nomenclature was also appropriated as not to become confused with sequence nomenclature of Kuhlmann and Wong, (2008) in the Netherlands North Sea or of Thöle et al. (2014) in German sector of the North Sea (Fig. 2.5).

The most important events in the basin to correlate were the Base Quaternary (MIS 103, regional flooding surface, *Top Plio 1*) and the following top glacial Marine Isotope Stages 100-92, which have been identified in Kuhlmann and Wong (2008); ten Veen et al. (2011) and Noorbergen et al. (2015) as regional high gamma ray spikes and strong amplitude seismic reflections with a very fine grained lithology.

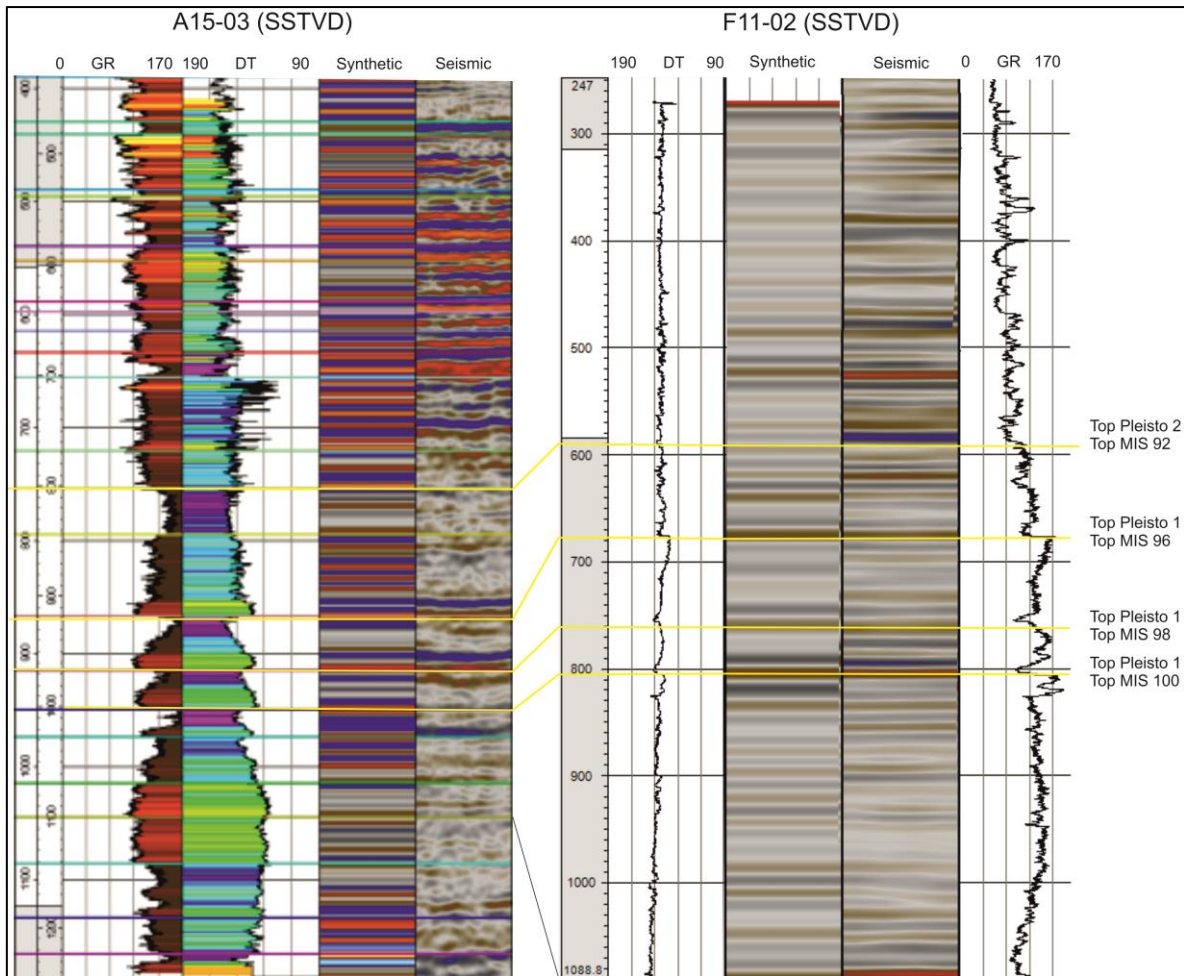


Figure 2.9 Synthetic seismogram for A15-03 and F11-02. Carried out using Synthetics module in Petrel for the purpose of identifying the seismic reflections associated with the well log correlation.

The correlation of these key seismic reflections, so important for linking our seismic section to a robust chronostratigraphic framework and ultimately to the global sea level curve, was initiated by identifying the same well log pattern in the gamma ray of other wells (Figs. 2.7 & 2.8). Tracing the important MIS 103-92 shale layers based on well log pattern was only clear in a similar basinal setting (Figs 2.7-2.9), basinwards of the base Quaternary shelf edge. This highlights the importance of correlating along strike as the same event is more likely to be of similar character in an area with a similar evolution and depositional environment. Then the correlation can be taken up dip and landwards, with the additional correlation aid of the seismic data to constrain the depositional geometries. This technique traced the events down to the SNS MegaSurvey dataset and to an area where the section from MIS 103-92 (base

Quaternary, 2.58 Ma to *Top Pleisto 2*, 2.35 Ma), is much expanded compared to the section in the A15 area (Fig. 2.6).

The correlation from well to seismic data is aided by the creation of synthetic seismograms (Fig. 2.9). Synthetic seismograms, created in Petrel seismic interpretation software calculate the acoustic impedance from the sonic log, an acoustic log that measures travel time of P waves against depth (Rider, 2002). The acoustic impedance log is then used to produce a seismic wavelet that can be compared to the original seismic data to confidently correlate surfaces identified in well logs to the seismic data. The quality of the well to seismic tie provided by TNO is highlighted in Fig. 2.10 where the mMU (mid Miocene unconformity) and the Top Chalk, regional seismic markers which are also clearly identifiable as gamma ray events, fit well. Therefore there is high confidence in the velocity model and correlation from the main chronostratigraphically significant wells to the rest of the basin.

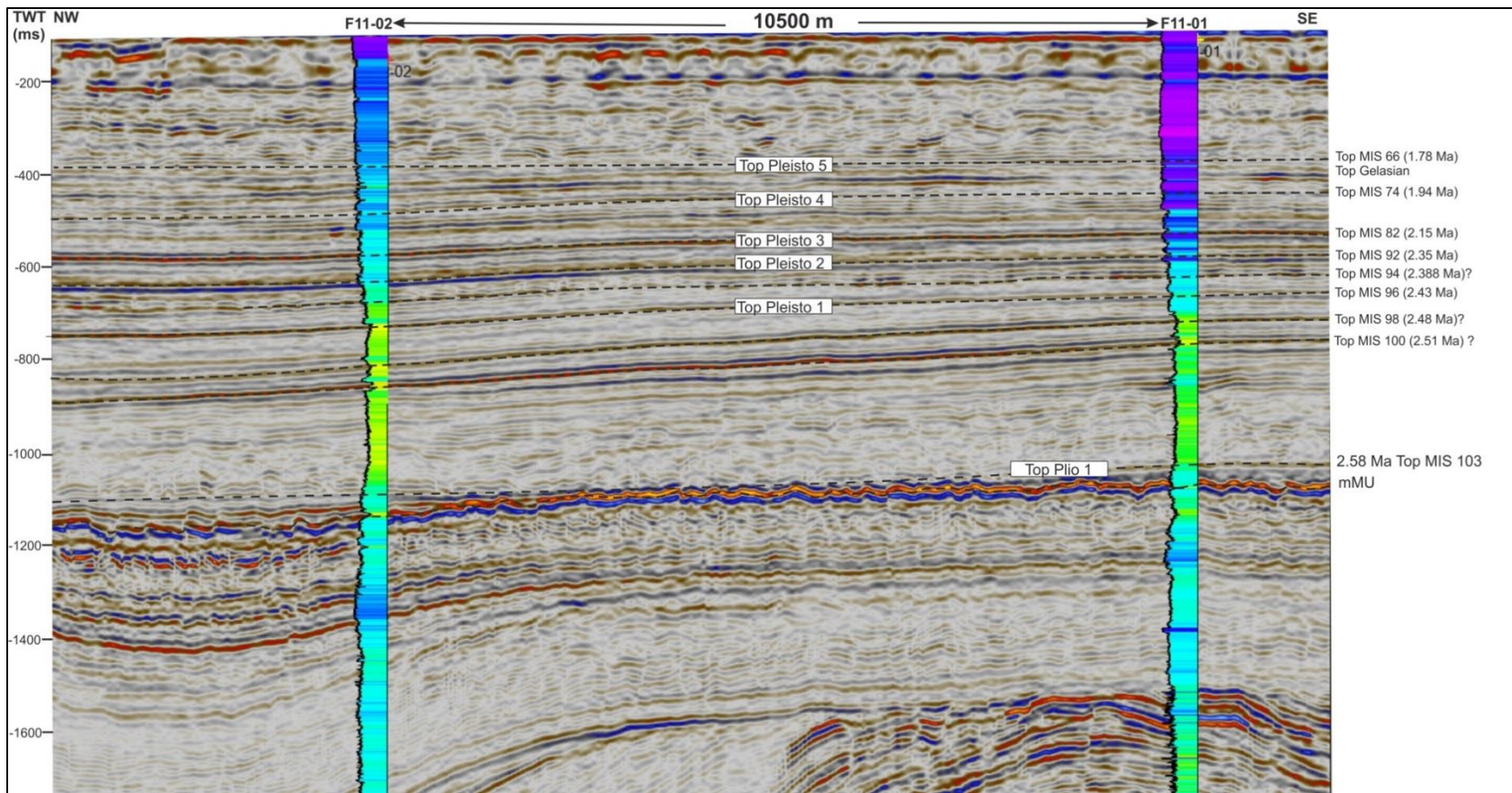


Figure 2.10 Gamma ray logs for Wells F11-02 and F11-01 (for location see Fig. 2.7) and the correlation to a NW-SE seismic cross section from the SNS MegaSurvey. Gamma ray logs are colour filled; darker colours represent lower gamma ray values whilst lighter colours represent higher gamma values, with yellow being the highest.

2.2 SEISMIC INTERPRETATION APPROACH

Several techniques were used to interpret the 3D seismic dataset. A combination of traditional horizon based seismic interpretation using Schlumberger Petrel v2013 and auto interpretation using Eliis PaleoScan software were used to map all reflections between picked horizons in a semi-automated fashion.

Key chronostratigraphic surfaces were correlated as far as possible across the basin using well and seismic correlation. Some of the reflections which were identified in Kuhlmann et al. (2006) did not extend across the dataset; however *Top Plio1*, *Top Pleisto 1* and *Top Pleisto 2* could be traced across the basin. Regional correlation landward of the shelf edge becomes more difficult in when chronostratigraphically significant reflections onlap underlying reflections, or are erosionally truncated or below seismic resolution. In order to be able to create the basin-wide chronostratigraphic framework, the reflection directly below had to be tracked. A chronostratigraphic surface within seismic data will not always be represented by one reflection and a geological model of the depositional system must be kept in mind when interpreting regionally.

Seismic stratigraphy was used to help determine sequences and key stratigraphic surfaces within the chronostratigraphic framework using the methodology of Mitchum et al. (1977). The aim was to pick strong regionally correlatable reflections which represent a change in deposition. Seismic events were rarely regional and difficult to follow for the entire basin and this is more the case for erosional surfaces such as sequence boundaries. In a shelf-prism setting, strong shale layers, which could represent Maximum Flooding Surfaces, were much easier to correlate over a wider area but still not the entire basin.

2.2.1 Imaging Techniques

For 3D visualisation and identification of key depositional features such as channels and lobes, seismic geomorphology techniques such as time slicing, stratal slicing and horizon slicing, were combined with RMS amplitude extractions and RGB blending

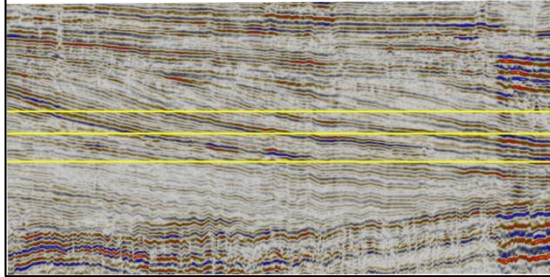
techniques using FFA Geoteric software (Fig. 2.11) (Posamentier and Kolla, 2003; Posamentier, 2004; Davies and Posamentier, 2005; Purves, et al., 2007). In vertical seismic cross section displays many of the stratigraphic features seen in amplitude maps are not easily identified due to their limited thickness relative to the seismic resolution whilst their spatial extent usually greatly exceeds the horizontal resolution.

Horizon slicing combined with seismic amplitudes in the most robust way of imaging the planform geomorphology of key reflections. Horizon slices are true to the geometry of seismic reflections and therefore in theory should represent a time line; whilst traditional time slices and stratal slicing to a lesser extent cross cuts stratigraphy and does not represent a time significant surface. Amplitude extractions are performed on a window below or above a seismic surface and therefore can represent more than a single time surface. In the example in Fig. 2.11 amplitude extractions are performed on a window 20-30 ms above the seismic surface.

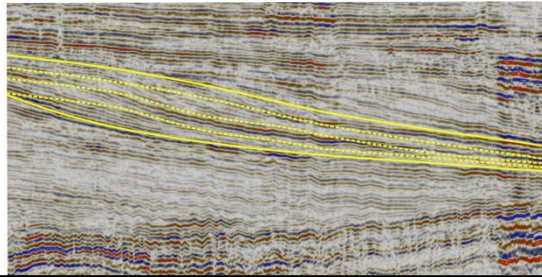
In the past horizon slicing would be impossible on the scale of the MegaSurvey as all the seismic reflections would have to be interpreted manually across the basin. Auto interpretation software, such as Eliis Paleoscan and Opendtect software allows the “quick” interpretation of reflections in between manually interpreted horizons which is imperative when using large datasets to identify areas of interests quickly, which can then be interpreted manually if needed.

Using these seismic geomorphology techniques allows us to attempt to understand the depositional environments and their evolution in the absence of diagnostic depositional environmental information from core data or outcrops. Depositional environments are interpreted from the seismic geomorphology by calibrating key features to well logs and lithological descriptions, and comparing them to analogues from the literature. Thickness maps and structure maps of key reflections and reflection-bound seismic units are utilised to place the key facies and architectures into the context of basin shape and main depocentre of the unit.

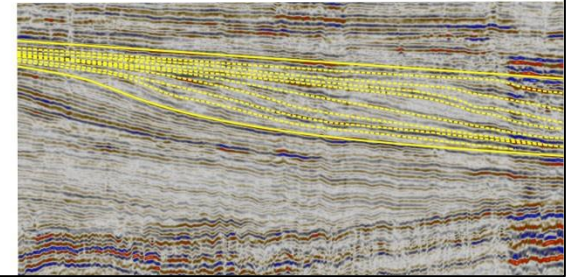
Time Slicing



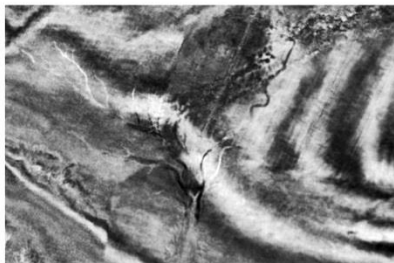
Stratal Slicing



Horizon Slicing

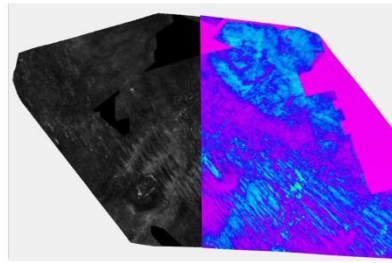


Seismic Amplitude



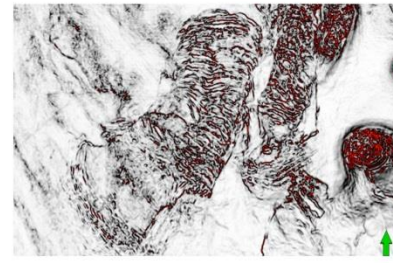
- Created using time-slice through seismic volume. Displayed using a black-grey-white colour bar.
- Shows lateral changes in acoustic impedance
- Ideal for first scan of geomorphological features.
- No additional processes to run.

RMS Amplitude



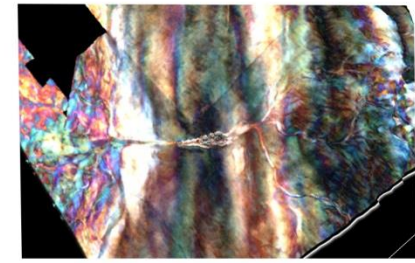
- Created using RMS attribute extracted onto a seismic surface. Petrel seismic attribute default colour bar to the right and black-grey-white colour bar to the left.
- Good for imaging stratigraphic features.
- RMS calculates the square root of the sum of squared amplitudes divided by the number of samples within the specified window used.
- Created by running surface attribute process in Petrel or alternately using the volume attribute tool to allow time-slicing through an RMS volume.

Variance Attribute



- Created by running seismic volume attribute process in Petrel.
- Can be used in time-slice or extracted onto a seismic surface.
- Variance compares trace by trace variability in acoustic impedance. Calculating dissimilarity in the seismic.
- Ideal for imaging structural features, salt diapirs, channel edges and chaotic features.

RGB Blending



- Created using RGB blended volume from Geoteric software.
- Used to image in more detail stratigraphic features.
- Best utilised on horizon slices/seismic surfaces.
- Frequency decomposition breaks down the seismic into component frequencies and allows the seismic response to be visualised in different frequencies.

Figure 2.11 Seismic interpretation and imaging techniques (previous page). **Above** slicing techniques **Below** Imaging techniques which can be used in conjunction with slicing to gain a planform view of the seismic geomorphology. Seismic amplitude and variance examples are performed on time slices which are associated with a specific plan view slice through the data. RMS amplitude example is extracted using a window of 30 ms above a gridded surface. RGB blending example is extracted onto a gridded surface using a 20 ms window above the surface.

In order to provide realistic clinoform trajectories from TWT (two-way time) seismic data the clinoforms should be back-rotated so their topsets are approximately horizontal and the clinoform height de-compacted (Pekar and Kominz, 2001; Patruno et al., 2014). Due to the role of loading on palaeotopography, topsets are largely less loaded than the bottomsets (Steckler et al., 1999) and therefore vertical differences between the topset and bottomset are exaggerated in TWT compared to the original depositional architecture (Miller et al., 2013). Flattening on overlying topsets in order to back rotate underlying topsets is carried out to understand depositional trajectories of the clinoforms. TWT is calibrated to depth using available industrial check shot data in the Netherlands North Sea (ten Veen et al., 2013).

2.2.2 Limitations

Utilising seismic data to understand depositional environments using seismic geomorphology techniques has limitations in comparison to using higher resolution datasets, e.g. from outcrop. Whilst seismic data can offer greater spatial coverage and allows interpretation in three dimensions, much detail about depositional processes and environment can be ascertained from outcrop data which is not possible from seismic. Individual sand bodies and architectural elements on a meter scale are not possible to image in the 3D seismic dataset used in this study (Fig. 2.12). Figure 2.12 indicates the level of heterogeneity within a 30 m high outcrop and compares this to a seismic section from the SNS MegaSurvey (Fig. 2.4).

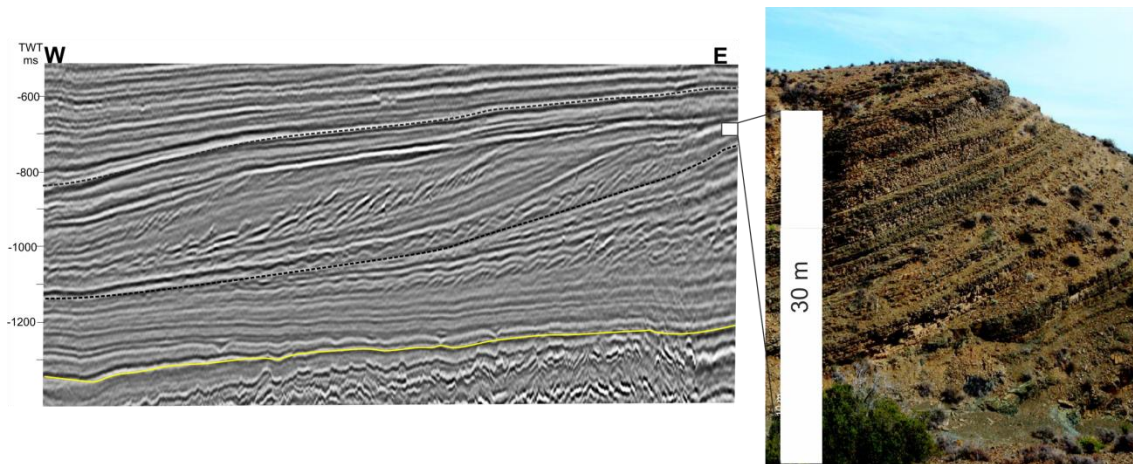


Figure 2.12 Comparison of clinoforms from seismic data to outcrop. Left seismic example of shelf prism clinoforms from SNS Megasurvey used in this study. Right outcrop example of clinothem from the Waterford Formation Laingsburg depocentre Karoo basin South Africa from Jones et al. (2013).

It is likely that the hierarchy of architectural elements or geobodies such as channels, levees and lobes identified in seismic data are not of the same order as those identified in outcrop and core which have a resolution of meter scale or better. For instance in a terrestrial to deltaic setting, individual delta top channels or incised valleys are not likely to be identified in seismic and are likely to be stacked channels, channel belt complexes or incised valley fills (Heldreich et al., 2013) (Fig. 2.13). In deep water settings individual architectural elements which comprise a turbidite stage will not be imaged in seismic. Turbidite stages may be present as an individual seismic loop and it will be turbidite systems and complexes which will be well imaged in seismic data (Prather et al., 2000). In sequence stratigraphy, several orders of sequences are described in the literature, from sequences, composite sequences and composite sequence sets (Neal and Abreu, 2009; Flint et al., 2011). Parasequences and sequences are resolvable at the outcrop and well log scale, however in the seismic dataset used in this study sequence sets or composite sequence sets are represented.

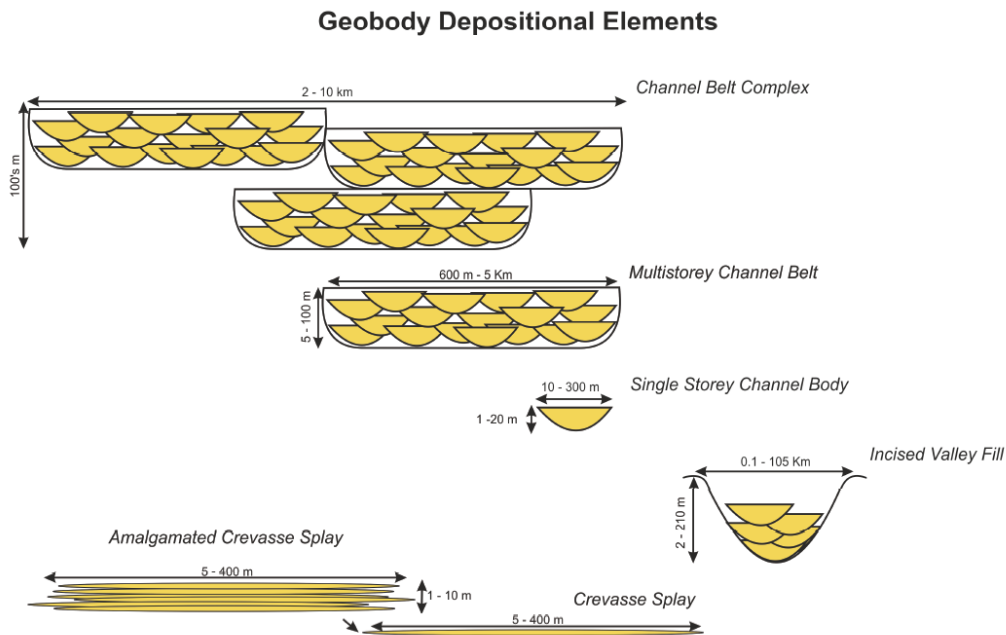


Figure 2.13 Hierarchies of channel geobodies. From Heldreich et al. (2013).

Data quality issues could also affect the identification of key seismic features and increase the difficult of correlation across the region. Noise and disturbed reflections are greatest in the upper 200-300 ms below the sea bed in the SNS and CNS MegaSurveys. Glacial related features such as tunnel valleys which erode into the shelf prism up to 500 ms below the seabed and strong amplitude channels in the top 50 ms affect the imaging of the underlying strata. The data quality towards the south west of the SNS MegaSurvey degrades and therefore there is less certainty that all relevant key seismic architectures and facies have been imaged and identified in that region. The inconsistency in wavelet character (Fig. 2.2) and seismic resolution which is due to induvial seismic volumes, acquired at different times being merged together for the MegaSurvey by PGS also creates uncertainty in the continuity of interpretation of key seismic reflections. These issues with polarity were mitigated as much as possible by understanding the wavelet character of key regional seismic reflections such as the sea bed Top Chalk and the mMU to check the polarity across the dataset and therefore understand where there are changes in the dataset.

2.3 REFERENCES

- Benvenuti, A, Kombrink, H., Ten Veen, J.H., Munsterman, D.K., Bardi, F., Benvenuti, M., 2012. Late Cenozoic shelf delta development and Mass Transport Deposits in the Dutch offshore area – results of 3D seismic interpretation. *Netherlands journal of Geosciences* 91, 591–608.
- Davies, R.J., Posamentier, H.W., 2005. Geologic processes in sedimentary basins inferred from three-dimensional seismic imaging. *GSA Today* 15, 4–9.
- Flint, S.S., Hodgson, D.M., Sprague, a. R., Brunt, R.L., Van der Merwe, W.C., Figueiredo, J., Pr  lat, A., Box, D., Di Celma, C., Kavanagh, J.P., 2011. Depositional architecture and sequence stratigraphy of the Karoo basin floor to shelf edge succession, Laingsburg depocentre, South Africa. *Marine and Petroleum Geology* 28, 658–674.
- Heldrich, G., Redfern, J., Gerdes, K., Legler, B., Taylor, S., Hodgetts, D., Williams, B. 2013. Analysis of geobody geometries within the fluvio-deltaic Mungaroo Formation, NW Australia. *West Australian Basin Symposium Abstract*.
- K  the, A., 2012. A revised Cenozoic dinoflagellate cyst and calcareous nannoplankton zonation for the German sector of the southeastern North Sea Basin. *Newsletters on Stratigraphy* 45, 189–220.
- Kuhlmann, G., Langereis, C., Munsterman, D., Jan van Leeuwen, R., Verreussel, R., Meulenkamp, J., Wong, T., 2006b. Chronostratigraphy of Late Neogene sediments in the southern North Sea Basin and paleoenvironmental interpretations. *Palaeogeography, Palaeoclimatology, Palaeoecology* 239, 426–455.
- Kuhlmann, G., Langereis, C., Munsterman, D., Jan van Leeuwen, R., Verreussel, R., Meulenkamp, J., Wong, T., 2006a. Chronostratigraphy of Late Neogene sediments in the southern North Sea Basin and paleoenvironmental interpretations. *Palaeogeography, Palaeoclimatology, Palaeoecology* 239, 426–455.
- Kuhlmann, G., Langereis, C.G., Munsterman, D., Leeuwen, R. Van, Verreussel, R., Meulenkamp, J.E., Wong, T.E., 2006. Integrated chronostratigraphy of the Pliocene-Pleistocene interval and its relation to the regional stratigraphical stages in the southern North Sea region. *Netherlands Journal of Geosciences* 85-1, 19-35.
- Kuhlmann, G., Wong, T.E., 2008. Pliocene paleoenvironment evolution as interpreted from 3D-seismic data in the southern North Sea, Dutch offshore sector. *Marine and Petroleum Geology* 25, 173–189.
- Miller, K.G., Mountain, G.S., Browning, J. V., Katz, M.E., Monteverde, D., Sugarman, P.J., Ando, H., Bassetti, M. A., Bjerrum, C.J., Hodgson, D., Hesselbo, S., Karakaya, S., Proust, J.N., Rabineau, M., 2013. Testing sequence stratigraphic models by drilling Miocene foresets on the New Jersey shallow shelf. *Geosphere* 9, 1236–1256.

- Mitchum Jr., R.M., Vail, P.R., Sangree, J.B., 1977. Seismic stratigraphy and global changes of sea level, Part six: stratigraphic interpretation of seismic reflection patterns in depositional sequences. *Seismic Stratigraphy — applications to hydrocarbon exploration* 117–134.
- Møller, L.K., Rasmussen, E.S., Clausen, O.R., 2009. Clinoform migration patterns of a Late Miocene delta complex in the Danish Central Graben; implications for relative sea-level changes. *Basin Research* 21, 704–720.
- Noorbergen, L.J., Lourens, L.J., Munsterman, D.K., Verreussel, R.M.C.H., 2015. Stable isotope stratigraphy of the early Quaternary of borehole Noordwijk, southern North Sea. *Quaternary International* 386, 148–157.
- Patrino, S., Hampson, G.J., Jackson, C. A-L., Whipp, P.S., 2014. Quantitative progradation dynamics and stratigraphic architecture of ancient shallow-marine clinoform sets: A new method and its application to the Upper Jurassic Sognefjord Formation, Troll Field, offshore Norway. *Basin Research* 27 (4), 412–452.
- Pekar, S.F., Kominz, M. A., 2001. Two-Dimensional Paleoslope Modeling: A New Method for Estimating Water Depths of Benthic Foraminiferal Biofacies and Paleoshelf Margins. *Journal of Sedimentary Research* 71, 608–620.
- Posamentier, H.W., 2004. *Seismic Geomorphology: Imaging Elements of Depositional Systems from Shelf to Deep Basin Using 3D Seismic Data: Implications for Exploration and Development*. Geological Society, London, Memoirs 29, 11–24.
- Posamentier, H.W., Kolla, V., 2003. Seismic Geomorphology and Stratigraphy of Depositional Elements in Deep-Water Settings. *Journal of Sedimentary Research* 73, 367–388.
- Purves, S.J., Henderson, J., Leppard, C., 2007. RGB Visualisation Based Delineation of Geological Elements from Volumetric Spectral Decomposition of 3D Seismic Data. Extended abstracts EAGE 69th Conference & Exhibition London, UK, 11 - 14 June.
- Rasmussen, E.S., Vejbaek, O. V, Bidstrup, T., Piasecki, S., Dybkjær, K., 2005. Late Cenozoic depositional history of the Danish North Sea Basin: implications for the petroleum systems in the Kraka, Halfdan, Siri and Nini fields. Geological Society, London, Petroleum Geology Conference Series 6, 1347–1358.
- Rider, M.H., 2002. The petrophysical interpretation of well logs. Rider-French Consulting Ltd 42–66.
- Steckler, M.S., Mountain, G.S., Miller, K.G., Christie-Blick, N., 1999. Reconstruction of Tertiary progradation and clinoform development on the New Jersey passive margin by 2-D backstripping. *Marine Geology* 154, 399–420.
- Ten Veen, J.H., Geel, C.R., Kunakbayeva, G., Donders, T.H., Verreusel, R.M.C.H., 2011. Property prediction of Plio-Pleistocene sediments in the A15 shallow gas systems. TNO Report. TNO-060-UT-2011-01184/C.

Thöle, H., Gaedicke, C., Kuhlmann, G., Reinhardt, L., 2014. Late Cenozoic sedimentary evolution of the German North Sea? A seismic stratigraphic approach. *Newsletters on Stratigraphy* 47, 299–329.

CHAPTER 3

REGIONAL EVOLUTION OF A SHELF-PRISM IN
THE LATE CENOZOIC: EUSTACY, SEDIMENT
SUPPLY AND SUBSIDENCE IN THE SOUTHERN
NORTH SEA

CHAPTER 3: REGIONAL EVOLUTION OF A SHELF-PRISM IN THE LATE CENOZOIC: EUSTACY, SEDIMENT SUPPLY AND SUBSIDENCE IN THE SOUTHERN NORTH SEA

Rachel Harding¹, Mads Huuse¹, Rob Gawthorpe², Johan ten Veen³

¹School of Earth, Environmental and Atmospheric Sciences, University of Manchester

²Departments of Earth Sciences, University of Bergen, Norway

³TNO, Netherlands Geological Survey, Utrecht, Netherlands

3.0 ABSTRACT

The Late Cenozoic southern North Sea shelf-prism represents an expanded record of depositional environments and climate for an important time period in global history, the descent into icehouse conditions. The study aimed to unravel the controlling factors on the evolution of a large shelf-prism on the basin and to take a step towards better visualisation of the lateral variation of sequences within a basin. Continuous 3D seismic data across the southern North Sea and high resolution chronostratigraphic control enables a correlation of sequences, seismic architectures, geomorphology and seismic facies with full 3D control, to eustatic change, subsidence and sediment supply.

The study found that eustacy was the main control on regional sea level and climate in the early Gelasian (2.58 Ma – 2.15 Ma) with accelerated subsidence in the late Gelasian overriding the eustatic signal (2.15-1.78 Ma). Sediment supply (amount and proximity to the source), local subsidence and underlying geomorphology of the shelf create variability in how eustacy is expressed within the sedimentary architecture of the SNS. The variation in the expression of a glacial-interglacial cycle within the seismic stratigraphy of the southern North Sea highlights the need for 3D large scale seismic

interpretations to understand the regional over local base level trends and their link to global sea level.

3.1 INTRODUCTION

Sedimentary basins preserve expanded regional records of climate and sea level change and therefore are invaluable in understanding important periods of the earth's past, such as the descent into icehouse conditions in the Late Cenozoic. Siliciclastic shelf systems have gained a large amount of interest due to hydrocarbon prospectivity of several elements of the system. The ability to predict the locations of reservoir sand bodies (from mouth bars to basin floor fans) and other elements of the petroleum play has been a key aim of sequence stratigraphy since the 1970's (Vail et al. 1977; Posamentier & Vail 1988; Posamentier et al. 1992; Neal & Abreu 2009). The prediction of sediment partitioning across a shelf-prism has been one of the main aims of clinoform trajectory analysis since the 1990's (Helland-Hansen and Gjelberg 1994; Helland-Hansen and Hampson 2009; Steel et al., 2010). The majority of the studies which have tested these methods have focused on regional 2D seismic lines, individual 3D seismic surveys or outcrop analogues (Steckler et al., 1999; Porebski and Steel, 2006; Miller et al., 2013; Fongngern et al., 2015).

Continuous 3D PGS MegaSurvey seismic data spanning the Netherlands, UK and part of the Danish southern North Sea (sNS) basin and a high density of borehole penetrations have recorded an expanded sedimentary record for the Late Cenozoic with unprecedented spatial detail and basin-wide coverage. The Late Cenozoic is a period of frequent, high-amplitude climate changes and associated glaciation-driven global sea level change (Pekar et al., 2002; Miller et al., 2005;). Up to 1500 m of Late Cenozoic sediments are preserved within the study area. The offshore seismic expression of the sediment input is in the form of largely low angle (1-2°) large scale clinoforms (100-400 m in height), downlapping on to the mid-Miocene Unconformity (mMU), a basin wide unconformity and regional seismic marker (Gołędowski et al., 2012; Huuse and Clausen, 2001; Jordt et al., 1995). Regionally, shallow gas and oil discoveries have increased the interest in the shallow section of the sNS, with several commercial gas discoveries in the last 10 years (ten Veen et al., 2011; Trampe et al., 2013).

The purpose of this study is to present a regional correlation of a high resolution chronostratigraphic framework (Kuhlmann and Wong, 2008; Kuhlmann et al., 2006a) utilizing

a basin-wide continuous 3D seismic dataset that allows an understanding of the palaeoenvironments throughout the succession to be gained at a high spatial and temporal detail. The chronostratigraphic control enables a correlation of sequences, seismic architectures, geomorphology and seismic facies with full 3D control, to eustatic change, subsidence and sediment supply.

This study utilises the wealth of data, including a continuous 3D seismic Mega Survey dataset covering 55,000 sq. km with continuous seismic data using state of the art seismic interpretation software and techniques to understand in fine detail the evolution of the geomorphology of the southern North Sea area during the study period and how this can be linked to existing chronostratigraphy and climate proxies to link to the global sea level curve. This then allows the second part of the paper which is understanding in broad terms the lateral variability in the seismic architecture such as clinoforms and key features, because we have a link to the global sea level curve and we have such a large area, we are able to discount lobe switching because we can follow the depocentres around the basin, we have a large enough area so that there are areas with subsidence and areas without, and have a broad range of proximity to sediment supply and underlying geomorphology situations to compare in order to comment on the controls on seismic architecture within a basin.

The Late Cenozoic southern North Sea shelf-prism represents an expanded record of depositional environments and climate for an important time period in global history, the descent into icehouse conditions. Decades of hydrocarbon exploration in the North Sea has led to unprecedented seismic coverage, calibrated to high density borehole penetrations and high resolution chronostratigraphy and climate proxies. This study utilises the wealth of data, including a continuous 3D seismic MegaSurvey dataset covering 55,000 sq. km combined with the use of state of the art seismic interpretation software and seismic interpretation techniques to image in fine detail the evolution of the geomorphology of the southern North Sea area. The chronostratigraphic control enables a correlation of sequences, seismic architectures, geomorphology and seismic facies with full 3D control, to eustatic change, subsidence and sediment supply.

The study aimed to unravel the controlling factors on the evolution of a large shelf-prism on the basin and to take a step towards better visualisation of the lateral variation

of sequences within a basin. The study found that eustacy was the main control on regional sea level and climate in the early Gelasian (2.58 Ma – 2.15 Ma) with accelerated subsidence in the late Gelasian overriding the eustatic signal (2.15-1.78 Ma). Sediment supply (amount and proximity to the source), local subsidence and underlying geomorphology of the shelf create variability in how eustacy is expressed within the sedimentary architecture of the SNS. The variation in the expression of a glacial-interglacial cycle within the seismic stratigraphy of the southern North Sea highlights the need for 3D large scale seismic interpretations to understand the regional over local base level trends and their link to global sea level.

3.1.1 Geological Setting

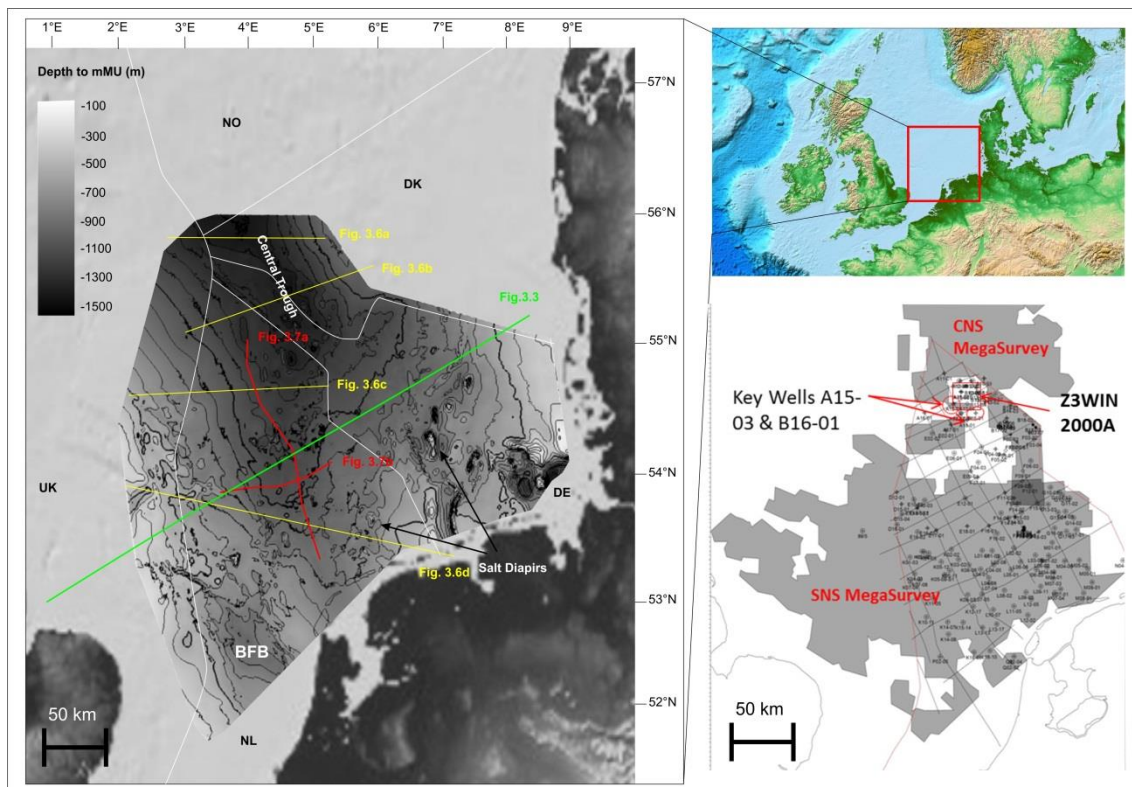


Figure 3.1 Regional setting and dataset map. Left: Mid Miocene Unconformity (mMU) depth structure map. Map is the result of seismic interpretation from this study, (UK, NL and DK sectors) combined with the German mMU structure map from Geopotenzial Deutch Nordsee project (www.gpdn.de). Deepest parts of the map show where the greatest sediments have been preserved since the mMU. Key areas of accommodation creation marked, Central Trough and BFB (Broad Fourteens Basin). NL Netherlands; DE Germany; DK Denmark; NO Norway. Locations of Fig.3.6 seismic cross sections shown in yellow. Top Right: GEBCO bathymetry for North Sea showing location of dataset within the contemporary setting.

Bottom Right: Dataset map. Grey areas represent 3D seismic coverage. 2D seismic lines and key boreholes used for chronostratigraphic framework also shown.

The southern North Sea is characterized by the interaction of structural elements associated with the E-W trending Southern Permian Basin and the NW-SE/NNE-SSW Mesozoic sub basins, which were inverted during the Late Cretaceous/Early Paleogene (Fig. 3.2) (Ziegler, 1992; Remmelts, 1995). The main structural elements that exert control on Late Cenozoic deposition in the SNS are the Mesozoic Central Graben, above which an intracratonic sag basin developed in the Cenozoic (Huuse and Clausen, 2001), referred to as the Central Trough (Fig. 3.1). The Broad Fourteens Basin (labelled BFB in Fig. 3.1) also exerts control on deposition and is a Mesozoic element which was inverted during the Oligocene (Nalpas et al., 1995). Salt structures are a key feature of the southern North Sea. Halokinesis of the Permian Zechstein salt layer occurred during both the Mesozoic and Cenozoic (Remmelts, 1996), and continued to the Quaternary and recent times in some areas (Harding and Huuse, 2015; ten Veen et al., 2012). Salt tectonics locally can create and destroy accommodation and therefore affect sediment pathways and depocentre locations (Gee and Gawthorpe, 2006; Hudec and Jackson, 2007).

During the early Miocene the North Sea basin was an epeiric sea covering most of present day Denmark, northern Poland, Germany and the Netherlands (Ziegler, 1992; Huuse, 2002; Knox et al., 2010). By the Late Miocene the SNS basin was the southern part of a north-south elongate basin characterized by strong tidal regimes (Galloway, 2002).

The Cenozoic SNS was dominated by a large clastic depositional system draining Fennoscandia and Northern Europe depositing into the subsiding basin (Huuse and Clausen, 2001; Kuhlmann and Wong, 2008; Overeem et al., 2001; Sørensen and Michelsen, 1995). In the Palaeocene-early Eocene there was a dominance of clinoforms and fans prograding from the NW due to uplift and igneous activity associated with the Iceland Plume (White and Lovell, 1997; Ziegler, 1990). Progradation was dominantly from the NE in the Danish and Norwegian sectors in the Oligocene-Miocene (Clausen et al., 1999; Huuse et al., 2001; Rasmussen et al., 2005); the NE and east in the late Miocene-Pliocene in the German sector and Dutch sectors (Thöle et al., 2014); and from the east- SE in the Netherlands sector in the Pleistocene (Anell et al., 2012; Kuhlmann and Wong, 2008; Overeem et al., 2001).

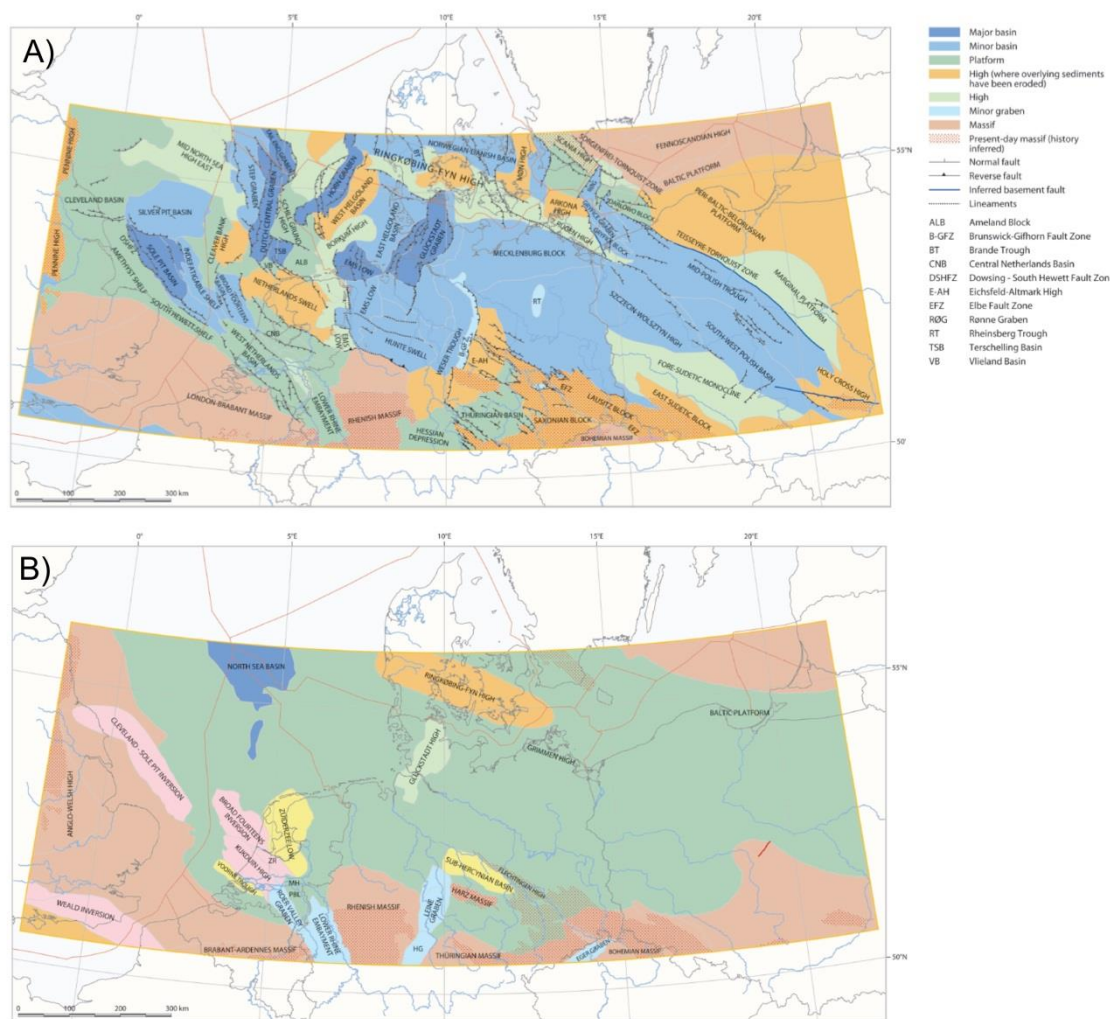


Figure 3.2 Structural Domains within southern North Sea. A) Late Triassic B) Cenozoic. From Pharaoh et al., 2010.

From the Middle Miocene to the Middle Pleistocene deposition was dominated by the Baltic River System (Bijlsma, 1981; Gibbard et al., 1991) Sediment provenance suggests contributions from the proto-Rhine, Meuse and Scheldt (Huisman and Klaver, 2007); Weser and Elbe drainage systems (Kuhlmann et al., 2004). The basin infill, dominated by marine to fluvio-deltaic sediments and the grain size is predominantly clay to very fine sands (Cameron et al., 1987; Overeem et al., 2001; Kuhlmann et al., 2006).

During the Late Cenozoic, climate cooled from subtropical to icehouse conditions (Buchardt, 1978; Anell et al., 2012) with long-term eustatic lowering (Miller *et al*, 2005) (Fig. 3.4). Intensification of global cooling occurred between 3.1 to 2.75 Ma (Maslin et al., 1998) with early Quaternary global sea level cycles dominated by 41,000 year eccentricity Milankovich cycles, (Ruddiman et al., 1986). Onshore and offshore paleoclimate and sea level indicators for

the Gelasian in the NL North Sea, (2.58 Ma – 1.8 Ma) have been studied in detail (Kuhlmann et al., 2006a; Kuhlmann et al., 2006b; ten Veen, et al, 2013), and suggest the regional Northern Hemisphere climate on both land and sea surface varies in tandem with local sea level with a small lead of temperature over Northern Hemisphere ice sheet growth at sea level (Donders et al., in prep).

The driver behind the large clastic input into the SNS during the Cenozoic is still a contentious issue in the literature. Renewed Neogene (~4 Ma) uplift of the Scandinavian topography as a cause for increased denudation and sediment supply to the basin has been proposed (Japsen and Chalmers, 2000; Rasmussen et al., 2005; Japsen et al., 2007). In contrast Clausen et al. (1999); Huuse, (2002); Nielsen and Clemmensen, (2009) and Gołędowski et al. (2012), suggest that the increased sediment supply to the North Sea basin during the Late Cenozoic was more likely climate driven as it coincides with long-term climatic deterioration and in particular the onset of extensive northern hemisphere glaciations (Huuse et al., 2001; Nielsen and Clemmensen, 2009). In this model, long-lived Scandinavian topography of Caledonian origin was rejuvenated when the erosional regime changed from fluvial to glacial, resulting in peak uplift and increased local relief during overall lowering of topography as fjords were over-deepened. Subsidence patterns in the North Sea Basin can in this model be explained to a first order by infilling of a deep epeiric basin by basin-marginal progradation varying in age along the basin margin (Gołędowski et al., 2012; Huuse, 2002).

Differential subsidence occurs across the region, focused over the regions of the Central Graben and the Broad Fourteens Basin (Figs. 3.1, 3.3). Subsidence accelerated greatly in the Pleistocene in the Netherlands and German sectors of the SNS (Koyi, 2001). In the German North Sea post-Pliocene subsidence increased by an order of magnitude from 36.95m/Ma to 323.07m/Ma (Brückner-Röhling et al., 2005). This has been linked with uplift on the basin margins, (Kooi et al., 1991; Kockel, 2002;), although long- and short term eustatic lowering may contribute to an impression of ‘uplift’ (Huuse 2002). The net effect on subsidence of repeated ice cover, erosion and sedimentation events across glacier covered and fore bulge areas during the mid- and late Pleistocene glaciations is as yet poorly understood (Moreau et al. 2015).

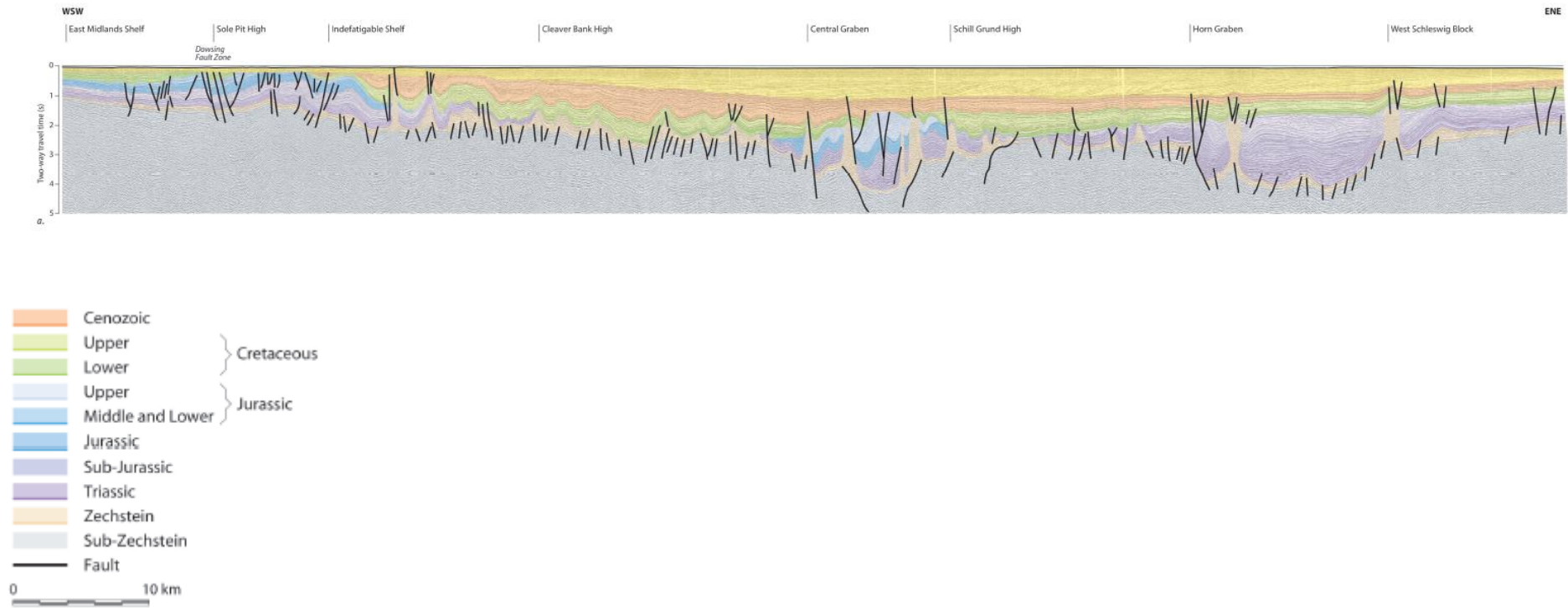


Figure 3.3 Regional cross section through the southern North Sea. For location see Fig.3.1. WSW-ESE seismic line through UK, Netherlands and German North Sea sectors. From Pharaoh et al., 2010.

3.1.2 Chronostratigraphic Framework

The stratigraphy of the Plio-Pleistocene Netherlands North Sea is constrained by high resolution chronostratigraphic, lithological, quantitative palynological and geochemical data from core and palaeomagnetic logs for wells *A15-03 and A15-04* in the north Netherlands North Sea (Kuhlmann et al., 2006ab; ten Veen et al., 2013). Biostratigraphy and benthic stable isotope analysis in the Noordwijk borehole, onshore Netherlands, has also been carried out (Meijer et al., 2006; Noorbergen et al., 2015) (Fig. 3.4).

Linking local climate and sea level change events from palynology and geochemical studies from the Netherlands North Sea and onshore Netherlands to the Marine Isotope Stages (MIS) of the global oxygen isotope curve (Lisiecki and Raymo, 2005) has allowed further dates to be identified and suggests a complex relationship between glacioeustasy and the sedimentary record in the SNS (Meijer et al., 2006; Kuhlmann et al., 2006ab; Noorbergen et al., 2015; Donders et al., in prep).

Terrestrial to marine ratios indicate proximity of the coast in the Netherlands North Sea, which transits landwards and basinwards in accordance to early Gelasian glacial-interglacial cycles (MIS 103-92), which suggests that relative minimum and maximum sea level in the SNS is as expected for icehouse conditions and governed by eustasy. The global oxygen isotope records (Lisiecki and Raymo, 2005) are strikingly similar to the benthic stable isotope record from onshore Netherlands (Noorbergen et al., 2015), well enough that they can be tuned to the global standard. This confirms that the regional glacial-interglacial cycles match that of the global response and it is valid to attempt to understand relative sea level and basin infill in the North Sea in relation to the global sea level curve, at least for the early Gelasian time period.

Sea level curves are scaled from oxygen isotope values from 57 globally distributed benthic ^{18}O records from (Lisiecki and Raymo, 2005) using assumptions given in (Miller et al., 2005) and (Miller et al., 2011) (Fig. 5.2).

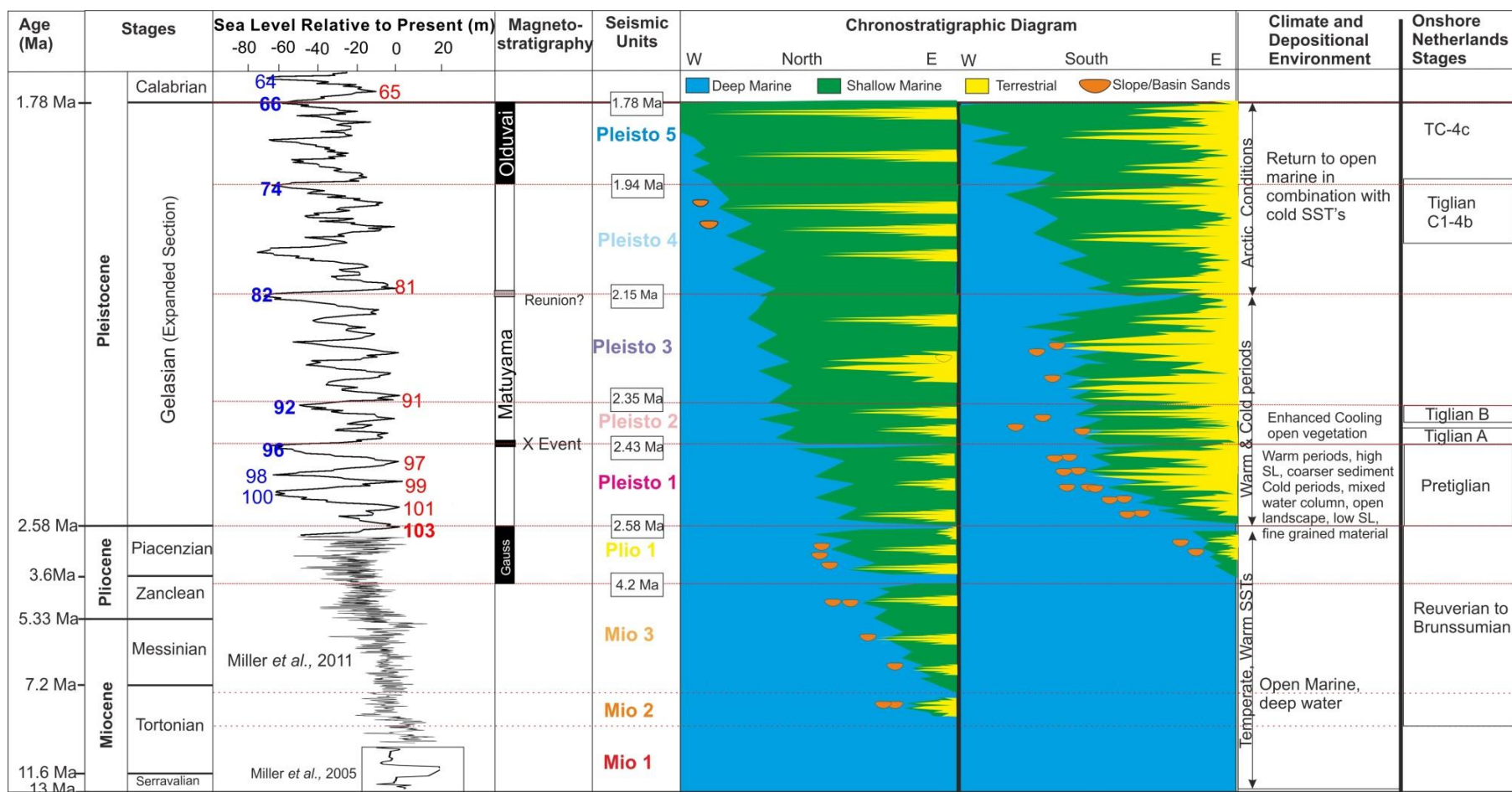


Figure 3.4 Chronostratigraphic framework (previous page). Eustatic Sea Level for the period 13 - 1.78 Ma. Sea level curves scaled from oxygen isotope values from 57 globally distributed benthic 180 records from Lisiecki and Raymo (2005) using assumptions given in Miller *et al.* (2005; 2011). Sea level is relative to present day. Interglacial Marine Isotope Stages (MIS) in red; Glacial MIS in blue. Ages given on left hand side are discussed in the data and methodology section, age scale is non-linear in order to visualise the study period in one figure. Linking the section to the magnetostratigraphy, Netherlands onshore stages and climate and depositional environment adapted from Kuhlmann *et al.* (2006ab) and ten Veen *et al.*, (2013).

A reverse coupling of sediment grain size and sea level in the basin is noted by Kuhlmann and Wong, (2008); Noorbergen *et al.* (2015) and Donders *et al.* (in prep). Finer grained sediment is associated with the glacial cold conditions and low sea level. The finest grained material, which is interpreted to enter the basin towards the glacial stage termination, is the product of weathering metamorphic rocks of Scandinavia and a long transport route (Kuhlmann *et al.*, 2004; Noorbergen *et al.*, 2015). The finest grained sediments (glacial terminations) are linked to the gamma ray log and seismic character in the north Netherlands North Sea (Kuhlmann and Wong, 2008; ten Veen *et al.*, 2011; 2013) and identified as gamma ray peaks, and are correlated to strong amplitude, semi-regional continuous seismic reflections. Coarser material associated with low gamma ray values are related to warm interglacial conditions and higher relative sea level. Therefore, though regional base level reflects glacioeustasy during the earliest Gelasian (2.58-2.35 Ma), grain size is not directly controlled by it (ten Veen *et al.*, 2013; Donders *et al.*, in prep).

In the Netherlands North Sea the majority of post mid Miocene Unconformity sedimentation consists of Gelasian sedimentation from 2.58 Ma (base Quaternary) and the Top Gelasian at 1.78 Ma. Several key chronostratigraphic surfaces are identified in the literature from the study period (Cande and Kent, 1995; Kuhlmann *et al.*, 2006ab; Noorbergen *et al.*, 2015; Donders *et al.*, in prep) (Fig. 3.4). The base Quaternary (2.58 Ma) corresponds to the Gauss-Matuyama magnetic reversal, an event in the pollen record which correlates to climatic degradation and the last occurrence of *Monspeliensina pseudotepida*, benthic foraminifera. In the Netherlands North Sea the surface is recognised as a regional flooding event and the top MIS 103 interglacial. The X event at 2.43 Ma is a regional strong amplitude shale layer and gamma ray peak and is correlated to the termination of glacial MIS 96. Two additional regional strong shale layers between the Gauss-Matuyama magnetic reversal and the X-event correspond to

the termination of glacial period MIS 100 (~2.51 Ma) and 98 (~2.48 Ma). An additional shale layer corresponds to a change in palynology and is correlated to the termination of MIS 92 and therefore gives an additional date at 2.35 Ma.

The Reunion event dated at ~2.15 Ma may corresponds to MIS 82 (Kuhlmann, et al., 2006ab). The top and base of the Olduvai event within the Matuyama epoch gives additional dates at 1.96 Ma and 1.78 Ma, corresponding with the Top Gelasian (Kuhlmann et al., 2006ab).

3.1.3 Clinoform Terminology

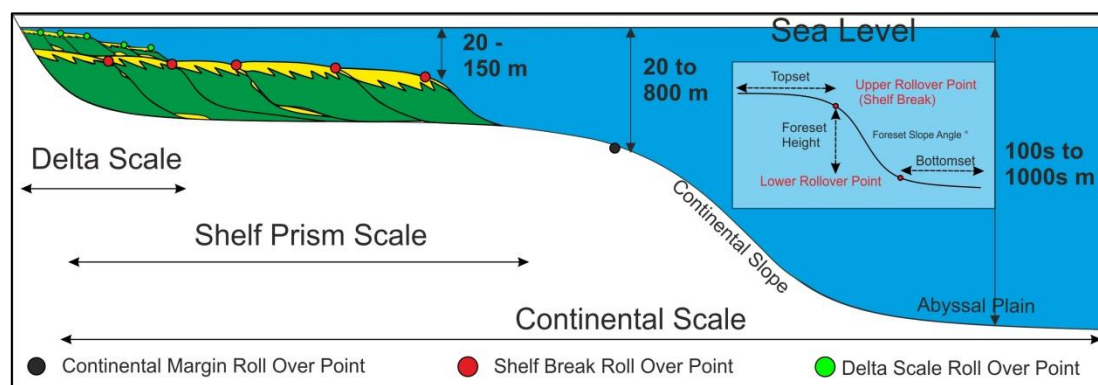


Figure 3.5 Clinoform nomenclature. Key definitions used in this paper. Adapted from Helland Hansen and Hampson (2009) and Patruno et al. (2015). Measurements on the delta scale, basin margin scale and the continental scale clinoform are regarding the water depth.

Climoforms within a basin can be of several spatial and temporal scales from subaerial delta, subaqueous delta, shelf-prisms and continental margins (Olariu and Steel, 2009; Patruno et al., 2015). The terms for the clinoforms can vary and the terminology used in this paper is illustrated in Fig. 3.5. Shelf-prism clinoforms (Henriksen et al., 2009) are large scale clinoforms (150-500 m) where the main rollover point separates neritic conditions from bathyal regimes (Steel and Olsen, 2002), and is known as the shelf edge, though not to be confused as continental shelf edge, though they can be coincidental, they can be an order of magnitude difference in size (Miller et al 2013). Delta scale clinoforms (< 150 m) can be superimposed on the larger scale clinoforms. The two scales of clinoforms converge where the delta system becomes entrenched at the shelf edge and deposition occurs as a shelf edge delta (Henriksen et al., 2011).

Distinguishing between the different scale clinoforms is important for the depositional environment interpretation and only the clinoform rollover point of the subaerial delta can be used to denote the shoreline, which is of key importance in sequence stratigraphy, facies prediction and palaeo-environmental reconstructions (Mitchum et al., 1977; Van Wagoner et al. 1988; Patruno et al., 2015). The nomenclature of the rollover point of the shelf-prism clinoforms in this study is termed the shelf break.

Shelf-prisms are built out basinwards by continuous transits of the shoreline across the shelf (Steel and Olsen, 2002). Shelf edge trajectories generally represents lower order cycles than the shoreline trajectory, largely 3rd order or longer which occur over 1-10 million years (Henriksen et al., 2011). Larger scale clinoforms are less likely to be affected by the autogenic processes (Steel and Olsen, 2002). The architecture of the clinoforms can be indicative of the sediment partitioning landwards and basinwards of the shelf edge. Sigmoidal clinoforms, with high topset preservation and ascending shelf edge trajectories, are indicative of sediment being trapped on the shelf, (Henriksen et al., 2011) and therefore accommodation on the shelf (Jones et al., 2015). Oblique tangential clinoforms, with no topset preservation and flat lying to descending shelf edge trajectories, suggest little to no accommodation on the shelf and sediment partitioning basinwards of the shelf edge and shelf bypass (Helland-Hansen and Hampson, 2009; Ryan et al., 2009).

The clinoform geometry is affected by sediment grain size, environmental forcings and basin physiography and post-depositional subsidence and compaction (Patruno et al., 2015). The trajectory of shelf-prism clinoforms, how they stack up with relation to each other, can give us information about the base level. Shelf edge trajectory generally represents lower order cycles than the shoreline trajectory is less likely to be affected by the autogenic processes.

Lateral, along strike variation in expression of sequences within a basin infill has long been identified (Dixon et al., 2012; Gawthorpe et al., 1994; Jones et al., 2015; Martinsen and Helland-Hansen, 1995) and this is integrated into interpretive methodologies, such as sequence stratigraphy and clinoform trajectory, which are largely associated with vertical and down dip stacking is still an ongoing process. Recent studies of clinoforms and basin infill has seen a shift from using the traditional sequence stratigraphy

techniques to more descriptive methodology including detailed qualitative and quantitative observations of clinoform architectures (Ryan et al., 2009; Anell and Midtkandal, 2015; Fongngern et al., 2015; Patruno et al., 2015, 2014) and the better integration seismic geomorphology techniques (Posamentier, 2004; Davies and Posamentier, 2005; Fongngern et al., 2015).

3.2 DATA AND METHODOLOGY

3.2.1 Data

The seismic dataset for this study comprises PGS (Petroleum Geo-Services) SNS MegaSurvey, covering 40,000 km² of the Netherlands and United Kingdom sectors of the southern North Sea (Fig. 3.1) and part of the PGS CNS MegaSurvey covering ~15,000 km² of the Netherlands, Danish and German sectors. The bin spacing is 50 m x 50 m, sampling rate 4 ms TWT with a vertical resolution of maximum 10-15 m in the top 1500 m (average velocity 1.8 ms⁻¹, ten Veen et al., 2013). The MegaSurvey data is complemented by individual 3D seismic surveys from TNO-DINO. These surveys are 12.5 x 12.5 bin spacing, with a similar vertical resolution to the MegaSurveys and SNST 83 and SNST 87 2D surveys which are of variable vintage. Well data consists of well logs, including gamma ray, sonic log and cuttings descriptions from commercial well reports for 172 wells in the Netherlands North Sea (Fig. 3.1).

Additional chronostratigraphic information is gained from seismic correlation to Late Cenozoic studies in the Danish sector (Rasmussen et al., 2005; Møller et al., 2009), German Sector (Köthe, 2012; Thöle et al., 2014) in the SE Netherlands sector wells *G10-01*, *G10-02*, *G16-06* and *M07-01* (Benvenuti et al., 2012) and to the UK central North Sea Josephine well (Chapter 6.1). Biostratigraphically derived dates for the Top and Base Gelasian (2.58 & 1.78 Ma) in wells G17-01, M08-02, P09-02 and P09-04 plus additional Intra Zanclean date at 4.2 Ma in well B17-01, B17-02, F02-01, F02-03 (Chris King *pers comm*, 2013).

3.2.2 Methodology

The base of study section is labelled mMU (mid Miocene Unconformity) which is a basin wide seismic stratigraphic surface (Fig. 3.4). The post mMU section up to the Top

Gelasian (1.78 Ma) is divided into nine seismic units, *Mio 1* to *Pleisto 5* (Figs. 3.4 & 3.6). Seismic stratigraphy methodology of Mitchum et al. (1977) was used to define regionally significant surfaces, largely using laterally extensive downlap surfaces. Chronostratigraphically significant seismic reflections from Kuhlmann and Wong (2008) were traced throughout the MegaSurvey in order to create a regional chronostratigraphic framework at unprecedented spatial and temporal resolution and spatial coverage. However, a first principles approach, using the observation based approaches of (Helland-Hansen and Hampson, 2009; Neal and Abreu, 2009; Miller et al., 2013), is utilised to analyse clinoform geometries and relationships, such as stacking patterns and clinoform trajectories. This approach does not press upon the observations the physical controls on sequence formation (Helland-Hansen and Hampson, 2009) unlike traditional sequence stratigraphic terms such as “highstand” and “lowstand” which suggest sea level being the dominant control.

Several techniques are used to interpret the 3D seismic dataset. A combination of traditional horizon based seismic interpretation using Schlumberger Petrel v2013 and auto interpretation using Eliis PaleoScan software was used to map all reflections between picked horizons in a semi-automated fashion. For 3D visualisation and identification of key depositional features such as channels and lobes, seismic geomorphology techniques such as time slicing, stratal slicing and horizon slicing, are combined with RMS amplitude extractions and RGB blending techniques using FFA Geoteric software (Posamentier and Kolla, 2003; Posamentier, 2004; Davies and Posamentier, 2005 ; Purves, et al., 2007).

In vertical seismic cross section displays many of the stratigraphic features seen in amplitude maps are not easily identified due to their limited thickness relative to the seismic resolution whilst their spatial extent usually greatly exceeds the horizontal resolution. Identifying seismic facies using seismic geomorphology techniques, calibrating them to well logs and lithological descriptions and comparing them to analogues from the literature is used in the absence of direct geological information to give an interpretation of the depositional environment. Thickness maps and structure maps of key reflections and reflection-bound seismic units are utilised to place the key facies and architectures into the context of basin shape and main depocentre of the unit.

Calibrated TWT to Depth plotted from available industrial check shot data in the Netherlands North Sea from ten Veen *et al.*, 2013 (TNO Report) is utilised.

The relationship is

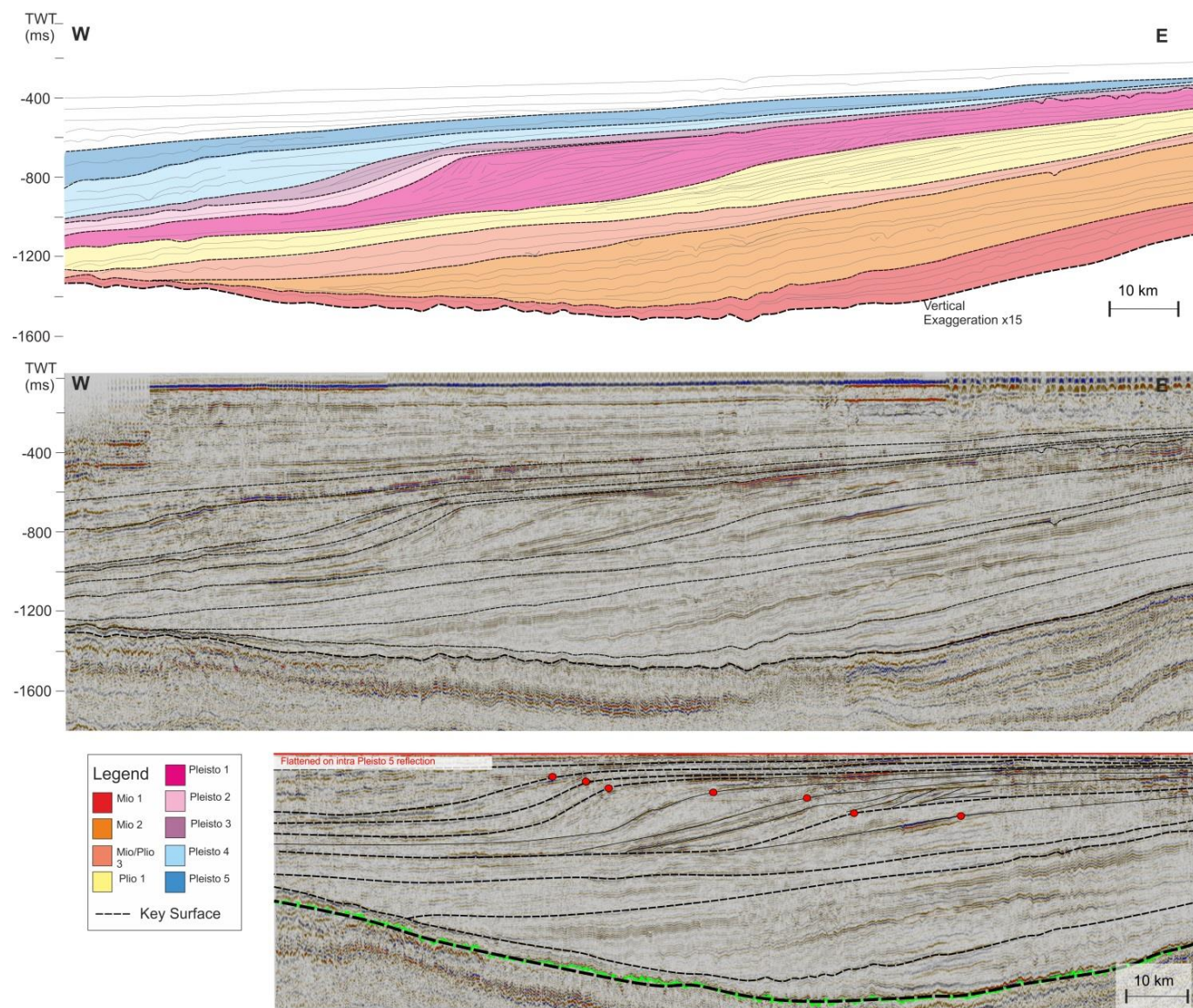
$$\text{Depth (m)} = 80.232 \times \text{TWT (s)}^3 - 28.734 \times \text{TWT (s)}^2 + 882.33 \times \text{TWT (s)}$$

3.3 STRATIGRAPHIC FRAMEWORK

In this section *Mio 1* to *Pleisto 5* the nine seismic units which comprise the post mMU section to the Top Gelasian (1.78 Ma) are described, the depositional environment interpreted and placed within the chronostratigraphic framework described in Section 3.12. In order to visualise the seismic and well log character of the seismic units four seismic cross sections (Figs. 3.6 a-d) and two well correlation panels are presented (Figs. 3.9 a&b). The cross sections have been chosen to represent the variation of the overall character across the basin but also to capture the most expanded parts of the main depocentres through the Pliocene and Pleistocene. In Figs. 3.6 a&b, flattening on topsets in the youngest part of our study period was done in order to restore the *Top Plio 1-Pleisto 3* topsets to horizontal, their likely original depositional geometry. This is because the clinoforms of the northern area of the dataset represented in Figs. 4 a&b appear to have undergone a greater amount of post depositional tilting compared to the southern area.

In order to understand the evolution of the basin fill through time and the evolution of depositional environments the most commonly recurring seismic architectures and seismic facies are described in Figs. 3.8 & 3.9 and in the next two sections. The key seismic architectures and facies are the building blocks of the sedimentary section and the distribution across the basin throughout the study period is discussed further in the 3.3.2 *Unit Descriptions* section.

Figure 3.6 Seismic cross sections (following page). Vertical exaggeration x 15 therefore clinoform angles greatly exaggerated. Locations of seismic lines shown in Fig. 3.1. **a)** East- west seismic cross section from the CNS MegaSurvey in the Danish sector, top interpreted seismic line; *centre*: un-interpreted seismic line; *bottom* flattened section. Flattening on seismic reflection within seismic unit *Pleisto 5* restores the topsets of the *Plio 1 to Pleisto 4* to horizontal (the original geometry); red dots represent the shelf-prism clinoform roll over point.



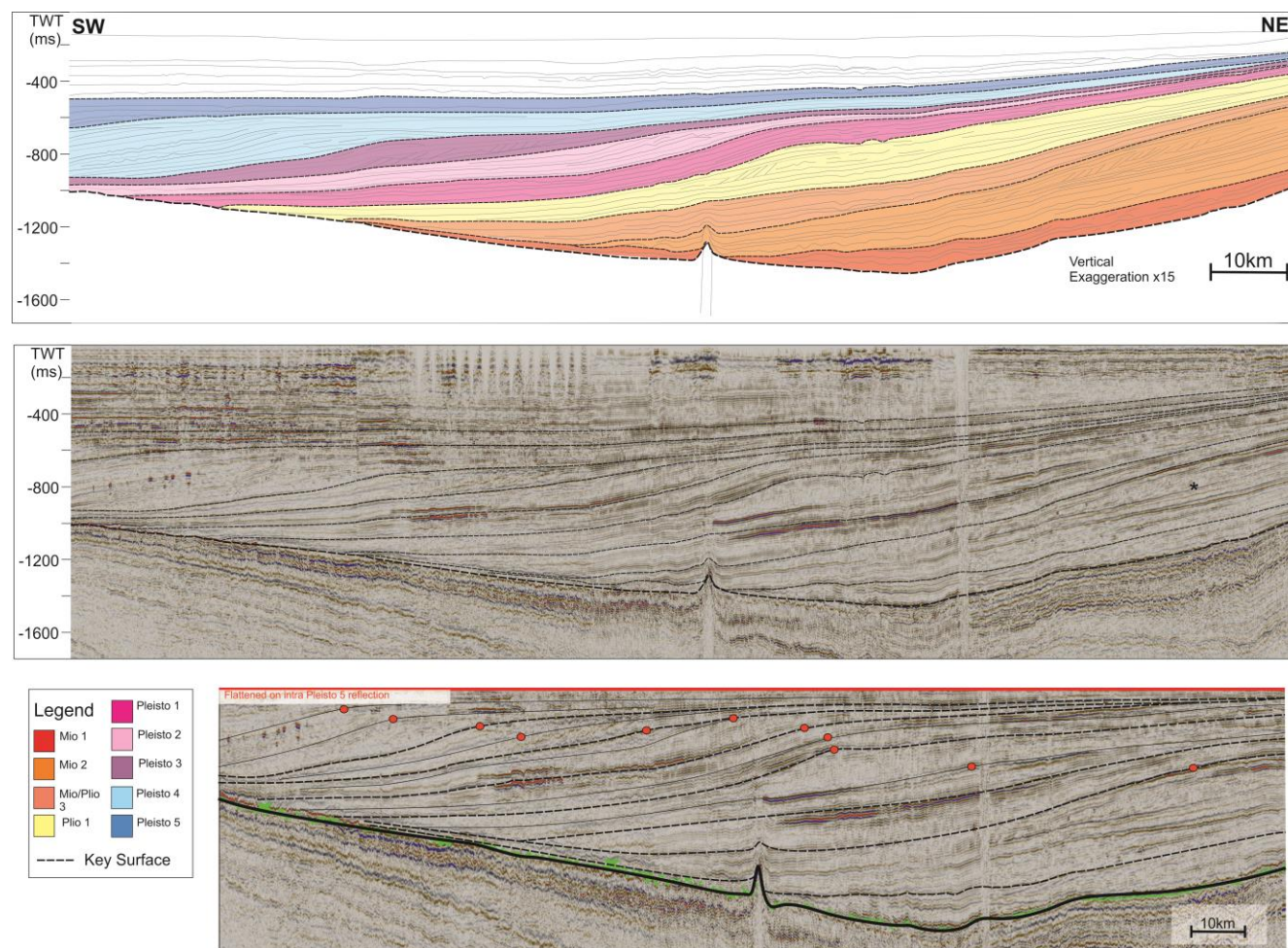


Figure 3.6 cont. b) NE-SW seismic cross section from the CNS MegaSurvey, *top* interpreted seismic line; *centre* un-interpreted seismic line; *bottom* flattened on seismic reflection within seismic unit *Pleisto 5*.

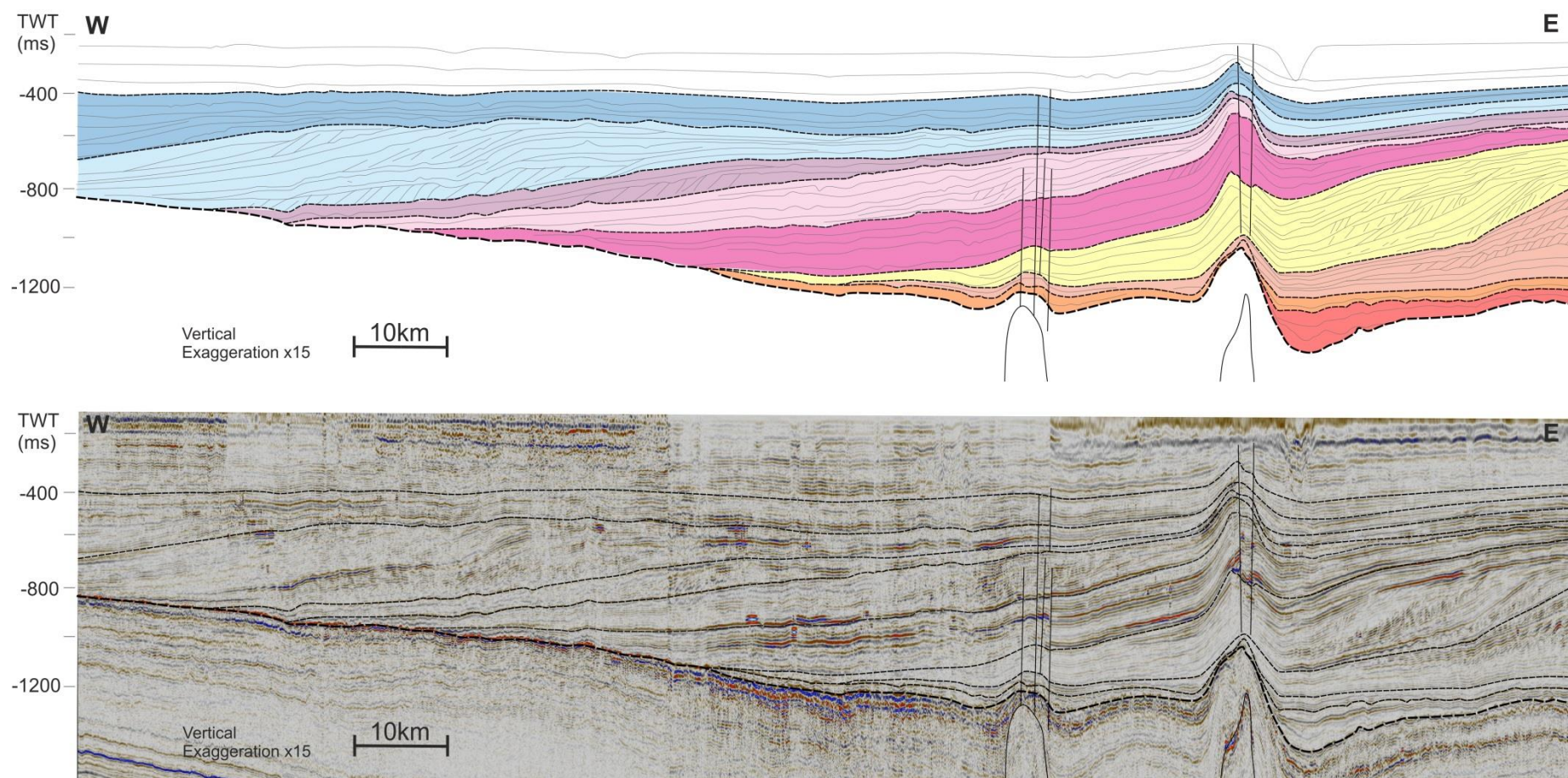


Figure 3.6 cont. c) East- west seismic cross section from the CNS MegaSurvey in the Netherlands sector of the North Sea. *top* interpreted seismic line; *bottom* un-interpreted seismic line.

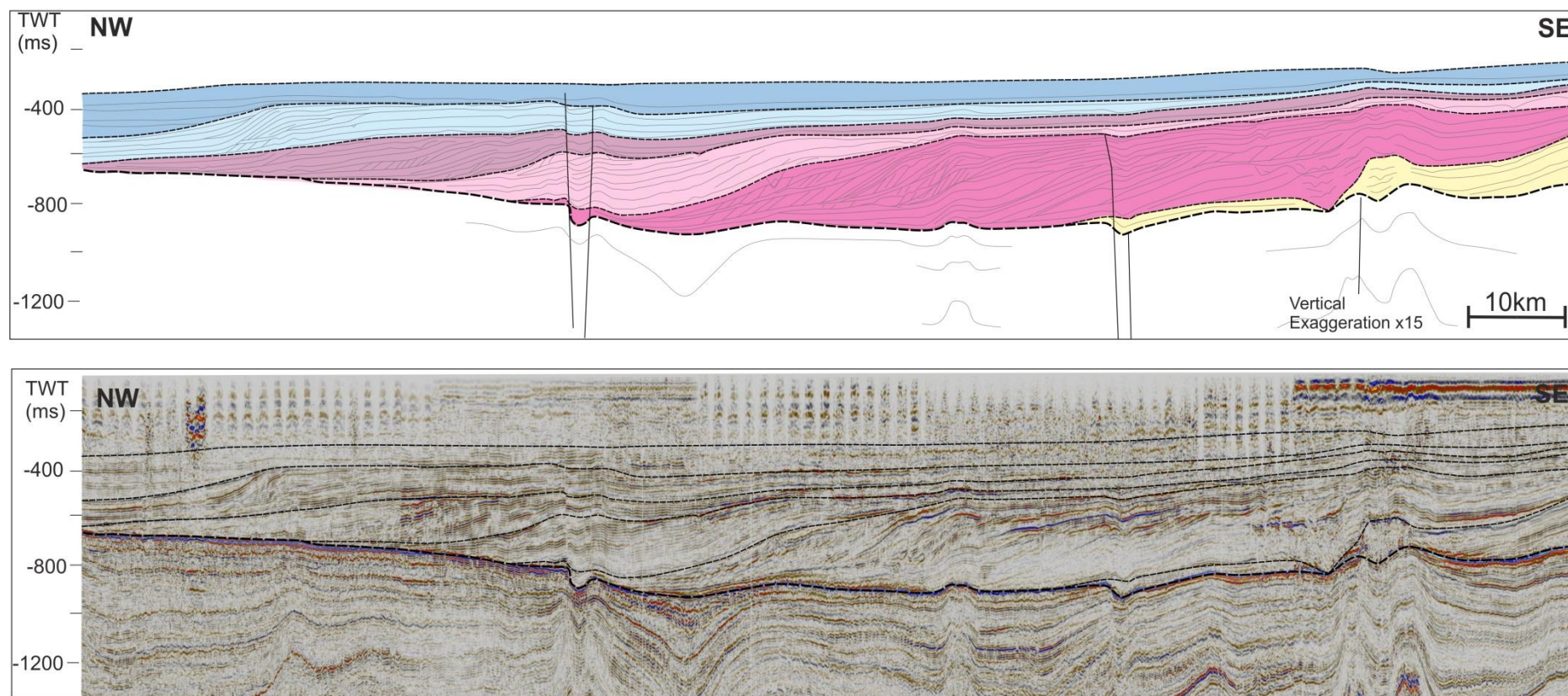


Figure 3.6 cont. d) NW-SE seismic cross section from the SNS MegaSurvey. *Top* interpreted seismic line; *bottom* un-interpreted seismic line.

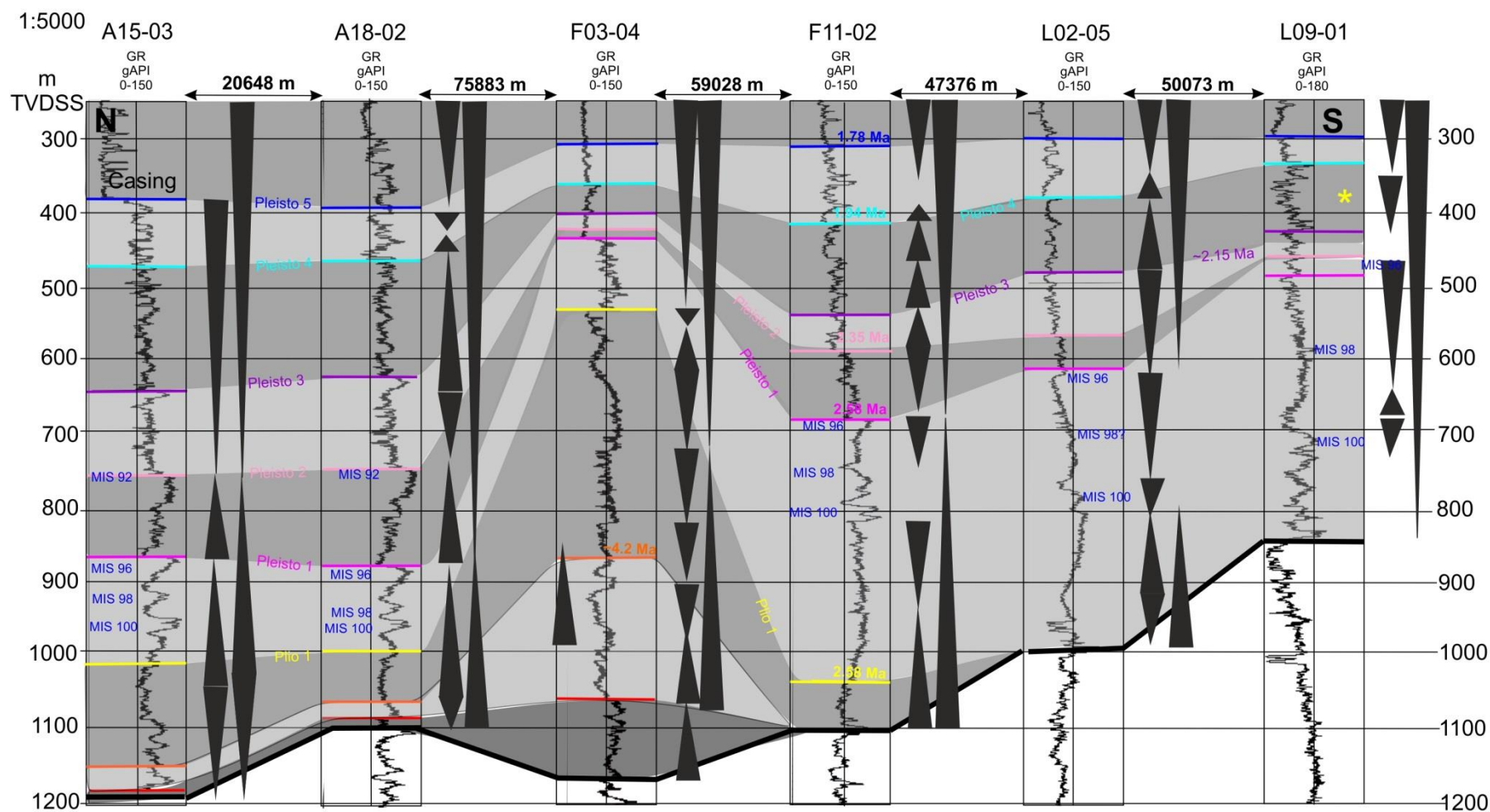


Figure 3.7 Well log correlation. a) North-South gamma ray well log correlation along strike of the depositional system. Black line at base represents the mMU, mid Miocene Unconformity. The correlated surfaces are the tops of the seismic units. Fining upwards and coarsening upwards well log motifs are identified and illustrated by the black triangles. Well distances are equalised. Location of well correlation shown in Fig. 3.1

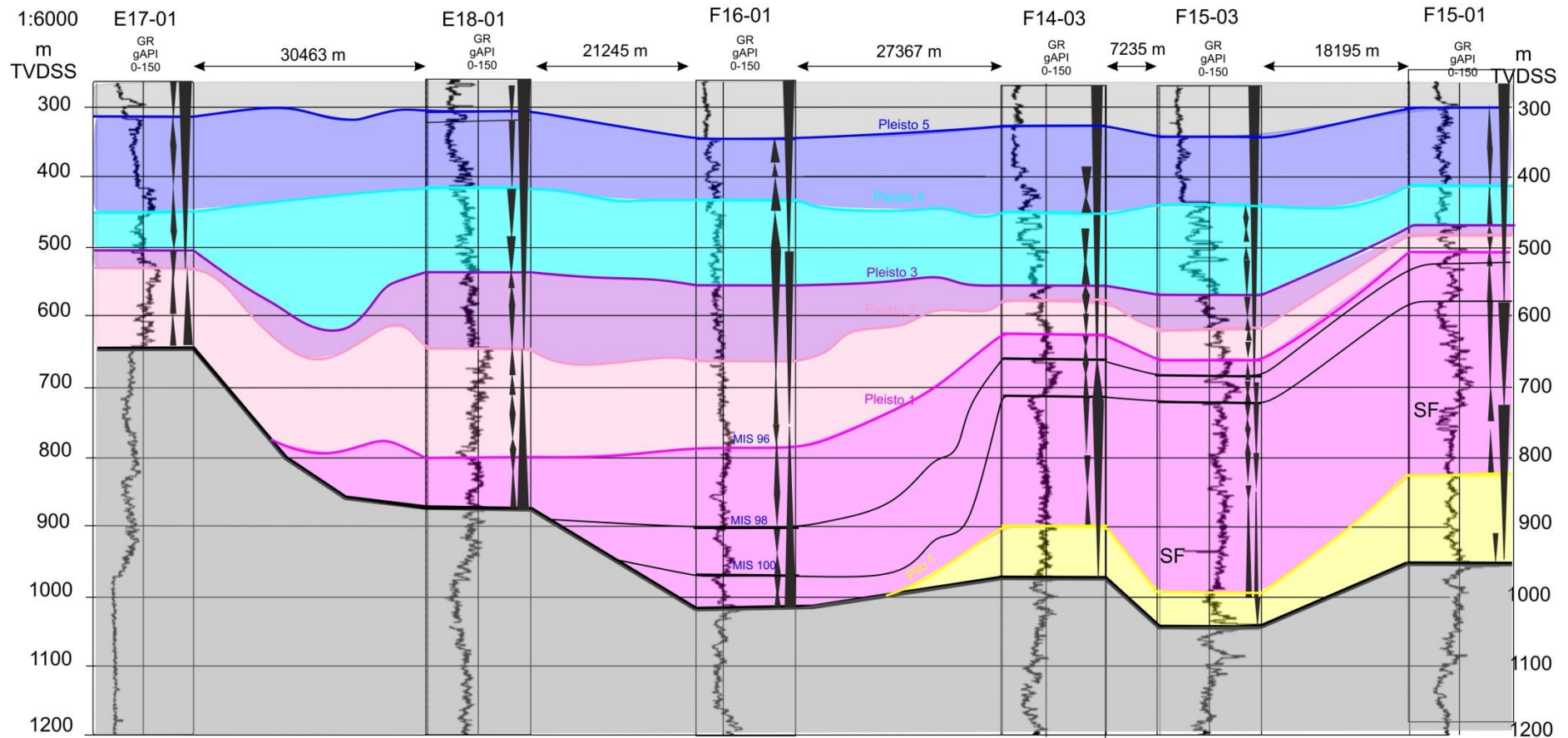


Figure 3.7 Well log correlation b) East-West gamma ray well log correlation along dip of the depositional system. Black line at base represents the mMU, mid Miocene Unconformity. The correlated surfaces are the tops of the seismic units. Fining upwards and coarsening upwards well log motifs are identified and illustrated by the black triangles. Well distances are proportional in order to visualise the depositional system. Location of well correlation shown in Fig. 3.1. SF highlights the well log character related to Seismic Facies 3 in Fig. 3.9.

3.3.1 Key to Unit Descriptions

The unit descriptions provide a comprehensive overview of each of the nine seismic units *Mio 1-Plesito 5* (Fig.3.4). The seismic reflection character, well log character and lithological information are combined to understand the depositional environment how the unit varies in character across the basin. For each unit the interpretation is placed within the context of the existing literature and chronostratigraphic framework. As there are many seismic facies and seismic architectures which are identified many times across the basin fill, the most common are identified and described in detail in Figs. 3.8 & 3.9 instead of being described each time in the unit descriptions. The distribution of the most common seismic architecture and seismic facies for each unit is mapped with the units thickness map in order to aid basin infill interpretation and visualisation of the lateral variation in basin infill across the SNS (Figs 3.10 & 3.11).

3.3.2 Seismic Architecture

Seismic architecture in this paper refers to the dominant seismic reflection geometries recorded in this dataset. Clinoforms are the dominant architecture in the study period and several criteria are used to distinguish seven key seismic architectures in the basin (Fig. 3.8). The clinoform shape, presence of topset and bottomset, foreset height and dip angle, plan view geometry and relationship to surrounding reflections are the key criteria, used to distinguish them from each other in (Figs. 3.5 & 3.8). There are two general scales of architectures identified: *Small Scale* clinoforms SA1-3 are generally <100 m and are superimposed on the *Large Scale* clinoforms SA4-7. SA6 *Oblique Tangential* or SA7 *Sigmoidal* clinoforms large scale clinoforms are the most dominant architectures (Figs. 3.8 & 3.10). The *Oblique Tangential* architecture also encompasses complex oblique sigmoidal which denotes sections dominated by oblique clinoforms but periodically are separated by a sigmoidal clinoform. The reason the dominance of SA6 or SA7 is of importance and mapped for each unit (Fig. 3.10) is that in SA6 *Oblique Clinoforms* generally preserve little or no topset and indicate bypass. The SA7 *Sigmoidal Clinoforms* generally have thicker topsets deposition and is preserved and therefore dominance of SA6 or SA7 can indicate whether there is accommodation on the shelf at

the time of deposition and therefore indicate the state of base level in the basin at the time (Anell and Midtkandal, 2015; Henriksen et al., 2011; Jones et al., 2015).

3.3.3 Seismic Facies

The seismic facies in this paper is defined as the key seismic features that are cyclically superimposed onto the seismic architectures (Figs. 3.9 & 3.11). The seismic facies are easily identified using seismic geomorphology techniques, where 2D cross sections are used in combination with 3D techniques seismic such as attribute extractions on horizon slices and time slices (Fig. 3.9). The position of each seismic facies along the clinoform aids interpretation of depositional environment in the absence of direct geological data such as core and outcrop. Specifically the distribution of *SF4 Topset Facies* which is interpreted as being indicative of terrestrial influence and subaerial exposure; and *SF6 Iceberg Scours*, which only occur in marine conditions are utilised to constrain the extent of marine and terrestrial conditions and therefore the maximum and the minimum regressions for each unit (Figs.3.9 & 3.10).

SF4 Topset Facies represent the continuous transit of the shorelines across the shelf and the shift between shallow marine and terrestrial conditions (Steel and Olsen, 2002). Within *SF4* coastal feeder systems can be well persevered, as in the example in Fig. 3.9, but largely the case is that successive transits cannibalise previous feeder systems creating a cross cutting of multi directional channels, representing successive regressions of the shoreline (Porębski and Steel, 2003). Seismic analogues for the cross crossing channels which have been linked to core and confirmed as terrestrial in the Mahakam Delta, NE Gulf of Mexico and the Mungaroo Fm in NW Australia (Crumeyrolle et al., 2007; Sylvester et al., 2012; Heldreich et al in prep). *SF6 Iceberg Scours* are only formed under marine or lacustrine conditions (Dowdeswell and Ottesen, 2013), and therefore where they are mapped for any given unit there must have been marine incursion at least to the extent of the mapped iceberg scours.

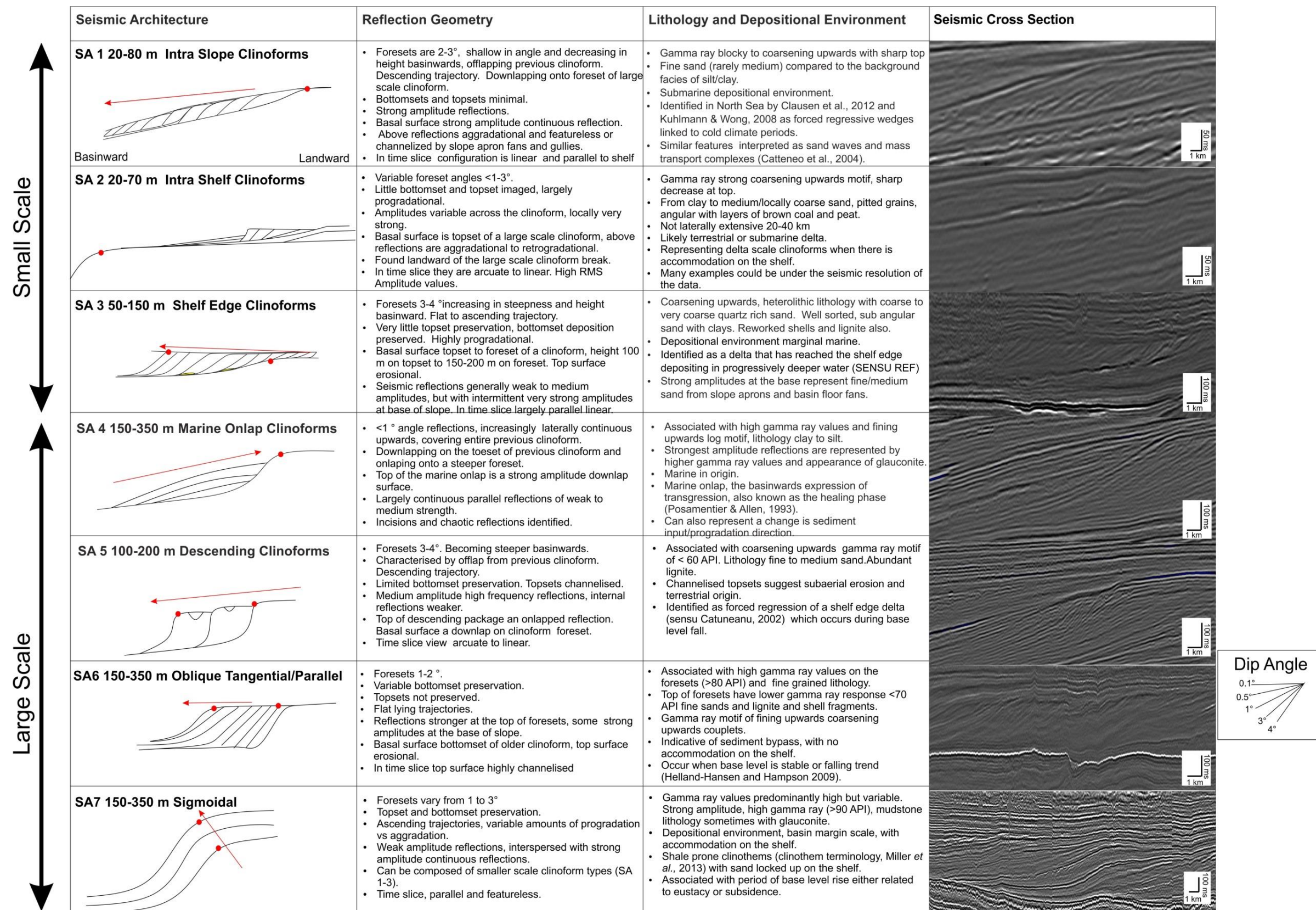


Figure 3.8 Seismic architectures. Description of the main seismic architectures within seismic units *Mio 1 to Pleisto 5*.

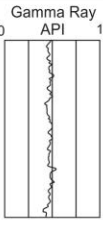

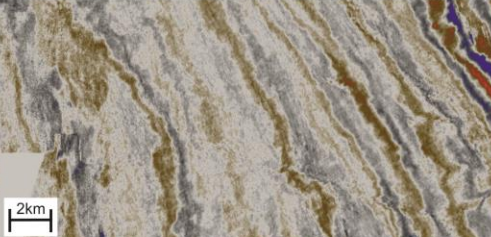
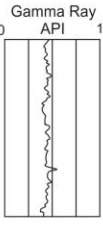
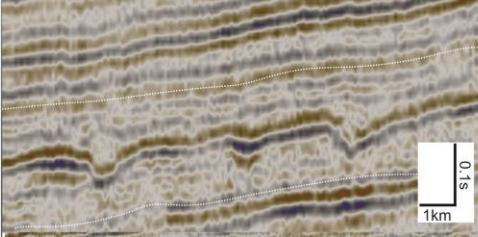
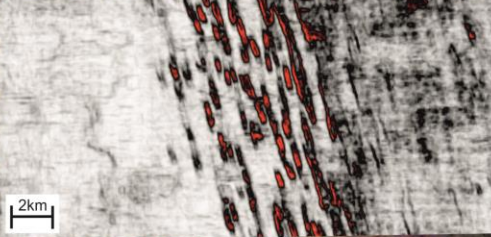
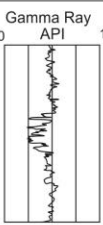
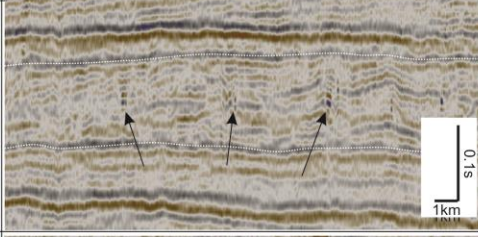
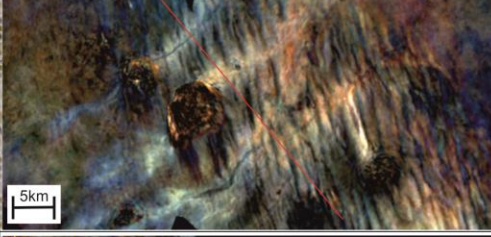
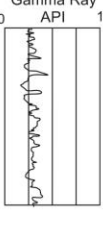
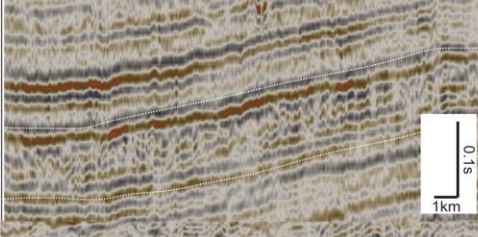

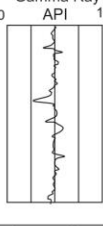

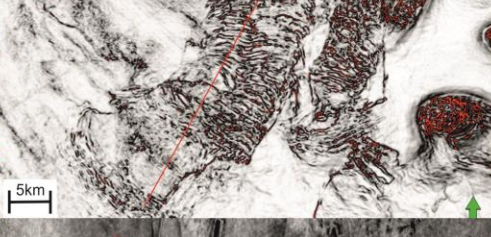
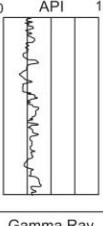
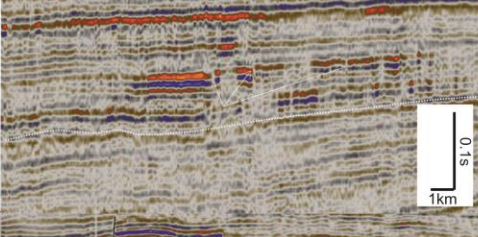
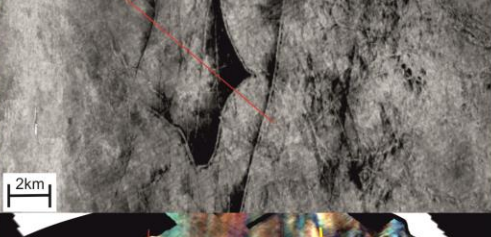
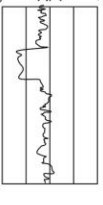
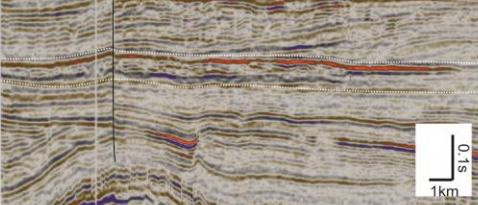
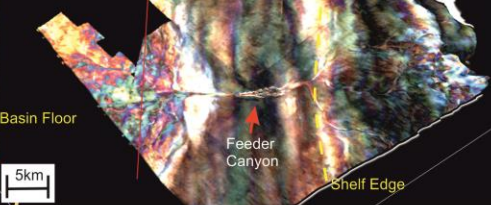
Seismic Facies	Reflection Geometry and Characteristics	Well Log Signature and Lithology	Example Cross Section	Example Time Slice
SF1 Marine Clinoforms (Background Facies)	Weak amplitude, low frequency, continuous reflections. Some stronger amplitude. Featureless, draping the underlying topography. Reflections are >150 m in height with a dip angle of 1°. In plan view, appear linear, parallel to the strike of the shelf. Downlapping onto the mMU. Representing bottomset reflections, basinwards of the shelf break. Stronger continuous reflections represent condensed sections.	 <p>Uniform gamma ray response greater than 70 API. Lithology: clays and silts. Clays vary from grey to dark green with glauconite.</p> <p>Deep marine environment 150-350 m</p>	 <p>0.1s 1km 2km</p>	
SF2 Lower Slope Current Incisions	Medium amplitude reflections within SF1 with depressions of 50-100 m. Variable shape from U shaped to V shaped. Variable infill from divergent prograding fill to a simple onlap fill. In plan view the depressions are circular to elongated, 1-3 km wide and can be up to 3 km in long axis. Composite features can be 10's km. Typically occur on the lower foreset, strike parallel to the shelf edge. Features described in the North Sea previously in several papers (Andresen et al. 2008; Kilhams et al, 2011; Stuart & Huuse 2012).	 <p>Similar lithology to SF1 with small increase in grain size. Interpreted as evidence of strong currents at the base of slope during formation.</p> <p>Deep marine environment 150-350 m</p>	 <p>0.1s 1km 2km</p>	
SF3 Multiple Source Slope Channels	Isolated strong amplitudes on the foreset and bottomset, sometimes confined within a V shaped incision. Some have small 2-5 km fans attached at the base of slope. In plan view, the features are perpendicular to the shelf edge, 20-40 km in length. Depth of features from 30 m but can be stacked up to 100 m. This encompasses several types of channel features from slope gullies, canyons, channel-levee complexes and slope fans (described in greater detail in Harding et al. (in Prep b)).	 <p>Decrease in gamma ray (to 30-40 API) is identified compared to a background high gamma ray value. Lithology fine (sometimes medium) sand on a background of grey clay.</p> <p>Slope 50-350 m</p>	 <p>0.1s 1km 5km</p>	
SF4 Topset Facies	Variable seismic characteristics, heterogenous weak and strong amplitude parallel continuous reflections found landwards of the shelf break. Chaotic, incised reflections common (see example) and isolated very strong amplitudes. In plan view incisions/chaotic reflections appear as multi directional/cross cutting channels. In some cases (see plan view example) individual channels can be imaged. These are interpreted as terrestrial delta top channels. This facies is used to identify the maximum regression of the coastlines during each unit.	 <p>Sawtooth gamma ray response 30-70 API. Lithology varies from clay to fine-medium sands (some coarse). Lignite, wood fragments and oyster beds identified.</p> <p>Shallow marine to terrestrial 0-100 m.</p>	 <p>0.1s 1km 5km</p>	 <p>Shoreline</p>
SF5 Mass Transport Complexes	Heterogenous reflection strength and chaotic in character. The seismic geometry is usually strong amplitude top and erosional base, truncating underlying reflections. The plan view shows extensional ridges nearer the shelf break, and compressional features at the base of slope. The mass transport complexes detach on strong amplitude continuous reflections. Found in areas of steep gradient foresets 3-4°. Described previously in Benvenuti et al. 2012.	 <p>Log character erratic and variable, dependant on the parent shelf/slope. Can have a blocky log appearance also.</p> <p>Slope 50-350 m</p>	 <p>0.1s 1km 5km</p>	
SF6 Iceberg Scours	Weak amplitude negative features within topsets. Depressions maximum 100 m wide, depth 30-50 m. In plan view feature are linear to curvilinear. Orientation variable N-S, NW-SE, NE-SW, striking parallel to the shoreline can be 10's km long. Identified previously in the study area in Kuhlman & Wong, 2008 and Dowdeswell & Ottesen, 2013. Greater detail of iceberg scours from this study in Newton et al. (in prep). Interpreted as marine iceberg ploughmarks. Used in this study to identify transgressions of the coastline in the upper units.	 <p>Has little effect on gamma ray response. Occurs on topsets. Marine depositional environment as icebergs are marine features.</p> <p>Shallow marine 10-100 m</p>	 <p>0.1s 1km 2km</p>	
SF7 Single Source Basin Floor Fans	Present across the entire clinoform. Incised topsets, preserved incisions parallel to the shelf edge, some perpendicular, feeding into a single canyon at the upper slope, 60-70 m deep. The canyon truncates underlying reflections and is infilled with ~30-50 m clinoforms. The canyon is 7-10 km in length and feeds at the base of slope, a 20-30 km wide channelized fan (noted by bidirectional downlap). Seismic amplitude is stronger within the incisions and fan than the surrounding reflections. More detail in Harding et al. (in prep b).	 <p>Canyon and basin floor fan show blocky decrease in gamma ray, sharp top and base. Fine to medium sand. Abundant lignite, wood fragments and macro and micro fossils.</p> <p>Terrestrial to deep marine 0-200 m</p>	 <p>0.1s 1km 5km</p>	 <p>Basin Floor Feeder Canyon Shelf Edge</p>

Figure 3.9 Seismic facies. Properties of seismic facies encountered in the seismic units.

3.3.2 Unit Descriptions

Miocene Unit 1 (Mio 1)

Seismic and Well Observations

Bounding Surfaces The base of *Mio 1*, the mMU, is known as a major regional downlap surface (Figs. 3.1 & 3.6) and marks the basal surface of the large scale clinoforms of seismic units *Mio 1* to *Pleisto 5*. Across the basin the mMU changes character and does not appear the same reflection across the entire basin.

The top surface of *Mio 1*, (*Top Mio 1*), (Figs. 3.6a&b; Fig. 3.11a) is a continuous positive reflection of moderate amplitude which drapes the underlying topography and is downlapped by overlying reflections. The reflection dips $<1^\circ$ to the SW. The extent of the reflection is confined to the NE part of the dataset in the DK and the NE NL sector (Fig. 3.11a). *Top Mio 1* is deepest (1300-1450 ms TWT; 1275-1460 m) within the DK sector and follows the trend of the Central Trough (Fig. 3.1). The surface gradually shallows to the south, west and east to 800-900 ms TWT (730-830 m). *Top Mio 1* is largely characterised as a sharp increase in gamma ray values from 70 API to 100 API.

Internal Character *Mio 1* thickens to the NW to a maximum of 200 ms (175 m) (Fig. 3.10a). The main depocentre strikes NNW-SSE in the eastern part of the dataset in the DK sector. The average thickness is 80 ms (70 m). *Mio 1* is locally absent on top of salt diapirs and unit reflections truncate onto the salt structures.

Internally, the seismic character of *Mio 1* is predominantly weak, parallel reflections (*SF1* Fig. 3.9) with no clinoformal geometry. Elongated depressions identified as *SF2 Elongated Current Scours* in *Mio 1* are 2-10 km in length; striking $140-160^\circ$, their spatial distribution is shown in Fig. 3.11. Gamma ray shows a serrated medium to high gamma ray motif with values between 75-100 API. Gamma ray values overall decrease upwards in unit *Mio 1* suggesting a coarsening upwards clay/silt heterolithic lithology in wells from the North NL sector. In the extreme east of the NL sector an increasing upwards (fining upwards) motif is identified (Fig. 3.7).

Correlation

Mio 1 correlates to unit S1 in Kuhlmann and Wong, (2008); Composite sequence I-III in Sørensen and Gregersen, (1997); SU1-3 in Thöle et al. (2014) and within the later part of Sequence E of the Gram Formation in Rasmussen et al. (2005).

Sequence E is dated at 15-11 Ma from micropaleontological dating in several wells by Konradi, (1996) in the DK Sector. Kuhlmann et al. (2006b) identified the onset of sedimentation onto the mMU as approximately 12 Ma (Middle Serravallian) recovered foraminifera *A. spiridoides*, *P. ventricosum* and *U. aquaeductum*. The *Top Mio 1* is likely Middle- Late Tortonian in age (from correlation with Rasmussen et al., 2005; Thöle et al., 2014).

Interpretation

The mid Miocene Unconformity (mMU) is the base of a mega-sequence and is a regionally correlatable composite downlap surface which becomes an onlap surface towards the DK onshore (Huuse and Clausen, 2001). In the southern North Sea Basin, the mMU represents a significant hiatus that spans 5-12 Ma which becomes younger towards the west of the North Sea basin (Anell et al., 2012; Huuse and Clausen, 2001). The mMU seismic reflector is interpreted as a combined Middle Miocene transgressive and Mid-Late Miocene erosive surface (ten Veen *et al.*, 2013). *Top Mio 1* is interpreted as a seismic downlap surface and therefore is interpreted as a maximum flooding surface (MFS).

NNE-SSW trending lower slope current incisions (*SF2*, Fig. 3.9) suggest strong currents within the basin during deposition and suggest that the shelf edge was trending NNE-SSW at the time, though laying eastwards DK sector at the time (Figs. 3.11a & 3.12a). Thickness maps from (Rasmussen et al., 2005; Sørensen and Gregersen, 1997; Thöle et al., 2014) show during the same period up to 1000 m of deposition occurred to the east of the study area within two main depocentres.

The weak seismic character of the unit, lack of clinoform geometry and the high gamma ray values suggests this unit represents condensed bottomsets of a depositional system in a distal deep marine environment, representing several million years of deposition.

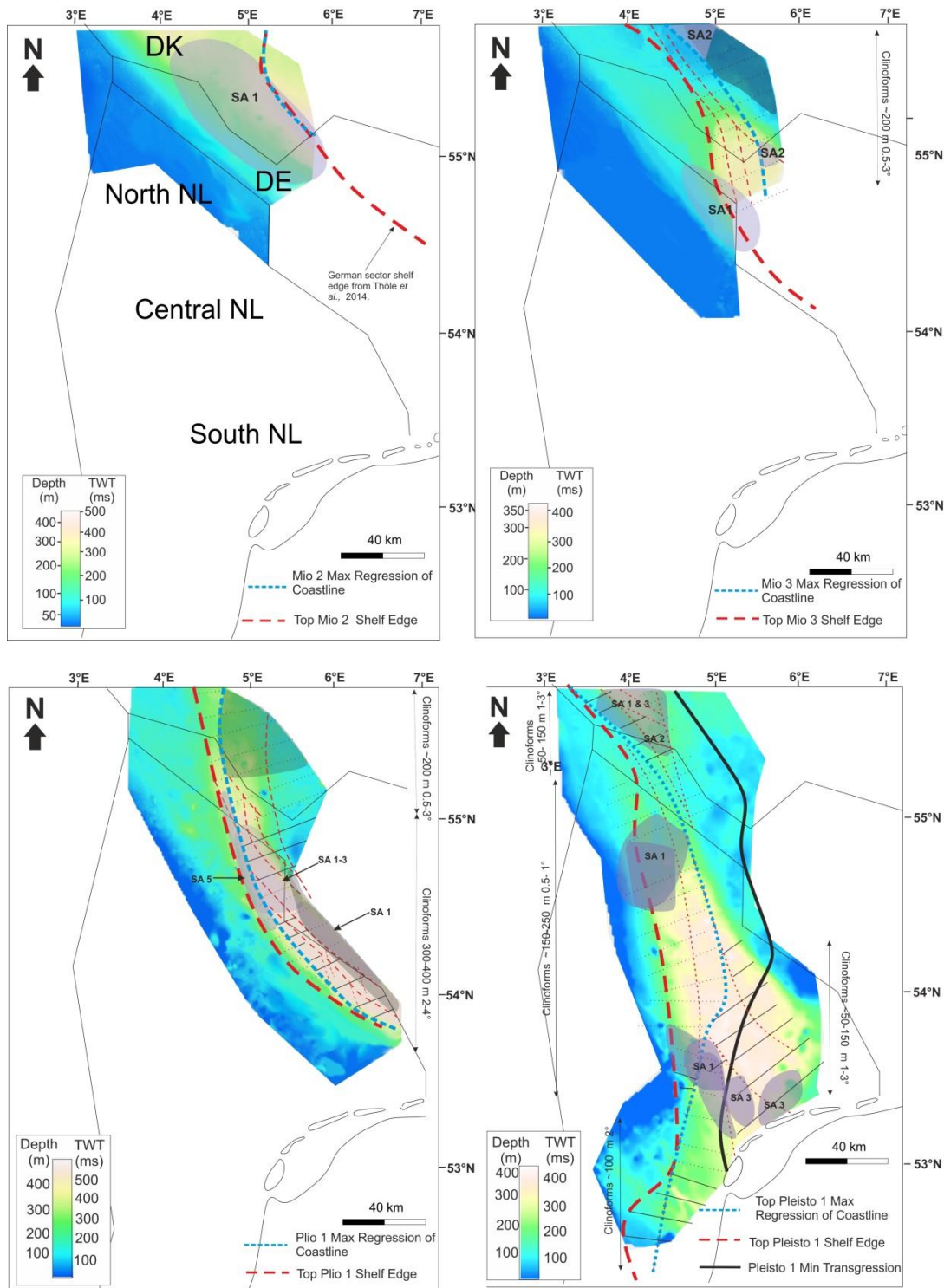
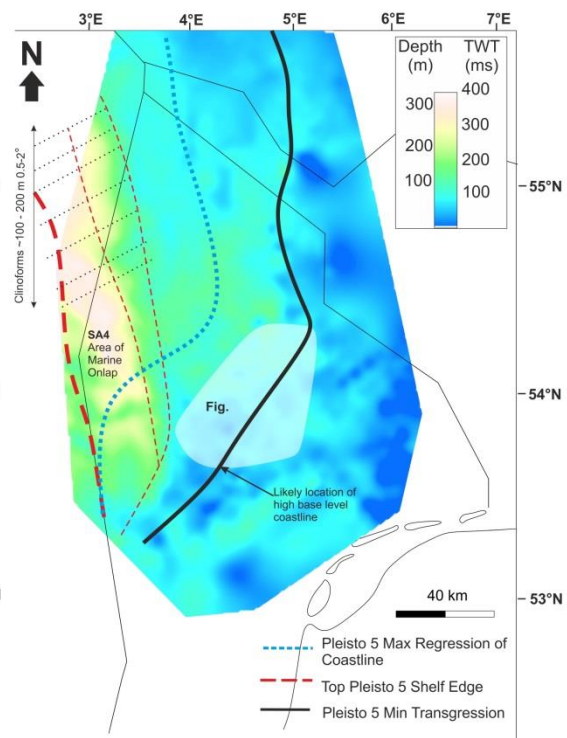
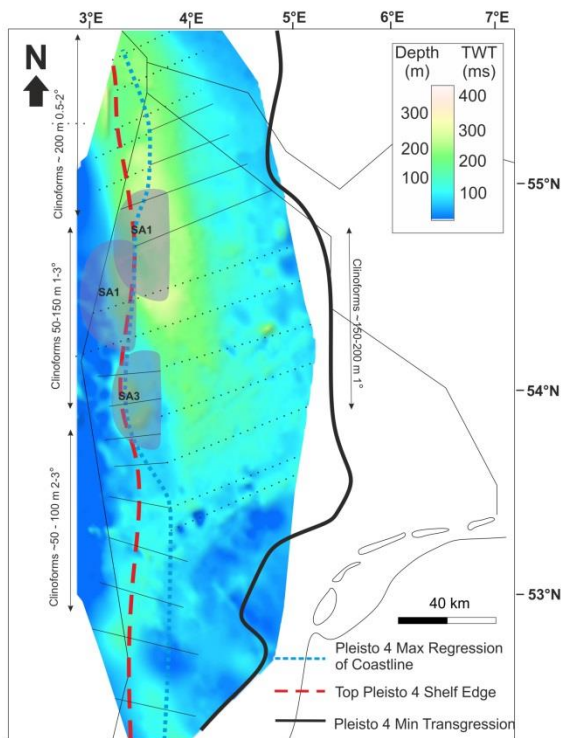
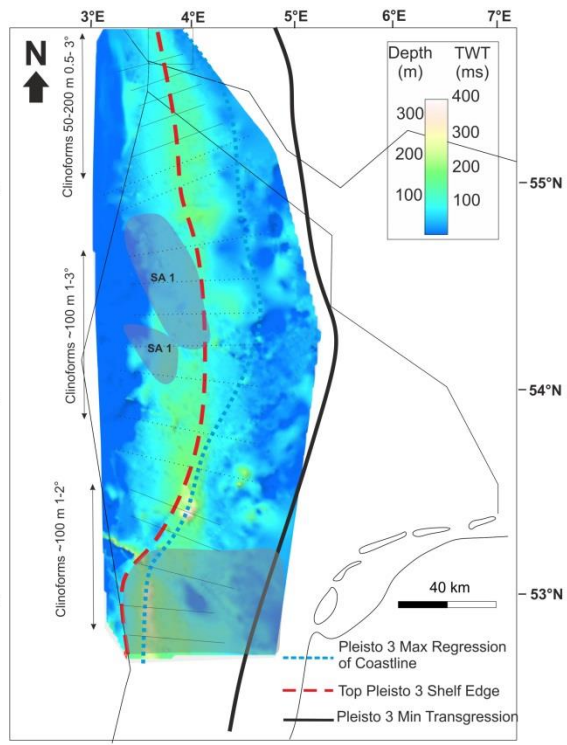
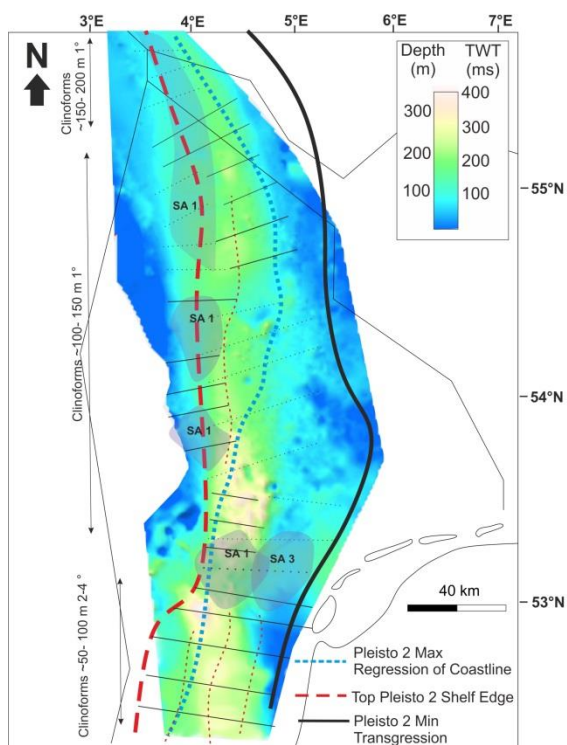


Figure 3.10 Unit thickness maps with seismic architecture distribution (above and following page). Thickness in TWT (ms) and depth (m). Solid and dotted lines represent the dominant large scale clinoforms. Shaded areas are the locations of smaller scale clinoforms described in Fig. 3.8. Final shelf edge of the unit and maximum regression within the unit is illustrated. Where possible (post *Pleisto 1*) the minimum transgression is shown. This relates to the minimum point that marine conditions could have occurred during the unit as iceberg scours require marine conditions to occur



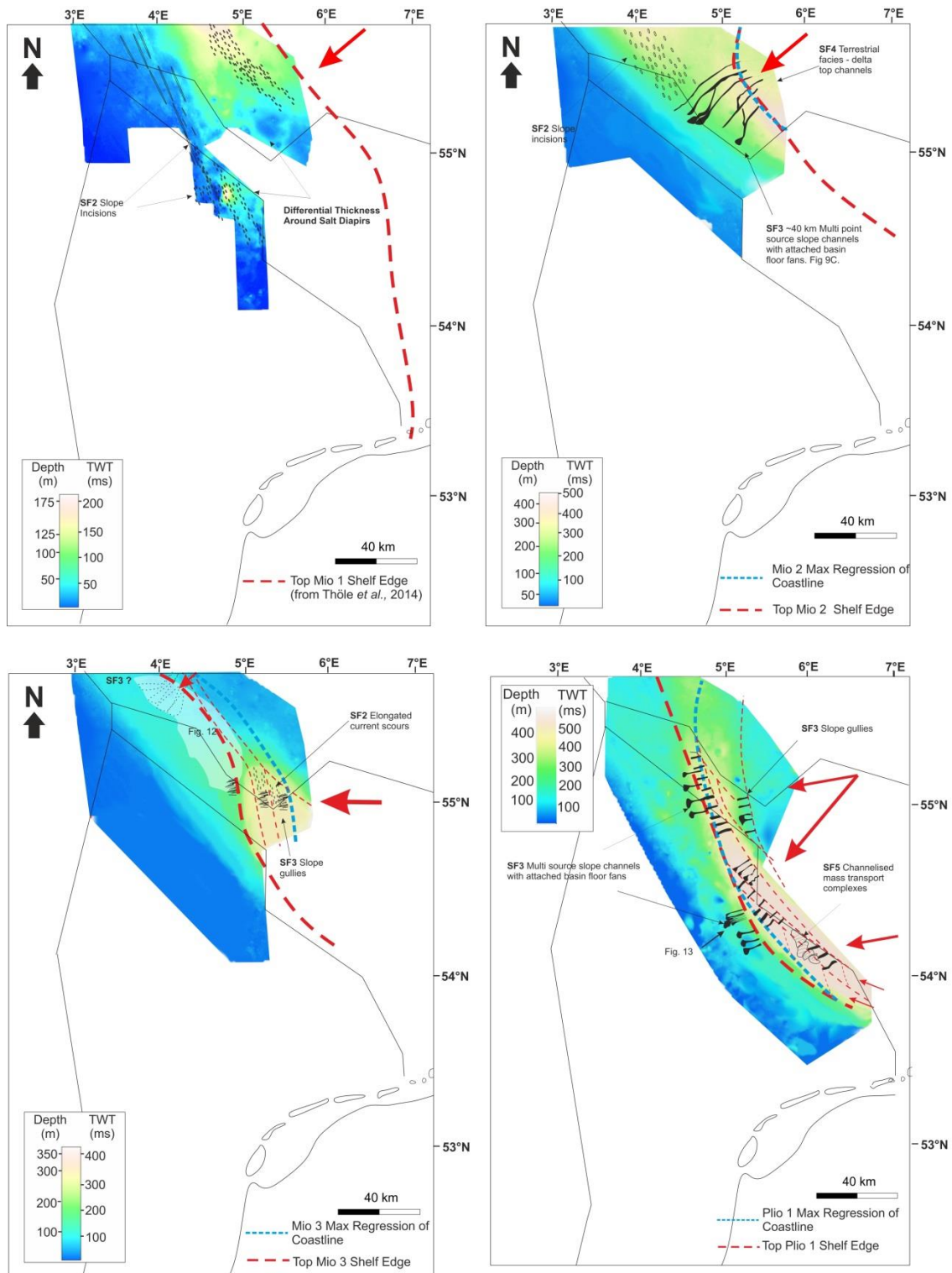
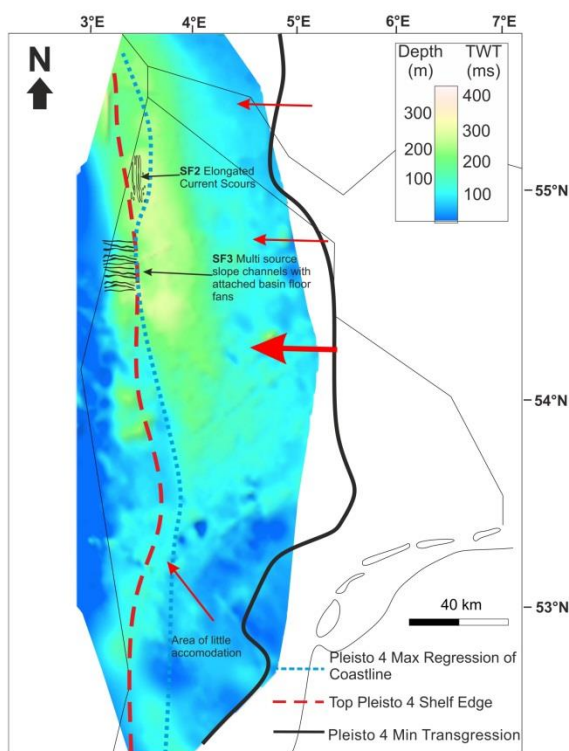
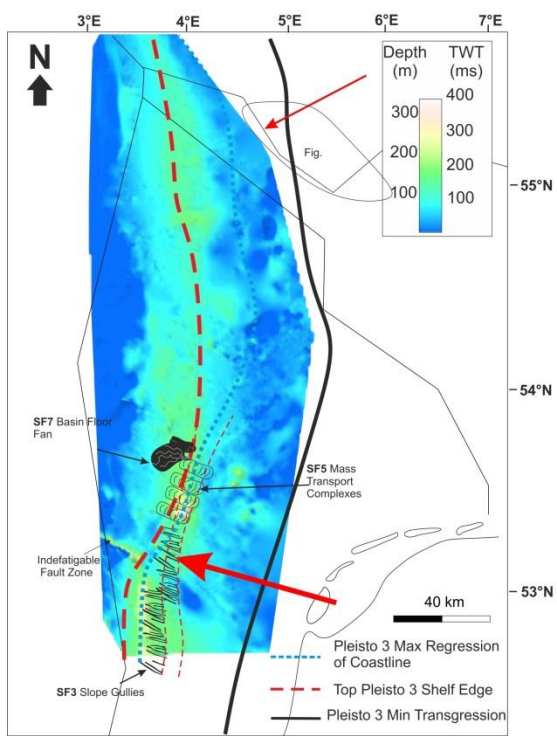
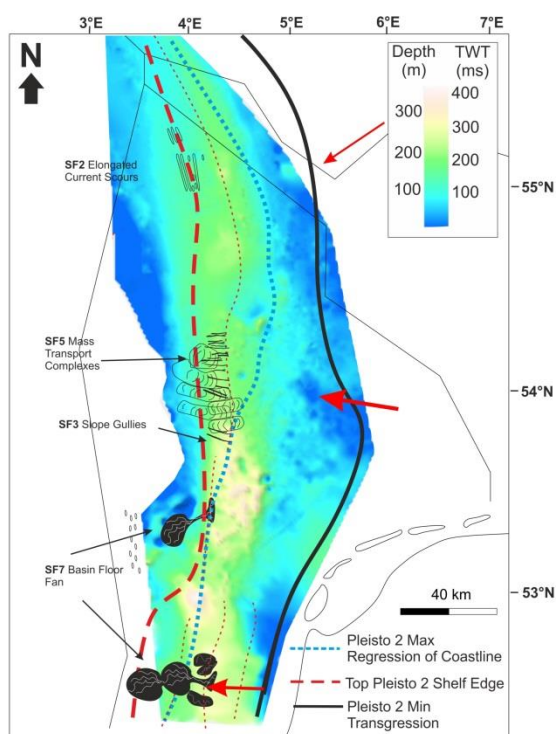
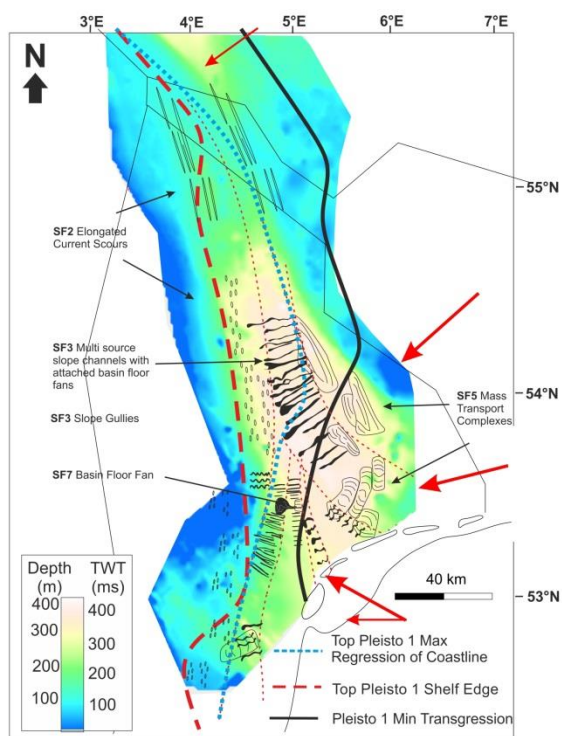


Figure 3.11 Unit thickness maps with seismic facies distributions Thickness in TWT (ms) and depth (m). Distribution of seismic facies described in Fig. 3.9 illustrated. Figures are an illustration of the relative size and distribution of key seismic facies but not exactly to scale. Final shelf edge of the unit and maximum regression within the unit is illustrated. Where possible (post Pleisto 1) the minimum transgression is shown. This relates to the minimum point that marine conditions could have occurred during the unit as iceberg scours require marine conditions to occur.



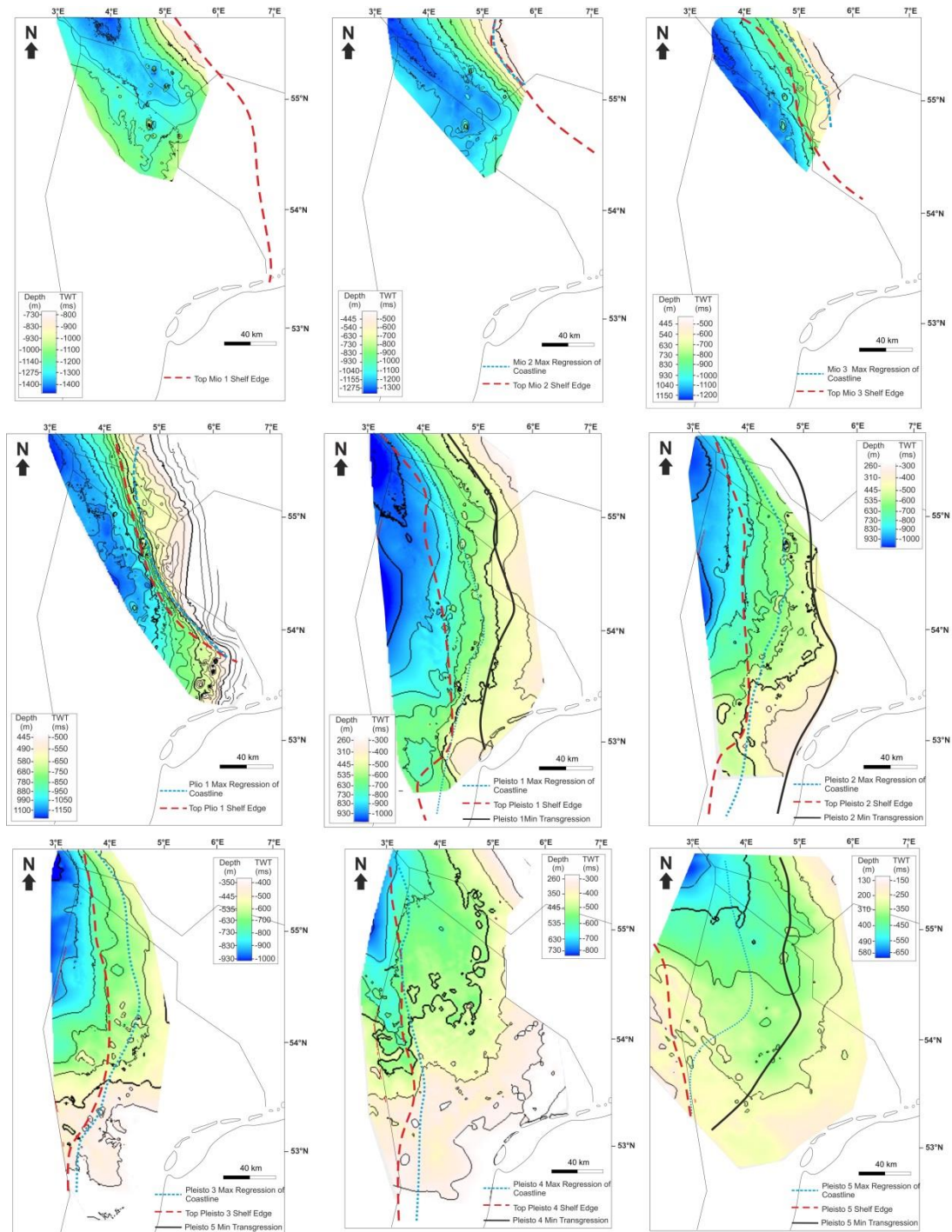


Figure 3.12 Structure maps. Maps for the Top of each seismic unit *Mio 1-Pleisto 5*. Both TWT (ms) and depth (m) given. Final shelf edge of the unit and maximum regression within the unit is illustrated. Where possible (post *Pleisto 1*) the minimum transgression is shown. This relates to the minimum point that marine conditions could have occurred during the unit as iceberg scours require marine conditions to occur.

Miocene Unit 2 (Mio 2)

Seismic and Well Observations

Bounding Surface: The *Top Mio 2* (Fig. 3.12b) is weak/medium negative amplitude reflection, confined to the NE of the dataset and parallel to underlying reflections (Figs. 3.6a&b). Large scale *SA7* sigmoidal clinoforms of the *Mio 3* unit downlap onto the *Top Mio 2* surface. Subsequent units, *Mio 3* and *Plio 1*, onlap onto the reflection in the NE (Fig. 3.6). The reflection has clinoform geometry in the NE and a $\sim 1^\circ$ foreset dip. In the rest of the area the surface is a low angle inclined surface of $<1^\circ$ degree.

The shallowest point of the reflection is in the NE of the dataset at 500 ms (~ 445 m), the unit deepens to the SW to 1300 ms (~ 1275 m) (Fig. 3.12b). *Top Mio 2* is defined by sharp decrease upwards in gamma ray values at the top of an increasing (fining) upwards package (Fig. 3.7).

Internal Character: *Mio 2* thickens towards the NE. Two NW-SE trending depocentres 400-450 ms (350-400 m) thick are imaged in the DK sector, separated by a thinner area of 300 – 350 ms (265-310 m) (Figs. 3.10a & 3.11b). Local anomalies in thickness around some salt diapirs are evident in the DK/DE sector.

The first 100 m of the unit are characterised by weak, heterogeneous and chaotic reflections (*SF1*) interspersed with individual stronger amplitude reflections eroded by NNW -SSE trending *SF2 Elongated Current Scours* (Fig. 3.9). The facies distribution map (Fig. 3.11b) shows *SF2* in the NE of the dataset is present basinwards of *SF2* in *Mio 1*. The following 70-100 m is weak amplitude, parallel, continuous reflections (*SF1*) with some *SF2* present.

The upper part of the unit comprises two stacked packages of *SA1 Intra Slope Clinoforms* (20-60 m each), separated by a truncation surface and a downlap surface (Fig. 3.6b). The foresets have a 3° dip maximum. Isolated strong amplitudes are identified at the termination of the package basinwards, and in the far NE. The top of the second package is an erosional truncation surface, onlapped by subsequent reflections. RMS Amplitude extraction on the top 20 ms (Fig. 3.13) of the upper *SA1* package shows in the northern depocentre *SF2* are incising into the clinoforms in a NW-SE direction (along strike). In

the southern depocentre low sinuosity *Multiple Line Source Slope Channels* (*SF3*) incise the *SA1* clinoforms in a NE-SW direction (down dip). The slope channels are ~40 km average length, with a maximum incision of 60 m. *SF3* emanate from an area of stronger amplitude to the NE with an arcuate front (Fig. 3.13), interpreted as the shelf edge. *SF4* (*Topset Facies*) is identified landward of the proposed shelf edge. The RMS amplitude map shows that some *SF3* channels have been pierced by post *Mio 2* salt diapirs.

The top 50-100 m of the unit is only present in the far east of the dataset and shows a set of backstepping reflections each downlapping the previous one eastwards (Fig. 3.13). Gamma ray values from the distal part of this unit are >80 API with 20-30 m increasing (fining) upwards packages. No wells from this study penetrate the *SA1* clinoforms. *SA2 Intra Shelf Clinoforms* exhibit low angle ~1° sigmoidal geometry and occur at the upper 100 m of the unit.

Correlation

Mio 2 corresponds to the early S2 (Kuhlmann and Wong, 2008); early Composite Sequence IV in (Sørensen and Gregersen, 1997); upper Sequence F in (Rasmussen et al., 2005) and ~SU3-4 in (Thöle et al., 2014).

Correlating to (Rasmussen et al., 2005) *Mio 2* is Upper Miocene in age, likely Late Tortonian. *Top Mio 2* correlates to nr Top Tortonian (7.8-7.1 Ma) well marker B14-03 (Chris King *pers comms*), (Fig. 3.1). The *SA1* clinoforms correspond to what is described as “Late Miocene delta complex” in (Møller et al., 2009).

Lithological information from cuttings descriptions of wells Adda-1 and E1-X (Møller et al., 2009) that penetrate the *SA1* units comprise grey-green mica rich largely clay to silt fraction sediment with very thin beds of fine grained sand. Though well NX-1 suggests a coarse grained fraction at the basinwards termination of the package.

Interpretation

Top Mio 2 is a seismic downlap surface the top of a transgressive systems tract (Fig. 3.13) and therefore interpreted as a MFS. *Top Mio 2* is also an onlap surface in the NE of the dataset, which reflects a likely change in direction of sedimentation post *Mio 2*. The strike of the depocentres and the orientation of the *SF2* and *SF3* suggest a sediment input from the NE with an arcuate shelf edge trending NW-SE (Figs. 3.10a & 3.11b). Up

to 1000 m of sediment are deposited during *Mio 2* largely in a N-S trending depocentre in the DE sector just east of the NL sector, (comparing SU3-4 thickness maps in (Thöle et al., 2014)).

The majority of the unit is interpreted as deep marine, distal from the sediment source (which is concentrated in the south of the DE sector, >100 km away), however the identification of *SA1* plus *SF3* & *SF4* in the study area suggest regression of the coastline into the basin. Though the *SA1* clinoforms are identified as subaerial deltaic in (Møller et al., 2009) there is no evidence of subaerial erosion on the topsets of *SA1* and without lithological information diagnostic of terrestrial facies it is inconclusive. Erosion into the topsets of *SA1* is consistent with the geometry of *SF3 Slope Channels* which are interpreted as submarine channels formed by and conveying sediment-gravity flows, (Janocko et al., 2013) and not fluvial in origin. During this time the terrestrial facies, *SF4* are confined landward of the shelf edge, and *SF3* slope channels emanate from the terrestrial facies. (Clausen et al., 2012) investigates similar geometry clinoforms eroded by submarine channels from the Oligocene Danish North Sea, suggesting they were deposited under marine condition associated with glacial maxima climate conditions. The depositional environment of these intra slope clinoforms is discussed further in *Chapter 5*. Whether *SA1* is terrestrial or not this subunit represents a dramatic regression and the appearance of the coastline into the study area. The backstepping of reflections at the top of the unit represents a transgression and a return to deep marine conditions.

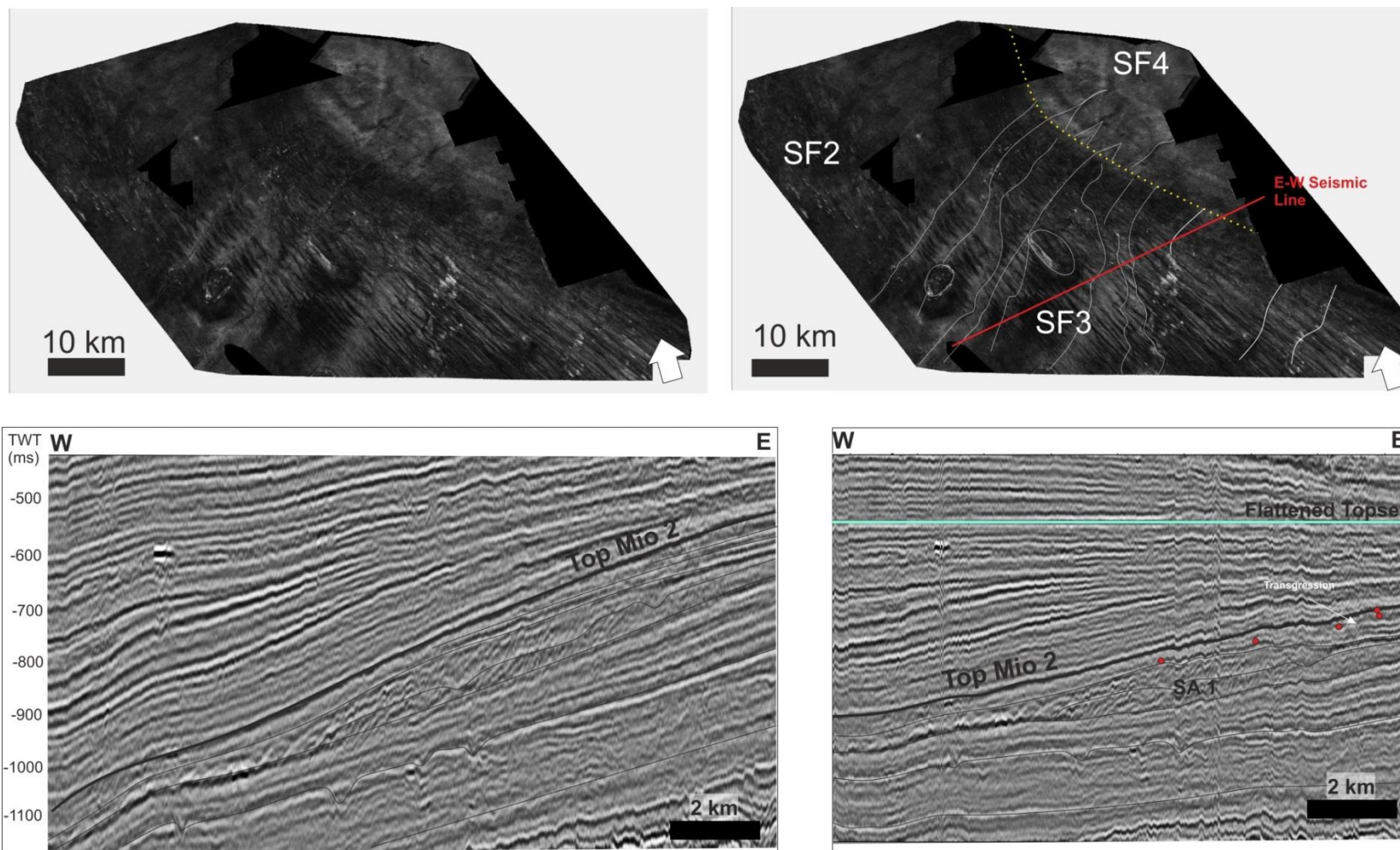


Figure 3.13 Mio 2 example of SA1 Intra Slope Clinoforms. *Top left* un-interpreted RMS Amplitude extraction onto horizon slice. *Top right* Interpreted RMS Amplitude extraction highlighting key features and seismic facies identified. Yellow dotted line represents the proposed shelf edge. Salt diapirs are highlighted. *Bottom left* E-W seismic cross section through SA1 clinoforms. *Bottom right* E-W seismic cross section through SA1 clinoforms, flattened on later surface. Location of seismic cross section is shown in *top right*.

Miocene/Pliocene Unit 3

Seismic and Well Observations

Bounding Surface: The top of *Mio 3* (Fig. 3.12c) is a positive amplitude reflection, (Figs. 3.6 a-c) confined to the NE of the dataset. In the NE the reflection is weak, increasing in strength southwards (Fig. 3.6b). The reflection erosionally truncates the *Mio3* unit in the NE (Fig. 3.10b) and is parallel to underlying reflections elsewhere. In the east of the NL the reflection is just above a clear truncation surface. The *Top Mio 3* downlaps onto the mMU in the NE NL sector. In the DK sector the reflection is a downlap surface for overlying large scale clinoforms (Figs. 3.6b). On the border of the NL and DE sector the *Top Mio 3* is onlapped on the foreset and is a downlap surface on the bottomset, (downlap area marked SA1 in Fig. 3.11c). The reflection is low angle ($<1^\circ$) in the north (Figs. 3.6a&b). Further south, towards the main depocentre the reflection has clinoform geometry with a foreset angle of $\sim 2-3^\circ$ (Figs. 3.6c, 8b, 9c).

The reflection is shallowest in the NE at 470 ms (390 m) deepening SE-wards to 1200 ms (935 m) (Fig. 3.12c). Local elevation variations of up to 200 m are identified in the NE of the NL sector around salt structures. Gamma ray response at the *Top Mio 3* reflection (Fig. 3.7) in wells near the main depocentre show a peak of 90 API separating 50-100 m units of 50 API. The shelf edge at the *Top Mio 3* is arcuate and is present in the DK sector and just enters the NL sector of SNS trending NW-SE (Fig. 3.10b, 3.11c, 3.12c).

Internal Character: *Mio 3* has a maximum thickness within the dataset of 350 ms (310 m) trending NW-SE (Fig. 3.10b, 3.11c). The unit thins to the north (area of the *Mio 1* depocentre), east and westwards and the depocentre is situated south of the previous two units.

The dominant seismic architectures are SA7 *Sigmoidal Clinoforms* and SA1 *Intra Slope Clinoforms*. Large scale SA7 clinoform heights are a maximum of 200 m within the study area and steepen from 0.5 to 2° towards the main depocentre (Fig. 3.11b). In the DE sector, the reflections are characterised by weak wavy- parallel reflections (SF1), sometimes chaotic with isolated strong amplitudes across the clinoform. The amplitude strength increases towards the top of the unit across and evidence of erosional truncation on the topsets increase.

In the area of the main depocentre focused in the DK sector, three packages of *SF3 Multi Source Slope Channels* within *SA7* clinoforms are identified (Fig. 3.11c). The channels are oblique to the shelf edge, trending east-west, each package develops westwards of the previous. The first package of *SF3* appears to emanate from an area of strong amplitudes at the shelf edge. Between the packages of *SF3*, parallel reflections and reflections with *SF2 Current Scours* occur on the lower foreset/bottomset which is correlated with the strongest amplitudes on the topset. *SF4 Topset Facies* is also identified (Fig. 3.11c).

Several packages of stacked *SA1 Intra Slope Clinoforms* are identified SW of the main depocentre in the NL sector, (Figs. 3.6c & 3.10b), the *SA1* clinoforms exhibit up to 3° foreset angle and are not followed by clear *SA3* slope channel erosion like in *Mio 2*, though strong amplitudes are seen at the base of slope so the channels might be below seismic resolution.

The gamma ray logs available have a clear character especially in the area of *Mio 3* maximum thickness. The character is decreasing upwards packages (coarsening upwards) capped by a sharp increase (flooding surface) (Fig. 3.7). The most proximal wells show increases of 50-70 to 110 API, in more distal wells the difference is 100-130 API. The more vertically extensive coarsening upwards packages are linked to the *SA1* clinoforms.

In the top 40 m of *Mio 3*, a very strong positive seismic reflection is identified; 100 km in lateral extent, to the north of the main depocentre (Fig. 3.14 RMS amplitude horizon slice extraction). It occurs on the foreset and bottomset and has an irregular basinwards termination with possible *SF3* in the north. No available borehole information penetrates the strong amplitude therefore it is difficult to ascertain the lithology. The reflection corresponds to an increase in acoustic impedance (hard event) which has the same polarity as gas bearing sands in the NL sector (ten Veen *et al.*, 2013).

Correlation

The *Top Mio 3* correlates to 4.2 Ma from biostratigraphy (wells B17-01, B17-02 and F02-03 Chris King *pers comms*, Appendix A). Therefore the unit is largely Latest Miocene (Messinian) to Mid Pliocene (Late Zanclean). *Mio 3* correlates to late S2 in (Kuhlmann and Wong, 2008), within Composite Sequence IV in Sørensen *et al.* (1997), lower part of Sequence G in (Rasmussen *et al.*, 2005) and SU5/SU6 in the (Thöle *et al.*, 2014). The unit corresponds to the Reuverian to Brunssumian onshore Netherlands Stages (Fig. 3.4).

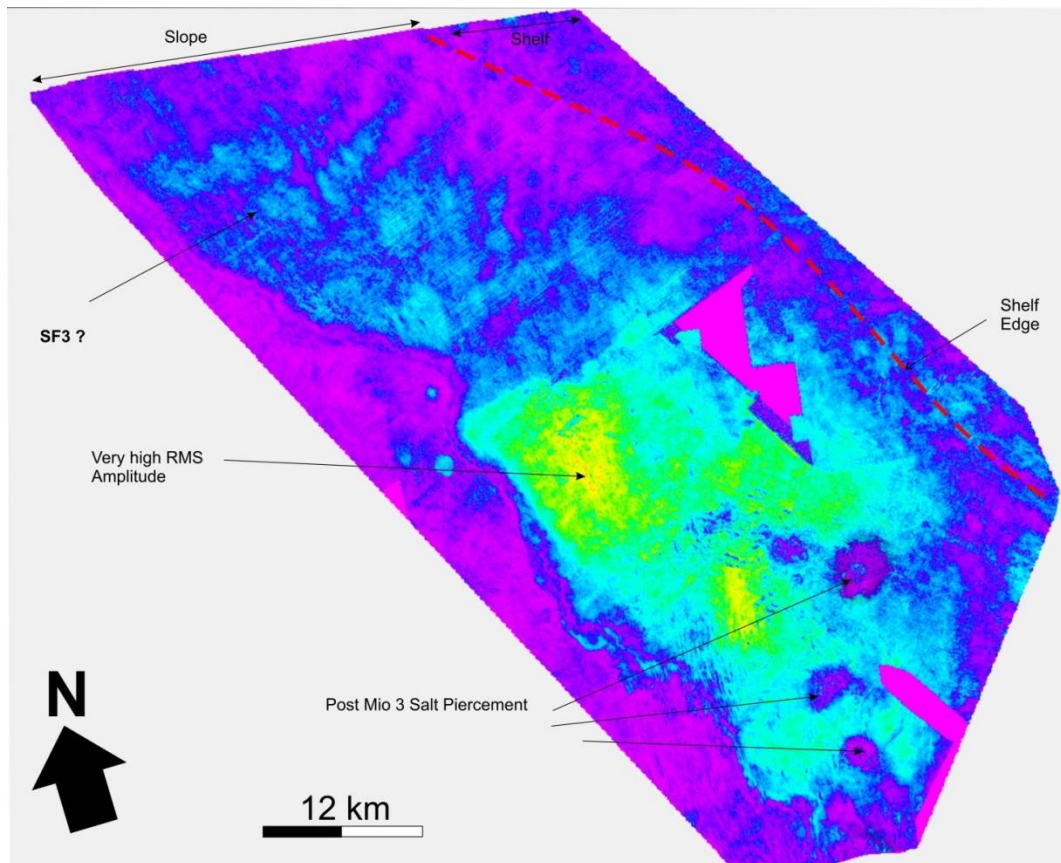
Interpretation

Top Mio 3 basinwards of the shelf edge is a major downlap surface and identified as a MFS. In the very NE of the dataset (DK) the surface is erosive surface and onlapped which are both indicative of a Sequence Boundary (SB). In the east of the NL sector a SB is just below the MFS. This could suggest that in the east the rise in base level that created the MFS did not flood back the shelf entirely. The top of the unit corresponds to a fining upwards and deepening of the basin.

The strike and position of the depocentre plus the orientation of the *SF2* and *SF3* (Fig. 3.11c) suggests sediment input was focused within the DE sector of the dataset south west of previous units. The full depocentre is within the DE sector to the east of the central NL sector, striking NW-SE (Thöle *et al.*, 2014). (Sørensen and Gregersen, 1997) shows that the unit extends into the Norwegian sector. The increase in foreset angle of the large scale clinoforms (Fig. 3.10b) and increased internal clinoforms into the DE sector suggesting closer to the sediment source. The provenance of sediment input is from the E to NE (Fig. 3.11c). Intra Shelf Clinoforms (*SA2*) exist to the east of the dataset in the German sector are shown in cross section Fig. 3 in Thöle *et al.*, (2014).

The increase in stronger amplitudes throughout the unit and the increase in magnitude of the coarsening upwards parasequences in gamma ray suggest the unit is overall regressive and the depositional environment is becoming proximal, however the unit is still dominated by deep marine facies and slope/basinal processes. The dominance of sigmoidal clinoforms suggests accommodation on the shelf during the unit. The westwards progression of the *SF2/SF3* facies suggests progradation is dominant at the time of deposition (Fig. 3.11c). The stacking of the *SA1* clinoforms packages (Fig. 3.6c) with the final *SA1* downlapping onto the previous suggests a more aggradational

character to the unit in the north NL sector (Fig. 3.10b). The depth to mMU (Fig. 3.1) suggests less accommodation in the area where the *Mio 3 SF2/SF3* are identified as the location is on the flank of the Central Trough. The location of the *SA1* is within the Central Trough area. This suggests that the underlying geology and differential subsidence is affecting the shelf trajectory at this time.



Figure

3.14 Top Mio 3 surface. RMS amplitude horizon slice extraction -50 ms from Top Mio 3 surface

The alternation of *SF2 Slope Current Incisions*, which are correlated with strong amplitudes on the topsets and *SF3 Multiple Slope Channels* which are associated with strong amplitudes on the bottomsets suggests that there is a switching between the capture of sediment on the shelf with basinal processes dominant lateral to the shelf edge and then bypass of the shelf with conduits delivering sediment to the basin floor. The *SA1* packages are also associated with coarser material being deposited basinwards of the shelf break and therefore along with *SF3* will be related to the sediment system getting closer to the shelf edge, either through increase in sediment supply or fall in base level

The lack of dating means that this unit cannot be confidently linked to the global sea level curve (Fig. 3.4) however the overall trend of the unit coarsening upwards and therefore likely shallowing upwards correlates to the general global sea level trend of the ~30 m during the *Mio 3* unit.

Pliocene Unit 1 (Plio 1)

Seismic and Well Observations

Bounding Surface: The top of the unit, *Top Plio 1*, in the DK sector is a weak amplitude, continuous, positive reflection (Figs. 3.6a-d; 3.12d). In the NL sector the reflection is medium amplitude, low frequency and continuous which becomes very strong towards the east NL sector. Towards the south of NL sector the surface is discontinuous on the topsets and bottomsets as it is eroded by *Pleisto 1* events. The *Top Plio 1* reflection downlaps onto the mMU in the eastern NL North Sea and has clinoform geometry throughout the basin. Basinwards of the clinoform break point, the reflection is a downlap surface. In the very NE of the dataset the surface is an erosional truncation surface, truncating on the topset and foreset positions of the clinoform (Fig. 3.10c), indicating deep marine erosion of previous clinoforms. Towards the south the surface represents the top of a marine onlap unit (*SA4*, Fig. 3.8) and is parallel to underlying reflections. The *Top Plio 1* clinoform is greater in height and steeper in the south of the dataset than in the north. In the south the maximum *Top Plio 1* clinoform height is 450 ms (400 m) and 4° average foreset angle (Fig. 3.6c). In the north the clinoform height is 200-300 ms (170-250 m) with a foreset angle 2-3° (Figs. 3.6 a&b).

The maximum depth of the *Top Plio 1* reflection is 1168 ms (1120 m) and minimum depth is 325 ms (285 m). The surface shallows eastwards. Salt diapirs in the SE of the NL sector affect the topography of *Top Plio 1* and result in local differences in the structure map (Fig. 3.12d) of up to 100 m. The *Top Plio 1* shelf edge is arcuate and strikes NNW-SSE in the very east of the NL sector.

Top Plio 1 character in gamma ray logs is consistent across most wells in the east of the NL sector as the top of an increasing upwards (fining upwards) package or a sharp increase upwards (typically 30-50 API) in gamma ray or the top of the *Plio 1* unit (Fig. 3.7).

Internal Character: The maximum thickness of *Plio 1* (Figs. 3.10c & 3.11d) is 500 ms (440 m) and forms an arcuate 20 km wide NNW/SSE striking depocentre along the eastern border of the NL North Sea. The unit thins to the north and to the east and the depocentre occurs to the west of the *Mio/Plio 3* depocentre. Local thickness anomalies of ~100 m are identified around active salt diapirs. No longer are the northern salt diapirs (DK sector) appearing to alter the topography of *Plio 1* reflections.

The dominant large scale seismic architectures of *Plio 1* are *SA6 Oblique Clinoforms* & *SA7 Sigmoidal Clinoforms* (Figs.6; 9c). In the north (DK/DE sector), a clinoform rollover is present in the study area only towards the top of the unit (Fig. 3.6a) where 200-250 m aggradational sigmoidal clinoforms (*SA7*) dominate (Fig. 3.11c). The inclination westwards of the *Plio 1* topsets is associated with post depositional tilt. The general seismic character is homogeneous, weak, parallel to discontinuous reflections in the DK/DE sectors apart from in the upper *Plio 1* in the very east of the dataset where more heterogeneous character of occasional strong discontinuous amplitudes are present and erosional topsets (Fig. 3.6a).

Within the northern NL sector *Plio 1* is dominated by *Oblique Tangential SA6* followed by *Sigmoidal Clinoforms SA7* (Fig. 3.6c). Clinoform heights in this area are 250 m increasing to up to 400 m at the top of the unit. The stacking pattern of the large scale clinoforms show a progradation followed by aggradation, an ascending regressive shelf edge character. This is most clearly seen in Fig. 3.6c, *Seismic Line 3* which intersects the *Plio 1* depocentre (Figs. 3.10c & 3.11d) but is also apparent in *Seismic Line 2* north of the main depocentre (Fig. 3.6b). The thickness of the aggradational topsets (associated with *SA7*) of the upper part of *Plio 1* decreases northwards and southwards from the main depocentre. Towards the depocentre in the NL sector strong amplitude continuous reflections become more prevalent along with increased topset preservation (Fig. 3.6c), especially the case towards in the top 100 m of the unit. The clinoform foreset angle steepens from 2° to 3-4° towards the depocentre. The highest foreset angles are associated with the oblique (*SA6*) clinoforms.

In the NL North Sea the internal character of the depocentre varies from the north to the south. In the northern area of the depocentre (Fig. 3.6c) the oblique tangential large scale clinoforms comprised of *SA1 Intra Slope Clinoforms* downlapping on the foresets of

SA6 and later in the unit *SA3 Shelf Edge Clinoforms* at the shelf break and upper foreset. Each package of *SA1/SA3* has prograded progressively basinwards. *SA2 Intra Shelf Clinoforms* downlap onto *SA7* topsets in the top 150 m of *Plio 1*. An example of *SA2* from *Plio 1* is shown in Fig. 3.15. The subunits of the small scale clinoforms can be traced only locally and are not as laterally extensive as the large scale clinoforms (Fig. 3.6).

SF3 and *SF4* seismic facies are present across the depocentre from the DE sector to the southern NL, basinwards and landwards of the shelf break respectively. Nine events are identified with differing geometries. Some are straight gullies with no evidence for strong amplitudes at the base; others are more sinuous with strong amplitude lobes at the base of the foreset. In the north the *SF3* can be linked to *SA2* clinoforms updip (Fig. 3.15a) which are part of larger scale *SA7 Sigmoidal Clinoforms*. There is evidence of differential thickness towards salt diapirs and pooling of strong amplitudes within salt withdrawal related lows surrounding the salt diapirs (Fig. 3.15a).

In the southern NL sector, aggradational *SA7* is followed by dominantly progradational *SA6*, (with single sigmoidal clinoforms separating packages of *SA6*). An onlap surface separates this A-P stacking pattern from a largely flat trajectory progradation package of *SA6* which is followed by a package of aggradational *SA4 Marine Onlap* (Fig. 3.8). The large scale clinoform heights decrease in height from 300-400 m in this area in early *Plio 1* to 200 m, returning to the higher values towards the very end of the unit. . There is no clear delta scale (*SA2*) clinoforms feeding the *SF3* channels in the south.

Reflections become chaotic and discontinuous in the area of the Mass Transport Complexes (MTC's, *SF5* Fig. 3.9). Clinoform heights downlapping on top of the *SF5* MTCs are <100 m. The degree of post depositional tilting of topsets is minimal compared to the northern NL sector and the DK sector.

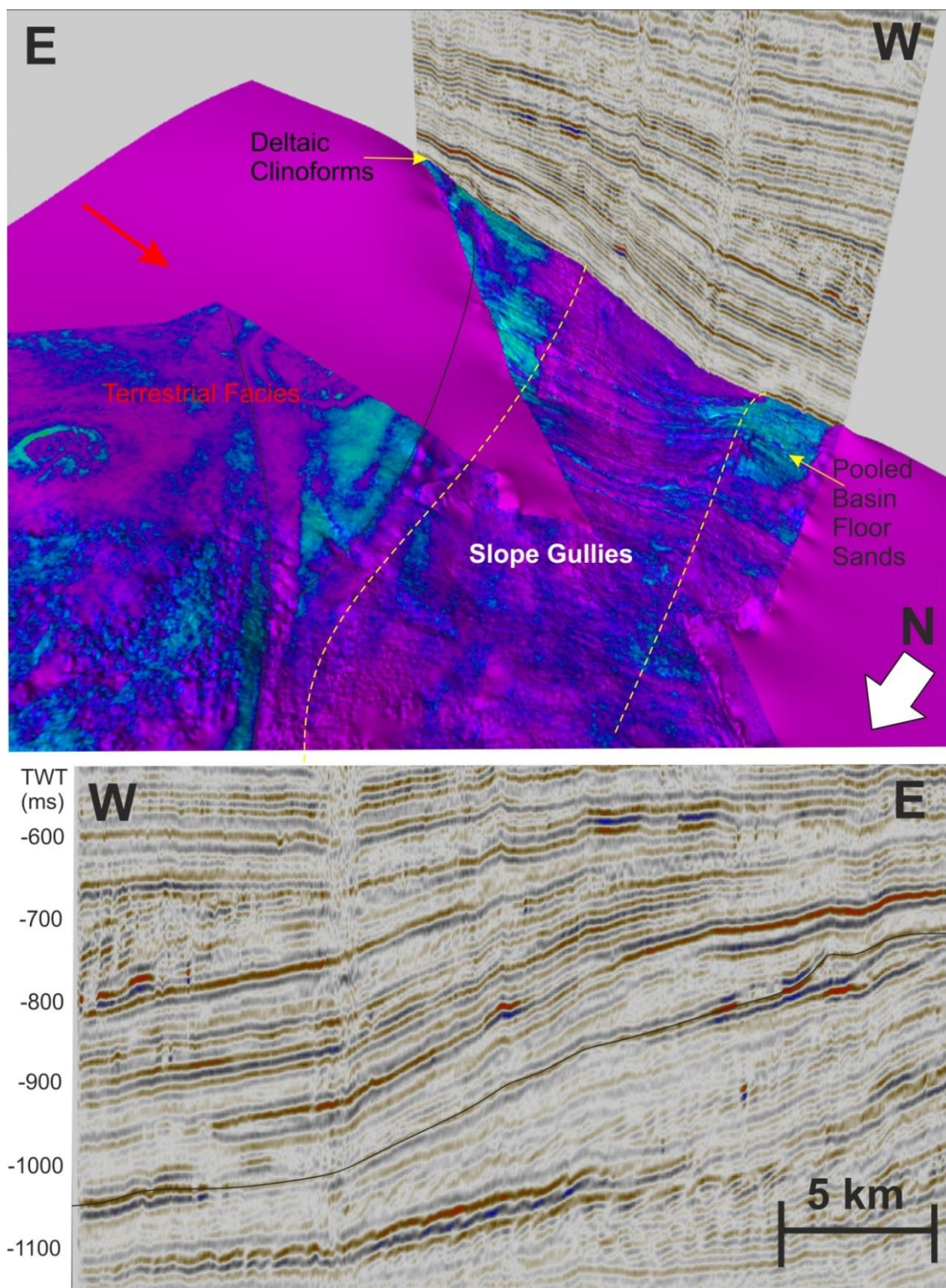


Fig. 3.15 Plio 1 SF2 Intra Shelf Clinoform example

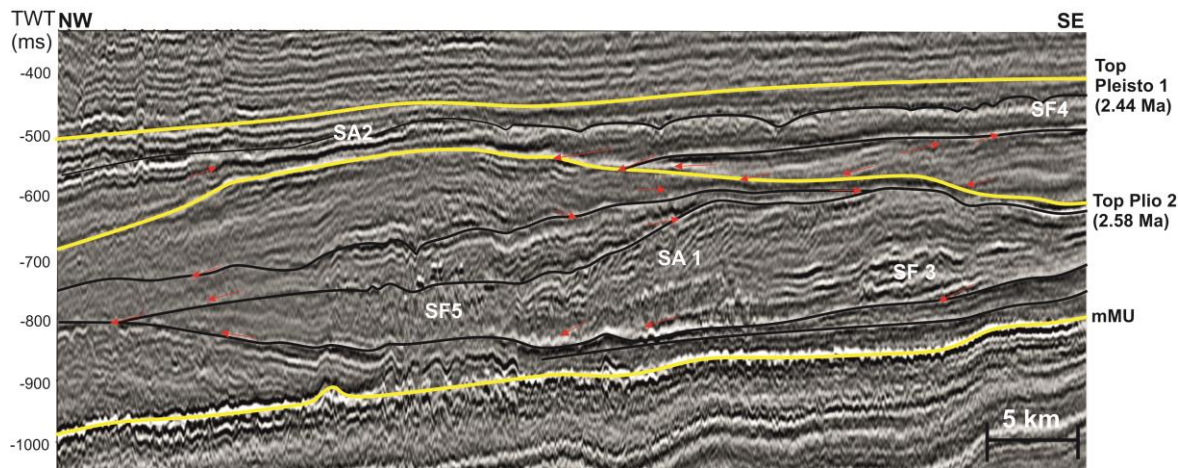


Figure 3.16 Cross section through lobate geometry of *Plio1*. Location in the south of the Netherlands North Sea.

In 3D view, this unit displays a series of arcuate, lobate geometry shelf breaks across the depocentre which are individually up to 80 km maximum in length (Figs. 3.10c, 3.11d). The lobate shelf breaks are variable in strike, most prominently in the south where two dominant directions occur striking NW-SE, with smaller arcuate shelf edges (<40 km extent) striking almost N-S. A seismic cross section through this area (Fig. 3.16) shows a series of at least four stacked lobes with various internal geometries (small scale clinoforms *SA1*; terminal slope fans *SF3*; MTC's *SF5*) indicating varying progradation directions and clinoforms heights, separated by strong amplitude downlap surfaces. The two main lobes imaged have strong amplitudes at the base associated with *SF3* in 3D view with *SA1* and *SF4* towards the top of the unit, capped by a strong amplitude continuous reflection. This lobate character appears within the tallest and steepest clinoforms of *Plio 1* and is not seen elsewhere in this dataset.

The gamma ray log signature of *Plio 1* shows a coarsening upwards (decreasing upwards) motif is and part of an overall coarsening upwards phase which ends at the top of the unit (Fig. 3.7). *Plio 1* comprises 30-50 m units of coarsening upwards package separated either by a fining upwards package or a sharp increase in gamma ray. The *SA1* and *SA3* clinoforms are represented by a gradually coarsening upwards package with a sharp increase at the top. The *SA2* have a sharp base and sharp top, with low gamma values (~50 API). Lithological descriptions from B14-03 suggest medium/coarse sandstone with evidence of peat and brown coal.

Correlation

The *Top Plio 1* reflection corresponds to base Quaternary at 2.58 Ma from correlation with (Kuhlmann et al., 2006a) in the A15 wells which corresponds to Gauss-Matuyama magnetic polarity reversal. The age and correlation base Quaternary in the Central and Southern North Sea is discussed further in Chapter 6.2. The *Top Plio 1* corresponds to MIS stage 103 (Fig. 3.4). This unit therefore is ~4.2 Ma- 2.58 Ma representing 1.62 Ma of the Zanclean and Piacenzian.

The *Top Plio 1* correlates to Top S4 and the seismic units S3 & S4 in (Kuhlmann and Wong, 2008); composite sequence V in (Sørensen and Gregersen, 1997) and within SU7 of (Thöle et al., 2014).

Interpretation

Top Plio 1 is identified as an MFS across the majority of the dataset. It is the top of a transgressive unit which manifests itself in different ways across the basin. In the south of the basin as Marine Onlap (*SA4*) and increase in the thickness in topsets towards the top of the unit and as backstepping of *SA2 Intra Shelf Clinoforms* in the north of the basin. The surface is a sequence boundary in the very NE of the DK sector and the east of the south NL sector, the former exhibiting marine erosion basinwards of the shelf edge. The clinoform height difference in the north and the south suggest the basin was deeper in central/south NL sector than it is in the north NL and DK sectors at the Base Quaternary. Backstripping the base Quaternary shows the average water depth across the dataset is 300 m with original clinoform heights of 200-250 m in the central North Sea and 250-300 m in the southern North Sea (Chapter 6.2). The steepest clinoforms of the whole study are found in the central/south NL at the beginning and are likely because a sediment depositional system building out into very deep water ~300 m. The character of the clinoforms is accommodation driven.

The dominant sediment input directions (Fig. 3.11d) are ENE-WSW in the north and NE-SW further south. Clinoform progradation directions and the orientation of *SF5 Mass Transport Complex* with *SF3* channelling into them suggest a SE-NW sediment input also. The shelf edge shape is consistently arcuate/lobate throughout the unit and the coastline is identified at the shelf edge (via mapping of *SA2* and *SF4* Terrestrial Topsets)

several times throughout the unit. (Sørensen and Gregersen, 1997) shows that the *Plio 1* depocentre imaged in this study extends into the Norwegian sector trending NW-SE.

The depositional environments encountered cover a full range from open marine (basinwards of the shelf edge) to terrestrial and shallow marine on the shelf. The lobate character suggests that though the individual river system/delta are not imaged that there was at least one river system depositing on the shelf during this time and that the shelf edge was built out by the river system switching lobes in order to create the elongate depocentre and the lobate shelf edge. Depositional systems are dominant over basinal processes during *Plio 1* and this is highlighted by the lack of *SF2 current scours* identified.

The shelf edge trajectory is dominated by a progradational followed by aggradational stacking pattern with an increase in accommodation on the topsets throughout the unit. However, sediment bypass to the basin floor via *SF3* occurs throughout the unit regardless of the type of large scale clinoform (*SA6* or *SA7*). An increase in base level towards the top of the Piacenzian, most notably in the north/central east NL and DE sectors is interpreted. This is also coupled with a supply driven depositional system which can reach the outer shelf and shelf edge even when the base level is rising. Global sea level is generally higher in the late Piacenzian (Fig.3.1) with a 50 m increase at the Top *Plio 1* than in the early Piacenzian and there is evidence for a regional transgression towards the top of the unit which suggests an allocyclic control.

Pooling of basin floor fans associated with *SF3* within the salt withdrawal basins (Fig. 3.15a) and the thinning of sediments towards salt diapirs during *Plio 1* is suggestive of salt being present at the sea floor affecting topography, locally creating accommodation for these to accumulate in.

Pleistocene Unit 1 (Pleisto 1)

Seismic and Well Observations

Bounding Surfaces: The top of the unit, (*Top Pleisto 1*, Fig. 3.12e), is a negative amplitude continuous reflection, basinwards of the clinoform rollover. The reflection is present in the DK/DE sector and across the east and south of the NL North Sea and

downlaps onto the mMU. The reflection has the strongest amplitude in the central part of the NL sector (Fig. 3.6c). In the central/southern NL *Top Pleisto 1* reflection is discontinuous on the topsets (Figs. 3.6c&d). On the foreset and bottomset the reflection is parallel to underlying reflections.

In the central NL sector the reflection is downlapped by overlying *SA1* reflections (Fig. 3.6c). In the southern NL sector the *Top Pleisto 1* reflection is overlapped by overlying *Pleisto 2* reflections. The reflection has *SA7* sigmoidal clinoform geometry across the basin with an average foreset height of (350 m) in the DK sector (2-3° foreset angle), 150 ms (200 m) in the northern NL sector and in the south 170 ms-230 ms (150 m-200 m) 1-2° foreset angle.

The maximum depth of the *Top Pleisto 1* (Fig. 3.12e) is 1100 ms (1040 m) in the NE, the area of the Central Trough (Fig. 3.1). In the area of the BFB (Fig. 3.1) the reflection is at 740 ms (670 m). The reflection is shallowest to the east and SE at 300 ms (265 m). The shape of the shelf edge is concave (Fig. 3.10e) which indicates a change from earlier arcuate convex, lobate shelf edges (Figs. 3.10a-d). In the north of the dataset the shelf is trending NW-SE, and in the south it is trending from the NE-SW. Salt diapirs create local anomalies in the TWT structure map (locally 100-150 ms above regional datum).

The gamma ray character of *Top Pleisto 1* corresponds largely to high gamma ray values >70 API, before a sharp decrease in gamma ray upwards. Lithological description from A15-03 core shows the *Top Pleisto 1* reflection correlates to a mudstone layer.

Internal Character: The *Pleisto 1* thickness map (Figs. 3.10d & 3.11e) shows a wide area (80 km) of maximum thickness (~400 m) trending NNW-SSE across the southern NL sector, becoming narrower towards the north. The unit thins NE and westwards. A secondary depocentre in DK sector, trends NW-SE and has a maximum thickness 300 m and extends north of the dataset.

In 3D, the shelf edge during *Pleisto 1* has arcuate geometry in the DK depocentre and in southern NL sector the geometry changes from arcuate to a linear/concave shelf edge towards the top of the unit (Figs. 3.11e). The reflection geometry of this unit is highly variable across the study area.

In the DK sector, representing the northern depocentre the clinoform break point progrades up to 40 km westwards during *Pleisto 1* (Fig. 3.6a Figs. 3.10d & 3.11e). The DK *Pleisto 1* shows an overall aggradational to progradational stacking pattern with an increase in foreset angle up the unit. Three packages can be distinguished.

The first package is aggradational, sigmoidal SA7 large scale clinoforms with internal strong amplitudes. The second package downsteps from the first, and consists of flat trajectory weak amplitude SA6 Oblique Tangential about half the height of the previous package followed by SA7 sigmoidal clinoforms and capped by a strong amplitude sigmoidal reflection. The package has a progradation-retrogradation stacking pattern. The third package is identical to the second but with an increased foreset dip. In 3D the SA7 clinoform breaks in 3D are arcuate whilst SA6 are linear, SF4 *Terrestrial Topsets* are identified >70 km landward of the large scale clinoform break and SF6 *Iceberg Scours* are also identified.

In the north-central NL sector (Figs. 3.6b&c), representative of the area between the two depocentres of *Pleisto 1*, and represented by the A15 wells, (Figs. 3.10d & 3.11e) many of the subunits of the DK sector are not present, and the unit has less internal character. The unit comprises SA7 *Sigmoidal* clinoforms and the shelf edge progrades less than 10 km westwards during *Pleisto 1*. Thickening of *Pleisto 1* reflections occur to the east in the NL/DK sector with SF4 and SF6 again identified.

The southern NL sector seismic line shows an expanded section of *Pleisto 1* (Figs 3.6d). The unit in the south of the dataset is highly progradational. The increased progradation can be visualised in 3D by the distance of progradation of the shelf edge from east to west during the unit (Fig. 8d & 9e) which is a maximum of 80 km in the very south of the NL sector. The early part of the unit is dominated by with strong amplitude relatively high angle (4°) reflections of oblique tangential SA6 with SF4 *Terrestrial Topsets* are identified in 3D. Chaotic and heterogeneous packages are identified which thickens basinwards which in 3D is identified as SF5 *Mass Transport Complexes* (Fig. 3.7). Strong bottomsets correspond in 3D SF3 *Multi Source Slope Channels*.

Sigmoidal clinoforms (SA7) are more dominant in the second half of the unit. Two very strong amplitude reflections are identified within this part of the unit, similar to the

Pleisto 1 reflection. In between these reflections in the north of the dataset there is little seismic character. Further south however, in between the reflection, internal character (largely *SA1* and *SF3*) are identified (Fig. 4d). *SF6 Iceberg Scours* are identified in the upper half of the aggradational unit only associated with the strong amplitude reflections.

Correlation

The *Top Pleisto 1* reflection corresponds with the X-event, a brief magnetic reversal in the A15 wells (Gesa Kuhlmann et al., 2006a) which is given an age of 2.43 Ma. The base of the unit is the base Quaternary (*Top Plio 1*) at 2.58 Ma therefore *Pleisto 1* unit is deposited within 150,000 years. The *Pleisto 1* unit has a distinct character which has enabled clear, regionally correlatable claystone layers to be linked via seismic to gamma ray correlation specifically to MIS glacial stages 100, 98 and 96 (Fig. 15). The MIS are identified in core via geochemical and palynological analysis within the NL A15-03 – A15-4 wells (Kuhlmann et al. 2006); ten Veen et al. 2013; Donders et al. in prep) and the Noordwijk borehole onshore NL sector (Noorbergen et al., 2015). Via this seismic and well correlation across to the southern part of the SNS basin, this has given us two more dates for the top of stage 100 ~2.51 Ma and the top MIS 98 at ~2.48 Ma. The MIS are annotated in Figs. 3.4 & 3.7 where possible. *Top Pleisto 1* corresponds to MIS 96. This also allows high resolution linking of the stratigraphy within the basin to eustacy, regional climate and local sea level.

Top Pleisto 1 corresponds to the Top S5 horizon and the S5 unit in (Kuhlmann and Wong, 2008) and Composite Sequences VI & VII in (Sørensen and Gregersen, 1997). The unit corresponds to the Pretiglian Netherlands Quaternary phase and the Pre-Ludhamian British Stage associated with the Red Crag deposits of Norfolk.

Interpretation

Pleisto 1 unit represents a large change in the character of sediment deposition in the basin. It is clear that between the base Quaternary, *Top Plio 1*, and the seismic reflection which represents MIS 100 there is an order of magnitude increase in sedimentation. The sub unit covers one-and-a-half glacial- interglacial cycles (Fig. 3.4) and comprises dominantly oblique clinoforms which prograde westwards in the southern Netherlands

North Sea by >67 km during this sub unit, a rate of regression of over a kilometre per 1000 years. Progradation rates decrease to <20 km per glacial-interglacial cycle for the rest of the unit. The amount of sediment delivery basinwards of the shelf edge, in its various forms (SF3 Multi Source Slope Channel, SF5 Mass Transport Complexes and SA1 Intra Slope Clinoforms) is very high during the entire unit in the southern depocentre, suggesting there was a sediment delivery system at or near the shelf edge during this time. The *Pleisto 1* thickness maps indicates for the first time that there is clearly more than one depocentre present in the basin and therefore likely more than one feeder system, one emanating from the NE and another from the SE.

Top Plesito 1 likely represents the glacial termination of MIS 96, in some places is indistinguishable from a downlap surface which represents the maximum flooding surface. It is a regionally continuous reflection basinwards of the shelf edge and therefore represents a regional event.

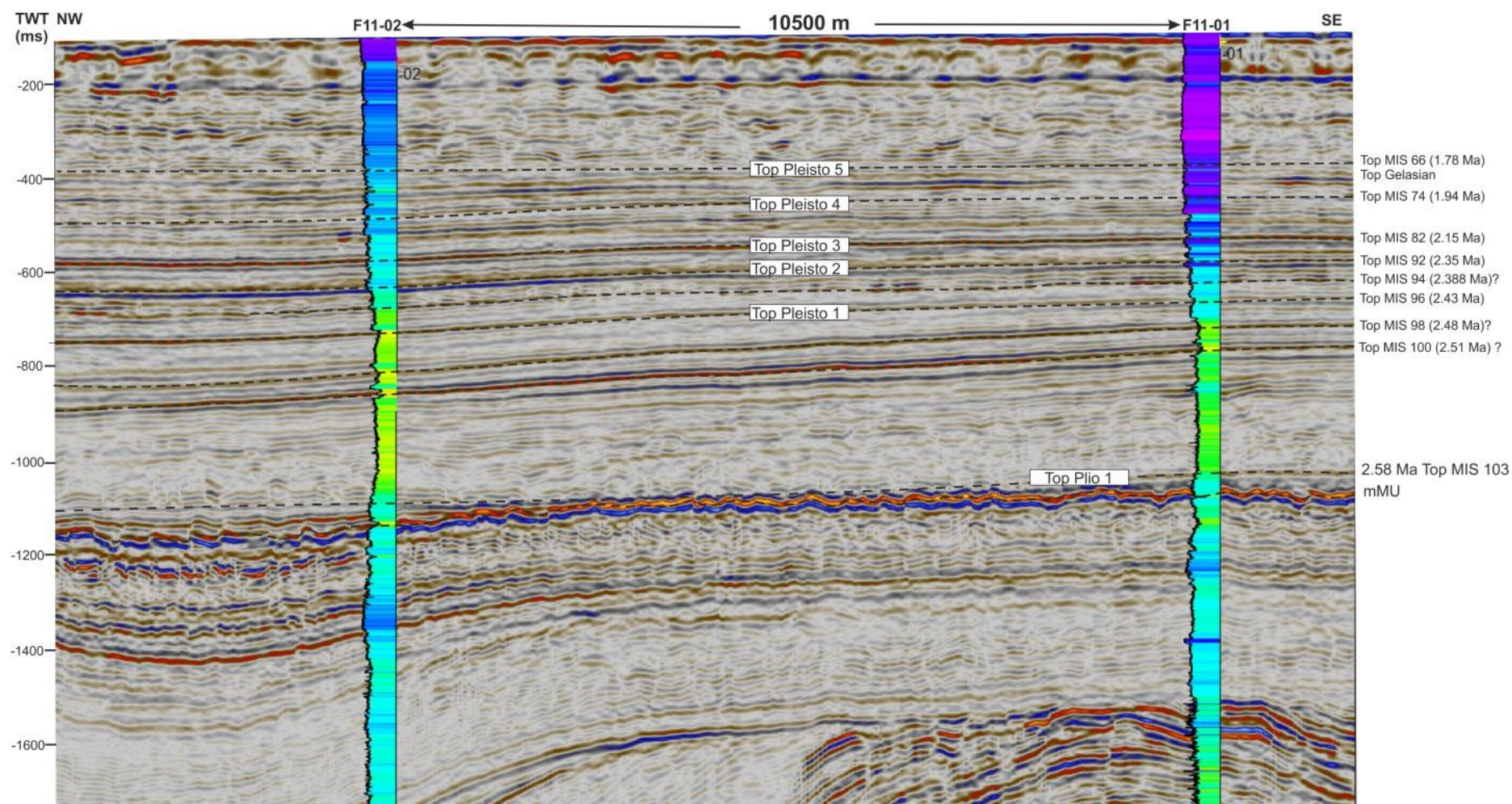


Figure 3.17 Gamma ray logs for Wells F11-02 and F11-01 and the correlation to a NW-SE seismic cross section from the SNS MegaSurvey. Gamma ray logs are colour filled; darker colours represent lower gamma ray values whilst lighter colours represent higher gamma values, with yellow being the highest.

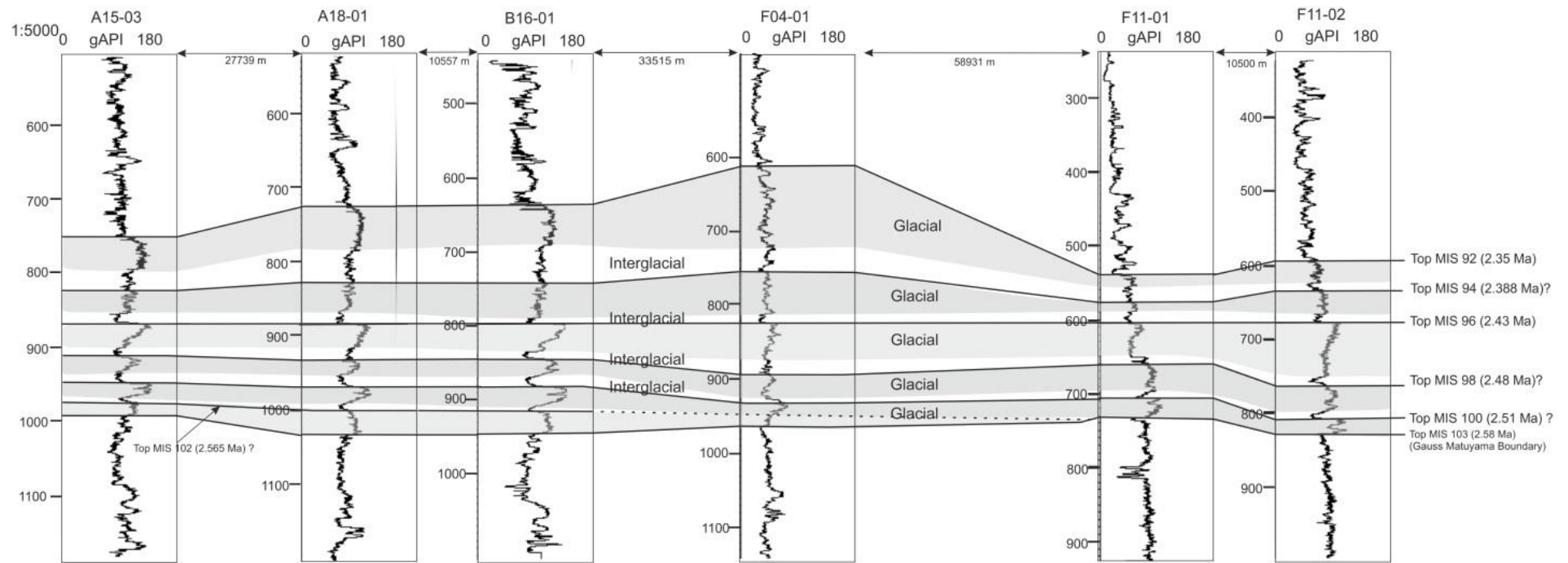
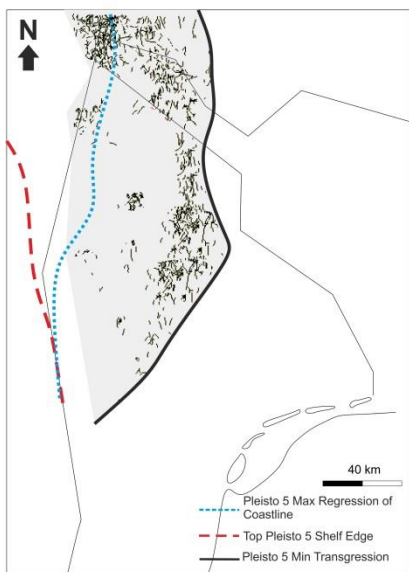
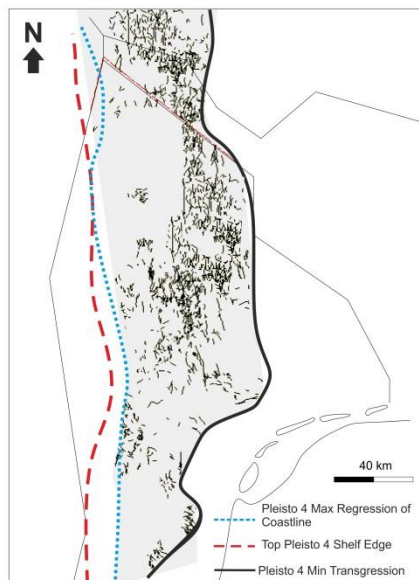
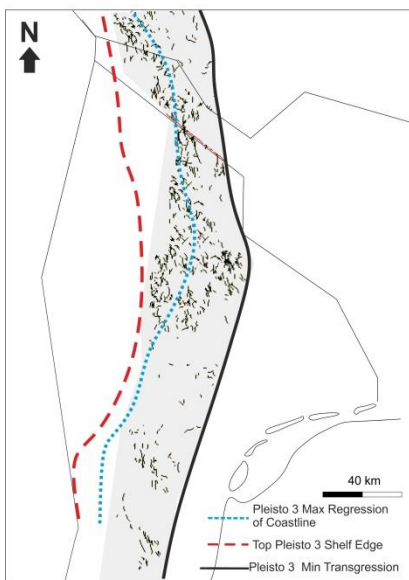
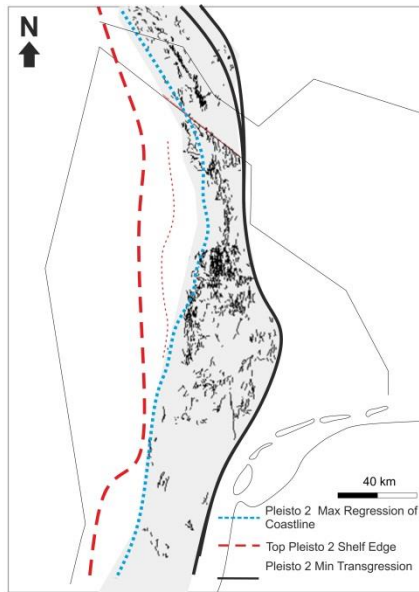
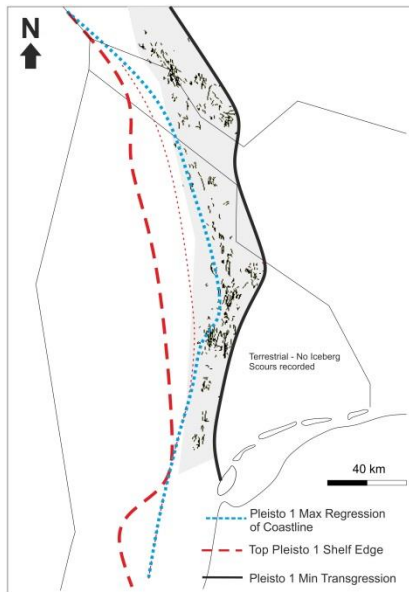


Figure 3.18 Well correlation along strike basinwards of the shelf edge. Linking A15-03 and SNS MegaSurvey area. Locations of the wells are shown in Fig. 2.7.

Figure 3.19 Iceberg scours (following page). Black lines represent iceberg scours mapped within unit. Scours mapped using a combination of traditional seismic interpretation and auto interpretation of horizons using Paleoscan software. The iceberg scours have been used to create the minimum transgressions in Fig. 3.10-3.12.



Pleistocene Unit 2 (Pleisto 2)

Seismic and Well Observations

Bounding Surfaces: *Top Pleisto 2* (Fig. 3.12f) is a regionally correlatable, continuous, strong positive amplitude reflection basinwards of the shelf break. The reflection is weaker, discontinuous and more heterogeneous on the topset. The reflection is strongest in amplitude in the NL sector, weaker in the DK sector and is not present in the very NE of the dataset (Fig. 3.6a). The reflection has sigmoidal clinoform geometry across the dataset (Figs. 3.6a-d). The reflection is concordant with underlying reflections on the foreset and bottomset but in the east and the south, landward of the shelf break, the underlying reflections have truncation relationship with *Top Pleisto 2*. In the DE sector *Top Pleisto 2* is eroded by younger terrestrial channel systems. Overlying reflections downlap onto *Top Pleisto 2*, basinwards of the shelf break.

The *Top Pleisto 2* clinoform is greatest in height in the north NL sector (Fig. 3.6c), (300-350 m) and foreset angle 1°. Towards the DK sector and in the southern NL sector the height decreases to 150-200 m and an average 2° foreset angle. The maximum depth of the *Top Pleisto 2* reflection is 1000 ms (930 ms) and the minimum is 300 ms (260 m) (Fig. 3.12f). The surface shallows to the east and in the south of the NL sector. The shelf edge is almost N-S trending except in the south where the shelf edge trends NE-SW. Salt structures displace this reflection up to 300 m in the largest salt structures in the SW of the unit.

Top Pleisto 2 gamma ray character across the basin is marked by a sharp decrease upwards of 20-60 API at top of an increasing upwards package. This is most pronounced in the A15- A18 wells (Fig. 3.7) which is representative of a basinal depositional environment.

Internal Character: *Pleisto 2* thickness map (Figs. 3.10e & 3.11f) shows the depocentre strikes N-S across the entire NL Sector. The unit is thickest in the south in the area of the Broad Fourteens Basin (BFB) at 400 ms (350 m). In the north of the NL sector the maximum thickness is 190 ms (165 m). The unit thins to the east and west. Anomalies in the central NL sector part of *Pleisto 2* thickness map are due to the differential accommodation creation and destruction by active salt diapirs.

The dominant seismic architecture in the DK /DE and the northern part of the NL sector is *SA7 Sigmoidal Clinoforms*. The unit in this location (Figs. 3.6a&b) is thin (~100 m thick) and progradation dominated (Figs. 3.10e & 3.11f). The unit thins towards the east. Clinoform heights and foreset angles are homogeneous at ~150-200 m with angle 1-2°. The seismic character in this area is largely of weak amplitude, in some places discontinuous reflections. On the topsets 30-50 km eastwards of the shelf break isolated strong amplitudes occurs. Isolated very strong amplitude, low frequency reflections early in the unit are identified on the bottomsets in the northern NL sector is associated in plan form with SF2 lower slope current scours in Fig. 9f.

The character of the unit is similar throughout the most of the northern and central NL, though becoming more expanded to the south with several elements varying. The general trend shows a *Pleisto 2.1* sigmoidal subunit (SA7) which are up to 200-300 m in the central NL sector with topsets that have been eroded to some extent, which thins to the east (landwards). This subunit is aggradation dominated and topped with a strong amplitude continuous reflection. *Pleisto 2.2* sub unit is only present in the area of the main depocentre and has stronger amplitude reflections and though is still SA7, it is more progradational. *Pleisto 2.3* is present across the majority of the NL sector and is a unit of oblique clinoforms (SA6) 100-150 m which downlaps onto the top of the previous subunit. The geometric relationship between *Pleisto 2.1/2.2* and *Pleisto 2.3* subunits changes towards the south. In the north NL the second unit is less extensive than the first, downlapping and onlapping onto subunit 1 reflections (See Fig. 3.6c), almost embedded on top of subunit 1, further south the unit downlaps onto the mMU and rather than onto the previous units bottomsets, but still onlaps onto the subunit 1 reflections, downstepping. The top of the unit corresponds to a sigmoidal clinoform and evidence of thickening landwards.

Packages of *SA1 Intra Slope Clinoforms* are present at the base of the first two subunits downlapping onto the strong amplitude continuous reflections, the first package downlapping onto the *Top Pleisto 1* (Fig. 3.10e). The internal character of *Pleisto 2.3* has internal small scale downstepping (30-50 m). The seismic character of *Pleisto 2* in the NL sector broadly increases in amplitude strength, and the second subunit with SA7 has stronger amplitudes, though a return to weaker amplitudes is associated with the *SA4/SA7* clinoforms at the top of *Pleisto 2*. Strong amplitudes at or near the shelf edge

are associated with sub unit 2. Both SF3 Multiple Line Source slope channel and SF7 Single Source basin floor fans are identified in this unit, associated with downstepping clinoforms.

Correlation

Top Pleisto 2 is dated to 2.35 Ma via seismic to gamma ray correlation with MIS 92 glacial stage in A15-03 well which has been determined by geochemical and palynology analysis (ten Veen et al., 2013 and Donders et al., in prep) (Fig. 2). The strong amplitude continuous reflection which separates sub units of Pleisto 2 could tentatively be associated with MIS 94. The base of the unit is dated at 2.44 Ma and therefore the duration of the unit is 90,000 years. *Pleisto 2* unit corresponds to S6 in (Kuhlmann and Wong, 2008) with *Top Pleisto 2* corresponding to Top S6. In (Sørensen and Gregersen, 1997) it corresponds to the early part of Composite Sequence VIII. Onshore Netherlands Stages Tiglian A and B are within *Pleisto 2* seismic unit (Fig. 3.4).

Interpretation

Pleisto 2 unit represents a change in depositional style from *Pleisto 1*. As shown in Figs. 3.10 & 11, the unit thickness maps show a change in character to a linear N-S depocentre which appears to be an amalgamation of three separate depocentres. The geometric relationship between the *Pleisto 2* sub units also suggests a series of separate depocentres interfingering and alternating in terms of which are most active. In the north of the dataset the condensed nature of this unit could be related to the restriction of the most northern depocentre by glacial conditions. There is evidence of a sediment source on the shelf in the Danish sector of the study area, identified from strong amplitudes and channel features, however this is up to 70 km away from the *Pleisto 2* shelf edge, therefore little sediment is available at the shelf break to build out the shelf prism. This suggests that there was not just one sediment source feeding into the basin at the time but more likely a series of river systems feeding the basin in a line source manner. Topsets are little preserved, especially in the north of the dataset suggesting less accommodation on the shelf during this period. Clinoform heights decrease from 200 m to <100 m by the end of the unit in the SNS MegaSurvey area, which suggests the decrease in accommodation in the SNS basin and infill by the previous units.

Top Pleisto 2 is interpreted as being a significant regional downlap surface basinwards of the shelf edge. Many *SA1 Intra Slope Clinoform* packages of *Pleisto 3* downlap onto the *Top Pleisto 2* across the study area indicating a regionally important change in deposition type and is interpreted as a maximum flooding surface. Landwards of the shelf edge, especially in the south of the dataset the reflection is indistinguishable from a major erosional surface which represents a sequence boundary.

Pleistocene Unit 3 (Pleisto 3)

Seismic and Well Observations

Bounding Surfaces: *Top Pleisto 3*, (Figs. 3.6 & 3.12g), is a positive medium to strong amplitude, low frequency reflection that is continuous across the underlying clinoforms. The reflection is a downlap surface, basinwards of the *Top Pleisto 3* shelf edge in the north and in the south east it is a downlap surface also landwards of the shelf edge as *Pleisto 4* reflections downlap on the topsets of *Top Pleisto 3*. The surface is a truncation surface to the west and south (Fig. 3.10f). It's a clear onlap surface towards the north (Fig. 3.6a). The reflection has clinoform geometry (~200 m in the DK/north NL to 100 m in the south NL sector) and is tilted in the south west to the east by post depositional deformation as are the following units, this mostly affects the bottomset. The reflection downlaps onto the mMU on the border of UK/NL sectors. The reflection foreset angle is greatest in the DK sector at 2-3 ° whilst everywhere else it is ~1°. The *Top Pleisto 3* surface (Fig. 3.12g) is shallowest to the south and west, at 346 ms (305 m) and deepest just NW of the border between UK and NL at 968 ms (900 m). On the topset the gamma ray response of the *Top Pleisto 3* is a sharp decrease upwards of gamma ray at the top of a decreasing upwards (fining upwards) package.

Internal Geometry: *Pleisto 3* thickness map depocentre trends almost N-S (~200 m thickness) to the west of the *Pleisto 2* depocentre (Figs. 3.10f, 3.11g). The maximum thickness (350 ms, 310 m), which is slightly offset from the rest of the main depocentre, occurs in the very south of the NL sector, to the west of present day onshore NL. Local thickness variation is due to large salt structures and active faults (Indefatigable Fault Zone, Fig. 3.10f & 3.11g). The dominant seismic architectures in *Pleisto 3* are *SA6 Oblique Tangential* and *SA7 Sigmoidal* clinoforms. Small scale clinoforms *SA1* are

observed in the central NL sector. Overall the unit has thin topset preservation (0-50 m). In the DK/north NL sector post depositional tilting (2°) of the topsets is identified towards the west (Fig. 3.6a&b).

In the DK sector the unit is thin, with less than 5 km of progradation of the shelf edge during the unit and sigmoidal *SA7* in character (Fig. 3.6a). In the north NL sector the unit commences with $\sim 3^\circ$ *SA1 Intra Slope Clinoforms* downlapping onto the *Top Pleisto 2* foreset. The remaining unit is aggradational (*SA7*) $\sim 1^\circ$ in character. The distance of progradation of the shelf edge in comparison to the DK sector is much greater at ~ 30 km. The seismic character of the reflections is low frequency, largely weak amplitude continuous, apart from where *SA1* which are associated with stronger discontinuous reflections (Figs. 3.6a-c). Stronger isolated amplitudes on the topsets are offset from the shelf edge by several 10's km and 3D appears as clear channel geometries on the topset (SF4). The erosional channels cut down into *Pleisto 2* unit but are thought to be of *Pleisto 3* age. In the top 30 ms of the unit in the north NL the indentations in the reflections are associated in plan form with SF6 Iceberg Scours which are only imaged at the top of this unit. Overall in the south (Fig. 4d) the unit is overall stronger in amplitudes, especially on the foresets and near the shelf edge and the dominant seismic architecture is flat lying oblique tangential clinoforms

The seismic facies identified in the south of the dataset include SF2 Lower Slope Current incisions and SF3 Slope Channels, associated where the oblique clinoforms (Fig. 3.10f & 3.11g). *SA1 Intra Slope Clinoforms* are not identified in the south but are found in the north where the sigmoidal clinoforms are dominant. SF4, terrestrial facies dominant over a large area in this seismic unit and this is reflected in the position of the maximum regression (Fig. 3.10f & 3.11g).

Correlation

Top Pleisto 3 is tentatively dated to around 2.13-2.15 Ma from seismic correlation to the Reunion magnetic reversal (Kuhlmann and Wong, 2008). As the base of the unit (*Top Pleisto 2*) is dated at 2.35 Ma the duration of the unit is around 200,000 years. This unit corresponds to the later part of Composite Sequence VIII (Sørensen and Gregersen, 1997) and units S7 and S8 of (Kuhlmann and Wong, 2008).

Interpretation

Pleisto 3 is a seismic unit which appears to have been deposited under limited accommodation conditions on the shelf. *Top Pleisto 3* is a SB in the very north. At the base of the unit Intra Slope Clinoforms downlap on the *Top Pleisto 2* across the entire depocentre, suggesting a period a major regional base level fall and sediment partitioning basinwards of the shelf break.

The *Top Pleisto 3* was picked as a significant surface as in the north of the dataset it is a downlap surface for small scale clinoforms across the basin and in the south of the dataset it is an unconformity where shelf margin clinoforms prograde on top of the earlier set of large scale clinoforms. (Sørensen and Gregersen, 1997) indicates a secondary depocentre just in the north of the dataset, likely the same source as the secondary depocentre seen during *Pleisto 1*. It's most likely that the northern depocentre is fed by another river system to the one that is feeding the main depocentre.

Pleistocene Unit 4 (Pleisto 4)

Seismic and Well Observations

Bounding Surfaces: The top of the unit, *Top Pleisto 4* (Fig. 3.12h), is a strong amplitude positive continuous reflection. It has clinoform geometry in the east of the dataset. In the north the reflection is largely parallel to underlying reflections (Fig. 3.6a). In the central part the reflection has a truncating relationship to underlying reflections on the topset, but is a downlap surface basinwards of the shelf break (Fig. 3.6c). In the south it is denoted as the top of a package of *SA4 Marine Onlap* (Fig. 3.6d & Fig. 3.6) and is onlapped by overlying reflections (Fig. 3.6d).

The deepest part of the *Top Pleisto 4* is a 100 m across narrow basin trending NNW-SSE reflection trends straddling the border of the UK and the NL sectors with a maximum depth of 800 ms (730 m). The reflection shallows to the east and the south to a minimum of 250 ms (220 m) (Fig. 3.12h). The reflection is deformed in the south east. *Top Pleisto 4* clinoform height is ~ 200 m in the north and 1-2° foreset height when flattened on a *Pleisto 5* topset (Fig. 3.6b), in the south where *Top Pleisto 4* is the top of a *SA4* package, the foreset is 3°.

Gamma ray logs indicate a sharp decrease of 30-50 API at the *Top Pleisto 4* at the top of a fining upwards sequence (Fig. 3.7) across the majority of the basin. On the foresets where *Top Pleisto 4* is most expanded the opposite occurs and it is represented by a sharp increase in gamma ray. The final shelf edge position is linear, N-S trending except in the very south NL where it becomes NE-SW trending (Figs. 3.10g, 3.11h).

Internal Geometry: *Pleisto 4* has a NNW-SSE trending maximum thickness in the east of the NL sector of 350 ms (310 m) thinning east, west and to the south (Figs. 3.10g & 3.11h). In the SW of the dataset a large area of minimal thickness (labelled in Fig. 3.11h) corresponds to previous depocentres suggesting this is an area of bypass during *Pleisto 4*. The unit is expanded in the NW with large preservation of topsets (Figs. 3.6a-d) across the DK, north and central NL sectors. This can be contrasted to previous units thickness maps where top the east of the main depocentre of thickness >100 ms (Figs. 3.11g&3.12h). The shelf edge prograded westwards 50 km across the main depocentre during *Pleisto 4* whilst to the south and north this is reduced to ~20 km.

In the DK/north NL sector *Pleisto 4* is dominated by *SA6 Oblique Tangential* followed by *SA7 Sigmoidal Clinoforms* ~200 m in height (0.5-2° foreset angle) (Figs. 3.6b&3.11g). Seismic character is homogenous weak amplitudes on the foresets with stronger discontinuous reflections on the topsets. The switch between the progradational *SA6* to aggradational *SA7* stacking pattern is separated by a stronger amplitude continuous reflection. Isolated <1 km across bright spots at the base of the *SA7* package in 3D correspond to *SF2* lower slope current features (Figs. 3.9 & 3.11h).

In the central NL sector (Fig. 3.6c); towards the most expanded part of the unit, *SA7* clinoforms largely 100-150 m (1-3°) dominate. The reflections are heterogeneous in seismic amplitude, with variation of internal architectures (*SA1*, *SA3*; Fig. 3.11g). Strong amplitudes on the topsets correlate with the tops of *SA1* packages on the foresets. This is followed by *SA6* clinoforms with less topset preservation, weaker amplitudes, with a flat to downstepping trajectory and evidence of *SF4* Terrestrial Facies. *SF3 Multiple Source Slope Channels* are identified in the downstepping part of the unit. The aggradational *SA7* and the progradational *SA6* stacking patterns are divided by a clear downlap surface in the centre of the unit. This is the opposite pattern to the DK sector described above. *SA1* is also identified within the *SA7* package. *SA4 Marine Onlap* is

identified at the top of the unit. Three *SA1* packages are identified in all over the *Pleisto 4* unit. Overall there is a decrease in seismic amplitude throughout the unit in the depocentre.

In the southern NL sector, early *Pleisto 4* weak amplitude *SA6* low angle (1°) clinoforms downlap onto *Top Pleisto 3*, landward of the shelf break. Overall clinoforms are less extensive in height (50-150 m). Clinoforms dramatically increase in foreset dip from 1° to 3° towards the top of the unit with the top 100 m of the unit characterised by strong amplitude reflections two erosional surfaces that truncate these earlier low angle reflections. An *SA4* package tops the unit. Amplitudes are stronger down south. In the south pre *Top Pleisto 3* bottomsets are tilted towards the east post-deposition, however the topsets and bottomsets of *Pleisto 4* are less deformed with the topsets almost horizontal.

Across the basin seismic amplitudes progressively weaken towards the top of the unit and towards the top of the unit either *SA6* aggradation or *SA4 Marine Onlap* top the unit. Topsets are irregular and eroded by terrestrial channels (*SF4*), and iceberg scours (*SF6*). Terrestrial facies is identified almost up to the final shelf break as are the iceberg scours. The iceberg scours extend across the dataset but are absent in the SE (see Minimum Transgression in Figs. 3.10g & 3.11h and Iceberg Scours Fig. 3.19d). At least four large scale iceberg scouring events, *SF6* are identified within the unit across the basin.

The *Pleisto 4* gamma ray response to the unit is largely <70 API and generally lower ~ 40 API in the east and overall coarsening upwards. In the wells that penetrate *Pleisto 4* topsets the unit is characterised by either fining upwards, coarsening upwards, couplets of 30-50 m (associated with delta plain/channels coupled with shallow marine deposits) or 50-100 m funnel shaped log motifs coarsening upwards, associated with delta fronts sensu (Olariu et al., 2012). In the central NL blocky low gamma ray packages of 50 m associated with *SA1* separated by fining upwards packages (Fig 3.7). The E18-01 well which penetrates the weak amplitude foresets suggests a higher API than the topsets of >70 API.

Correlation

Top Pleisto 4 corresponds to 1.94 Ma, the base of the Olduvai magnetic stage (Kuhlmann and Wong, 2008). The unit's duration is ~ 200,000 years. *Pleisto 4* correlates to units ~S8-11 in (Kuhlmann and Wong, 2008). Tiglian C1-4b NL onshore stage is correlated within this unit (Fig. 3.4). The *SF2* current scours of *Pleisto 4* are discussed in (Stuart and Huuse, 2012).

Interpretation

The *Top Pleisto 4* is interpreted as a sequence boundary because there is a strong increase in grain size (decrease in gamma ray values) upwards and an onlap surface and truncation surface within the dataset.

The *Pleisto 4* unit denotes a change in the style of deposition in the study area. The main depocentre has shifted from the south NL to the North/Central NL, where internal small scale clinoforms plus *SF3 Multiple Source Slope Channels* (Fig. 3.11g) are concentrated. This is reflected in the chronostratigraphic diagram (Fig. 3.4). Clinoform heights and lithology suggest larger accommodation in the north and central NL basinwards of the shelf edge. The shelf edge appears linear N-S and sediment input from but likely from the upper part of the unit

Pleisto 4 is different from *Pleisto 2-3* units in that there is greater accommodation on the shelf, landward of the shelf break. This suggests a deepening between *Top Pleisto 3* (~2.15 Ma) and *Top Pleisto 4* (1.94 Ma). This is also apparent due to the shift landwards (east) of the large scale clinoforms, with the *Pleisto 4* reflections downlapping onto of the *Top Pleisto 3*. In comparison to *Pleisto 2 & 3* the unit has a greater amount of aggradation, most notably in the north of the dataset. Weaker seismic amplitudes across the main depocentre finer grained sediment are the building block for the shelf-prism. Depositional environment is broad as we have distal deep marine bottomsets, nearshore environments and shelfal environments.

Pleistocene Unit 5 (Pleisto 5)

Seismic and Well Observations

Bounding Surfaces: The top of the unit is *Top Pleisto 5* (Fig. 3.12i), a strong amplitude positive reflection which is continuous across the basin and parallel to underlying

reflections. The reflection is inclined in the north towards the west at 1-2 ° due to post depositional tilting. The overlying reflections are parallel to *Top Pleisto 5*. The shallowest point of the reflection is 160 ms (140 m) in the central/south NL sector (Figs. 3.6c&d, 3.12i). The reflection is 670 ms (550 m) at its deepest in the NW of the dataset forming an NW-SE trending basin to the west of the Central Trough (Fig. 3.1). The reflection is disturbed by local salt tectonic related uplift largely in the east of the dataset. Gamma ray logs indicate a sharp decrease in gamma ray values at *Top Pleisto 5* (Fig. 3.7). The shelf edge at the top *Pleisto 5* is within the UK sector and trending NNW-SSE.

Internal Geometry: *Pleisto 5* (Fig. 3.10h) main depocentre trends NNW-SSE in the border of the NL and UK sectors. The maximum thickness is 350 ms (300 m), east and south of the depocentre the unit thins from 150 ms (130 m) to 0 ms. The unit is laterally continuous across the basin, thinning landwards, but with substantial 50-100 m topset thickness. In the UK sector clinoforms are post depositionally deformed/tilted. The toesets have been post-depositionally inclined west to east at an angle of 1-2°.

The seismic architecture of the unit is dominated by parallel continuous reflections with variable amplitude. In the area of the main depocentre (Fig. 3.6c) *SA7 Sigmoidal Clinoforms* followed by *SA4 Marine Onlap* (Fig. 3.8) are identified. Further to the south only *SA4* is present (Fig. 3.6d). The sigmoidal clinoforms are from 150 ms (130 m) to 200 ms (170 m) in height. The main depocentre *SA7* has weak amplitudes but with strong amplitudes on the topsets in the east (Fig. 3.6b). The character of the large scale clinoforms are ascending regressive, with aggradation being dominant.

The dominant facies within the limits of the dataset is Topset Facies (SF4, Fig. 3.9). Some of the parallel topset reflections exhibit erosional characteristics. RMS amplitude extraction on horizon 30 ms above *Top Pleisto 4* identifies large scale (2-20 km wide) channels eroding into the topsets from the S and SE. The smaller scale 2-3 km wide SE-NW trending channels appears to be older than the larger (5-20 km wide) S-N trending.

The topset facies is presented as a serrated style gamma ray motif (Fig. 3.7), with alternating high/low gamma ray values which includes fining upwards and coarsening upwards packages of 30-60 m. In general *Pleisto 5* is overall coarsening upwards the gamma ray values are <60 API suggesting an overall coarser grained lithology than

previous units. Lithological information from well cuttings landwards of the shelf break suggest three dominant lithologies; white medium to coarse well sorted, pitted, sand; fine to very fine subangular sands, and light grey mudstones. Closer towards the depocentre the medium to coarse sands are not present.

SF6 Iceberg Scours seismic facies are widespread across the northern and central parts of the dataset (Fig. 3.19e) largely scouring from NNE-SSW. Several events of iceberg scouring have occurred during this unit. The presence of the iceberg scours show that marine conditions occurred many times across a large part of the northern and central study area.

Correlation

The top of the unit, *Top Pleisto 5* corresponds to Top S13 seismic surface and the base of the unit, *Top Pleisto 4* corresponds to Top S11 in (Kuhlmann and Wong, 2008). This correlates with top and base of the Olduvai subchron, *Top Pleisto 5* ~1.942 Ma (Top Gelasian) and the *Top Pleisto 4* at ~1.785 Ma. The unit therefore represents 157,000 year time period. The dating is corroborated by biostratigraphy Top Gelasian in many wells across the dataset (Chris King *pers comms*, see Appendix). The Tiglian C-4c onshore NL stage is within this unit.

Interpretation

Top Pleisto 5 is interpreted as a sequence boundary due to the sharp decrease in gamma ray values across this reflection, plus it is interpreted to be a regional event as it is a laterally continuous reflection across the basin. The units' main depocentre is now outside the NL sector. Largely weak amplitudes, thickness of topsets on the shelf and lithological information suggest to the NE that there is accommodation creation on the shelf throughout the unit and the minimum transgression shows us where a minimum point of where the highstand coastline was during this unit and indicates a broad shelf in the north between the shelf edge and the highstand coastline. Further south, medium to coarse grained lithology suggests a more proximal setting, the well log feature of fining upwards and coarsening upwards motifs suggest switching from coastal plain and channels (FU) to fluvial dominated deltas (CU) sensu (Olariu et al., 2012) which is verified by the Fig. 14e where the lack of marine conditions in the south suggests a highstand coastline closer to the shelf edge.

Pleisto 5 exhibits an ascending shelf edge trajectory aggradational in character. The unit is deeper than previous Pleistocene units. Therefore in the north the unit is described as open marine and the more proximal area in the south is transitional (between shallow marine and delta plain). To the east of max transgression line is likely the high stand position of the coastline within the study area and therefore is described as terrestrial. The maximum regression for the entire unit is close to the shelf edge in the south but is offset to the east in the north of the dataset, suggesting that river systems were not completing the cross shelf transit to the shelf edge in this area because sediment rate could not keep up with base level increases. It therefore suggests that there was an increase in relative sea level regionally over the unit with the north becoming deeper than the south however in the south of the NL sector is more proximal to the main sediment input into the basin at the time.

The smaller SE-NW trending 2-3 km channel systems in the central NL sector (Fig. 3.20) are interpreted as likely delta top distributaries and the S-N trending larger laterally accreting channels (5-20 km wide) could represent the proto Rhine. This is the only time in the study period where a river system of this magnitude is imaged. This suggests a substantial regression of the coastline occurred during the early part of the unit followed by a transgression for the rest of the unit to exhibit iceberg scours at the same location. However the preservation of large channels could be inhibited elsewhere in this unit due to degradation of the seismic quality at the top of the surveys and the heavy scouring by iceberg scours.

The geomorphology of the basin at the time is likely a very narrow deep basin of several hundreds of meters with a broad and shallow shelfal sea of 50-100 m. Progradation directions and sediment input, because the depocentre is elongate NNW -SSE suggests an sediment direction from the east but also the orientation of clinoforms and topset channel systems suggest SE-NW, S-N influence. The main area of accommodation in the basin at the time of *Pleisto 5* will be to the east of the *Pleisto 4* depocentre (Fig. 3.10g, 3.11h) and in this case the main thickness area appears not dominated by the present sediment input directions but by the geomorphology that the previous depocentres created.

The *SA4 Marine Onlap* architecture is likely caused by a change in progradation direction rather than a eustatically derived transgression, likely ongoing change in direction of dominate clinoform progradation direction. Strike lines show an increase in progradation from the south from late *Pleisto 4*.

Palynological assemblages in A15 wells (Fig. 3.1) indicate open marine conditions in combination with cold sea surface temperatures (Kuhlmann et al., 2006a) during *Pleisto 5*. This indicates that relative sea level was high during a glacial period, which is not the case during many of the other glacial periods in the study. This has been suggested to be due to a melting event (ten Veen *et al*, 2013) but this could also be caused by accelerated subsidence during this time period. The tilting basinwards of topsets that would have been originally deposited horizontally.

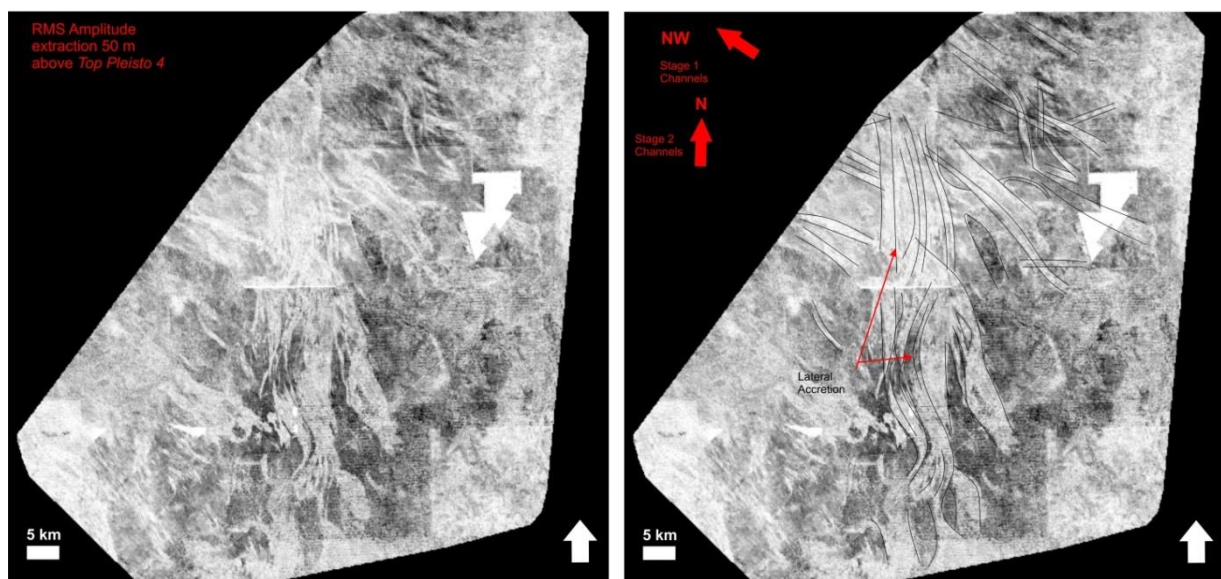


Figure 3.20 Large scale river channel systems during *Pleisto 5*. Likely proto-Rhine.

3.4 BASIN INFILL AND DEPOSITIONAL MODEL

3.4.1 Basin Infill

The observation of seismic geomorphology and trends in seismic reflection architecture, placed within the chronostratigraphic framework, allows new insights into the evolution of the Late Cenozoic southern North Sea basin. In this section a brief summary of this evolution derived from the detailed unit descriptions is given.

Providing a summary of depocentres, key basin changes, large scale trends in facies and architecture.

The well log correlations indicate two major trends in depositional upwards fining and an upwards coarsening character (Fig. 3.7). This represents a change in the depositional environment and is not representative of a single event across the basin but of the shelf-prism clinoforms prograding across the basin. The shelf-prism clinoforms are associated with many depositional environments from deep marine to slope to shelf/terrestrial conditions and the change from fining upwards to coarsening upwards identified the transition at the well between the depositional environments.

The post mMU section was divided into nine seismic units, dependent on the well log and seismic characteristics; and chronostratigraphic significance of normally laterally extensive downlap surfaces.

Mio 1 (mid-late Tortonian) seismic unit depocentre strikes NNW-SSE in the eastern part of the dataset in the DK sector with a shelf edge trending NNE-SSW laying eastwards DK sector at the time (Figs. 3.11a & 3.12a). Thickness maps from (Rasmussen et al., 2005; Sørensen and Gregersen, 1997; Thöle et al., 2014) show during the same period up to 1000 m of deposition occurred to the east of the study area within two main depocentres. The weak seismic character of the unit, lack of clinoform geometry and the high gamma ray values suggests this unit represents condensed bottomsets of a depositional system in a distal deep marine environment, representing several million years of deposition.

Mio 2 (nr top Tortonian) consist of two NW-SE trending depocentres in the DK sector with a sediment input from the NE and an arcuate shelf edge trending NW-SE (Figs.

3.10a & 3.11b). Up to 1000 m of sediment are deposited during *Mio 2* largely in a N-S trending depocentre in the DE sector just east of the NL sector (Thöle et al., 2014). The majority of the unit is interpreted as deep marine, distal from the sediment source (which is concentrated in the south of the DE sector, >100 km away), however the identification regression of the coastline into the basin does occur during the unit (Figs. 3.10 & 3.13). A transgression occurs at the top of the unit which coincides with a shift in depocentre.

Mio 3 (~7.2 Ma – 4.2 Ma) full depocentre is within the DE sector and extends into the Norwegian sector, striking NW-SE (Sørensen and Gregersen, 1997; Thöle et al., 2014). Sediment input was focused within the DE sector of the dataset south west of previous units and provenance of sediment input is from the E to NE (Fig. 3.11c).

The increase in stronger amplitudes throughout the unit and the increase in magnitude of the coarsening upwards parasequences suggest the unit is overall regressive and the depositional environment is becoming proximal, however the unit is still dominated by deep marine facies and slope/basinal processes. The top of the unit corresponds to a fining upwards and deepening of the basin in the north east of the dataset and Top *Mio 3* is correlated to a shift in depocentre southwards.

Plio 1 seismic unit (4.2 Ma-2.58 Ma) is 1.62 Ma in duration and deposition was focused in an arcuate shape, in the far east of the Netherlands North Sea along the boundary with the German sector (Fig. 3.10c). Clinoform architectures are dominantly sigmoidal towards the north and oblique tangential towards the centre and the south of the depocentre. Intra shelf clinoforms are preserved on the topsets of shelf-prism clinoforms suggesting high accommodation on the shelf at the time. Slope angles of large scale clinoforms are a maximum 4° in the southern part of the Netherlands North Sea.

Top *Plio 1* is marked by a transgression and corresponds to the Gauss magnetic reversal and the termination of interglacial MIS 103 (base Quaternary, 2.58 Ma). Top *Plio 1* corresponds to a shift of depocentre further south in the Netherlands sector and to an E-W sediment input direction compared to NE-SW previously. Basin bathymetry changes significantly across the base Quaternary as at 2.58 Ma the south of the NL sector clinoforms were >300 m compared to the north of the NL sector ~ 200 m but during the

early Gelasian (seismic units *Pleisto 1 -3*) the south shallows upwards during the Gelasian (2.58-1.78 Ma) and the north deepens in relative depth (Chapter 6.2). This is associated with the greater accommodation creation in the north of the Netherlands North Sea due to differential subsidence.

The *Pleisto 1* seismic unit (2.58 Ma – 2.43 Ma) is very well constrained. *Top Pleisto 1*, a regional strong amplitude reflection and shale layer, corresponds to a maximum flooding surface. The top of *Pleisto 1* corresponds with a North Sea magnetic reversal event at 2.43 Ma (X event, Cande and Kent, 1995; Kuhlmann et al., 2006; Noorbergen et al., 2015) which is correlated to the termination of glacial MIS 96 (Donders et al., in prep). Two additional regional strong amplitude shale layers within *Pleisto 1* correspond to the termination of glacial period MIS 98 and 100. The correlation of regional shale layers within *Pleisto 1* allows the unit to be subdivided (Figs. 3.17 & 3.18). In most cases this surface appears to coincide or occur just below the maximum flooding surface which is identified as regional downlap surfaces basinwards of the shelf edge. The unit represents an expanded section in the SNS and shows a greater than order of magnitude increase in sedimentation (from ~3 km³ per 1000 years to ~55 km³ per 1000 years) and a change from an arcuate convex to a linear concave shelf edge from *Plio 1* to *Pleisto 1* (Figs. 3.10d & 3.11e), which suggests a change from river dominated to wave/storm dominated systems (Hampson et al., 2015).

Lateral variability of the seismic units across the dataset increases after the base Quaternary with *Pleisto 1* exhibiting exceptional progradation rates of the shelf-prism in the south of the dataset, prograding ~100 km from east to west within 150,000 years, most of which occurred within the first 70,000 years of the unit. This is not as clear in the north Netherlands North Sea, in the area of A15-03 well where <20 km progradation occurred during the same time period (Fig. 4b).

The first major fall in global sea level within the Quaternary occurs in *Pleisto 1*. The first sub unit, MIS 103-100 (2.58 Ma to 2.51 Ma), covers one and a half glacial interglacial cycles and is 62,000 years in duration. The shelf edge progrades westwards in the southern Netherlands North Sea by >67 km during this sub unit, over a kilometre every 1000 years. The sub unit is dominantly oblique clinoforms. There is a dramatic change to a very high sediment supply and this is reflected in the first major basin deposition

event of the Pleistocene and large mass transport complexes are associated with this section. The second sub unit is from MIS 100-98 (2.51-2.48 Ma) and covers ~ 37,000 years. The maximum progradation is ~20 km and therefore a progradation rate of 540 m every 1000 years. The sediment rate has reduced from the last cycle and there is greater preservation of topsets and the presence of sigmoidal clinoforms.

The third sub unit is from MIS 98-96 and is 55, 000 years in length and covers 23,000 km of progradation, 420 m per 1000 years. During *Pleisto 1* a secondary depocentre in the very north of the dataset in the DK sector indicates a second river system which progrades 40 km into the basin from the NE during the unit. The progradation rates of this magnitude suggest both are supply driven sedimentary systems, but the system that is supplying the main depocentre has a larger sediment supply than most ancient and modern systems (Carvajal et al., 2009)

The *Pleisto 2* and *Pleisto 3* seismic units shelf edges are linear and their depocentres trend north-south across the central Netherlands North Sea (Fig. 4.3). *Top Pleisto 2* is a strong amplitude downlap surface and is linked to the glacial termination of MIS 92 at 2.35 Ma. *Pleisto 3* corresponds to a downlap surface in the north Netherlands North Sea at ~2.15 Ma, and is possibly linked to the glacial termination of MIS 82. *Pleisto 3* is a seismic unit which appears to have been deposited under limited accommodation conditions on the topsets and low base level. Intra Slope Clinoforms downlap on the *Top Pleisto 2* across the entire depocentre, suggesting a period a major regional base level fall and sediment partitioning basinwards of the shelf break. The *Top Pleisto 3* was picked as a significant surface as in the north of the dataset it is a downlap surface for small scale clinoforms across the basin and in the south of the dataset it is an unconformity where shelf margin clinoforms prograde on top of the earlier set of large scale clinoforms. Sørensen and Gregersen, (1997) indicates a secondary depocentre just in the north of the dataset, likely the same source as the secondary depocentre seen during *Pleisto 1*.

The *Pleisto 4* unit (~2.15-1.94 Ma) denotes a change in the style of deposition in the study area. The main depocentre has shifted from the south NL to the North/Central NL, are concentrated Fig. 3.11g. This is reflected in the chronostratigraphic diagram (Fig.

3.4). Clinoform heights and lithology suggest larger accommodation in the north and central NL basinwards of the shelf edge.

Pleisto 4 is different from *Pleisto 2-3* units in that there is greater accommodation on the shelf, landward of the shelf break. This suggests a deepening between *Top Pleisto 3* (~2.15 Ma) and *Top Pleisto 4* (1.94 Ma). This is also apparent due to the shift landwards (east) of the large scale clinoforms, with the *Pleisto 4* reflections downlapping onto of the *Top Pleisto 3*. In comparison to *Pleisto 2 & 3* the unit has a greater amount of aggradation, most notably in the north of the dataset. Weaker seismic amplitudes across the main depocentre finer grained sediment are the building block for the shelf-prism. Depositional environment is broad as we have distal deep marine bottomsets, nearshore environments and shelfal environments.

Pleisto 5 (1.94-1.78 Ma) main depocentre resided to the east of the NL sector. Largely weak amplitudes, thickness of topsets on the shelf and lithological information suggest to the NE that there is accommodation creation on the shelf throughout the unit and the minimum transgression shows us where a minimum point of where the highstand coastline was during this unit and indicates a broad shelf in the north between the shelf edge and the highstand coastline. Further south, coastal plain and channels, fluvial dominated deltas suggest proximal setting.

Pleisto 5 exhibits an ascending shelf edge trajectory aggradational in character. The unit is deeper than previous Pleistocene units. It therefore suggests that there was an increase in relative sea level regionally over the unit with the north becoming deeper than the south however in the south of the NL sector is more proximal to the main sediment input into the basin at the time. Large scale river systems (5-20 km wide) are identified within this unit for the first time in the study period in the central NL sector (Fig. 3.20) and could represent the proto Rhine. Palynological assemblages in A15 wells (Fig. 3.1) indicate open marine conditions in combination with cold sea surface temperatures (Kuhlmann et al., 2006a) during *Pleisto 5*. This indicates that relative sea level was high during a glacial period, which is not the case during many of the other glacial periods in the study. This has been suggested to be due to a melting event (ten Veen et al., 2013) but this could also be caused by accelerated subsidence during this

time period indicated by tilting of topsets which would have been deposited horizontally (Fig.3.4).

3.4.2 Depositional Model

This section focuses on the depositional model for the basin derived from the observations of basin infill and distribution of seismic facies.

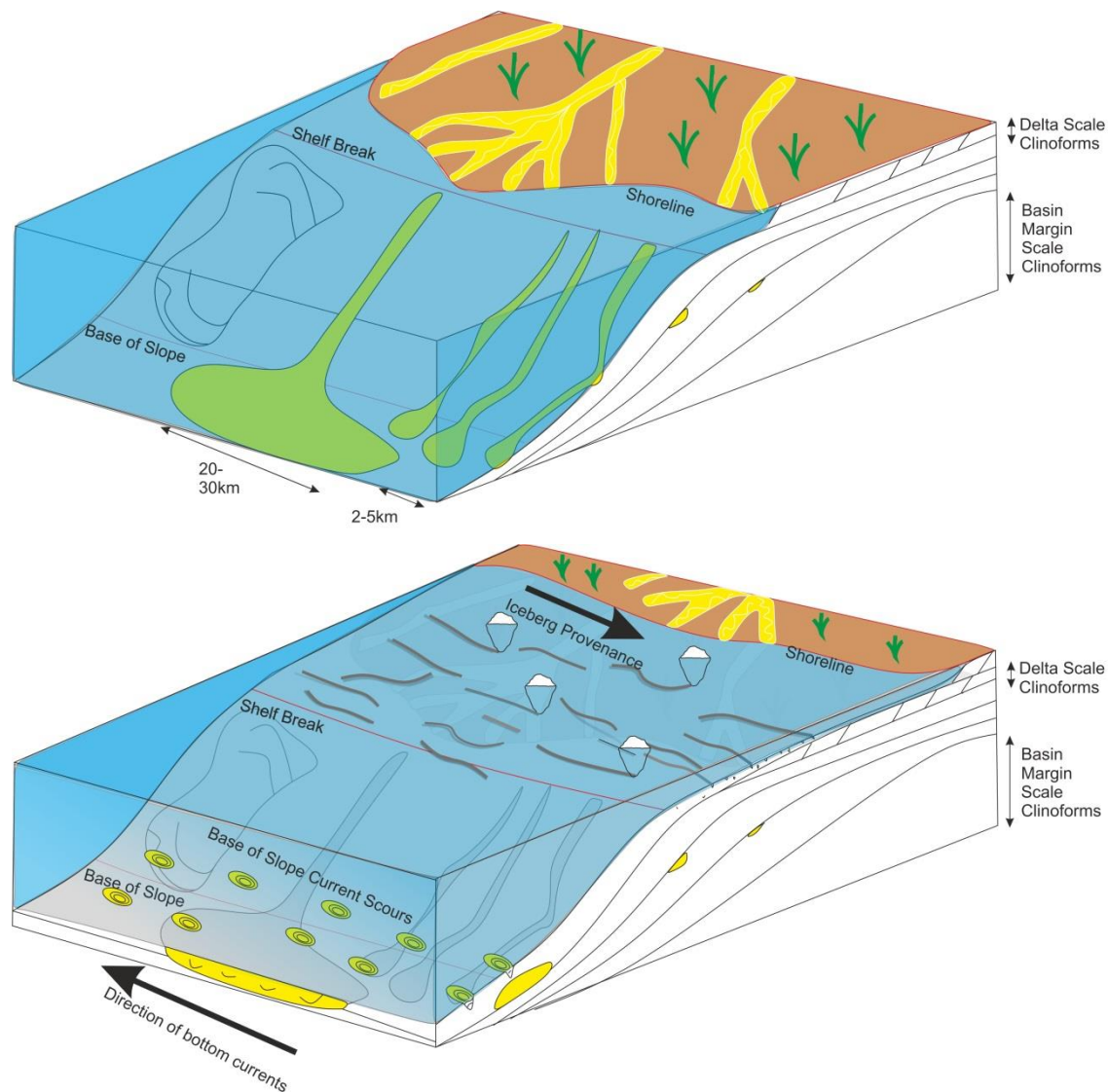


Figure 3.21 Depositional models. Left: Delta at/near shelf edge. Right: Flooded Shelf. The depositional models are based on observations from distribution of key seismic facies across the basin. The models are not linked to sea level changes or sediment supply as they are non-unique and can occur during differing scenarios. Basin margin scale clinoforms are another term for shelf-prism clinoforms.

The dominant seismic architecture of the SNS during the study period is of highly progradational sigmoidal and oblique shelf-prism clinoforms, 100-400 m high, downlapping on to the mid Miocene Unconformity (mMU). The depositional environment of the shelf-prism scale clinoform is determined as the topset, foreset and bottomset representing the shelf, slope and basin floor respectively and the shelf-prism clinoform roll over point representing the shelf edge. The roll over points of the small scale clinoforms (<150 m in foreset height) may represent the coastline. Delivery to the basin floor occurs in three main ways, via mass transport complexes on the slope, slope channel levee systems feeding 2-5 km wide basin floor fans and large individual canyons feeding 20-30 km wide basin floor fans. Overall the basin is shallowing and coarsening upwards during the study period. Along slope currents are strong at times when base level is high (Fig. 3.21).

Direct evidence of glaciation is seen from *Pleisto 1* onwards, as abundant iceberg scouring events are identified (Fig. 3.16 & Chapter 6.1). Iceberg scouring events, as they are marine features, have enabled the extent of transgressions to be quantified (Fig. 3.21). During *Pleisto 1-3* the shelf floods back almost the same place in the south eastern Netherlands North Sea throughout the Gelasian, and that there is a clear area that is permanently emerged in the south east from early in *Pleisto 1* (after MIS 100, location indicated in Fig. 3.10 & 3.11).

The distribution of slope channel and basin floor fan systems indicates that after *Plio 1* sediment inputs were focused in the south. The north of the data set is largely devoid of sediment delivery to the basin floor. This is likely because the shelf was wider and subsidence in this area meant the river systems were not able to reach the shelf edge in order to supply basin floor fans.

The distribution of deep water sedimentation indicates a relationship to the proximity of the coastline to the shelf edge and the reason why slope and basin floor deposition reduces through time (Fig 3.11) is because the shelf-prism is building out and infilling the SNS basin but each time there is a transgression the coastline is being pushed back to the same place each time, thus requiring increased sediment supply and increased base level fall to reach the shelf edge in the future.

3.5 DISCUSSION

The detailed analysis of the Late Cenozoic section across the SNS has identified great regional variability in clinoform architecture and seismic geomorphology within seismic units. The seismic units are dated and tied to the global sea level curve (Fig.3.4). The chronostratigraphic control enables a correlation of sequences, seismic architectures, geomorphology and seismic facies with full 3D control, to eustatic change, subsidence and sediment supply.

The discussion focuses on highlighting the controlling factors on the evolution of a large shelf-prism in context of external forcings such as eustasy and more local forcings such as sediment supply, subsidence and basal geomorphology.

3.5.1 Eustatic Control

Previous palynological and geochemical analysis of the SNS show that the regional proximity to the coastline and climate is governed by eustatic glacial –interglacial cycles (ten Veen et al., 2011; Donders, et al., in prep; Noorbergen et al., 2015). Regional base level is said to reflect glacioeustasy during the earliest Gelasian (2.58-2.35 Ma), though grain size is not directly controlled by it (ten Veen et al., 2013; Donders et al, in prep). The identification of regional shale layers and clinoform architectures in this study in the early Gelasian shows that this is reflected to some extent in the seismic stratigraphy of the basin. The ability in this study to be able to correlate the key shale layers linked to the termination of glacial period across 100 km of basin does suggest that eustasy does govern the development of some key sequence stratigraphic surfaces (Fig. 3.18).

Not all units can be linked to the global sea level curve however large swings in eustasy manifest themselves in the sequences preserved within the basin. An example of this is the transition from *Plio 1*-to *Pleisto 1* is a regional flooding event. This corresponds with an increase in global sea level and a period at the beginning of *Pleisto 1* where the sea level is generally higher. Clinoform stacking patterns (sensu Neal and Abreu, 2009) within *Pleisto 1* and *Pleisto 2* correlate well to the eustatic curve in the south of the dataset, where the section is most expanded. Clinoform architecture and foreset heights reflect eustatic rises and falls in conjunction with glacial-interglacial cycles.

3.5.2 Sequence Variability

Early sequence stratigraphy models suggested that sequence development was governed by eustasy (Haq, 1988; Posamentier and Vail, 1988; Vail et al., 1977). If eustasy was the only forcing on the stratigraphic architecture of the basin then there would be very little variation in architecture across the. The seismic architectures and seismic facies described in Section 3.3 show there is a large amount of variation in the expression of sequences for each seismic unit and this corroborates findings from 1990's which identified that sequence stratigraphic framework did not account for lateral variation and other forcings on sequence development (Cartwright et al., 1993; Gawthorpe et al., 1994; Helland-hansen and Gjølberg, 1994; Martinsen and Helland-Hansen, 1995; Posamentier and Allen, 1993).

There are clear examples within the dataset where sequence architectures do not correspond to the global sea level. For instance, from *Pleisto 3- Pleisto 5* (2.15-1.78 Ma) there is a switch across the region to ascending trajectories, sigmoidal clinoforms (Fig. 3.10) and a greater preservation of topsets. This is at odds with the global sea level curve which indicated global sea level is lowering. Biostratigraphy from Kuhlmann et al. (2006ab) and ten Veen et al. (2011) also show a return to largely open marine conditions. The distribution of key seismic facies such as the Multiple Line Source and Single Feeder deep water sedimentary systems throughout time also indicate that sedimentation is uniform across the basin and that additional forcings are responsible for the positioning of these systems (Figs. 3.9 & 3.11).

3.5.3 Subsidence and Tectonics

Differential subsidence is identified as one of the key factors in affecting the sequence variability across the basin. This is identified by comparing the north of the dataset in the area of the Central Trough (Fig. 3.1) where the basal surface, the mMU shows heavy tilting towards the axis of the Central Trough (most notable in Figs. 3.6b&c) and a greater sediment accumulation in the Late Cenozoic with the southern area of the dataset where the mMU appears relatively flat and similar to its original depositional state (Fig. 3.6d). The main differences in depositional style between the two structural domains are that in the North, sigmoidal shelf-prism scale clinoforms are dominant

whilst in the south oblique shelf-prism scale clinoforms are dominant (Fig. 3.10) and seismic amplitude and lithological difference from north to south and the lack of basin depositional events in the north after *Plio 1*.

On a more local scale accommodation creation and destruction is associated with active salt tectonics which affects seismic architectures on a local scale of 5-10 km around the salt structures it is affecting the sediment sequence and a large amount of the post mid Miocene salt movement, especially in the west of the dataset is younger than our study period. Areas which are tectonically active during the Late Cenozoic such as the Broad Fourteens Basin (Fig. 3.1) appears to have more active basin deposition and this can be identified in Fig. 3.11f.

3.5.4 Sediment Input and Shelf Geomorphology

The ability of the sediment supply systems to reach the shelf edge in different relative sea level to be the main driver of whether there is coarser grained material delivered to the basin floor. The distribution of slope channel and basin floor fan systems indicates that after *Plio 1* sediment inputs were focused in the south. The north of the data set is largely devoid of sediment delivery to the basin floor. This is likely because the shelf was wider and subsidence in this area meant the river systems were not able to reach the shelf edge in order to supply basin floor fans.

The distribution of deep water sedimentation indicates a relationship to the proximity of the coastline to the shelf edge and the reason why slope and basin floor deposition reduces through time (Fig 3.11) is because the shelf-prism is building out and infilling the SNS basin but each time there is a transgression the coastline is being pushed back to the same place each time, thus requiring increased sediment supply and increased base level fall to reach the shelf edge in the future.

The lack of sediment supply to the basin floor also correlates to the proximity of the terrestrial facies to the shelf edge. In the north the maximum regression for the units does not meet the shelf edge whilst in the south the terrestrial facies is identified at the shelf edge (Figs. 3.10 & 3.11) There are several river systems feeding the basin and are imaged (See unit descriptions), the southern system linked to the 'Baltic River System' is highly supply dominated (>100km progradation in 1mya) especially during *Pleisto 1*

where the system is at or near the shelf edge for the majority of the unit. River systems are identified in the north also during the Gelasian but generally are > 50 km eastwards of the shelf edge.

Therefore progressively through *Pleisto 1-5*, the shelf edge is continuing to build out to the west, however the river systems, in order to reach the shelf edge during lower relative sea level conditions, have to travel further each time from their higher relative sea level position (the shelf is getting wider). This may help explain the lack of delivery of coarser grained material to the basin floor that being via turbidity currents and landslides by the later units and in the north, throughout the time period.

3.6 CONCLUSIONS

- The high resolution chronostratigraphic framework for the north Netherlands North Sea based on biostratigraphy and magnetostratigraphy was extended across the area of the SNS MegaSurvey in the Netherlands North Sea and into Danish North Sea. Nine seismic units were identified and correlated across the basin.
- The importance of correlating well logs along strike when correlation across clinoformal geometry and the importance of integrating the seismic geometries into the correlation to guide the interpretation was identified. The gamma ray signal of glacial terminations of MIS 100, 98, 96 and 92 can be traced over 500 km along strike of the depositional trend from the A15-03 well in the Netherlands North Sea to the Noordwijk borehole onshore Netherlands, via wells in the southern North Sea all of which inhabit a similar depositional environment on the basal Quaternary shelf-prism. However the clear gamma ray character is hard to trace even 50 km landwards or basinwards.
- The identification of a range of clinoform architectures and seismic facies in planform using seismic geomorphology and the mapping them for each seismic unit against the respective thickness map highlighted the lateral variation of basin infill within the study period.
- The seismic geomorphology was utilized to identify depositional environments in the absence of direct geological observation; along with the seismic

architectures an idea of the position of the coastline was taken. A novel way of measuring the extent of transgressions of the shelf during base level highs was developed using the mapping of iceberg scours across the shelf during the Gelasian. As iceberg scours can only form in subaqueous conditions, these were key indicators that the shelf was flooded. Mapping the seismic facies and seismic architecture has also enabled visualisation of the lateral variation of seismic units.

- Eustacy is the main control on regional sea level and climate in the early Gelasian (2.58 Ma – 2.15 Ma) with accelerated subsidence in the late Gelasian overriding the eustatic signal (2.15–1.78 Ma).
- Sediment supply (amount and proximity to the source), local subsidence and underlying geomorphology of the shelf create variability in how eustacy is expressed within the sedimentary architecture of the SNS.
- The variation in the expression of a glacial-interglacial cycle within the seismic stratigraphy of the southern North Sea highlights the need for 3D large scale seismic interpretations to understand the regional over local base level trends and their link to global sea level.

3.7 REFERENCES

- Anell, I., Midtkandal, I., 2015. The quantifiable clinothem – types, shapes and geometric relationships in the Plio-Pleistocene Giant Foresets Formation, Taranaki Basin, New Zealand. *Basin Research*.
- Anell, I., Thybo, H., Rasmussen, E., 2012. A synthesis of Cenozoic sedimentation in the North Sea. *Basin Research* 24, 154–179.
- Benvenuti, a, Kombrink, H., Ten Veen, J.H., Munsterman, D.K., Bardi, F., Benvenuti, M., 2012. Late Cenozoic shelf delta development and Mass Transport Deposits in the Dutch offshore area – results of 3D seismic interpretation. *Netherlands journal of Geosciences* 91, 591–608.
- Bijlsma, S., 1981. Fluvial sedimentation from the Fennoscandian area into the North-West European Basin during the Late Cenozoic. *Geologie en Mijnbouw/Netherlands Journal of Geosciences* 60, 337–345.
- Brückner-Röhling, S., Forsbach, H., Kockel, F., 2005. The structural development of the German North Sea sector during the Tertiary and the Early Quaternary. *Zeitschrift der Deutschen Gesellschaft für Geowissenschaften* 156, 341–356.

- Buchardt, B., 1978. Oxygen isotope palaeotemperatures from the Tertiary period in the North Sea area. *Nature* 275, 121-123.
- Cameron, T.D.J., Stoker, M.S., Long, D., 1987. The history of Quaternary sedimentation in the UK sector of the North Sea Basin. *Journal of the Geological Society* 144, 43-58.
- Cartwright, J. A., Haddock, R.C., Pinheiro, L.M., 1993. The lateral extent of sequence boundaries. *Geological Society, London, Special Publications* 71, 15-34.
- Carvajal, C., Steel, R., Petter, A., 2009. Sediment supply: The main driver of shelf-margin growth. *Earth-Science Reviews* 96, 221-248.
- Clausen, O.R., Gregersen, U., Michelsen, O., Sorensen, J.C., 1999. Factors controlling the Cenozoic sequence development in the eastern parts of the North Sea. *Journal of the Geological Society* 156, 809-816.
- Clausen, O.R., Śliwińska, K.K., Gołdowski, B., 2012. Oligocene climate changes controlling forced regression in the eastern North Sea. *Marine and Petroleum Geology* 29, 1-14.
- Crumeyrolle, P., Renaud, I., Suiter, J., 2007. The use of two- and three-dimensional seismic to understand sediment transfer from fluvial to deepwater via sinuous channels: example from the Mahakam shelf and comparison with outcrop data (south central Pyrenees). *Geological Society, London, Special Publications* 277, 85-103.
- Davies, R.J., Posamentier, H.W., 2005. Geologic processes in sedimentary basins inferred from three-dimensional seismic imaging. *GSA Today* 15, 4-9.
- Dixon, J.F., Steel, R.J., Olariu, C., 2012. Shelf-Edge Delta Regime As A Predictor of Deep-Water Deposition. *Journal of Sedimentary Research* 82, 681-687.
- Donders, T., Verreussel, R., van Helmond, N., Munsterman, D., Ten Veen, J., Speijer, R., Weijers, J., Sangiorgi, F., Reichart, G-J., Damsté, J-S., Lourens, L., Kuhlmann, G., Brinkhuis, H., n.d. Early Pleistocene glaciations exhibit predominant Northern Hemisphere forcing. In Prep.
- Dowdeswell, J.A., Ottesen, D., 2013. Buried iceberg ploughmarks in the early Quaternary sediments of the central North Sea: a two-million year record of glacial influence from 3D seismic data. *Marine Geology* 344, 1-9.
- Fongngern, R., Olariu, C., Steel, R.J., Krézsek, C., 2015. Clinoform Growth in a Miocene, Para-Tethyan Deep Lake Basin: Thin Topsets, Irregular Foresets, and Thick Bottomsets. *Basin Research*.
- Galloway, W.E., 2002. Paleogeographic Setting and Depositional Architecture of a Sand-Dominated Shelf Depositional System, Miocene Utsira Formation, North Sea Basin. *Journal of Sedimentary Research* 72, 476-490.

- Gawthorpe, R.L., Fraser, A.J., Collier, R.E.L., 1994. Sequence stratigraphy in active extensional basins: implications for the interpretation of ancient basin-fills. *Marine and Petroleum Geology* 11, 642–658.
- Gee, M.J.R., Gawthorpe, R.L., 2006. Submarine channels controlled by salt tectonics: Examples from 3D seismic data offshore Angola. *Marine and Petroleum Geology* 23, 443–458.
- Gibbard, P.L., West, R.G., Zagwijn, W.H., Balson, P.S., Burger, A.W., Funnell, B.M., Jeffery, D.H., de Jong, J., van Kolfschoten, T., Lister, A.M., Meijer, T., Norton, P.E.P., Preece, R.C., Rose, J., Stuart, A.J., Whiteman, C.A., Zalasiewicz, J.A., 1991. Early and early Middle Pleistocene correlations in the southern North Sea basin. *Quaternary International* 10, 23–52.
- Gołędowski, B., Nielsen, S.B., Clausen, O.R., 2012. Patterns of Cenozoic sediment flux from western Scandinavia. *Basin Research* 24, 377–400.
- Hampson, G.J., Graham, G.H., Holgate, N.E., Morris, J.E., Patruno, S., Sech, R.P., Petersen, S.A., Jackson, C.-L., Jackson, M.D., Johnson, H., 2015. Sedimentological Characterisation, Impact and Modelling of Clinoforms in Shallow Marine Reservoirs. *Sedimentology of Paralic Reservoirs: Recent Advances and their Applications Conference Abstract*.
- Haq, B.U., 1988. Mesozoic and Cenozoic chronostratigraphy and cycles of sea-level change. *SEPM Special Publication* 42, 71–108.
- Harding, R., Huuse, M., 2015. Salt on the move: Multi stage evolution of salt diapirs in the Netherlands North Sea. *Marine and Petroleum Geology* 61, 39–55.
- Helland-Hansen, W., Gjelberg, J.G., 1994. Conceptual basis and variability in sequence stratigraphy : a different perspective 92, 31–52.
- Helland-Hansen, W., Hampson, G.J., 2009. Trajectory analysis: concepts and applications. *Basin Research* 21, 454–483.
- Henriksen, S., Hampson, G.J., Helland-Hansen, W., Johannessen, E.P., Steel, R.J., 2009. Shelf edge and shoreline trajectories, a dynamic approach to stratigraphic analysis. *Basin Research* 21, 445–453.
- Henriksen, S., Helland-Hansen, W., Bullimore, S., 2011. Relationships between shelf-edge trajectories and sediment dispersal along depositional dip and strike: A different approach to sequence stratigraphy. *Basin Research* 23, 3–21.
- Hudec, M.R., Jackson, M.P. a., 2007. Terra infirma: Understanding salt tectonics. *Earth-Science Reviews* 82, 1–28.
- Huisman, D.J., Klaver, G.T., 2007. Heavy Minerals in the subsurface: Tracking sediment sources in three dimensions, *Developments in Sedimentology, Developments in Sedimentology* 58, 869–885.

- Huuse, M., 2002. Cenozoic uplift and denudation of southern Norway: insights from the North Sea Basin. Geological Society, London, Special Publications 196, 209–233.
- Huuse, M., Clausen, O.R., 2001. Morphology and origin of major Cenozoic sequence boundaries in the eastern North Sea Basin: top Eocene, near-top Oligocene and the mid-Miocene unconformity. *Basin Research* 13, 17–41.
- Huuse, M., Lykke-Andersen, H., Michelsen, O., 2001. Cenozoic evolution of the eastern Danish North Sea. *Marine Geology* 177, 243–269.
- Janocko, M., Nemec, W., Henriksen, S., Warchoř, M., 2013. The diversity of deep-water sinuous channel belts and slope valley-fill complexes. *Marine and Petroleum Geology* 41, 7–34.
- Japsen, P., Chalmers, J. A., 2000. Neogene uplift and tectonics around the North Atlantic: Overview. *Global and Planetary Change* 24, 165–173.
- Japsen, P., Green, P.F., Nielsen, L.H., Rasmussen, E.S., Bidstrup, T., 2007. Mesozoic-Cenozoic exhumation events in the eastern North Sea Basin: A multi-disciplinary study based on palaeothermal, palaeoburial, stratigraphic and seismic data. *Basin Research* 19, 451–490.
- Jones, G.E.D., Hodgson, D.M., Flint, S.S., 2015. Lateral variability in clinoform trajectory, process regime, and sediment dispersal patterns beyond the shelf-edge rollover in exhumed basin margin-scale clinoforms. *Basin Research* 27 (6), 1–24.
- Jordt, H., Faleide, J.I., Bjørlykke, K., Ibrahim, M.T., 1995. Cenozoic sequence stratigraphy of the central and northern North Sea Basin: tectonic development, sediment distribution and provenance areas. *Marine and Petroleum Geology* 12, 845–879.
- Knox, R.W.O.B., Bosch, J.H.A., Rasmussen, E.S., Heilmann-Clausen, C., Hiss, M., De Lugt, I.R., Kasiński, J., King, C., Köthe, A., Słodkowska, B., Standke, G. & Vandenberghe, N., 2010. Cenozoic. In: Doornenbal, J.C. and Stevenson, A.G. (editors): *Petroleum Geological Atlas of the Southern Permian Basin Area*. EAGE Publications b.v. (Houten): 211–223.
- Kockel, F., 2002. Rifting processes in NW-Germany and the German North Sea sector. *Geologie en Mijnbouw/Netherlands Journal of Geosciences* 81, 149–158.
- Konradi, P.B., 1996. Foraminiferal biostratigraphy of the post-mid-Miocene in the Danish Central Trough, North Sea. Geological Society, London, Special Publications 117, 15–22.
- Kooi, H., Hettema, M., Cloetingh, S., 1991. Lithospheric dynamics and the rapid pliocene-quaternary subsidence phase in the southern north sea basin. *Tectonophysics* 192, 245–259.

- Köthe, A., 2012. A revised Cenozoic dinoflagellate cyst and calcareous nannoplankton zonation for the German sector of the southeastern North Sea Basin. *Newsletters on Stratigraphy* 45, 189–220.
- Koyi, H. A., 2001. Modeling the influence of sinking anhydrite blocks on salt diapirs targeted for hazardous waste disposal. *Geology* 29, 387–390.
- Kuhlmann, G., de Boer, P.L., Pedersen, R.B., Wong, T.E., 2004. Provenance of Pliocene sediments and paleoenvironmental changes in the southern North Sea region using Samarium–Neodymium (Sm/Nd) provenance ages and clay mineralogy. *Sedimentary Geology* 171, 205–226.
- Kuhlmann, G., Langereis, C., Munsterman, D., Jan van Leeuwen, R., Verreussel, R., Meulenkamp, J., Wong, T., 2006a. Chronostratigraphy of Late Neogene sediments in the southern North Sea Basin and paleoenvironmental interpretations. *Palaeogeography, Palaeoclimatology, Palaeoecology* 239, 426–455.
- Kuhlmann, G., Langereis, C.G., Munsterman, D., Leeuwen, R. Van, Verreussel, R., Meulenkamp, J.E., Wong, T.E., 2006. Integrated chronostratigraphy of the Pliocene-Pleistocene interval and its relation to the regional stratigraphical stages in the southern North Sea region. *Netherlands Journal of Geosciences / Geologie en Mijnbouw* 85 (1), 19–35.
- Kuhlmann, G., Wong, T.E., 2008. Pliocene paleoenvironment evolution as interpreted from 3D-seismic data in the southern North Sea, Dutch offshore sector. *Marine and Petroleum Geology* 25, 173–189.
- Lisiecki, L.E., Raymo, M.E., 2005. A Pliocene-Pleistocene stack of 57 globally distributed benthic $\delta^{18}O$ records. *Paleoceanography* 20, 1–17.
- Martinsen, O.J., Helland-Hansen, W., 1995. Strike variability of clastic depositional systems: does it matter for sequence-stratigraphic analysis? *Geology* 23, 439–442.
- Maslin, M.A., Li, X.S., Loutre, M.-F., Berger, A., 1998. The contribution of orbital forcing to the progressive intensification of Northern Hemisphere glaciation. *Quaternary Science Reviews* 17, 411–426.
- Meijer, T., Cleveringa, P., Munsterman, D.K., Verreussel, R.M.C.H., 2006. The Early Pleistocene Praetigian and Ludhamian pollen stages in the North Sea Basin and their relationship to the marine isotope record. *Journal of Quaternary Science* 21, 307–310.
- Miller, K., Mountain, G., Wright, J., Browning, J., 2011. A 180-Million-Year Record of Sea Level and Ice Volume Variations from Continental Margin and Deep-Sea Isotopic Records. *Oceanography* 24, 40–53.
- Miller, K.G., Kominz, M.A., Browning, J. V, Wright, J.D., Mountain, G.S., Katz, M.E., Sugarman, P.J., Cramer, B.S., Christie-Blick, N., Pekar, S.F., 2005. The Phanerozoic Record of Global Sea-Level Change. *Science* 310, 1293–1298.

- Miller, K.G., Mountain, G.S., Browning, J. V., Katz, M.E., Monteverde, D., Sugarman, P.J., Ando, H., Bassetti, M. A., Bjerrum, C.J., Hodgson, D., Hesselbo, S., Karakaya, S., Proust, J.N., Rabineau, M., 2013. Testing sequence stratigraphic models by drilling Miocene foresets on the New Jersey shallow shelf. *Geosphere* 9, 1236–1256.
- Mitchum Jr., R.M., Vail, P.R., Sangree, J.B., 1977. Seismic stratigraphy and global changes of sea level, Part six: stratigraphic interpretation of seismic reflection patterns in depositional sequences. *Seismic Stratigraphy — applications to hydrocarbon exploration* 117–134.
- Møller, L.K., Rasmussen, E.S., Clausen, O.R., 2009. Clinoform migration patterns of a Late Miocene delta complex in the Danish Central Graben; implications for relative sea-level changes. *Basin Research* 21, 704–720.
- Nalpas, T., Le Douaran, S., Brun, J.-P., Unternehr, P., Richert, J.-P., 1995. Inversion of the Broad Fourteens Basin (offshore Netherlands), a small-scale model investigation. *Sedimentary Geology* 95, 237–250.
- Neal, J., Abreu, V., 2009. Sequence stratigraphy hierarchy and the accommodation succession method. *Geology* 37, 779–782.
- Nielsen, L., Clemmensen, L.B., 2009. Sea-level markers identified in ground-penetrating radar data collected across a modern beach ridge system in a microtidal regime. *Terra Nova* 21, 474–479.
- Noorbergen, L.J., Lourens, L.J., Munsterman, D.K., Verreussel, R.M.C.H., 2015. Stable isotope stratigraphy of the early Quaternary of borehole Noordwijk, southern North Sea. *Quaternary International*. 386, 148–157.
- Olariu, C., Steel, R.J., 2009. Influence of point-source sediment-supply on modern shelf-slope morphology: implications for interpretation of ancient shelf margins. *Basin Research* 21, 484–501.
- Olariu, M.L., Carvajal, C.R., Olariu, C., Steel, R.J., 2012. Deltaic process and architectural evolution during cross-shelf transits, Maastrichtian Fox Hills Formation, Washakie Basin, Wyoming. *AAPG Bulletin* 96, 1931–1956.
- Overeem, I., Weltje, G.J., Bishop-Kay, C., Kroonenberg, S.B., 2001. The Late Cenozoic Eridanos delta system in the Southern North Sea Basin: a climate signal in sediment supply? *Basin Research* 13, 293–312.
- Patruno, S., Hampson, G.J., Jackson, C. A L., Whipp, P.S., 2014. Quantitative progradation dynamics and stratigraphic architecture of ancient shallow-marine clinoform sets: A new method and its application to the Upper Jurassic Sognefjord Formation, Troll Field, offshore Norway. *Basin Research* 27 (4), 412–452.
- Patruno, S., Hampson, G.J., Jackson, C.A.-L., 2015. Quantitative characterisation of deltaic and subaqueous clinoforms. *Earth-Science Reviews* 142, 79–119.

- Pekar, S.F., Christie-Blick, N., Kominz, M. A., Miller, K.G., 2002. Calibration between eustatic estimates from backstripping and oxygen isotopic records for the Oligocene. *Geology* 30, 903–906.
- Porebski, S.J., Steel, R.J., 2006. Deltas and Sea-Level Change. *Journal of Sedimentary Research* 76, 390–403.
- Porębski, S.J., Steel, R.J., 2003. Shelf-margin deltas: Their stratigraphic significance and relation to deepwater sands. *Earth-Science Reviews* 62, 283–326.
- Posamentier, H.W., 2004. Seismic Geomorphology: Imaging Elements of Depositional Systems from Shelf to Deep Basin Using 3D Seismic Data: Implications for Exploration and Development. Geological Society, London, Memoirs 29, 11–24.
- Posamentier, H.W., Allen, G.P., 1993. Variability of the sequence stratigraphic model: effects of local basin factors. *Sedimentary Geology* 86, 91–109.
- Posamentier, H.W., Allen, G.P., James, D.P., Tesson, M., 1992. Forced regressions in a sequence stratigraphic framework: concepts, examples, and exploration significance. *American Association of Petroleum Geologists Bulletin* 76 (11), 1687–1709.
- Posamentier, H.W., Kolla, V., 2003. Seismic Geomorphology and Stratigraphy of Depositional Elements in Deep-Water Settings. *Journal of Sedimentary Research* 73, 367–388.
- Posamentier, H.W., Vail, P.R., 1988. Eustatic controls on clastic deposition II — Sequence and systems tract models. *SEPM Special Publication* 42, 125–154.
- Purves, S.J., Henderson, J., Leppard, C., 2007. Rgb Visualisation Based Delineation of Geological Elements from Volumetric Spectral Decomposition of 3d Seismic Data. Extended abstracts EAGE 69th Conference & Exhibition London, UK, 11 - 14 June.
- Rasmussen, E.S., Vejbaek, O. V, Bidstrup, T., Piasecki, S., Dybkjær, K., 2005. Late Cenozoic depositional history of the Danish North Sea Basin: implications for the petroleum systems in the Kraka, Halfdan, Siri and Nini fields. Geological Society, London, Petroleum Geology Conference series 6, 1347–1358.
- Remmelts, G., 1996. Salt tectonics in the southern North Sea, the Netherlands, in: *Geology of Gas and Oil under the Netherlands*. 143–158.
- Remmelts, G., 1995. Fault-Related Salt Tectonics in the Southern North Sea, The Netherlands. *AAPG Memoir* 65, 261–272.
- Ruddiman, W.F., Raymo, M., McIntyre, a., 1986. Matuyama 41,000-year cycles: North Atlantic Ocean and northern hemisphere ice sheets. *Earth and Planetary Science Letters* 80, 117–129.

- Ryan, M.C., Helland-Hansen, W., Johannessen, E.P., Steel, R.J., 2009. Erosional vs. accretionary shelf margins: The influence of margin type on deepwater sedimentation: An example from the Porcupine Basin, offshore western Ireland. *Basin Research* 21, 676–703.
- Sørensen, J., Gregersen, U., 1997. High-frequency sequence stratigraphy of Upper Cenozoic deposits in the central and southeastern North Sea areas. *Marine and Petroleum Geology* 14, 99–123.
- Sørensen, J.C., Michelsen, O., 1995. Upper Cenozoic sequences in the southeastern North Sea Basin. *Bulletin of the Geological Society of Denmark* 42, 74–95.
- Steckler, M.S., Mountain, G.S., Miller, K.G., Christie-Blick, N., 1999. Reconstruction of Tertiary progradation and clinoform development on the New Jersey passive margin by 2-D backstripping. *Marine Geology* 154, 399–420.
- Steel, R., Carvajal, C., Olariu, C., Petter, A., Plink-bjorklund, P., Sanchez, C., 2010. Shelf-Margin Trajectories : Significance for Sediment By-Pass. *Search and Discovery Article* 50297.
- Steel, R.J., Olsen, T., 2002. Clinoforms, clinoform trajectories and deepwater sands. *Sequence Stratigraphic Models for Exploration and Production: Evolving Methodology, Emerging Models and Application Histories* 367–381.
- Stuart, J.Y., Huuse, M., 2012. 3D seismic geomorphology of a large Plio-Pleistocene delta – “Bright spots” and contourites in the Southern North Sea. *Marine and Petroleum Geology* 38, 143–157.
- Sylvester, Z., Deptuck, M.E., Prather, B.E., Pirmez, C., O’Byrne, C., 2012. Seismic stratigraphy of a shelf-edge delta and linked submarine channels in the northeastern Gulf of Mexico, *SEPM Special Publication* 99, 31-59.
- Ten Veen, J.H., Geel, C.R., Kunakbayeva, G., Donders, T.H., Verreusel, R.M.C.H., 2011. Property prediction of Plio-Pleistocene sediments in the A15 shallow gas systems. TNO Report. TNO-060-UT-2011-01184/C.
- Ten Veen, J.H., van Gessel, S.F., den Dulk, M., 2012. Thin- and thick-skinned salt tectonics in the Netherlands; a quantitative approach. *Netherlands Journal of Geosciences* 91, 447–464.
- Ten Veen, J.H., Verweij, H., Donders, T., Geel, K., de Bruin, G., Munsterman, D., Verreussel, R., Daza Cajigal, V., Harding, R., Cremer, H., 2013. Anatomy of the Cenozoic Eridanos Hydrocarbon System. TNO Report R10060.
- Thöle, H., Gaedicke, C., Kuhlmann, G., Reinhardt, L., 2014. Late Cenozoic sedimentary evolution of the German North Sea? A seismic stratigraphic approach. *Newsletters on Stratigraphy* 47, 299–329.

- Trampe, A.F., Lutz, R., Franke, D., Thöle, H., Arfai, J., 2013. Shallow gas in Cenozoic sediments of the Southern North Sea, in: EGU General Assembly Conference Abstracts. p. 1835.
- Vail, I., Mitchum, R.M., Thompson, S., 1977. Seismic stratigraphy and global changes of sea level, Part IV: Global cycles of relative changes of sea level. In: Stratigraphic interpretations of seismic data. American Association of Petroleum Geologists 26, 83–97.
- Vail, P.R., Seismic Stratigraphy Interpretation Using Sequence Stratigraphy Part I : Seismic Stratigraphy Interpretation Procedure. AAPG Studies in Geology 27 (1), 1-10.
- White, N., Lovell, B., 1997. Measuring the pulse of a plume with the sedimentary record. Nature 387, 888–891.
- Ziegler, P. A., 1992. European Cenozoic rift system. Tectonophysics 208, 91–111.
- Ziegler, P.A., 1990. Tectonic and palaeogeographic development of the North Sea rift system, in: Tectonic Evolution of the North Sea Rifts. Oxford Science Publications Oxford, 1–36.

CHAPTER 4

DEEP WATER SEDIMENTARY SYSTEMS
LINKED TO SHELF EDGE TRAJECTORY AND
GLOBAL SEA LEVEL

CHAPTER 4: DEEP WATER SEDIMENTARY SYSTEMS LINKED TO SHELF EDGE TRAJECTORY AND GLOBAL SEA LEVEL

Rachel Harding¹, Mads Huuse¹, Rob Gawthorpe²,

¹School of Earth, Environmental and Atmospheric Sciences, University of Manchester

²Department of Earth Sciences, University of Bergen, Norway

4.0 ABSTRACT

In this study we use basin-wide 3D seismic data, calibrated by well data from the Plio-Pleistocene of the southern North Sea to link deep water sedimentary systems to marine isotope stages. The study focuses on *Single Feeder* basin floor fans and Multiple Line Source slope channel systems in the Netherlands North Sea between 4.2 Ma and 2.15 Ma, spanning the Late Pliocene to the Earliest Quaternary glacial-interglacial cycles. The systems are linked to their updip shelf properties and the trajectory of the shelf edge. *Single Feeder* systems comprise an incised valley system, canyon and basin floor fan and are associated with a descending shelf edge trajectory. Multiple Line Source systems comprise of many sediment input points along a slope and occur at several different shelf edge trajectory scenarios, suggesting that they can occur at many points of a base level curve. The link of the two types of system to the global sea level curve has shown that many more deep water depositional systems than there are eustatic cycles, which has implications for sequence stratigraphy. This study shows that sediment can be transported to the deep water when relative sea level is rising and sediment supply is high. The deposition of reservoir quality sediments basinwards of the shelf edge can be moderately predictable but knowledge of the regional lateral variability of the basin, seismic geomorphology of the shelf, sediment supply and knowledge of the basin relationship to the global sea level curve is imperative.

4.1 INTRODUCTION

Submarine channels are incised conduits for sediment transport downslope and act as the main transport mechanism for coarse-grained sediment from the shelf to the basin floor (Khripounoff et al., 2003; Gee and Gawthorpe, 2006; Piper and Normark, 2009). Ancient basin floor fans are a key target for hydrocarbon exploration due to their ability to stratigraphically trap hydrocarbons. Slope and basin floor depositional systems are affected by base level, sediment supply, shelf geomorphology and process type on the shelf and therefore the prediction of their place within the sequence stratigraphic framework can be complex (Vail et al., 1977; Posamentier and Vail, 1988; Carvajal and Steel, 2006; Steel et al., 2010; Flint et al., 2011; Dixon et al., 2012ab; Jones et al., 2015).

Early sequence stratigraphic models placed the sediment transfer basinwards of the shelf edge within lowstands of global sea level (Vail et al., 1977), and within the Lowstand Systems Tract (LST) comprising the basin floor fan, slope fan and prograding wedge (Posamentier and Vail, 1988). Fall in relative sea level below the shelf edge enables river systems to reach the shelf edge and directly supply coarse-grained sediment into deep water settings (Johannessen and Steel, 2005). Many modern submarine fans, such as the Indus, Amazon, Mississippi and Bengal, have become inactive during the Holocene highstand of sea level as sediment is stored on the shelf (Leeder, 2009). However, transfer of sediment to the basin floor occurs during the Highstand Systems Tract (HST) in ancient and modern systems with high sediment supply, narrow shelf width and tectonic uplift are identified as key factors which can override eustatic sea level (Kolla and Perlmutter, 1993; Gawthorpe et al., 1994; Burgess and Hovius, 1998; Carvajal and Steel, 2006; Covault et al., 2007; Henriksen et al., 2011). In supply driven systems, for instance, the coastline can reach the shelf edge regardless of the relative sea level condition (Porebski and Steel, 2006).

If the coastline is entrenched at the shelf edge during LST conditions this does not necessarily translate to significant sand volumes transferred to the basin floor (Dixon et al., 2012b). Delta process regime influences whether sediment is transferred past the shelf edge. River-dominated deltas are shown to transfer sediment regardless of base level, and wave-dominated and tidal-dominated deltas are less likely to have associated

basin floor deposition even in LST conditions (Dixon et al., 2012ab; Jones et al., 2015). Shelf-prisms are built out during lower order cycles than shorelines, largely occurring over 1-10 million year timescales (Henriksen et al., 2011) and are less likely than the shoreline to be affected by the autogenic processes (Steel and Olsen, 2002).

Studying the architecture of shelf-prism clinoforms can be indicative of the sediment partitioning landwards and basinwards of the shelf edge. Sigmoidal clinoforms, with high topset preservation and ascending shelf edge trajectories, are indicative of sediment trapped on the shelf (Henriksen et al., 2011) and therefore accommodation on the shelf (Jones et al., 2015). Oblique-tangential clinoforms, with no topset preservation and flat to descending shelf edge trajectories, suggest little accommodation on the shelf and sediment partitioning basinwards of the shelf edge (Helland-Hansen and Hampson, 2009; Ryan et al., 2009).

In this study we use basin-wide 3D seismic data, calibrated by well data from the Plio-Pleistocene of the southern North Sea to link deep water sedimentary systems to marine isotope stages (MIS) for the first time (Fig. 4.1). The study focuses on *Single Feeder* basin floor fans and Multiple Line Source slope channel systems in the Netherlands North Sea between 4.2 Ma and 2.15 Ma, spanning the Late Pliocene to the Earliest Quaternary glacial-interglacial cycles (Fig. 4.2).

Single Feeder systems refer to single incision into the slope, fed by an incising system on the shelf which deposits unconfined sediment at the base of slope. The Multiple Line Source systems refer to systems where there are multiple entry points along strike of the slope, mainly depositing confined and unconfined sediment on the lower slope.

Submarine channel and lobe architectures in slope to basinal settings can be directly linked to the shelf edge trajectory and shelf-prism clinoform stacking patterns, within a high resolution chronostratigraphic framework (<100,000 years). Palynological and geochemical proxies allow linkage of the depositional architectures to regional sea level and climate (Kuhlmann et al., 2006a; Donders et al., in prep). This allows an evaluation of the importance of eustacy on the delivery of sediment basinwards of the shelf edge. This has implications for sequence stratigraphic models and the prediction of reservoir sands.

4.1.1 Geological Setting

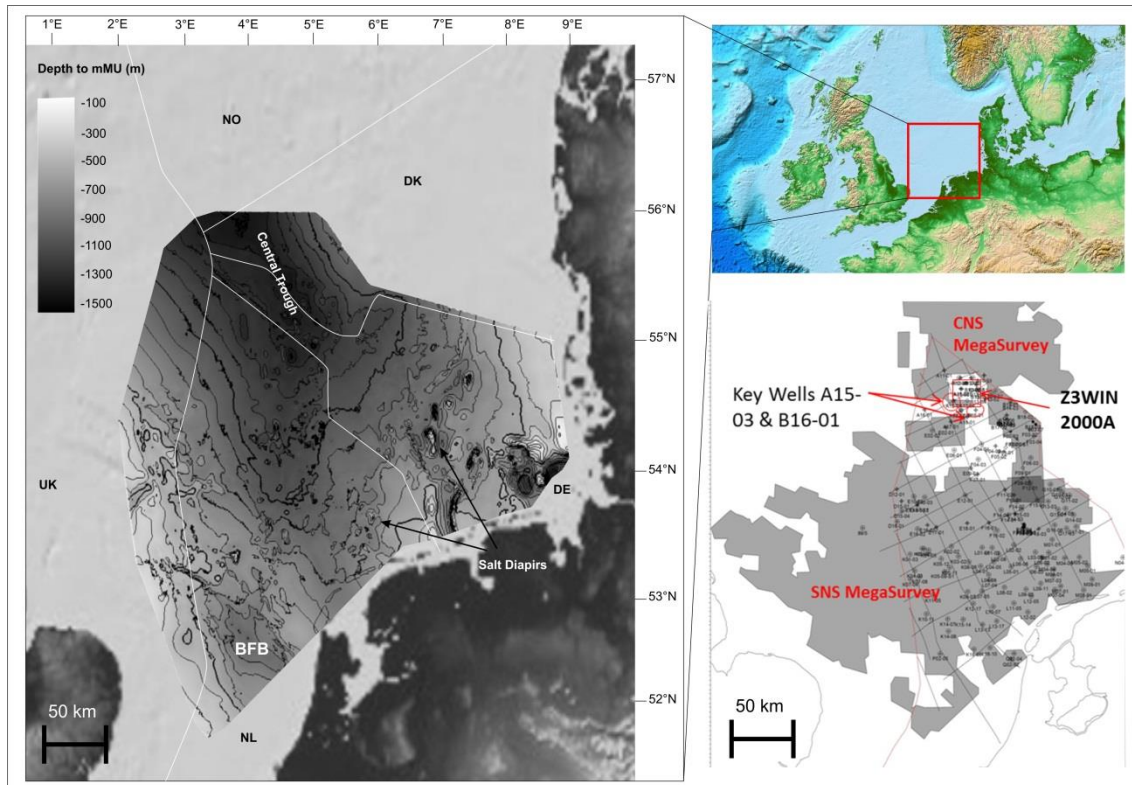


Figure 4.1 Regional setting and dataset map. Left: Mid Miocene Unconformity (mMU) depth structure map. Map is the result of seismic interpretation from this study, (UK, NL and DK sectors) combined with the German mMU structure map from Geopotenzial Deutsche Nordsee project (www.gpdn.de). Key areas of Late Cenozoic accommodation creation marked, Central Trough and BFB (Broad Fourteens Basin). NL Netherlands; DE Germany; DK Denmark; NO Norway. Top Right: GEBCO bathymetry for North Sea showing location of dataset within the contemporary setting. Bottom right: Dataset map. Grey areas represent 3D continuous seismic coverage. 2D seismic lines and key boreholes used for chronostratigraphic framework also shown.

The southern North Sea is an intra-cratonic basin, dominated by the interaction of structural elements associated with the E-W-trending Southern Permian Basin and the NW-SE/NNE-SSW Mesozoic rift basins which were inverted during the Late Cretaceous to Early Paleogene (Ziegler, 1992; Remmelts, 1995). Salt structures are a key feature of the southern North Sea. Halokinesis of halite from the Permian Zechstein supergroup occurred during both the Mesozoic and Cenozoic (Remmelts, 1996), and continued to the Quaternary and recent times in some areas (ten Veen et al., 2012; Harding and Huuse, 2015).

From the Late Miocene to Quaternary the southern North Sea was the southern part of an increasingly narrowing north-south elongate basin with a strong tidal regime (Galloway, 2002) dominated by fine-grained marine to fluvio-deltaic sediments (Cameron et al., 1987; Kuhlmann et al., 2006b) from the Baltic river system, (Bijlsma, 1981; Gibbard et al., 1991), with additional contributions from the proto-Rhine, Meuse, Scheldt, Weser and Elbe (Kuhlmann et al., 2006b; Huisman and Klaver, 2007).

Sediment input was from the NE and east in the late Miocene-Pliocene in the German and Dutch sectors, and from the E to SE in the Netherlands sector in the Pleistocene (Overeem et al., 2001; Kuhlmann and Wong, 2008; Anell et al., 2012; Thöle et al., 2014). The dominant seismic architecture of the Netherlands North Sea in the Plio-Pleistocene is of shelf-prism clinoforms 100-400 m high, downlapping on the mid Miocene Unconformity (mMU), a regional seismic reflection (Fig. 4.1). Within the dataset, delta-scale clinoforms (<100 m) are also identified, superimposed on larger shelf-prism clinoforms (Fig. 4.3).

4.1.2 Chronostratigraphic Framework

The linking of the deep water sedimentation to eustacy relies on a robust chronostratigraphic framework for the basin. The stratigraphy of the Plio-Pleistocene Netherlands North Sea is constrained by high resolution chronostratigraphic, lithological, quantitative palynological and geochemical data from core and palaeomagnetic logs for wells *A15-03* and *A15-04*, linked to the gamma ray log and seismic character in the north Netherlands North Sea (Kuhlmann et al., 2006ab; Kuhlmann and Wong, 2008). This is utilized in this study to create a basin-wide chronostratigraphic framework (Fig. 4.2). Additional work has been carried out by ten Veen et al. (2011, 2013) and Donders et al. (in prep) to expand and refine the framework and is now complimented by biostratigraphy and benthic stable isotope analysis from the Noordwijk borehole, onshore Netherlands (Meijer et al., 2006; Noorbergen et al., 2015).

Key dates used in this study correspond to magnetic reversals. The base Quaternary corresponds to the Gauss-Matuyama magnetic reversal, an event which correlates to

climatic degradation in the pollen record and the last occurrence of *Monspeliensina pseudotepida*, benthic foraminifera at 2.58 Ma. The Olduvai magnetic event within the Matuyama epoch is recognised also in the southern North Sea and is dated at 1.94 Ma at the base and 1.788 Ma at the top (Kuhlmann et al., 2006a). In the Netherlands North Sea the majority of post mMU sedimentation is dated between 2.58 Ma (base Quaternary) and 1.788 Ma (top Gelasian) (Fig. 4.2). Smaller scale magnetostratigraphic events, the X event at 2.43 Ma and the Reunion event at ~2.15 Ma give additional dates (Cande and Kent, 1995; Kuhlmann et al., 2006a; Noorbergen et al., 2015).

Linking patterns from palynology and geochemical studies from the Netherlands North Sea (Kuhlmann et al., 2006ab, Donders et al., in prep) and onshore Netherlands (Meijer et al., 2006; Noorbergen et al., 2015) to the Marine Isotope Stages (MIS) of the global oxygen isotope curve has allowed further dates to be identified and suggests a complex relationship between glacioeustasy and the sedimentary record in the southern North Sea (Lisiecki and Raymo, 2005).

Terrestrial to marine palynology ratios indicate proximity of the coast in the Netherlands North Sea, which transits landwards and basinwards in accordance to early Gelasian glacial-interglacial cycles (MIS 103-92) (Donder et al., in prep). This suggests that relative minimum and maximum sea level in the SNS is as expected for icehouse conditions and governed by eustasy. The similarity between the global oxygen isotope records (Lisiecki and Raymo, 2005) and the benthic stable isotope record from onshore Netherlands (Noorbergen et al., 2015) are close enough that they can be tuned to the global standard. This confirms that the regional glacial-interglacial cycles match that of the global response and thus, it is valid to attempt to understand relative sea level and basin infill in the North Sea in relation to the global sea level curve, at least for the early Gelasian time period. Sea level curves are scaled from oxygen isotope values from 57 globally distributed benthic ^{18}O records from (Lisiecki and Raymo, 2005) using assumptions given in Miller et al., (2011, 2005) (Fig. 4.2).

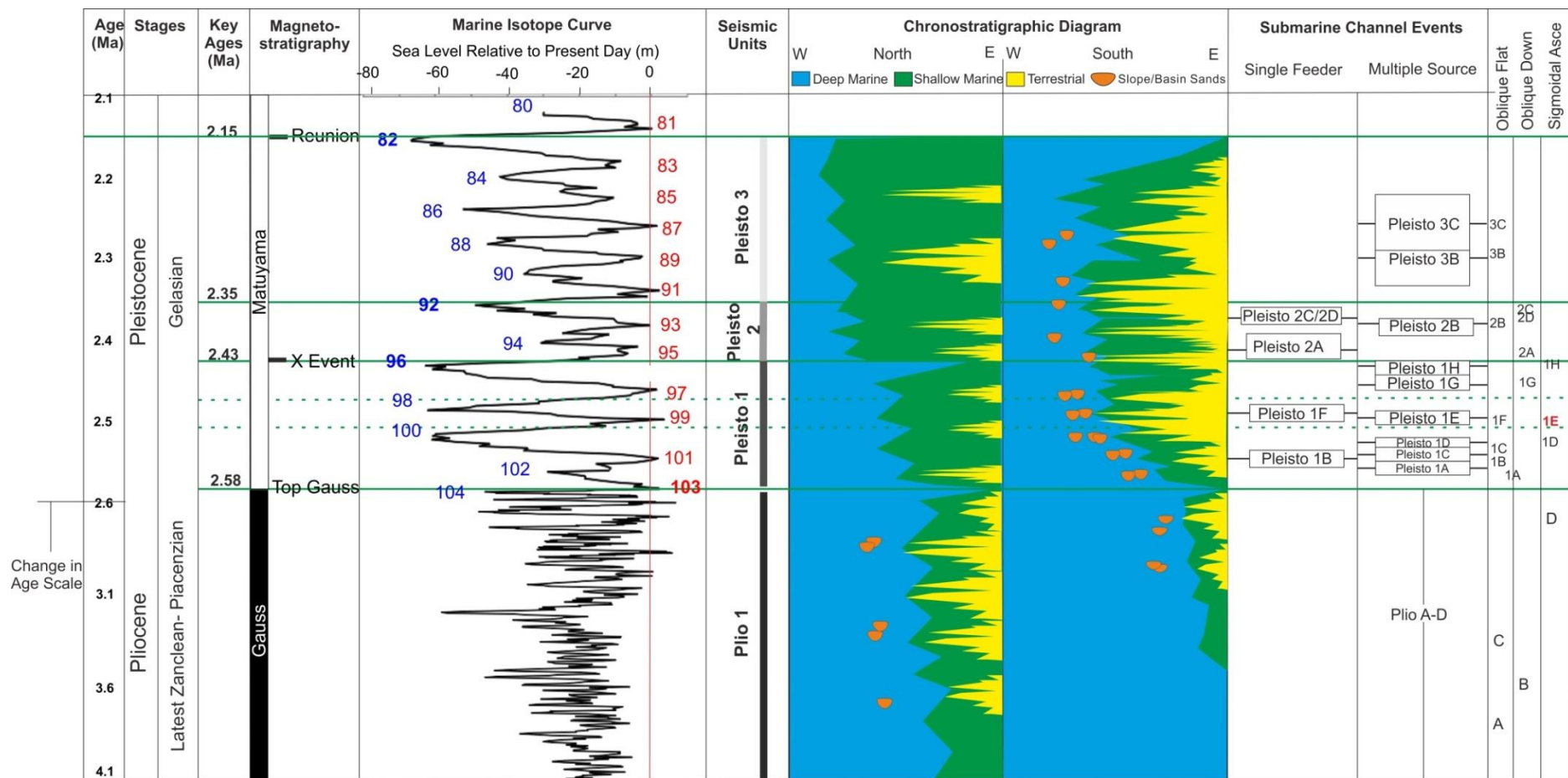


Figure 4.2. Chronostratigraphic framework (previous page). Eustatic sea level for the period 4.1-2.1 Ma. Sea level curves scaled from oxygen isotope values from 57 globally distributed benthic ^{18}O records from (Lisiecki and Raymo, 2005) using assumptions given in (Miller et al., 2011, 2005). Sea level is relative to present day. Interglacial Marine Isotope Stages (MIS) in red; Glacial MIS in blue. Green lines represent the terminations of stages. Age scale is non-linear in order to visualise the study period in one figure. Magnetostratigraphy from Kuhlmann et al. (2006a) and ten Veen et al. (2013). Seismic units discussed in greater detail in *Chapter 3*. Chronostratigraphic diagram is based on direct observations however no relative scale is intended. Submarine channel events are placed within the seismic unit at their relative position and the uncertainty is illustrated by the box outlining each event. The final column represents the shelf edge trajectories the events are associated with. Oblique Flat, Oblique Downstepping and Sigmoidal Ascending. The Sigmoidal Ascending clinoforms are associated with two different scenarios; deposited prior to a sequence boundary, (red) or where base level is rising towards a maximum flooding surface (black).

A reverse coupling of sediment grain size and sea level in the basin is noted by Kuhlmann and Wong, (2008); Noorbergen et al. (2015) and Donders et al. (in prep). Finer grained sediment is associated with the glacial cold conditions and low sea level. The finest grained material, which is interpreted to enter the basin towards the glacial stage termination, is the product of weathering metamorphic rocks of Scandinavia and a long transport route (Kuhlmann et al., 2004; Noorbergen et al., 2015). The finest grained sediments are linked to the gamma ray log and seismic character in the north Netherlands North Sea (Kuhlmann and Wong, 2008; ten Veen et al., 2011; 2013) and identified as gamma ray peaks, and are correlated to strong amplitude, semi-regional continuous seismic reflections. Coarser material associated with low gamma ray values are related to warm interglacial conditions and higher relative sea level. Therefore, though regional base level reflects glacioeustasy during the earliest Gelasian (2.58-2.35 Ma), grain size is not directly controlled by it (ten Veen et al., 2013; Donders et al, in prep). Sediment supply, local subsidence and underlying geomorphology create variability in how eustasy is expressed within the sedimentary architecture of the SNS (Chapter 3).

The base Quaternary (2.58 Ma) corresponds to a regional flooding event and top interglacial MIS 103. The X event at 2.43 Ma (Cande and Kent, 1995), a regional strong shale layer, is correlated to the termination of glacial MIS 96. Two additional regional strong shale layers between the Gauss-Matuyama magnetic reversal and the X-event correspond to the termination of glacial periods MIS 100 (~2.51 Ma) and MIS 98 (~2.48 Ma) (Kuhlmann et al., 2006a; Noorbergen et al., 2015). An additional shale layer

matches a change in palynology and is correlated to the termination of MIS 92 and therefore gives an additional date at 2.35 Ma (Donders et al., in prep).

4.2 DATASET AND METHODOLOGY

The seismic dataset for this study comprises PGS (Petroleum Geo-Services) SNS MegaSurvey, covering 40,000 km² of the Netherlands and United Kingdom sectors of the southern North Sea (Fig. 4.1) and part of the PGS CNS MegaSurvey covering ~15,000 km² of the Netherlands, Danish and German sectors. The bin spacing is 50 m x 50 m, sampling rate 4 ms TWT with a vertical resolution of maximum 10-15 m in the top 1500 m (average velocity 1.8 ms⁻¹, ten Veen et al., 2013). Well data consists of well logs, including gamma ray, sonic log and cuttings descriptions from commercial well reports for 172 wells in the Netherlands North Sea (Fig. 4.1).

Several techniques are used to interpret the submarine channel systems within the 3D seismic dataset. A combination of traditional horizon based seismic interpretation using Schlumberger Petrel v2013 and auto interpretation using Eliis PaleoScan software was used to map horizons and investigate reflections between picked horizons. For 3D visualisation, seismic geomorphology techniques such as time slicing, stratal slicing and horizon slicing, are combined with RMS amplitude extractions and RGB blending techniques using FFA Geoteric software (Posamentier and Kolla, 2003; Posamentier, 2004; Davies and Posamentier, 2005; Purves, et al., 2007).

Seismic stratigraphy was used to help determine sequences and key stratigraphic surfaces using the methodology of Mitchum et al. (1977). The approaches of Helland-Hansen and Hampson, (2009); Neal and Abreu, (2009) and Miller et al. (2013) are utilised to analyse clinoform geometries, stacking patterns and clinoform trajectories associated with the submarine channel events identified in this study.

In order to provide realistic clinoform trajectories from TWT (two-way time) seismic data the clinoforms should be back-rotated so their topsets are approximately horizontal and the clinoform height de-compacted (Pekar and Kominz, 2001; Patruno et al., 2014). Due to the role of loading on palaeotopography, topsets are largely less loaded than the bottomsets (Steckler et al., 1999) and therefore vertical differences

between the topset and bottomset are exaggerated in TWT compared to the original depositional architecture (Miller et al., 2013). Flattening on overlying topsets in order to back rotate underlying topsets is carried out to understand depositional trajectories of the clinoforms. The datum horizons which were chosen to flatten on were topset reflections which have little depositional thickness changes across the entirety of the underlying clinoform of interest. For different areas, different topset datums were chosen. The topsets which are made up of coastal plain and shallow marine shelf were likely deposited close to horizontal (shelf angle $< 0.1^\circ$) and therefore the clinoforms should have their topsets restored to horizontal if the original depositional architecture is to be understood. This is carried out to remove the effects of post depositional tilting from subsidence which followed the deposition of the clinoforms. TWT is calibrated to depth using available industrial check shot data in the Netherlands North Sea (ten Veen et al., 2013).

4.3 SEISMIC STRATIGRAPHIC FRAMEWORK

The seismic stratigraphic framework from this study provides the context for the deep water sedimentary systems. In this section, the key bounding surfaces, the link to well data and how the well data links to climate proxies within the Plio-Pleistocene shelf-prism is discussed. The study focuses on the time period between 4.2 Ma and ~2.15 Ma and a brief overview of the basin infill is provided. The post mMU seismic section is divided into four units, dependent on the well and seismic characteristics, *Plio 1* & *Pleisto 1-3* (Figs. 4.2 & 4.3).

The dominant seismic architecture of the SNS during the study period is of highly progradational sigmoidal and oblique shelf-prism clinoforms, 100-400 m high, downlapping on to the mid Miocene Unconformity (mMU). The depositional environment of the shelf-prism scale clinoform is determined in Chapter 3 as the topset, foreset and bottomset representing the shelf, slope and basin floor respectively and the shelf-prism clinoform roll over point representing the shelf edge (Fig. 4.4).

Plio 1 seismic unit (4.2 Ma-2.58 Ma) is 1.62 Ma in duration and is the least chronostratigraphically constrained unit. *Plio 1* deposition was focused in an arcuate shape, in the far east of the Netherlands North Sea (NL) along the boundary with the

German sector (DE) (Fig. 4.3). Clinoform architectures are dominantly sigmoidal towards the north and oblique tangential towards the centre and the south of the depocentre (Fig. 4.4). Slope angles of large scale clinoforms are a maximum 4° in the southern part of the Netherlands North Sea.

Top Plio 1 is marked by a transgression and corresponds to the Gauss magnetic reversal and the termination of interglacial MIS 103 (base Quaternary, 2.58 Ma). *Top Plio 1* corresponds to a shift of depocentre further south in the Netherlands sector and to an E-W sediment input direction compared to NE-SW previously. Basin bathymetry changes significantly across the base Quaternary as at 2.58 Ma the south of the NL sector clinoforms were >300 m compared to the north of the NL sector ~ 200 m but during the early Gelasian (seismic units *Pleisto 1 -3*) the south shallows upwards during the Gelasian (2.58-1.78 Ma) and the north deepens in relative depth (Chapter 6.2). This is associated with the greater accommodation creation in the north of the Netherlands North Sea due to differential subsidence.

The *Pleisto 1* seismic unit (2.58 Ma – 2.43 Ma) is very well constrained. *Top Pleisto 1*, a regional strong amplitude reflection and shale layer, corresponds to a maximum flooding surface. The top of *Pleisto 1* corresponds with a North Sea magnetic reversal event at 2.43 Ma (X event, Cande and Kent, 1995; Kuhlmann et al., 2006; Noorbergen et al., 2015) which is correlated to the termination of glacial MIS 96 (Donders et al., in prep, Chapter 3). Two additional regional strong amplitude shale layers within *Pleisto 1* correspond to the termination of glacial period MIS 98 and 100. The correlation of regional shale layers within *Pleisto 1* allows the unit to be subdivided (Figs. 4.2 & 4.11). In most cases this surface appears to coincide or occur just below the maximum flooding surface which is identified as regional downlap surfaces basinwards of the shelf edge. *Pleisto 1* seismic unit represents the first 150,000 years of the Quaternary and the ability to subdivide this unit into single eustatic glacial interglacial cycles using the shale layers correlated to Marine Isotope Stages places a constraint of where in a glacial-interglacial cycle deep water depositional events are occurring (Fig. 4.2). The unit represents an expanded section in the SNS and shows a greater than order of magnitude increase in sedimentation (from ~3 km³ per 1000 years to ~55 km³ per 1000 years) and a change from an arcuate convex to a linear concave shelf edge from

Plio 1 to *Pleisto 1* (Fig.4.3), which suggests a change from river dominated to wave/storm dominated systems (Hampson et al., 2015).

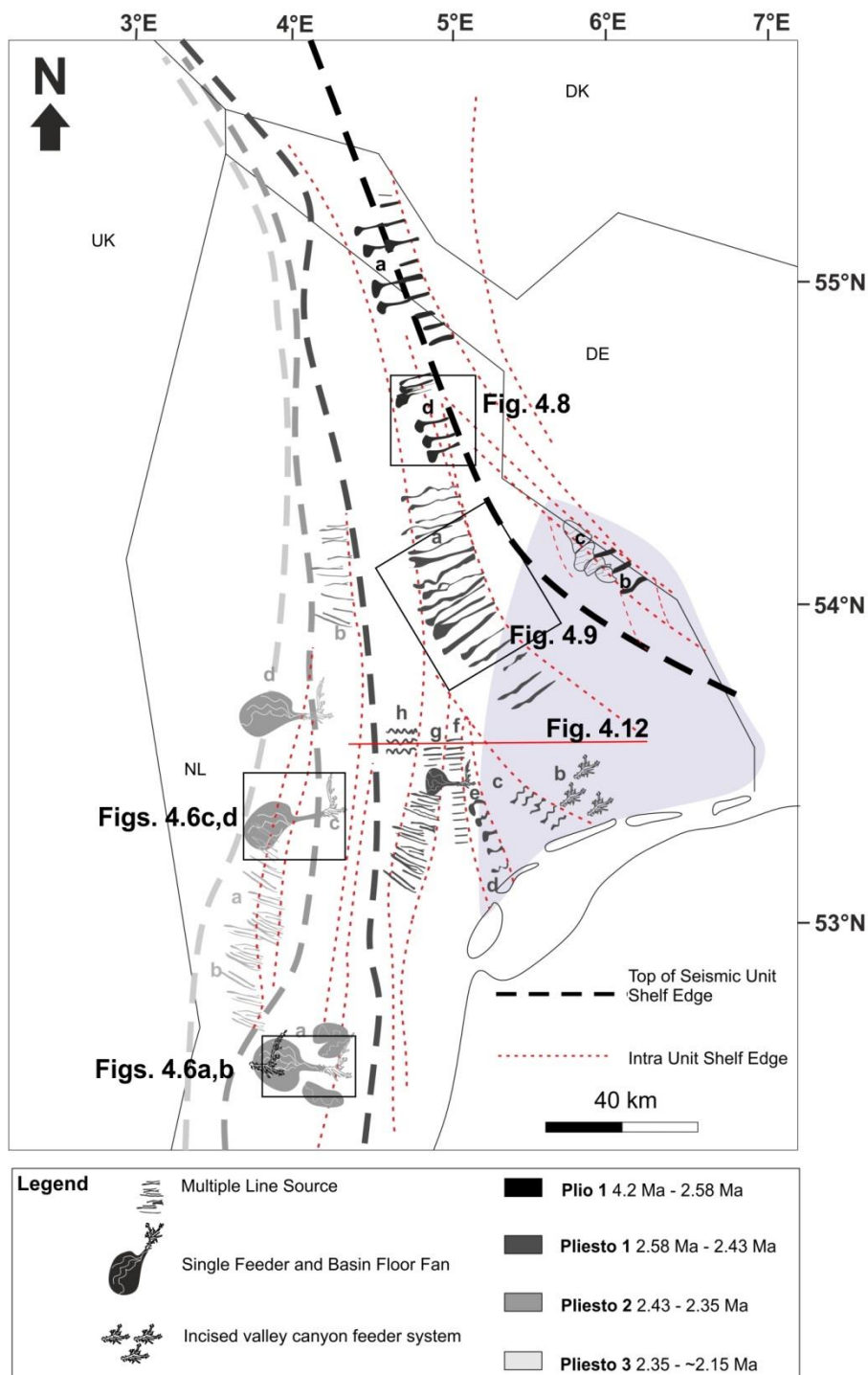


Figure 4.3 Submarine channel map (previous page). Distribution of submarine channels and adjoining basin floor deposition with relation to the seismic units. Events are labelled in the relative order of deposition. Relative positions correct, geometries implied. North Sea sectors labelled. NL Netherlands; DE Germany; DK Denmark; UK United Kingdom. Grey transparent area represents the area which is consistently terrestrial from MIS 100 to the top of the study period.

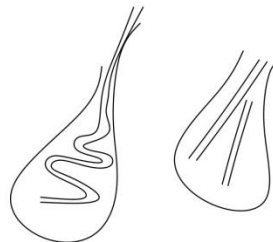
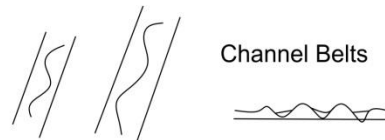
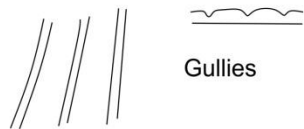
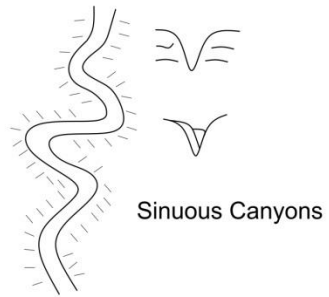
Lateral variability of the seismic units across the dataset increases after the base Quaternary with *Pleisto 1* exhibiting exceptional progradation rates of the shelf-prism in the south of the dataset, prograding ~100 km from east to west within 150,000 years, most of which occurred within the first 70,000 years of the unit (Chapter 3). This is not as clear in the north Netherlands North Sea, in the area of A15-03 well where <20 km progradation occurred during the same time period (Fig. 4.3).

The *Pleisto 2* and *Pleisto 3* seismic units shelf edges are linear and their depocentres trend north-south across the central Netherlands North Sea (Fig. 4.3). *Top Pleisto 2* is a strong amplitude downlap surface and is linked to the glacial termination of MIS 92 at 2.35 Ma. *Pleisto 3* corresponds to a downlap surface in the north Netherlands North Sea at ~2.15 Ma, and is possibly linked to the glacial termination of MIS 82.

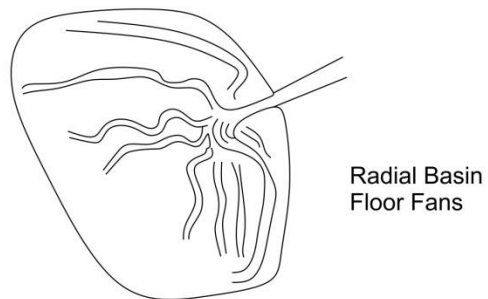
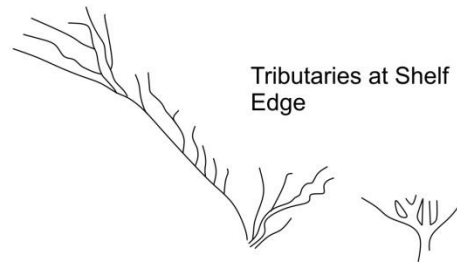
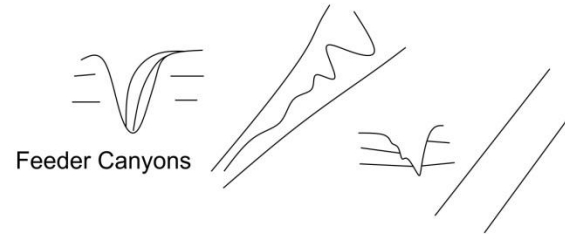
Direct evidence of glaciation is seen from *Pleisto 1* onwards, as abundant iceberg scouring events are identified (Fig. 3.19 & Chapter 6.1). Iceberg scouring events, as they are marine features, have enabled the extent of the minimum transgression to be quantified. During *Pleisto 1-3* the shelf floods back almost to the same place in the SE Netherlands North Sea throughout the Gelasian, and there is a clear area that is permanently emerged in the SE from early in *Pleisto 1* (after MIS 100, location indicated in Fig. 4.3). The distribution of deep water sedimentation and shelf edge position from *Plio 1* to *Pleisto 3* indicates the basin infill pattern (Fig. 4.3).

Figure 4.4 Seismic architectures and clinoform types (following page). Architectural elements identified within the dataset and main clinoform types identified. No scale implied. The architectural elements of the Multiple Line Source and Single Feeder Systems are found on the foreset and bottomset of the shelf-prism scale clinoforms apart from the incised valleys, present on the outer topset. Clinoform nomenclature used in this paper is illustrated on the sigmoidal clinoform architecture. Red dots represent the shelf edge.

Multiple Line Source Architectures

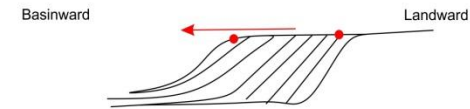


Single Feeder System Architectures

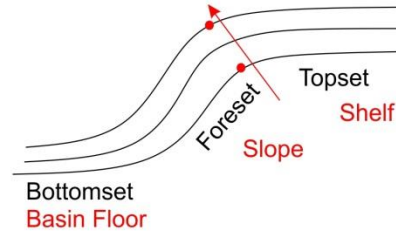


Shelf-Prism Clinoform Architectures

150-350 m Oblique Tangential/Parallel

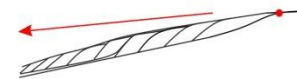


150-350 m Sigmoidal



Delta Scale Clinoform Architectures

20-80 m Intra Slope



20-70 m Intra Shelf



50-150 m Shelf Edge



4.4 DEEP WATER SEDIMENTATION

Single Feeder and *Multiple Line Source* systems identified in the southern North Sea are described in this section with relation to the reflection characteristic, reflection geometry and lithology of the systems and the link to shelf edge trajectory and proximity to coastal facies. The individual submarine channel events are detailed in Table 4.1 and Table 4.2 and the distribution is aerially and temporally mapped in Fig. 4.3. The relationship of the submarine channel systems to the architecture of the surrounding clinoforms and the shelf edge trajectories are focused on.

4.4.1 Single Feeder Systems

Five *Single Feeder* systems are described within the study period across the study area (Fig. 4.3; Table 4.1). The *Single Feeder* seismic character has three main components, present at the base of the slope (bottomset); on the slope (foreset) and on the shelf (topset) of the shelf-prism clinoform (Fig. 4.4).

The *Single Feeder* geometry at the base of slope is of strong amplitude, chaotic seismic reflections up to 50 m thick, bidirectionally downlapping onto an underlying reflection or pinching out into weak amplitudes (Figs. 4.5a & 4.6). In planform, the strong amplitudes are between 10-30 km in width and 10-18 km in length and have a channelized unconfined lobate geometry. Channels incise up to 20 m, and are infilled by strong or weak amplitudes (*Pleisto 2A* and *Pleisto 2C* examples, Fig. 4.6).

Strong amplitudes at the base of slope connect updip to a single 30-70 m deep incision into the upper slope, initiating at the shelf edge and shallowing down slope, that are typically 5-8 km in length (equal to the slope length). The incisions tend to narrow downslope from 1.5 km to 0.5 km wide. The change in incision width is associated with a change in cross section geometry from staggered sawtooth geometry on the upper slope changing to a simple “V” shaped thalweg on the lower foreset (Fig. 4.5). Chaotic reflections and smaller scale channels are identified within the incisions on the upper slope, together with individual small scale clinoforms (~50 m) which prograde down dip within the confines of the incision. The lower slope and base of slope *Single Feeder* are identified in well logs by a gamma ray decrease (60 to 30 API) with a sharp top and

base (SF7 in Fig. 3.9). Lithological descriptions through this part of the depositional system are characterised by clay interbedded with fine sand.

The *Single Feeder* Systems have a consistent seismic character on the outer shelf and at the shelf edge. The topset comprises well-preserved incised channels, exhibiting parallel to rectangular tributary planform geometry. Elongate channels, parallel to the shelf edge can extend along the shelf for up to 40 km and are either symmetrical, feeding the slope incision from both directions along the shelf, or largely from one direction (compare *Pleisto 2A* and *2C* in Fig. 4.6). Parallel channels are fed by a series of dendritic channels, shorter in length and oblique to the shelf edge (Fig. 4.6). The extent of incised systems landwards of the shelf edge is variable but typically between 5 and 20 km. The upper slope incision and tributaries are largely strong in amplitude. The shelf edge exhibits strong amplitudes in a linear band along the shelf edge (Fig. 4.6); the strong amplitudes are associated with fine to medium grained sedimentation, from calibration with lithological descriptions. Abundant wood fragments and lignite are encountered in channels on the shelf edge.

The depositional environment of the *Single Feeder* System components is described here. The incisions on the shelf are identified as incised valleys by the geometry and preservation of the dendritic tributaries valleys feeding into a main trunk valley, along the shelf edge (Posamentier, 2001). Subaerial erosion is suggested by the presence of lignite and wood fragments typical of delta plains and terrestrial settings within the tributaries on the shelf edge. Analogues for the *Single Feeder* examples in the SNS are identified off the southern coast of Brittany from the last glacial sea level fall. The Etel, Concarneau, Loreint and Villane incised valleys (Menier et al., 2006) are especially analogous in planform geometry to *Pleisto 2A* and *2C*. The incised valley feeds into an erosional slope canyon, which deposits an unconfined basin floor fan at the base of slope. Fine to medium grained sand is deposited at the base of slope, bypassing the shelf and the upper slope. The shelf is likely exposed during the incision of the incised valleys, and a river system is entrenched at the shelf edge at this time but the rest of the *Single Feeder* is submarine in origin and deposited in slope to basinal settings.

Age	Seismic Character	Input Direction	Dimensions	Maximum Slope Incision	Slope and Basin Floor Seismic Character	Shelf Seismic Character	Shelf Edge Trajectory	Sequence Position
Pleisto 1B (between MIS 103 and 100)	Incised valleys with no preserved canyon/fan. Three events on separate shelf edges.	NE-SW	Canyon 0.5 km width, 2.5 km of length preserved. tributaries cover 5 km on the shelf and are 100 m width.	46 m upper foreset.	Most of the feature is destroyed by subsequent events	Linear shelf edge. Active salt diapir topography on shelf. No topset preservation, evidence of terrestrial channels eroding topsets. Some strong amplitudes, channels weak.	Flat lying trajectory, oblique tangential clinoforms. Slope angle 3-4°.	Within expanded section of weak amplitude progradational oblique clinoforms. Likely part of one composite sequence. Constant exposure of the shelf.
Pleisto 1F (between MIS 100 and 98)	Incised valley tributaries, elongate along shelf edge feeding a single canyon to basin floor fan	E-W	Canyon 0.5 km maximum width, length of canyon 7.8 km. Basin floor fan largely not preserved. Tributaries symmetrical either side of canyon, 10 km along the shelf, tributaries normal to shelf edge maximum length 7km average 1 km length.	50 m upper foreset. 20 m on shelf.	Salt diapir later pierced through section therefore erosion of most of the basin floor fan. Estimated fan area 46.3 km ² . Some strong amplitudes on the slope associated with the canyon.	Linear shelf edge. Strong amplitudes associated with symmetrical tributaries at the shelf edge and on the outer shelf. The tributaries clearly erode the top of the underlying clinoforms.	Within a flat trajectory package of oblique clinoforms. Slope angle 2-3°.	The flat trajectory package occurs after a 40 m downstepping from aggradational sigmoidal clinoforms (associated with Pleisto 1E). Largely oblique/sigmoidal ascending clinoforms downlap onto the basin floor fan.
Pleisto 2A (between MIS 96 and 92)	Radial basin floor fan fed by single canyon with an incised valley system at the shelf edge. Main tributaries parallel to the shelf edge.	E-W	Canyon maximum width 1.5 km on the upper foreset, length of canyon 8 km. Basin floor fan max width 27 km by 17 km length. tributaries max width 1 km and extend landwards from the shelf edge 20 km and along the shelf 20 km. Fan area 280 km ² .	85 m at upper foreset, 30 m on the shelf, channels on the basin floor 20 m.	Strong amplitudes radiating from base of slope, reflections bidirectional downlap. Thickness 22 m. Weak amplitude basin floor distributary channels. Very strong amplitudes and clinoforms within canyon.	Linear shelf edge. Strong amplitude incisions parallel to the shelf, fed by tributaries that are perpendicular to the shelf edge all feeding into the canyon at the top of the foreset.	Descending (by 50 m) oblique clinoforms. Rising trajectory linked to late BF deposition and canyon infill lope angle 3-4°.	Tributaries and canyon are eroding into oblique clinoforms 50-100 m in height. Downlapping onto the basin floor fan are 100 m sigmoidal rising trajectory clinoforms.
Pleisto 2C (between MIS 96 and 92)	Radial basin floor fan fed by single canyon with an incised valley system at the shelf edge. Main tributaries parallel to the shelf edge to the north east of the canyon.	NE-SW	Canyon maximum width 1 km, length 5 km. Basin floor fan is 32 km width and 18 km in length. 20 km valley system extends along the shelf and 0.3 m width of tributaries. System extends from the shelf edge 15 km. Fan area 290 km ² .	50 m on upper foreset, 28 m on the shelf, basin floor 25 m.	Strong amplitudes on the outer fan at base of slope, distributary channels are weak amplitude. Very strong amplitudes within the canyon. Subsequent salt movement deformed fan. Thickness 53 m.	Linear shelf edge. Strong amplitude main tributaries are elongate along the shelf edge for 14 km to the NE from the canyon. Hinterland affected by salt tectonics.	Descending trajectory oblique ~70 m in height clinoforms with no little bottomset. Slope angle 1-2°.	Just above Pleisto 2B, to the north. Top Pleisto 2 MIS 92 surface is a sigmoidal clinoform of greater height covering entire area, which caps the basin floor fan system. Same event as Pleisto 2D.
Pleisto 2D (between MIS 96 and 92)	Radial basin floor fan fed by single sigmoidal canyon with an incised valley system at the shelf edge. Main tributaries parallel to the shelf edge to the south of the canyon.	E-W	Canyon maximum width 0.5 km, length 7 km. Basin floor fan estimated 10 km width by 11 km length. tributaries parallel to the shelf edge from the south for 10 km, and north for 6 km, average width 0.2 km. 140 km ² .	Canyon max on foreset 40 m, 30 m on the shelf.	Basin floor fan character bidirectional downlap of strong amplitude chaotic character pinching out into weak amplitude parallel reflections. Thickness 30 m.	Linear shelf edge. Salt diapir at the shelf edge, tributaries eminent from salt diapir. Strong amplitude main tributary runs parallel to shelf edges for 10km along the shelf	Descending trajectory clinoforms ~20-30 m followed by oblique clinoforms, 70 m in height. Slope angle 1-2°.	Sigmoidal clinoforms below, Oblique clinoforms followed by a sigmoidal aggradational clinoforms downlap on to the basin floor fan. Pleisto 2 MIS 92 surface caps the aggradation clinoforms.

Table 4.1 Description of Single Feeder Systems. Detailed descriptions of submarine channel events which consist of one main sediment entry point. Submarine channel events are labelled in order of the relative occurrence and therefore *Pleisto 1B* for example is the first single feeder system example but the second submarine channel event in *Pleisto 1* seismic unit.

Age	Description	Input Direction	Dimensions	Maximum Slope Incision	Slope and Basin Floor Seismic Character	Shelf Seismic Character	Shelf Edge Trajectory	Sequence Position
<u>Plio 1A</u>	Weak amplitude straight gullies, emanating from the shelf edge eroding into medium amplitude single reflection within package of low amplitude reflections.	ENE-WSW	System width >60 km. Gullies distributed every 1-2 km, average 1.4 km. Max width of channels 0.1 km. Length of gullies 40-50 km.	20 m	Base of slope strong amplitudes, but no clear fans, redistributed elongate to shelf. Pooling of strong amplitudes mid slope due to accommodation created by salt tectonic movement.	Arcuate shelf edge. Topset exhibits very strong amplitudes, and heavy channelisation near the shelf edge. Many salt diapirs present landward affecting topography.	Oblique clinoforms exhibiting descending trajectory <20 m. Slope angle 1-2°.	Package onlapping onto previous aggradational clinoforms. followed by progradation and ocean current scours. Salt tectonics affecting deposition locally.
<u>Plio 1B</u>	Weak amplitude straight gullies on the upper slope, strong amplitude unconfined lobes on the lower slope. Base of slope strong amplitude discontinuous reflections, thickness 50 m.	ENE-WSW	System width 13 km, distributed every 0.1-0.6 km. Max width gullies <0.1 km; lobes <0.6 km. Full length of channels <10 km.	22 m	Confined to the slope. Straight gullies at the upper slope and strong amplitude unconfined sinuous channels/lobes on the lower slope.	Arcuate shelf edge. Delta scale clinoforms (< 70 m) at shelf edge, Heterogenous amplitude strength. Channelized topsets.	Oblique clinoforms exhibiting descending trajectory. Slope angle 4°.	Package onlaps sigmoidal aggradational reflections associated with delta scale clinoforms on shelf. Oblique progradational but ascending clinoforms downlap onto the channel reflections.
<u>Plio 1C</u>	Highly sinuous strong amplitude channels emanating from headwall of mass transport complexes. Four separate packages of 30 m.	E-W	System width 20 km, distributed every 0.1-0.3 km. Maximum width 50 m. Length of channels 4-5 km.	32 m	Very strong amplitudes on the lower slope atop mass transport complexes. Sinuous channels present on the lower slope. Weak amplitudes on the upper slope.	Arcuate shelf edges. Weak amplitudes on the shelf and upper slope. Extensive channeling on the topsets.	Progradational oblique clinoforms exhibiting flat trajectory. Slope angle 4°.	Within expanded section of weak amplitude progradational oblique clinoforms with cyclical strong amplitude chaotic mass transport complexes followed by sinuous channels. Likely part of one composite sequence. Exposure of the shelf during channel deposition.
<u>Plio 1D</u>	Strong amplitude straight to mildly sinuous channels with unconfined pooled fans at the base of slope, thickness of package 30 m.	ENE-WSW	System width 20 km. Distributed every 1.2 km. Maximum width 0.3 km. 12 km maximum channel length, including base of slope fan, 15 km.	30 m	Very strong amplitudes on upper slope. Strong amplitude channels on foreset and lower slope. Strong amplitude amalgamated basin floor fan, pooled within salt withdrawal basin.	Arcuate shelf edge. Very strong amplitudes near the shelf edge associated with delta scale clinoforms. Terrestrial cross cutting channels of topset are widespread.	Sigmoidal shelf scale clinoforms with accommodation on the topset, rising trajectory. Delta scale clinoforms downstepping. Slope angle 2°.	Aggradational sigmoidal reflections below. Base of slope fans bidirectional downlap onto the same reflection as the delta scale clinoforms on shelf. Retrogradational package overlies the channels. Sediment supply reaching shelf edge regardless of increasing base level.
<u>Pleisto 1A (between MIS 103 and 100)</u>	Strong amplitude channel levee system. Stacked slope channels and fans. Unconfined lobes on lower slope and basin floor. Package up to 200 m thick on the lower slope, thinning landwards.	ENE-WSW	System width >80 km. At least 16 channel systems distributed every 2-6 km. Width of channels 0.5-1 km. Maximum width of unconfined fans 6 km. Maximum length of channels 40 km.	Individual channels, 35 m.	Chaotic heterogeneous seismic character. Early deposition focussed on lower slope and basin floor, unconfined strong amplitudes becoming weaker and more confined towards the top of the package. Channels exhibit increased sinuosity near salt diapirs	Arcuate shelf edge. Very strong amplitudes near the shelf edge. Landwards, terrestrial cross cutting channels of topsets are widespread.	Initiated by a descent in trajectory then dominated by aggradation on the slope. Slope angle <2°.	Strong continuous mudstone layers above and below. Slope apron package exhibits marine onlap onto a 220 m clinoform which may link to MIS stage 102. Marks a major increase in sedimentation rate. Overall an aggradational package on the slope. Mass Transport Complexes below, oblique shelf delta downlaps on top of the package.
<u>Pleisto 1C (between MIS 103 and 100)</u>	Very strong amplitudes at the base of slope incised by weak amplitude sinuous channels. Package 35 m.	NE-SW	System 16 km wide. Channels distributed every 0.5 km, average width of channel 0.15 km, Maximum length of channels 3.5 km.	34 m	Very strong amplitudes at base of slope and lower foreset, strong amplitudes confined to channels on upper foreset. Overall in a package of weak amplitude reflections.	Linear shelf edge. Clear terrestrial channelization up to the shelf edge, weak to medium amplitudes.	Flat trajectory oblique clinoforms, associated with shelf edge delta. Slope angle 4°. No topset preservation.	Within a highly progradational oblique clinoform unit of weak amplitude clinoforms increasing in height from 50-150 m. Channels occur within 150 m package. Mass transport complexes below. Continued oblique flat trajectory progradation above.

Table 4.2 Description of Multiple Line Source submarine systems. Detailed descriptions of submarine channel events which consist of more than one sediment entry point into the basin on the upper slope, continued on following page.

Age	Seismic Character	Input Direction	Dimensions	Maximum Slope Incision	Slope and Basin Floor Seismic Character	Shelf Seismic Character	Shelf Edge Trajectory	Sequence Position
Pleisto 1D (between MIS 103 and 100)	Channel belt of 50 m thickness, heterogeneous amplitude strength.	ENE-WSW	System 46 km wide. Channels distributed every 1-2 km, closer spaced towards the south. Maximum width of channel 0.15 km, some just above seismic resolution. Average channel length 8 km.	30 m	Little evidence of basin floor deposition, chaotic strong amplitudes on the slope. Stacked channels within low amplitude section.	Linear shelf edge. Strong amplitudes at the shelf edge, evidence of delta scale clinoforms near the shelf edge with foreset angle 1-2°.	Ascending trajectory, sigmoidal clinoforms slope angle 2°.	Incising into strong amplitude small scale Intra Slope clinoforms. Towards the top of an aggradational sigmoidal package but will little bottomset preserved.
Pleisto 1E (between MIS 100 and 98)	Weak amplitude straight gullies, single seismic cycle thickness ~ 20 m.	E-W	System 32 km wide. Channels distributed every 1-1.5 km. Maximum channel width 0.2 km. Average channel length 16 km.	20 m, V shaped incisions	No evidence of basin floor fans, largely weak amplitude slope reflections. Not erosionally truncated or channelized like previous examples.	Linear shelf edge. Strong amplitudes landwards of the shelf edge, not at the shelf edge.	Ascending trajectory sigmoidal clinoforms, one seismic cycle before the clear downstepping of >40 m. Slope angle 2°.	Previous reflections are aggradational sigmoidal, 150 m height. Event occurs just prior to a downstepping. Downlapping and onlapping onto the channel package is flat lying oblique clinoforms <100 m prograding wedge associated with Pleisto 1F. The ascending trajectory is half way between the maximum glacial MIS 100 and 98.
Pleisto 1G (between MIS 98 and 96)	Strong amplitude straight channel belts with internal sinuous channels. Thickness of package 40 m.	E-W; SE-NW	System width 40 km, channels distributed every 0.7-1.2 km, average width 0.3-0.7 km. 16 km max length of channels becoming shorter towards the north.	U- V shaped, 25 m	Strong amplitude reflections limited to the foreset.	Linear shelf edge. Strong amplitudes at the shelf edge. Iceberg scours trending N-S on the outer shelf. Strongest amplitudes further south.	Descending trajectory oblique clinoforms. Slope angle 1-2°.	Below is a package of aggradational sigmoidal and above is a flat lying trajectory, oblique tangential. The channels are onlapped and downlapped by the oblique reflections. The event is between MIS 98 and 96. Iceberg scouring event from two seismic cycles above.
Pleisto 1H (between MIS 98 and 96)	Medium amplitude sinuous canyons with internal lateral accretion.	ENE- WSW	System width 8km across slope, distributed 2-3 km apart, 1.5 km maximum width of canyon towards base of slope. maximum length 19 km.	V Shaped to flat bottomed incision, 60 m	Foreset based, no evidence of fans heterogeneous internal structure. Medium amplitude Salt diapirs on the slope.	Linear shelf edge. Weak shelf amplitudes and no evidence of strong terrestrial channelization of the topset. Active salt diapirs on the shelf.	Ascending trajectory. Progradational sigmoidal clinoforms. Slope angle 1-2°.	One seismic cycle below MIS 96, top Pleisto 1. Sigmoidal aggradational clinoforms above, chaotic/aggradational sigmoidal clinoforms with intra slope clinoforms, below.
Pleisto 2B (between MIS 94 and 92)	Medium amplitude channel belts 20-50 m thick.	E-W	System width 30 km across, average 2 km apart. Maximum slope channel width 0.5 km. Width basin floor fan 2-5 km. Maximum length 15 km.	20 m	Chaotic, channelized foresets, strong amplitudes across the foreset. Relatively straight channel edges but made up of sinuous channels within. Strong amplitudes at base of slope.	Linear shelf edge. Strong amplitudes on the shelf. Low angle delta scale clinoforms at the shelf edge and terrestrial channelling on the topsets.	Flat trajectory oblique clinoforms. Slope angle 1-2°.	Within strongly progradation oblique tangential final package of Pleisto 2. Iceberg scours into topsets on the shelf followed by a strong amplitude continuous basinwide event (Top Pleisto 2, MIS 92). Clinoform heights <100 m.
Pleisto 3A (between MIS 92 and 82)	Medium amplitude, mildly sinuous stacked channel deposited of 50 m.	ESE-WNW	System width 53 km across. Distributed every 0.8 -1.3 km along slope. Width of channels range 0.15 to 0.25 km. Maximum length of channels 11 km.	28 m	Highly chaotic facies on foreset, with strong amplitudes on the upper foreset. Due to lack of accommodation clinoforms are <100 m.	Linear shelf edge. Strong amplitudes on the upper foreset and topset, No evidence of associated topset terrestrial channelization.	Minor descending to flat trajectory oblique clinoforms. Slope angle 2-3°.	Within strongly progradational oblique tangential package, prior to and following an aggradational sigmoidal package. Clinoform heights <100 m.
Pleisto 3B (between MIS 92 and 82)	Medium amplitude, mildly sinuous stacked channel deposited of 50 m.	ESE-WNW	System width 38 km across, distribution every 1-1.4 km. Width of channels range from 0.15-0.3 km. maximum length 12 km.	25 m	Highly chaotic, weak amplitude channelized facies on the foresets. No evidence of basin floor fans. Clinoforms <100 m.	Linear shelf edge. Strong amplitudes on upper foreset and shelf edge.	Flat trajectory. Progradational oblique clinoforms. Slope angle 1-2°.	Within a strongly progradational oblique tangential package with little change before or after, most of topsets eroded. Clinoform heights <100 m.

Table 4.2 Description of Multiple Line Source submarine systems. Detailed descriptions of submarine channel events which consist of more than one sediment entry point into the basin on the upper slope.

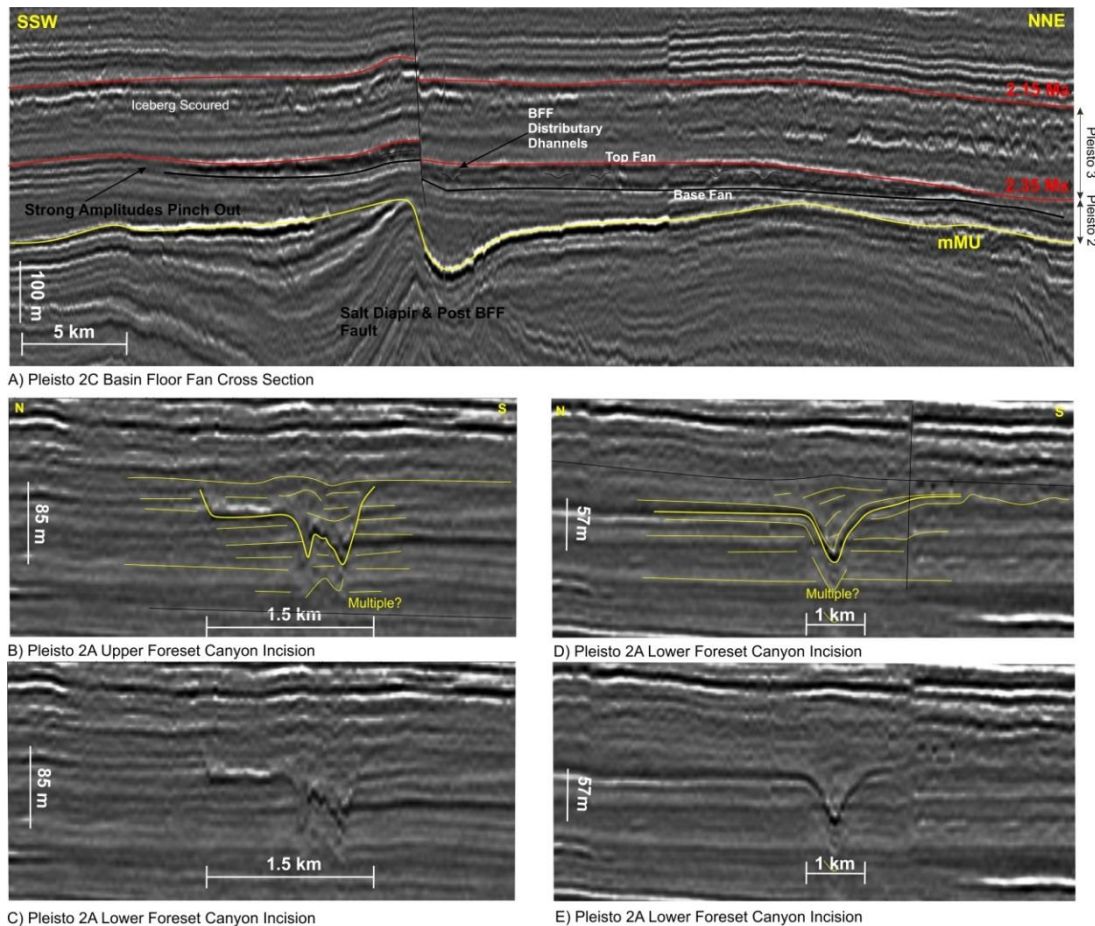
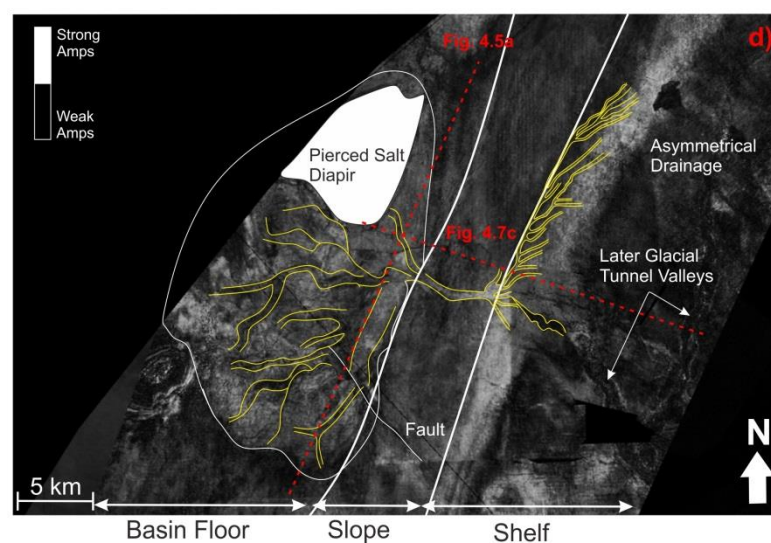
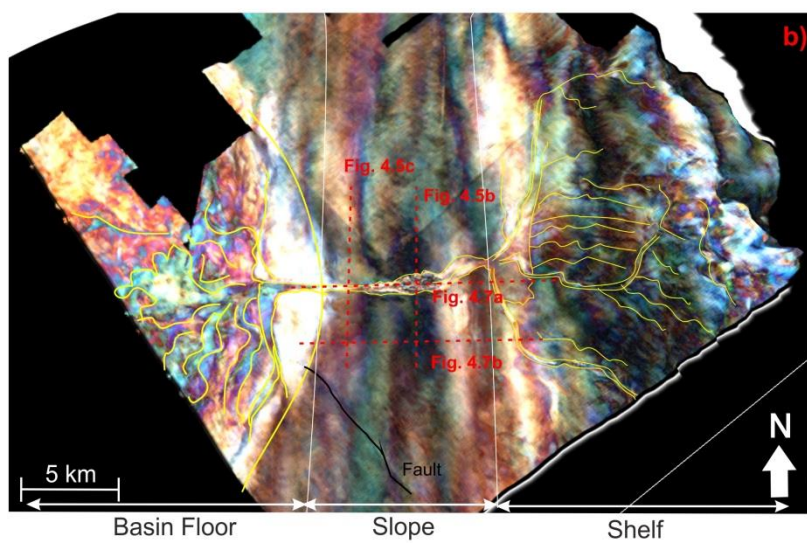
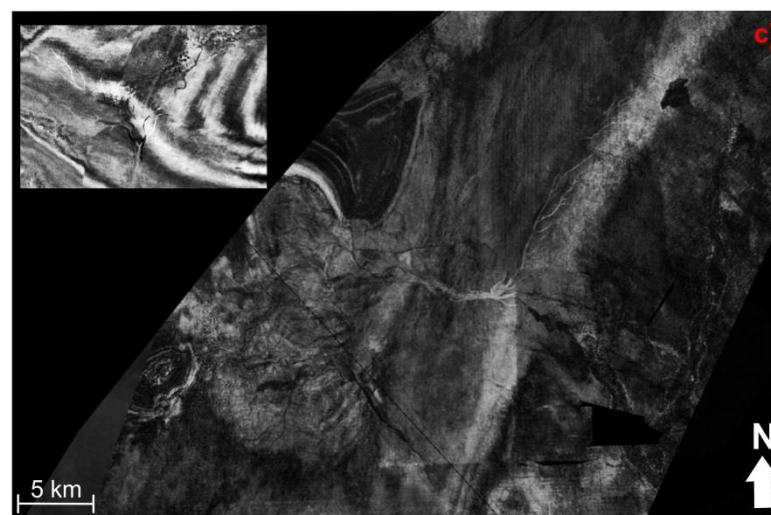
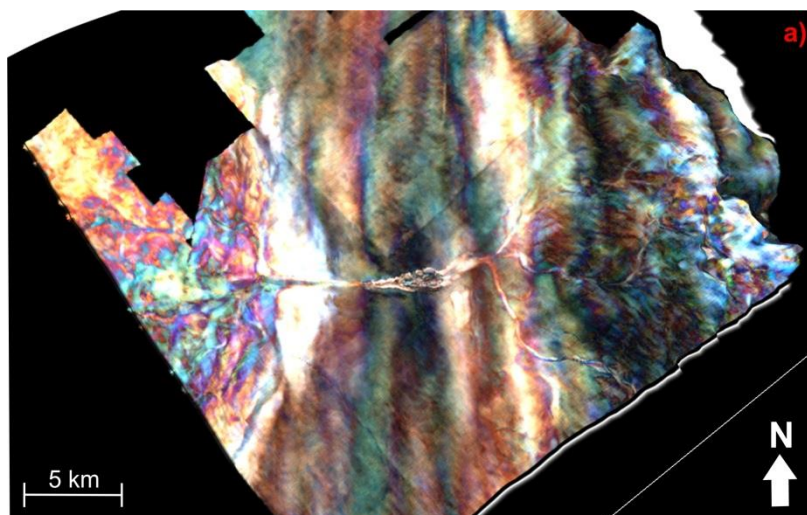


Figure 4.5 Single Feeder System seismic cross section examples **a)** *Pleisto 2C* basin floor fan SSW-NNE seismic cross section. mMU = mid Miocene Unconformity. Key dated reflections annotated. **b)** *Pleisto 2A* upper foreset canyon incision. Interpreted seismic cross section. **c)** *Pleisto 2A* upper foreset canyon incision. Uninterpreted seismic cross section. The scales represent the depth and width of the canyon. **d)** *Pleisto 2A* lower foreset canyon incision. Interpreted seismic cross section. **e)** *Pleisto 2A* lower foreset canyon incision uninterpreted seismic cross section. Locations of cross sections shown in Fig. 4.6. All vertically exaggerated.

Figure 4.6 Single feeder system 3D examples. (Following page) **a)** *Pleisto 2A* 3D uninterpreted RGB blend (Over a ~60 m interval between top and base basin floor fan interpreted surfaces) extracted onto a seismic surface. **b)** *Pleisto 2A* 3D interpreted RGB blend extracted onto a seismic surface. Position of the shelf, slope and basin floor identified and key features highlighted in yellow. Locations of Figs. 4.5b & c shown in red. **c)** *Pleisto 2C* 3D uninterpreted RMS amplitude extraction (using base basin floor fan reflection with a -50 ms interval) using black-grey-white colour scale onto a seismic surface. *Inset* Expanded view of incised valley feeder system, a timeslice through the seismic amplitude volume. **d)** *Pleisto 2C* 3D interpreted RMS amplitude extraction. Position of the shelf, slope and basin floor identified and key features are highlighted in yellow. Location of Fig. 4.6a seismic cross section shown in red. See Fig. 4.3 for locations of *Pleisto 2A* and *2C* single feeder systems.



4.4.2 Single Feeder System Clinoform Architectures

The *Single Feeder* systems are consistently placed within a sequence of clinoforms architectures. Below, sigmoidal clinoforms with ascending shelf edge trajectories are dominant, displaying an aggradational to progradational form. The *Single Feeder* system is linked updip with a set of clinoforms which have a descending shelf edge trajectory exhibiting a progressive reduction in slope height basinwards, or a flat shelf edge trajectory (Fig. 4.7). This is most apparent in *Pleisto 1F* and *Pleisto 2A*, where slope height decreases from 200 m to 100 m (Fig. 4.7a). The slope angles of the clinoforms associated with the *Single Feeder* events are variable, but relatively steep ranging from 2-4°. Progradational, oblique clinoforms which increasingly become aggradational, sigmoidal clinoforms downlap on to the top of the *Single Feeder* basin floor fan. The top of the sequence is strong amplitude, continuous reflection, which correlates with high gamma ray values and mudstone lithology in boreholes. Local clinoform architectures are identified to change with faulting and with local paleo topography.

Pleisto 1B (Fig. 4.3), is a series of incised valleys within a flat trajectory prograding set of largely oblique shelf-prism clinoforms. This example differs from the other *Single Feeder* System examples in that the aerial extent of the tributaries on the shelf is limited to and emanating from a salt related topographic high. *Pleisto 1B* appears related to reducing accommodation on the shelf locally to large active salt diapirs in the hinterland. The outer shelf topography in the cases of *Pleisto 1B*, *2C* and *2D* is affected by active salt tectonics at the time of deposition and this is likely to have affected the drainage pattern of the incised systems. In the case of *Pleisto 2A* no salt tectonics is present but it is within the area of the Broad Fourteens Basin (BFB in Fig. 4.1) which does exhibit active faulting during the Quaternary.

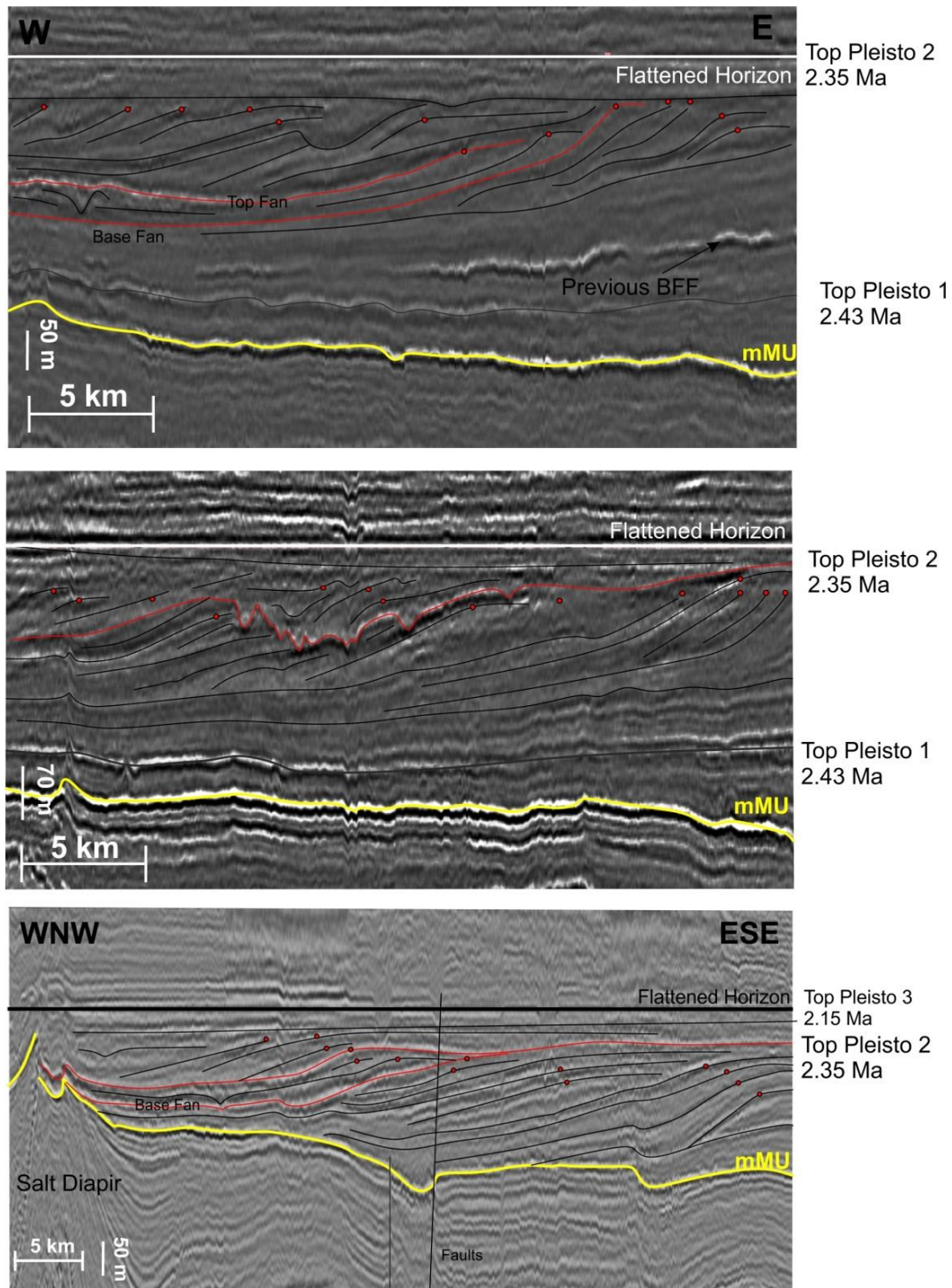


Figure 4.7 Single feeder system shelf edge trajectories. a) Seismic dip cross section of *Pleisto 2A* off canyon axis. b) Seismic dip section of *Pleisto 2A* near canyon axis. c) Seismic dip section *Pleisto 2C*. Section locations shown in Fig.4.6. BFF= Basin Floor Fan. mMU = mid Miocene Unconformity. Vertical exaggeration x15. All sections flattened on overlying topset reflections.

4.4.3 Multiple Line Source Systems

A minimum of thirteen Multiple Line Source systems occur during the study period (Figs. 4.2 & 4.3; Table 4.2.) Multiple Line Source systems are focused on the slope of the shelf-prism clinoform. The thickness of the package on the lower slope of each *Multiple Line Source* system can vary from one seismic cycle (<20 m) to 200 m thick. The width of the *Multiple Line Source* systems along strike can vary between 13 and 80 km. The narrowest systems are associated with slope dips of 3-4° (e.g. *Plio 1B*), whereas wider systems occur in lower gradient are related to slope angles of 1-2° (e.g. *Pleisto 1G*).

The Multiple Line Source systems are identified in seismic cross section by isolated strong amplitudes within a largely weak amplitude layer. They can be unconfined or confined strong amplitudes within a U to V shaped incisions (Figs. 4.8, 4.10, 4.11), distributed every 0.5-3 km along strike. In planform the incisions/isolated strong amplitudes trend at a right angle to the shelf edge and are identified as channels. Channel length is dependent on slope length and slope angle, but ranging from 5-50 km (Fig. 4.3). Channel width can range from 50 m to 1.5 km. The channels are normally at least incisional on the upper slope and the maximum incision on the slope is typically 20-30 m. Sinuosity of channels on the slope increases with three main conditions: towards the base of slope; when slope gradient decreases around salt related topography or with increased incision. Many of the examples show relatively straight channels (Fig. 4.4).

The gamma ray response to Multiple Line Source channels is a sharp decrease from background API of ~100 to 30-50 API followed by an increasing upwards motif. This represents a sharp increase in coarser sediments followed by cessation of coarser grained material delivery resulting in a fining upwards package. In the stacked examples the gamma ray shows a sawtooth motif between low and high gamma ray representing interbedded sands and shales. The lithology of the sediment deposited during the Multiple Line Source events are mainly fine grained sand with medium found only in the southern most events, surrounded by a general slope lithology of grey mudstone.

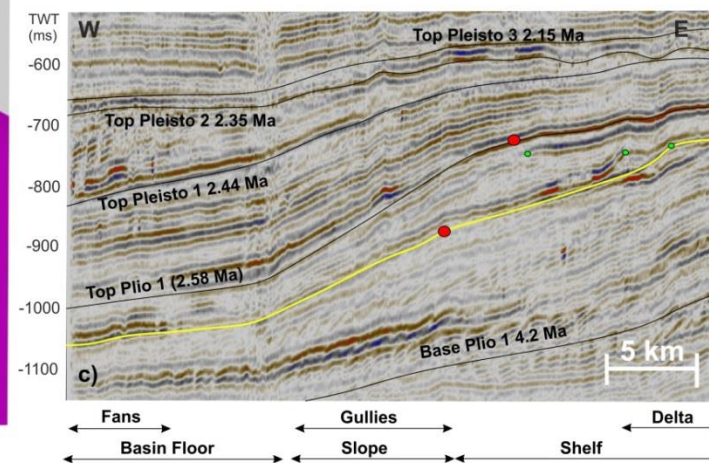
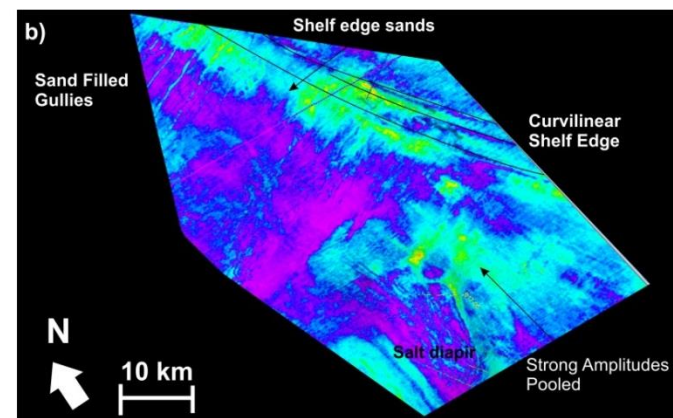
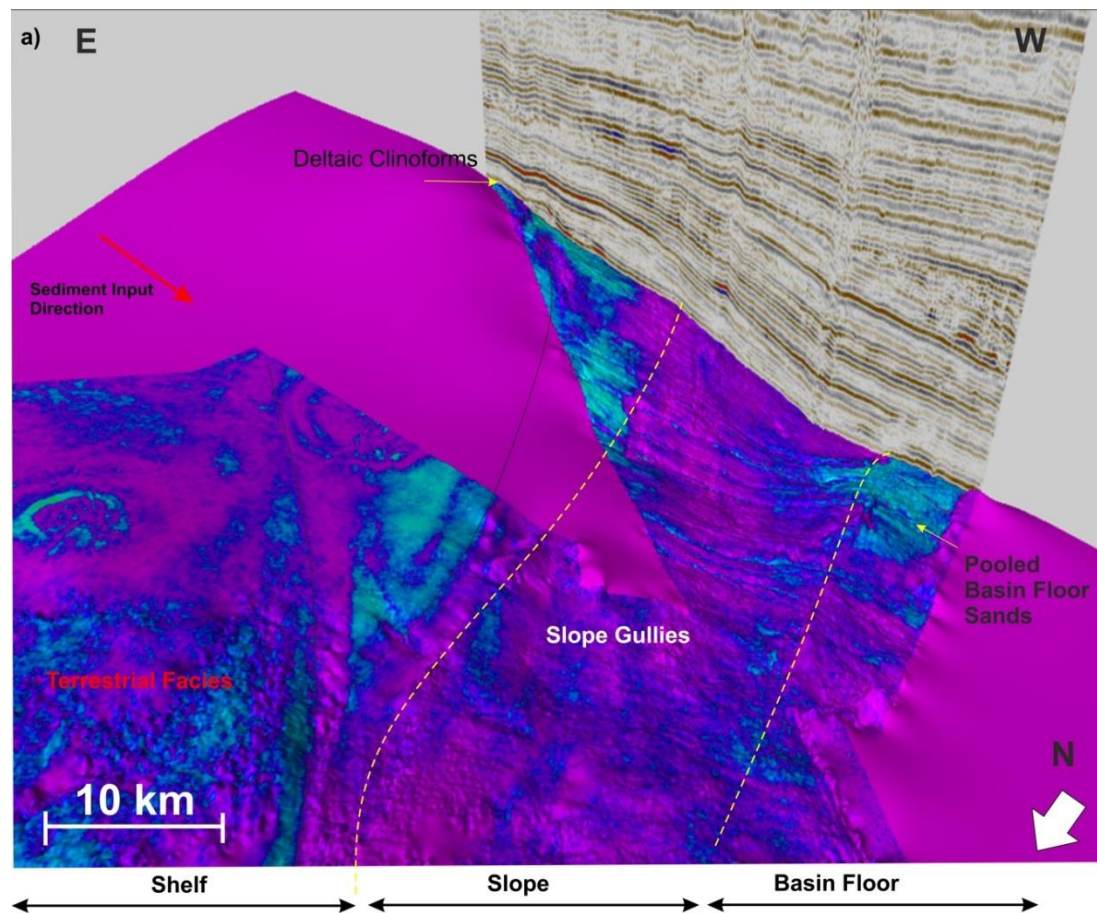


Figure 4.8 Multiple line source examples: *Plio 1D* gullies (previous page). a) 3D view of *Plio 1D*. RMS amplitude extraction on a seismic surface (shown in c). b) Zoomed out RMS amplitude extraction c) W-E seismic cross section covering the basin floor, slope and shelf parts of *Plio 1D*. Location shown in a). Black line represents the seismic surface used for amplitude extractions using an interval of -30 ms. Brighter blue colours represent sandy lithology. Seismic cross sections are vertically exaggerated between x 10 and x 15, 3D surfaces x 5.

The Multiple Line Source systems are only present on the foreset and the bottomset of the shelf-prism clinoform and generally do not have clear preserved feeder incisions on the shelf like in the *Single Feeder* Systems. The Multiple Line Source systems have a varied relationship to the seismic character of the outer shelf and shelf edge (Table 4.2). The seismic character at the shelf edge is of varied amplitudes from weak to strong. The shape of the shelf edge is arcuate with lobate forms (radius 20-40 km) at the shelf edge for *Plio 1* examples and *Pleisto 1A*, after which the shelf edge is linear. RMS amplitude extractions aid characterisation of the shelf area (Figs. 4.8 & 4.9).

Examples prior to MIS 100, within *Pleisto 1* seismic unit (Fig. 4.2), and the *Pleisto 2B* event are associated with a seismic facies that is heterogeneous and chaotic in 3D on the outer shelf, comprising many multi directional cross cutting channels, creating a “mottled” effect on the topsets (Figs. 4.8 & 4.9). This facies is associated with clay to fine-medium sands with some coarse grained material in the very south and lignite, wood fragments and oyster beds (SF4, Fig. 3.9, Chapter 3). This is identified as shallow marine to terrestrial and is interpreted as delta top channels. This is a very important interpretation as it gives an indicator of subaerial erosion which is imperative in understanding the position of the Multiple Line Source systems within the local base level curve.

A direct link between specific delta top channels and submarine channels is not imaged in this dataset however this could be due to seismic resolution issues as in the Fuji-Einstein delta complex in the NE Gulf of Mexico shows similar mottled effect channels converging at the shelf edge, directly linking and feeding coarser grained sediment to into slope gullies (Fig. 13 in Sylvester et al., 2012). Similar features are also identified in the Late Pleistocene Mahakam delta (Crumeyrolle et al., 2007).

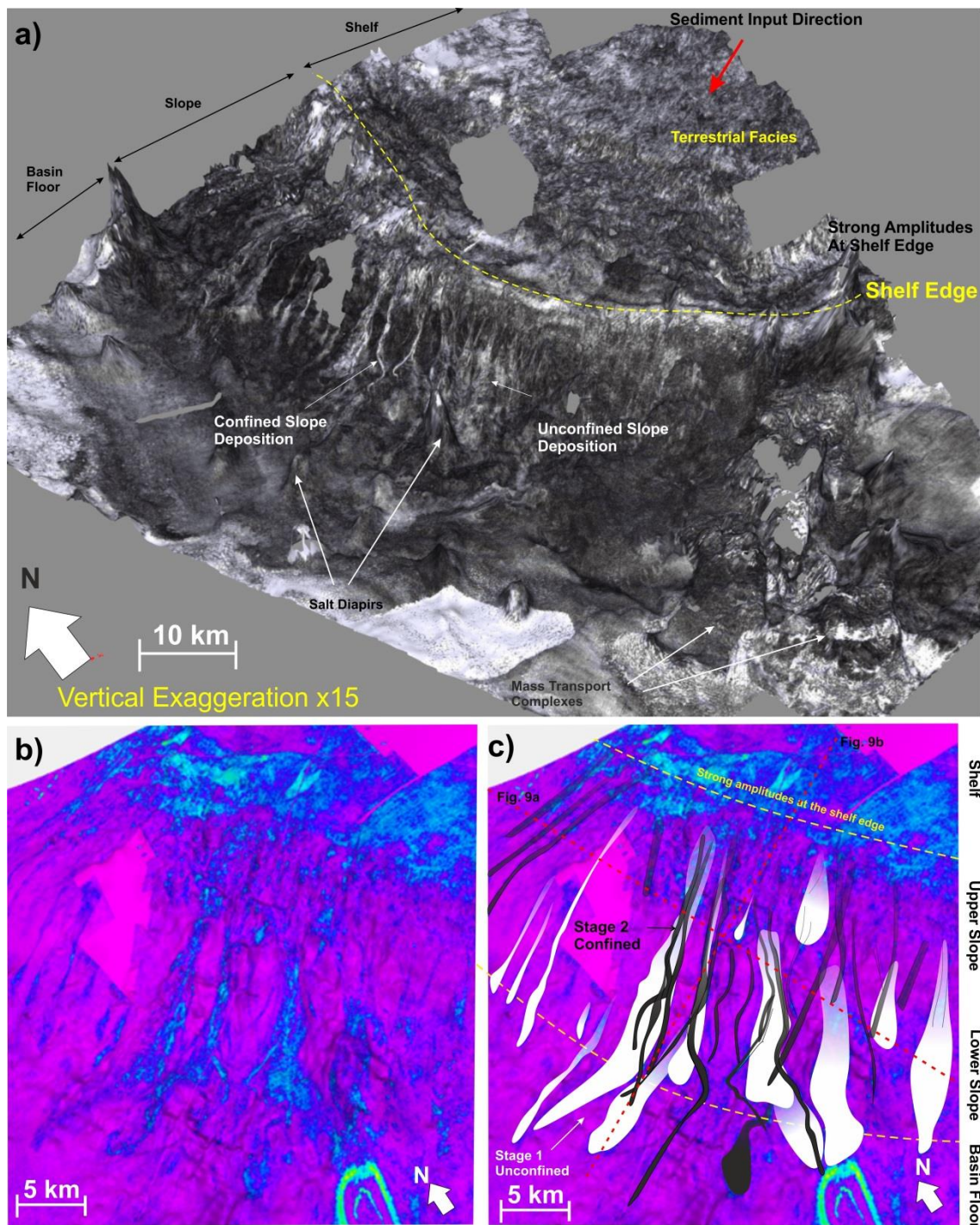


Figure 4.9 Multiple line source 3D example: *Pleisto 1A* channel levee complex. a) RMS amplitude extracted between Top and Base *Pleisto 1A* (RMS window used annotated on Fig. 4.9) onto a surface. Brighter, whiter areas represent sandy lithologies. Vertical exaggeration x 15. b) *left* Uninterpreted zoomed in RMS amplitude extracted on seismic surface (same extraction window used). Brighter colours such as blues represent coarser grained lithology. *Right* interpreted, zoomed in RMS amplitude extracted on seismic surface. White interpretations represent the first stage of coarser grained deposition basinwards of the shelf break which represents unconfined sediment at the base of slope followed by a

second stage where the deposition is more channelized (black interpretations). This is confirmed by taking stratal slices through the ~200 m of stacked channel levee deposits.

Three examples are focused on below representing the variability in the *Multiple Line Source* systems encountered. *Plio 1D* (Figs. 4.3 & 4.8, Table 4.2) is a set of largely strong amplitude straight gullies, 50 m maximum width, emanating from the shelf edge from an ENE direction. The thickness of the package is 30 m. The gullies attach at the base of slope to strong amplitudes pooled in a salt withdrawal minibasin. The gullies are interpreted as sand filled. To the south of the gullies, slope deposition is unconfined as very strong amplitudes are identified across the slope (Fig. 4.8b). Strong amplitudes, delta top facies and delta scale clinoforms are identified near the lobate shelf edge during *Plio 1* (Fig. 4.8). Single thread gullies are the least evolved submarine channel systems suggesting these are short lived events (Gee et al., 2007; Prather, 2003; Sylvester et al., 2012).

Pleisto 1A (Figs. 4.3, 4.9 & 4.10, Table 4.2) is an 150-200 m landward and northwards thinning channel-levee system deposited basinwards of the shelf break in the earliest Quaternary (first 60,000 years, Fig. 4.2) and is by far the largest slope deposition event during the study period. The channel system is 80 km across the slope and follows the arcuate shape of the shelf at the time (Fig. 4.9a). The channels are the greatest in length, up to 40 km. The slope geomorphology is variable due to active salt tectonics and prior mass transport complex deposits and this affects the geometry of the channels. Where slope grade decreases, sinuosity increases and channels actively deflect around the salt related topographic highs.

The stacked nature of the slope deposits is most clear within the central part of the slope where several generations of channels can be identified (Fig. 4.9). The channels and associated accretion of sediment in levees shows a stacking and migration upwards (Fig. 4.10a). RMS amplitude extractions on seismic surfaces through *Pleisto 1A* confirm the first 75 m of the unit is dominated by lower slope unconfined sediments (Stage 1 in Fig. 4.9b). In seismic cross section (Fig. 4.10a) this is indicated by more laterally extensive strong amplitudes of up to 6 km in width. The upper 75-100 m is dominated by confined strong amplitude slope deposits on the upper and lower slopes and greater abundance of clear incisions of less than 1 km wide (Stage 2 in Figs. 4.9b & 4.10). The unconfined to confined pattern is also observed in *Pleisto 1C* (Table 4.2) and in the

Laingsburg depocentre submarine events of the Karoo basin, South Africa (Flint et al., 2011). Strong amplitudes are identified in a narrow band at the shelf edge and to the north on the shelf.

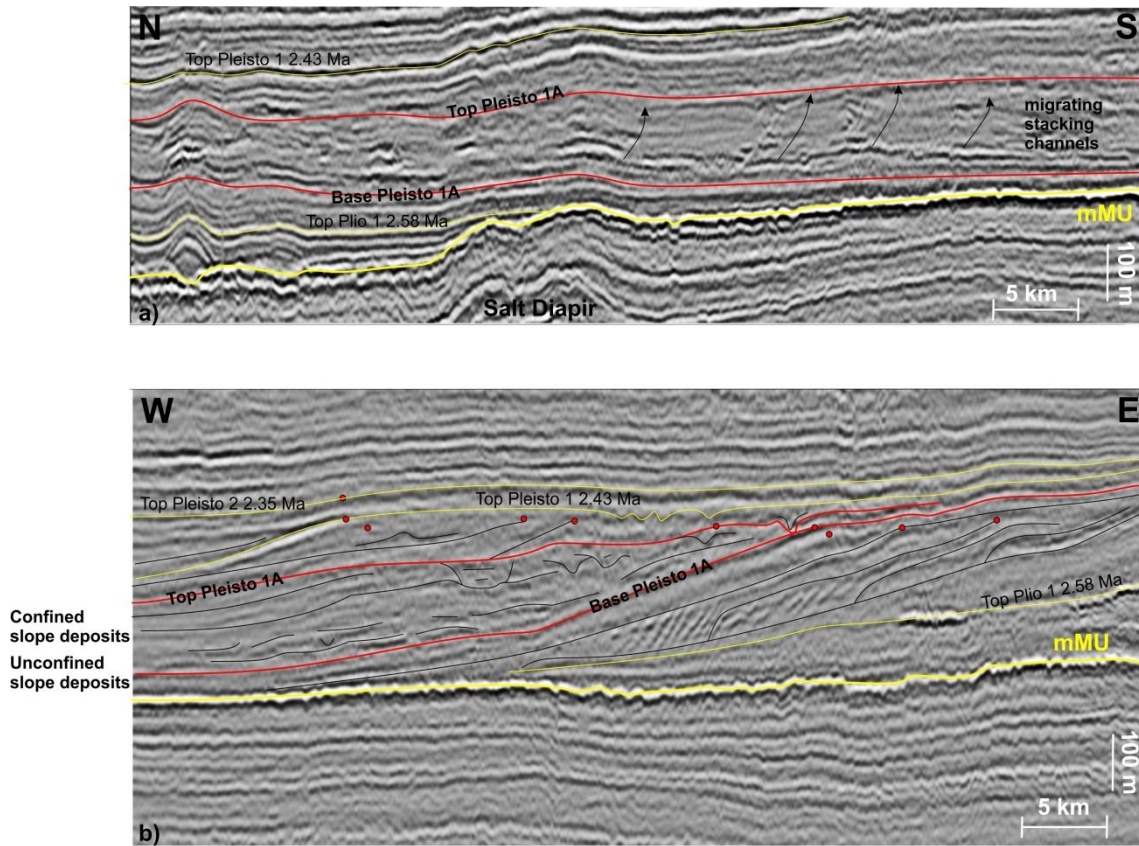


Figure 4.10 Seismic cross sections through *Pleisto 1A* channel levee complex a) N-S seismic cross section showing the migration and stacking patterns of the channel levee systems. Seismic window used for RMS extractions in Fig. 4.9 shown. b) W-E dip section showing the thickness of the complex and the evolution from unconfined slope deposits to confined slope deposits. Vertical exaggeration x10. Red circles represent clinoform roll over which represent the shelf edge used in order to map the shelf edge trajectory.

Pleisto 1H (Figs. 4.3, 4.11 & 4.12) represents highly sinuous channels emanating from ENE that incises the slope to a much greater than any other *Multiple Line Source* event in the study period. *Pleisto 1H* is recognised on the slope as steep walled “V” to “U” incisions, incising into underlying aggrading reflections or *Intra Slope Clinoforms* (Fig.4.4) up to a maximum of 60 m on the upper foreset. Each incision is up to 1.5 km across. The seismic character is largely strong amplitude infill with evidence of lateral accretion within, however they are incising into a sandy lithology package (*Intra Slope*

Clinofolds) and there is not necessarily a strong acoustic impedance contrast between the channel fill and the underlying incised package (Fig. 4.11). Lateral migration of the channel is identified in Fig. 4.11 and the shelf edge is characterised by weak amplitudes and shelf indents which are consistent in their spacing across the shelf and are only present on the upper slope. *Pleisto 1H* is the exception in the *Multiple Line Source* in that a connection to shelf channels is identified as one of the slope canyons appear to link to a 40 km long channel system emanating from the SE on the shelf (Fig. 4.11).

The *Pleisto 1H* example shows the link of channel systems to the local topography. In this case, the salt diapir which is now present on the slope (Fig. 4.11) was not affecting topography enough at the time of canyon incision to deflect the channel around the salt structure and the channel appears atop the salt diapir. The difference between a structurally restored and normal cross section through *Pleisto 1H* and the salt diapir indicate that the salt diapir on the slope is not as much of a topographic feature once structurally restored and must have been active later in the section (after the flattened horizon, therefore after the Gelasian). However, the salt diapir on the shelf, to the east of *Pleisto 1H* was a topographic feature of the shelf at the time.

Shelf feeder systems that clearly link to the slope channels are not defined in the majority of Multiple Line Source systems. This suggests the majority of the Multiple Line Source channels/incisions are created by retrogradational slumping on the upper slope, then capturing sediment from the staging area rather than directly linking to a river system as the *Single Feeder* systems and *Pleisto 1H* does. Iceberg scours are also prevalent features on the shelf after MIS 98 within *Pleisto 1* and *Pleisto 2* (Figs. 4.2 & 4.12) when the shelf is submerged and there is topset preservation.

Active salt diapirism is creating and destroying accommodation on the shelf in pulses during the study period. In the case of *Plio 1A* and *Pleisto 1H*, submarine channels are emanating from that part of the shelf that is affected by salt diapirism and is likely providing erosive material and/or instability on the upper slope for the submarine channels to form. Salt diapirs do affect the local topography, however can be ruled out as the main cause of the submarine channels as a whole as the area of the shelf, the dynamic topography affects, is much less than the width of the slope systems.

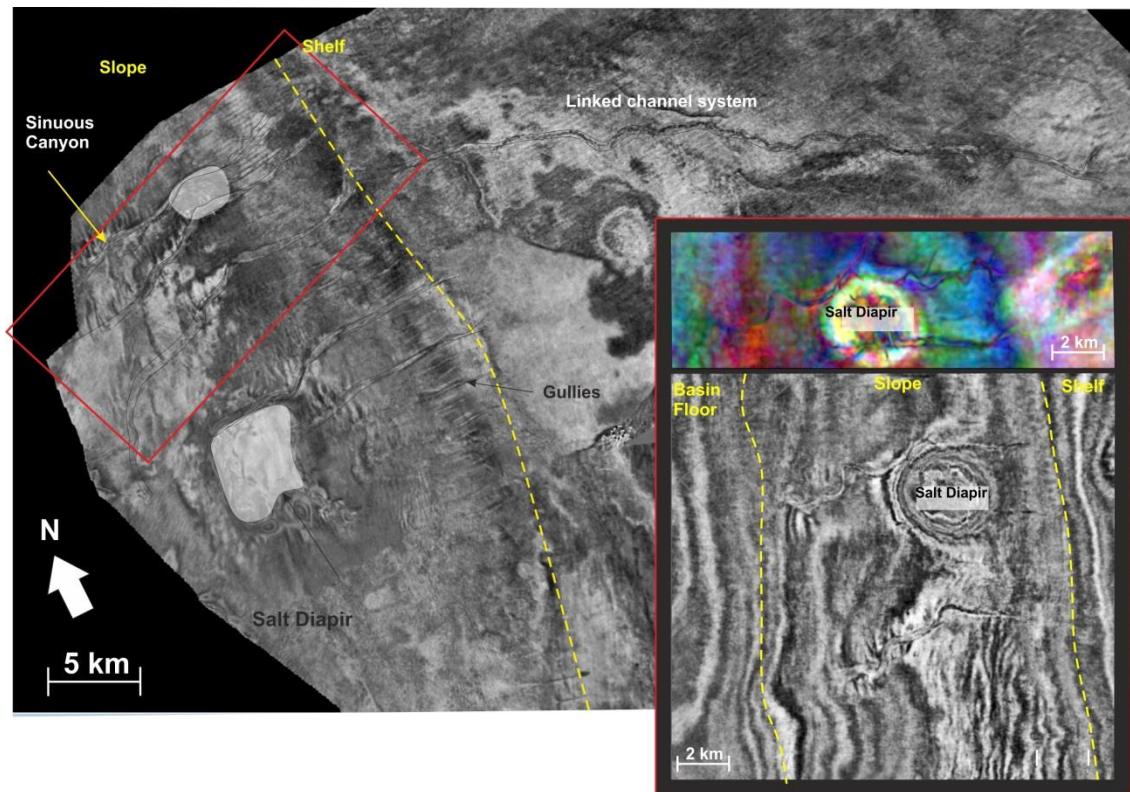


Figure 4.11 Multiple line source example *Pleisto 1H* sinuous canyons. Seismic amplitude extracted onto surface through *Pleisto 1H* canyons. Channels and canyons highlighted with black outline. *Inset* close up of sinuous canyon features using time slices *top* frequency decomposition volume (-720 ms timeslice), *bottom* RMS Amplitude volume (-730 ms timeslice). Location of inset within red box of main figure.

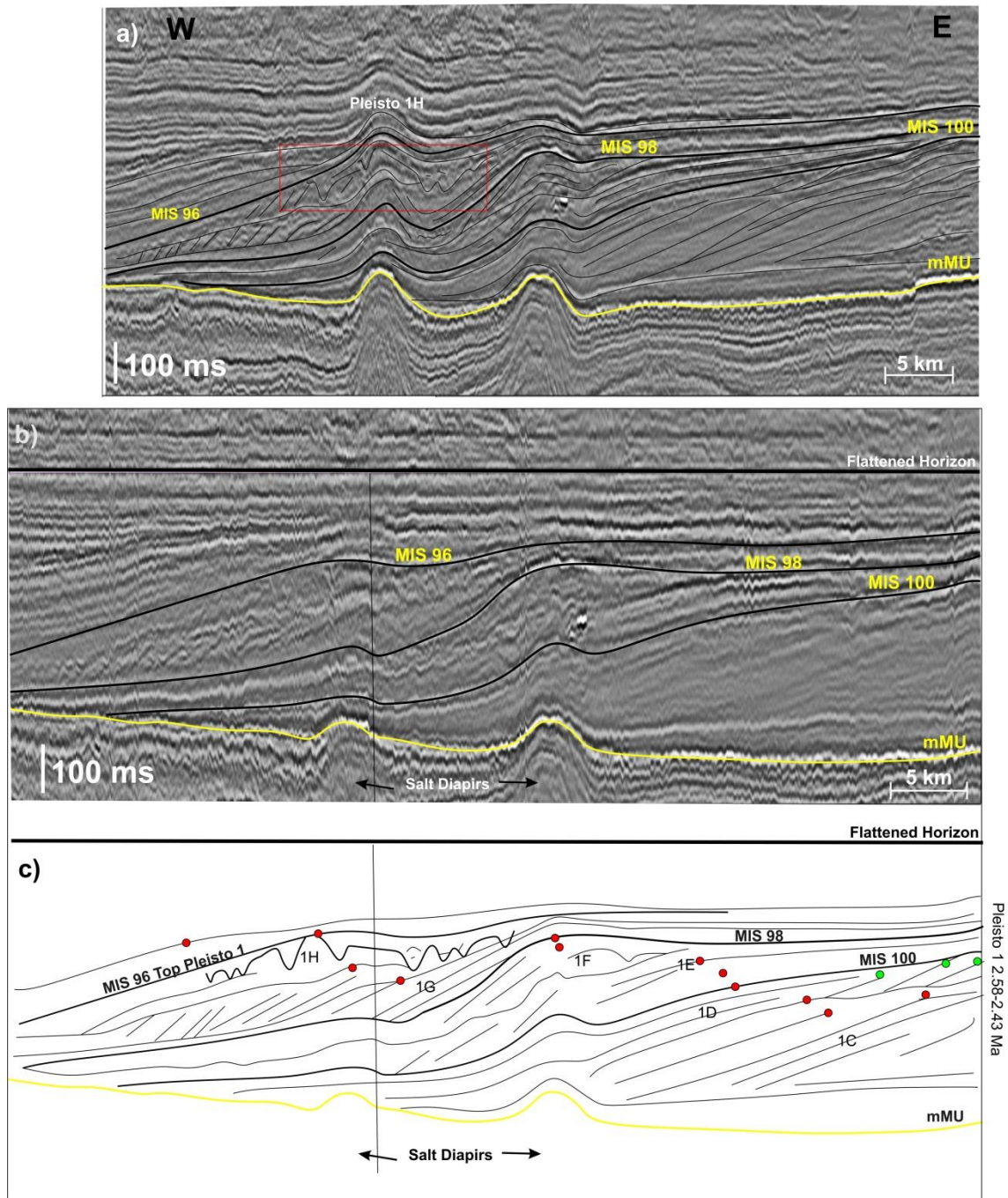


Figure 4.12 Seismic cross sections through *Pleisto 1*. Covering period from MIS 100-96, between ~2.51-2.43 Ma. Several channel systems identified including *Pleisto 1H*. Locations shown on Fig. 4.3. a) East-west interpreted cross section. b) East-west cross section flattened on overlying topset c) Outline of key geometries and trajectories based on flattened cross section. Red circles represent shelf break, the roll over point of shelf-prism scale clinoforms. Green circles represent delta scale clinoform roll overs and may represent the coastline. *Pleisto 1H* because the canyon is highly sinuous the cross section is cutting through the same channel several times therefore several incisions are seen, but are the same channel. mMU = mid Miocene Unconformity. Vertical exaggeration x15.

4.4.4 Multiple Line Source Clinoform Architectures

The seismic architectures and sequences associated with Multiple Line Source submarine systems are variable and less predictable in comparison to the *Single Feeder* systems. The basinwards deposition events are associated with: i) oblique-tangential clinoforms with a descending ii) oblique tangential flat trajectory, or iii) sigmoidal clinoforms with an ascending trajectory (Fig.4.2).

Multiple Line Source deposition associated with descending shelf edge trajectory is rare and share a similar position within the sequence as *Single Feeder* systems (*Pleisto 1A*, Fig.4.9; *Pleisto 1G*, Fig. 4.12). The examples are present lower angle slopes than the *Single Feeder* systems ($\sim 1-2^\circ$). Several examples of Multiple Line Source submarine systems occur within the latter parts of a set of highly progradational oblique clinoforms with a flat shelf edge trajectory and strong topset erosion (*Plio 1C*, *Pleisto 1C*, *Pleisto 2B*, *Pleisto 3A & B*; Fig. 4.12). There is little change in character of the clinoforms immediately before or after the Multiple Line Source deposition.

Channel systems associated with ascending shelf edge clinoforms are normally within a sigmoidal set of clinoforms where there is accumulation on the topset of the shelf-prism clinoform. The *Multiple Line Source* events can occur within a package just above an oblique clinoform wedge (Fig. 4.12), as is the case with *Pleisto 1D & 1H*. *Plio 1D* (Fig. 4.8) and *Pleisto 1D* (Fig. 4.11) are the clearest examples of where basin floor deposition can be linked to a well imaged shelf delta at a time when there is accommodation on the shelf. They can also occur at the top of a sigmoidal set just before a downward shift in trajectory as is the case in *Pleisto 1E* (Fig. 4.12 & 4.13).

The position of Multiple Line Source systems within the sequence of *Pleisto 1* seismic unit indicates that sediment is delivered to the slope and basin floor, not only under conditions of shelf bypass, but even when sediment is accumulating on the shelf during periods of high accommodation. The style of the line source events does not appear to be linked to the clinoform stacking pattern associated with it, as gullies, sinuous channels and channel belts all occur in both sigmoidal and oblique settings.

4.5 DISCUSSION

4.5.1 Deep Water Sedimentation and Glacial-Interglacial Cycles

The submarine channel systems are placed within the context of the global sea level curve (Fig. 4.2) by using their relative positions to key dated surfaces and their clinoform stacking patterns. This can be carried out with most confidence in *Pleisto 1 and 2* as they are the best constrained chronostratigraphically. Using the chronostratigraphic framework their relationship to eustasy is interpreted and their place within the sequence stratigraphic framework investigated.

The relative position of each submarine event has been linked to its position within the seismic units and with relation to the global sea level curve in Fig. 4.2. The first major fall in global sea level within the Quaternary of 70 m occurs in *Pleisto 1* between MIS 101 and MIS 100, (Fig. 4.2). The following two glacial-interglacial cycles MIS 99-98 and MIS 97-96 exhibit similar falls. MIS 100, 98 and 96 are the first large-scale glaciations with widespread vegetation change in the southern North Sea (Zagwijn, 1992).

Three *Multiple Line Source* and one *Single Feeder* systems are identified between the seismic reflections associated with the first sub unit of *Pleisto 1*, MIS 103-100 (2.58 Ma to 2.51 Ma). The sub unit covers one-and-a-half glacial- interglacial cycles (Fig. 4.2) and comprises dominantly oblique clinoforms which prograde westwards in the southern Netherlands North Sea by >67 km during this sub unit, a rate of regression of over a kilometre per 1000 years. *Pleisto 1A* occurs after a large amount of deposition has already occurred and *Pleisto 1B, C & D* are towards the upper part of the sub unit (Figs. 4.2 & 4.11).

Pleisto 1A-C are related to oblique clinoforms and which are likely related to a low relative sea level period. *Pleisto 1D* is associated with sigmoidal ascending clinoforms followed by the strong amplitude shale layer attributed to MIS 100. *Pleisto 1D* is linked to the increase in accommodation with relation to the glacial-interglacial transition. Strong topset erosion associated with *Pleisto 1B & C* can be linked to the Maximum Glacial where the sea level is lowest (Figs. 4.11 & 4.13a).

Multiple Line Source Pleisto 1E gullies and *Single Feeder Pleisto 1F* occur during the second sub unit, from MIS 100-98 (2.51-2.48 Ma). The maximum progradation is ~20 km, a rate of regression of 540 m per 1000 years. There is greater preservation of topsets and the presence of sigmoidal clinoforms. *Pleisto 1E* occurs during a base level rise above the Top MIS 100 (glacial termination). The downstepping and reduction in clinoform height from sigmoidal clinoforms associated with *1E* (190 ms foreset height) to oblique clinoforms associated with *1F* (80 ms foreset height), indicate a large reduction in basin accommodation. *Pleisto 1F* therefore is associated with a base level fall just after *Pleisto 1E*. *Pleisto 1E* could relate to the interglacial rise between MIS 100 and 99 and *Pleisto 1F* associated with the onset of base level fall associated with the transition between MIS 99 and 98 (Fig. 4.2).

Two Multiple Line Source events *Pleisto 1G* and *Pleisto 1H* are associated with the third sub unit is from MIS 98-96 (2.48-2.43 Ma). During the sub unit there is 23 km of progradation, 420 m per 1000 years. *Pleisto 1G* is associated with the aggradational to progradational unit just above Top MIS 98 (Fig. 4.12), in a similar position to *Pleisto 1E* in the previous sub unit. *Pleisto 1H* occurs within an aggradational stacking pattern and the incision is associated with the seismic reflections just below end of glacial period regional shale layer MIS 96 (*Top Pleisto 1*). The aggradational stacking patterns are separated by a series of oblique clinoforms with smaller foreset heights. There are no submarine events identified in this package.

The *Pleisto 2* unit (2.43-2.35 Ma) covers two smaller scale glacial-interglacial cycles of 30 m and 50 m magnitude respectively. *Pleisto 2A* appears linked to the earlier part of *Pleisto 2*, which could therefore be tentatively linked to MIS 94. It is possible that all *Pleisto 2* systems correlate to the MIS 93-92 (Fig. 4.2) which is the greater in magnitude of the two glacial-interglacial cycles which is also associated with the greatest amount of iceberg scours and therefore likely a regionally important glacial event (Chapters 3 & 6). Several other *Single Feeder* events are identified in the area of *Pleisto 2A* (within Block P of the Netherlands North Sea sector in the very south of the dataset, Fig. 4.3) which not covered entirely by the dataset and therefore have not been included. The first two are just above Top *Pleisto 1* and only the basin floor fan is imaged within the dataset. The geometry is elongate compared to the fan shape of *Pleisto 2A* and they occur before

Pleisto 2A. *Pleisto 2C* and *D* appear associated with the same downstepping of clinoforms and could be linked to the sea level drop of 50 m between MIS 93 and 92.

The two identified *Multiple Line Source* occur early in the seismic unit *Pleisto 3* (2.35-2.15 Ma) (Figs.4.2 & 4.3). They are thin events and not easily imaged. There is greater uncertainty as to which MIS they belong as the seismic unit represents a longer time scale than the previous units. Both are associated with flat lying trajectories and oblique clinoforms which suggest a lower base level. There are no *Pleisto 3 Single Feeder* systems identified. The lack of sediment being transferred basinwards of the shelf edge could be related to change in character in southern Netherlands North Sea, with greater topset accommodation, possibly linked to accelerated subsidence from this time could start to inhibit the river systems reaching the outer shelf.

4.5.2 Deep Water Sedimentation Model

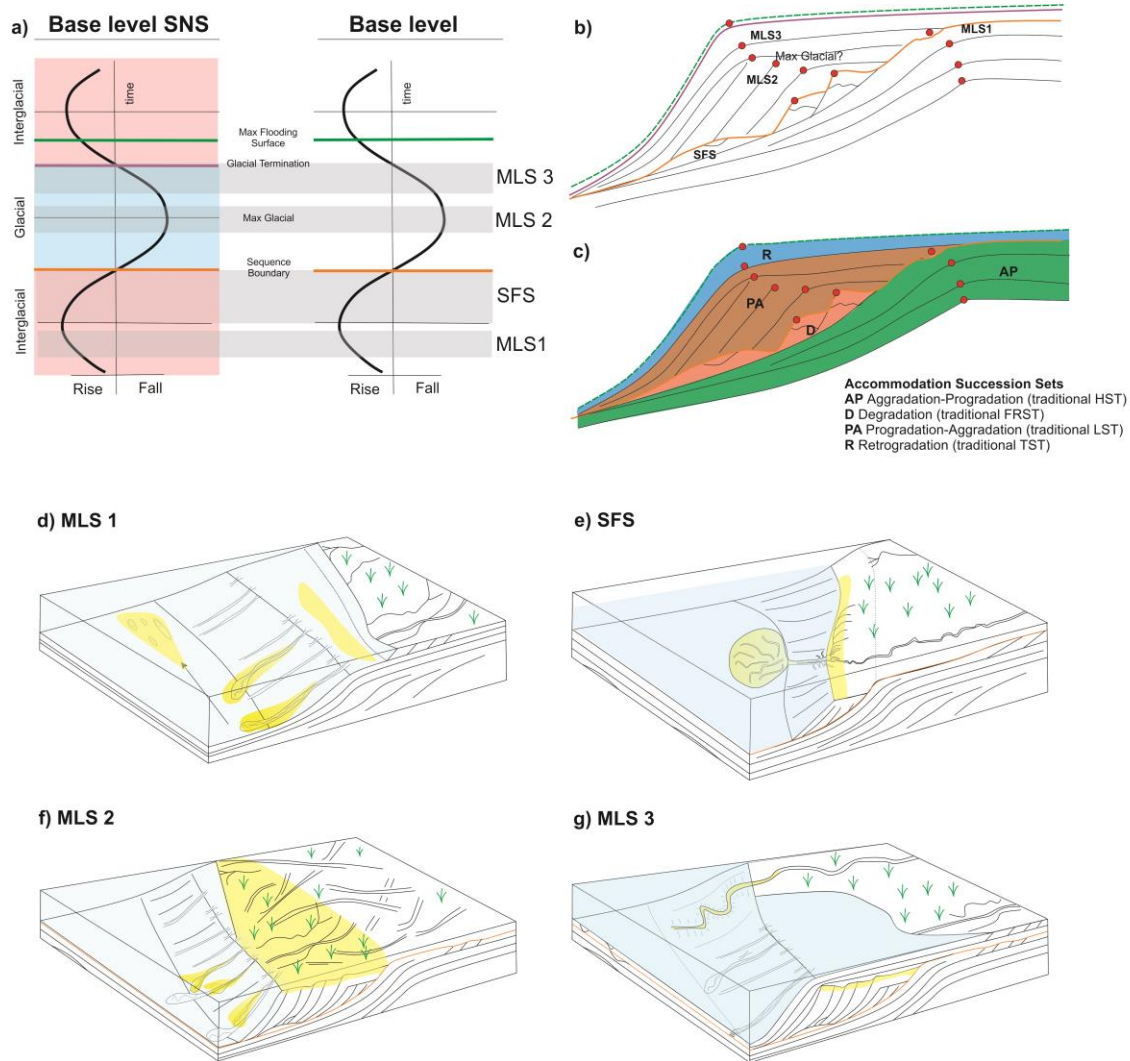
The key findings of linking the submarine channel events to the global sea level curve (Fig. 4.2) is that the distribution in time of submarine events does not match the amount of glacial-interglacial cycles. This is most clear in *Pleisto 1* seismic unit where there is the most robust control on the chronostratigraphy. Within this unit submarine channels occur throughout the base level cycle, several times in one glacial interglacial cycle (Figs. 4.2, 4.12 & 4.13).

A model is created to understand where in the accommodation succession (sensu Neal and Abreu, 2009) submarine events occur and in an ideal case, where in the base level curve the submarine events occur (Fig. 4.13). In this case, the idealised model represents an area of little overall tectonics and subsidence and the margin is supply driven (high sediment supply).

The *Multiple Line Source 1* (MLS1) events represent where sediment is delivered to the slope and basin floor via multiple submarine channels and is associated with an AP accommodation succession in an interglacial setting, the top of the AP succession is usually a sequence boundary (Fig. 4.13a-d). An example of MLS 1 is *Pleisto 1E*. *Single Feeder* scenario (SFS) represents where sediment bypassed the shelf via incised valley

systems, delivering sediment direct from the river system to the basin floor via a single feeder canyon system. This type of submarine channel is associated with a downstepping of clinoforms (degradation) and falling base level within the interglacial to glacial transition (Fig. 4.13a-c, e). *Multiple Line Source* systems also occur in this setting, but are more associated with wider and lower angle slopes than the SFS systems. *Multiple Line Source 2* (MLS2) sediment is delivered to the slope via multiple entries and terrestrial facies is observed up to the shelf edge, the shelf is exposed. Base level is interpreted to be at its lowest and under glacial conditions. The submarine channels are associated with the progradational part of a PA accommodation set (Fig. 4.13 a-c, f). Examples of this model are the most numerous and include *Plio 1C*, *Pleisto 1C*, *Pleisto 3A* and *3B*. *Multiple Line Source 3* (MLS3) is associated with rising base level in the glacial-interglacial transition, aggradational clinoforms in a later part of PA succession. Generally the coastline is far from the shelf edge (for example, in the nearside of the block model), however exceptional circumstances where channel systems reach the shelf edge in spite of the rising sea level develop longstanding, sinuous channel systems (far side of block model), e.g. *Pleisto 1H*. This could be due to increases run off during the glacial-interglacial transition. The models represent the ideal situation and *Pleisto 1* seismic unit within the south east of the Netherlands North Sea is the closest to this within the dataset. However in the dataset there are many examples of where the relationship to the base level breaks down.

Figure 4.13 Submarine channel link to global sea level curve (following page). **a)** base level curves (adapted from Bijkerk et al., 2014; Catuneanu et al., 2009) with key sequence stratigraphic surfaces annotated. *left* southern North Sea (SNS) base level model for “in phase sedimentation” *right* standard base level curve. **b)** Submarine channel event position within a common sequence using the trajectory analysis **c)** Accommodation succession sets in the style of Neal and Abreu, 2009, with the addition of a separate descending clinoform set, reference made to the four tract model of Hunt and Tucker, 1992) **d)** Multiple Line Source scenario 1 (MLS1) **e)** Single Feeder system scenario (SFS) **f)** Multiple Line Source scenario 2 (MLS2). **g)** Multiple Line Source scenario 3 (MLS3).



4.5.3 Role of Eustasy and Controlling Factors

A straightforward predictive relationship between rise and fall of eustasy and sediment delivery to the slope and basin floor is not found in this dataset. The mismatch between the global sea level curve and the submarine events could be because of many different external and local forcings. Each glacial-interglacial cycle has a unique depositional architecture and not one sequence is the same. If eustasy was the dominant factor affecting depositional architecture this would not be seen.

In the instance of the *Single Feeder* system, all the examples are associated with a drop in base level, as suggest by the reduction in clinoform height and downstepping shelf edge trajectory. However as shown in *Pleisto 2* (Top MIS 96- Top MIS 92), there are more basin floor fan events than there are eustatic sea level lows within the chronostratigraphically constrained seismic unit within the area of the Broad Fourteens

Basin (BFB). The BFB is the offshore extension of the West Netherlands Basin, which was a tectonically active basin during the Cenozoic (Nalpas et al., 1995) and an area of accommodation and greatest thickness of sediments during the Quaternary (Fig. 4.1). At least four *Pleistocene 2* age fans have been identified (Fig. 4.3). It is likely that the repeated incision of the shelf is due to uplift in the hinterland in this tectonically active area or than a narrower shelf than to the north means that the coastline is consistently nearer the shelf break so that there is a clearer response to higher order events than the glacial-interglacial stages in Fig. 4.2. The importance in understanding the tectonics of the area and associated the variation in sequences has been highlighted previously (Catuneanu et al., 2009)

Salt tectonics creates dynamic topography in the area surrounding an active diapir (Gee and Gawthorpe, 2006) and in this study there are numerous examples of active salt diapirs controlling sediment deposition and geometry of channels and basin floor events. However, the active salt diapirism can be ruled out in the majority of the cases in actually affecting the base level enough to trigger an event as usually the system width of the submarine channel events (Tables 4.1 & 4.2) are much greater than that which is affected by topography of the active salt diapirs.

Process regime at the shelf edge could also be crucial in understanding the lack of basinwards sedimentation in some low base level conditions and the presence of basinwards sedimentation in some high base level conditions. River dominated systems are the most efficient sediment distributors basinwards of the shelf edge (Dixon et al., 2012; Johannessen and Steel, 2005; Jones et al., 2015) and regardless of base level they can deliver sediment to the basin floor. What is intriguing about the SNS basin is that lobate shelf geometries, which are indicative of river dominated systems on the shelf (Hampson et al., 2015) are not recognised after *Pleistocene 1A*. They are abundant on the shelf during *Plio 1* seismic unit and during *Pleistocene 1* in the north of the Netherlands North Sea sector, where there is no evidence of submarine channel events. Straight geometries of the shelf edge and evidence of strong ocean currents indicate a wave dominated system after MIS 100 in *Pleistocene 1*.

The identification that the river system in the south of the Netherlands Sector was dominated by a high sediment supply rate and high progradation rates and can be identified as “supply dominated” sensu Porębski and Steel, (2003) during *Pleistocene 1*.

Rivers with sufficient sediment supply can reach the shelf edge even in icehouse conditions (Burgess and Hovius, 1998; Carvajal et al., 2009; Carvajal and Steel, 2006; Kolla and Perlmutter, 1993; Muto and Steel, 2000). This is in accordance to several studies including the Holocene California borderlands (Covault et al., 2007) and the Neogene Niger and Orinoco deltas which reached the shelf edge during “highstand” conditions to deposit sediment (Henriksen et al., 2011).

The capacity of the river systems to reach the shelf edge can be linked to the underlying geomorphology and width of the shelf at the point of the event (Jones et al., 2013). In this study, a progressively wide shelf during the study period in the south of the dataset and the ability of the shelf to flood back several hundreds of meters (Chapter 3, Iceberg Scours Fig. 3.19) suggests the river systems require more and more sediment supply to reach the shelf edge each time. This likely is a factor in why the submarine events decline after *Pleisto 2* seismic unit as the width of the shelf built out largely during *Pleisto 1* becomes a limiting factor in allowing coarser grained material reaching the shelf edge and depositing basinwards of the shelf edge. The inconsistency across the seismic units also highlights this, with *Pleisto 2 & 3* seismic units only exhibiting three *Multiple Line Source* events, compared to many more in *Plio 1 and Pleisto 1*. Differential subsidence across the SNS basin is a clear hinderance to sediment reaching the shelf edge in the Plio-Pleistocene and determines the distribution of channel events on a regional scale (Chapter 3 & Fig. 4.3).

The investigation of the maximum depths of incision has highlighted that using the geomorphology of submarine systems to understand the amount of base level fall, and specifically a eustatic fall is not fully understood. In the case of the *Multiple Line Source* events, it is likely that base level falls trigger a large amount of these events but there is little evidence to correlate the amount of incision to the eustatic falls. The *Single Feeder* systems are the same order of magnitude of the eustatic falls and therefore could represent a record of base level fall within the basin at the time and more examples across other basins would need to be looked at to confirm this.

4.5.4 Sequence Stratigraphic Context

The key finding of this study is that many more submarine channel depositional events are identified within the seismic record than there are glacial-interglacial cycles. Six *Multiple Line Source* events and at least two incised valley *Single Feeder* systems within 150,000 years are identified which are linked to three glacial-interglacial cycles. Unlike other studies, the scale and continuous coverage of the dataset eliminates to some extent, the likelihood of a submarine channel event being present in another part of the basin by lobe switching. Most of the submarine channel events are associated with evidence of periods of lower relative sea level. Most are associated with late interglacial (degradational clinoform trajectories) and the maximum glacial period where sea level is at its lowest (degradational/flat trajectory) (Fig. 4.13). This corresponds to the traditional view of when sediment bypass of the shelf would be predicted (Vail et al., 1977, Posamentier and Vail, 1988). Deposition basinwards of the shelf edge is more likely during periods of base level lows (Johannessen and Steel, 2005) and associated with descending trajectories (Henriksen et al., 2011). This study also highlights that in the SNS basinwards deposition can occur within many different base level scenarios (Fig. 4.13) including rising base level.

Each *Single Feeder* system appears to be predictably associated with a degradational stacking pattern; however that does not necessarily link to each individual fall in global sea level (Fig. 4.2). Each glacial-interglacial cycle does not correspond to a predictable set of basin deposition events. This is contradictory to the evidence that the regional markers of the glacial termination, the strong amplitude, high gamma ray shale layers which cap the glacial periods tell us. The predictability of sequence architecture in the basin is clearer than the predictability of basin deposition events. The magnitude of eustatic fall and rise appears to have little correlation to the type of deep water deposition present and how evolved the system will be (i.e. gullies, channel belts, or canyons). This points towards poor predictability of reservoir quality sands basinwards of the shelf edge if only talking eustasy into account.

A diagnostic of a sequence boundary is that it is the boundary of which a basin floor fans bidirectional downlaps on to. The presence of incised valleys associated with basin deposition expresses that the shelf is exposed and the river system is bypassing the

coastal prism. Type 1 sequence boundaries are placed at the incision surface and its correlative conformity, associated with the bidirectional downlap of the basin floor fan (Van Wagoner et al., 1990). The associated downstepping of clinoforms and reduction in clinoform height confirms that the sequence boundary is caused by a base level fall rather than a change in sediment load or hydrodynamics of the incising river system (Posamentier et al., 1992). Infill of the canyons is filled during the same time as the aggrading clinoforms and is completed by the strong amplitude continuous shale layer above.

This study shows there can be more than one basin floor fan deposition (*Single Feeder* system) within in a traditional sequence or a basin floor fan is not present at all. This suggests that interpreting sequence boundaries based on the presence of these channel or fan architectures can be misleading. Sequence boundaries are defined as regionally important boundaries rather than locally important and therefore, this highlights the imperative of understanding the local tectonics, seismic geomorphology and sediment supply system before attempting to apply sequence stratigraphy methodology to a basin. This study clearly shows that just using sequence stratigraphy and clinoform trajectory analysis should be supplemented with seismic geomorphology and investigation of sediment accumulation rates and progradation rates to analyse whether there is a supply dominated system. More commonly basinwards deposition appears associated with certain conditions on the outer shelf and shelf edge. Strong amplitudes at the shelf edge, delta scale clinoforms or heavily channelized outer shelves correspond with an area downdip where submarine channel events will occur. There can be more use in analysing the conditions on the outer shelf and shelf edge than using traditional prediction techniques (Dixon et al., 2012; Johannessen and Steel, 2005; Sømme et al., 2009).

The maximum incision of *Single Feeder* systems canyons reflect the changes in base level more effectively than that of the *Multiple Line Source* events, which appear consistent throughout the study period, regardless of larger base level changes from the base Quaternary onwards.

4.5.5 Implications and Limitations

Hydrocarbon discovery LilleJohn in the Miocene Ustira formation in the Danish Sector of the North Sea is associated with a basin floor sands play (Trampe et al., 2013). This is the first time slope channels and basin floor fans have been mapped in the Netherlands sector and now that these have been identified they could be used as an analogue for the earlier Ustira formation but also could possibly present viable hydrocarbon targets themselves. Individual *Multiple Line Source* channel basin floor deposition is small in compared to the *Single Feeder* radial basin floor fans however they become viable when active salt tectonics on the slope or basin floor creates accommodation and enables sediment ponding. The systems identified in this paper could also be provided as shallow analogies for deeper, less well imaged targets.

A limitation of any study of ancient clinoforms in seismic data is that geophysical representations of the clinoforms which are now buried at depth are being studied. This creates a twofold reason why the seismic may not represent the original depositional architecture at the time the clinoforms were deposited. The seismic data used in this study is in two way time rather than depth and therefore a depth conversion of the clinoforms could alter the clinoform architectures. The velocities of the Late Cenozoic section in the SNS are variable between 1700-2200 ms⁻¹ () and are well constrained from velocity studies and borehole data (van Dalfsen et al., 2007). Sensitivity analysis was carried out on the clinoforms to attempt to understand if clinoform geometries are distorted. Sonic log velocities were studied across a test sample of clinoforms along the clinoforms in different settings. Two distinct velocity layers could be distinguished; the “topsets facies” which are layercake interbedded terrestrial and marine deposits which had an average velocity of 1700-1800 ms⁻¹ and “foreset/bottomset facies” which would largely be made of hemipelagic muds and distal marine muds and silts which had a faster velocity of around 2000 ms⁻¹. The thickness of the topset facies across a set of clinoforms is between 20-30% compared to the thickness of the foresets, therefore even though the foreset/bottomset facies has a faster velocity it was found to cancel each other out when depth conversion was carried out across a test clinoform. The shift in depth was almost equal across the clinoform (within 5%). More detailed work should be carried out to understand the depth conversion in many different cases, e.g. oblique

clinoform dominated sections compared to sigmoidal clinoform dominated sections but the confidence is that there should not be a significant change in clinoform angles and it should not affect the relationship between the clinoforms (e.g the trajectory). Any distortion of the clinoform would largely affect the lower slope because of the faster velocities in that section may experience velocity pull up, so that the lower slope and bottomset appear shallower than they actually are.

The other important factor is restoring the clinoforms to their original depositional configuration. This requires detailed structural restoration and decompaction of the clinoforms similar to which has been carried out previously in New Jersey (Steckler et al., 1999), in the Troll Field North Sea (Patruno et al., 2014) and in this dataset (Lamb et al, in review; Chapter 6.2). This is important for this study because of the aim to understand the clinoforms original depositional architecture relative to each others, however after analysing the difference between the decompacted clinoforms in Lamb et al., compared to the TWT configuration of the clinoforms, it was found that the difference between the two was within 10% once depth converted and therefore should have minimal effect. For instance in the southern Netherlands North Sea the base Quaternary clinoform after backstripping was found to be of the order 250-300 m clinoform height, which after depth conversion is within the same range as the clinoform as it appears in the seismic. This is likely because of the opposite effect to the depth conversion. Due to the role of loading on palaeotopography, topsets are largely less loaded than the bottomsets (Steckler et al., 1999) and therefore vertical differences between the topset and bottomset are exaggerated in TWT compared to the original depositional architecture (Miller et al., 2013) and therefore has the opposite effect to the velocity effects. For more details on the Backstripping process in the area see Chapter 6.2. It was therefore decided that between the depth conversion and the decompaction the changes in the trajectories is minimal with a sensitivity of 10% or less, which is deemed not to distort the outcomes of this paper. Flattening on datum horizons to structurally restore clinoforms was deemed enough to be able to understand the original depositional history of the clinoforms.

4.6 CONCLUSIONS

- For the first time, Plio-Pleistocene submarine channels have been identified and imaged in the Netherlands North Sea. The events could be used as analogues for earlier Miocene submarine events which are found to be prospective in the Danish North Sea sector or even be targets themselves.
- The high resolution dating and correlation of key seismic reflections events to the Marine Isotope Curve has highlighted that at least eight distinct submarine channel systems occurred within three glacial-interglacial cycles. This has not been shown before.
- The most common shelf edge trajectory conditions for bypass of the shelf into the basin is flat lying to descending shelf edge trajectories of oblique tangential clinoforms with strong amplitudes found on the outer shelf.
- *Single Feeder* systems link to the traditional “LST” Lowstand Systems Tract, appears valid in relation to the seismic architecture, however when related to the global sea level curve it is clear that a basin floor fan is not present during every global sea level low, and in fact several can occur within one glacial interglacial cycle which makes clear that many other factors affect the chance of getting sediment to the basin and that sequence boundaries, should be based on clinoform architectures rather than the position of basin floor fans.
- Previous palynological and geochemical analysis of the SNS show that the regional sea level is governed by glacial –interglacial cycles and by the identification of regional shale layers and clinoform architectures this is reflected to some extent in the seismic stratigraphy of the basin. However it is clear from this study that the relationship between predicated base level falls and sediment being delivered to the basin floor is not straight forward.
- This paper supports that sediment can be transported to the deep water when relative sea level is rising when sediment supply is high enough. The deposition of reservoir quality sediments basinwards of the shelf edge can be moderately predictable but knowledge of the regional lateral variability of the basin, seismic geomorphology of the shelf, sediment supply and knowledge of the basins relationship to the global sea level curve is imperative.

4.7 REFERENCES

- Anell, I., Thybo, H., Rasmussen, E., 2012. A synthesis of Cenozoic sedimentation in the North Sea. *Basin Research* 24, 154–179.
- Bijkerk, J.F., ten Veen, J., Postma, G., Mikeš, D., van Strien, W., de Vries, J., 2014. The role of climate variation in delta architecture: Lessons from analogue modelling. *Basin Research* 26, 351–368.
- Bijlsma, S., 1981. Fluvial sedimentation from the Fennoscandian area into the North-West European Basin during the Late Cenozoic. *Geologie en Mijnbouw/Netherlands Journal of Geosciences* 60, 337–345.
- Burgess, P.M., Hovius, N., 1998. Rates of delta progradation during highstands: consequences for timing of deposition in deep-marine systems. *Journal of the Geological Society* 155, 217–222.
- Cameron, T.D.J., Stoker, M.S., Long, D., 1987. The history of Quaternary sedimentation in the UK sector of the North Sea Basin. *Journal of the Geological Society* 144, 43–58.
- Cande, S.C., Kent, D. V, 1995. Revised calibration of the geomagnetic polarity timescale for the Late Cretaceous and Cenozoic. *Journal of geophysical research* 100, 6093–6095.
- Carvajal, C., Steel, R., Petter, A., 2009. Sediment supply: The main driver of shelf-margin growth. *Earth-Science Reviews* 96, 221–248.
- Carvajal, C.R., Steel, R.J., 2006. Thick turbidite successions from supply-dominated shelves during sea-level highstand. *Geology* 34, 665–668.
- Catuneanu, O., Abreu, V., Bhattacharya, J.P., Blum, M.D., Dalrymple, R.W., Eriksson, P.G., Fielding, C.R., Fisher, W.L., Galloway, W.E., Gibling, M.R., Giles, K. A., Holbrook, J.M., Jordan, R., Kendall, C.G.S.C., Macurda, B., Martinsen, O.J., Miall, A. D., Neal, J.E., Nummedal, D., Pomar, L., Posamentier, H.W., Pratt, B.R., Sarg, J.F., Shanley, K.W., Steel, R.J., Strasser, a., Tucker, M.E., Winker, C., 2009. Towards the standardization of sequence stratigraphy. *Earth-Science Reviews* 92, 1–33.
- Covault, J. A., Normark, W.R., Romans, B.W., Graham, S. A., 2007. Highstand fans in the California borderland: The overlooked deep-water depositional systems. *Geology* 35, 783–786.
- Crumeyrolle, P., Renaud, I., Suiter, J., 2007. The use of two- and three-dimensional seismic to understand sediment transfer from fluvial to deepwater via sinuous channels: example from the Mahakam shelf and comparison with outcrop data (south central Pyrenees). *Geological Society, London, Special Publications* 277, 85–103.
- Davies, R.J., Posamentier, H.W., 2005. Geologic processes in sedimentary basins inferred from three-dimensional seismic imaging. *GSA Today* 15, 4–9.

- Dixon, J.F., Steel, R.J., Olariu, C., 2012. River-dominated, shelf-edge deltas: Delivery of sand across the shelf break in the absence of slope incision. *Sedimentology* 59, 1133–1157.
- Dixon, J.F., Steel, R.J., Olariu, C., 2012. Shelf-Edge Delta Regime As A Predictor of Deep-Water Deposition. *Journal of Sedimentary Research* 82, 681–687.
- Flint, S.S., Hodgson, D.M., Sprague, a. R., Brunt, R.L., Van der Merwe, W.C., Figueiredo, J., Pr  lat, A., Box, D., Di Celma, C., Kavanagh, J.P., 2011. Depositional architecture and sequence stratigraphy of the Karoo basin floor to shelf edge succession, Laingsburg depocentre, South Africa. *Marine and Petroleum Geology* 28, 658–674.
- Galloway, W.E., 2002. Paleogeographic setting and depositional architecture of a sand-dominated shelf depositional system, Miocene Utsira Formation, North Sea Basin. *Journal of Sedimentary Research* 72, 476–490.
- Gawthorpe, R.L., Fraser, A.J., Collier, R.E.L., 1994. Sequence stratigraphy in active extensional basins: implications for the interpretation of ancient basin-fills. *Marine and Petroleum Geology* 11, 642–658.
- Gee, M.J.R., Gawthorpe, R.L., 2006. Submarine channels controlled by salt tectonics: Examples from 3D seismic data offshore Angola. *Marine and Petroleum Geology* 23, 443–458.
- Gee, M.J.R., Gawthorpe, R.L., Bakke, K., Friedmann, S.J., 2007. Seismic Geomorphology and Evolution of Submarine Channels from the Angolan Continental Margin. *Journal of Sedimentary Research* 77, 433–446.
- Gibbard, P.L., West, R.G., Zagwijn, W.H., Balson, P.S., Burger, A.W., Funnell, B.M., Jeffery, D.H., de Jong, J., van Kolfschoten, T., Lister, A.M., Meijer, T., Norton, P.E.P., Preece, R.C., Rose, J., Stuart, A.J., Whiteman, C.A., Zalasiewicz, J.A., 1991. Early and early Middle Pleistocene correlations in the southern North Sea basin. *Quaternary International* 10, 23–52.
- Hampson, G.J., Graham, G.H., Holgate, N.E., Morris, J.E., Patruno, S., Sech, R.P., Petersen, S.A., Jackson, C.-L., Jackson, M.D., Johnson, H., 2015. Sedimentological Characterisation, Impact and Modelling of Clinoforms in Shallow Marine Reservoirs. *Sedimentology of Paralic Reservoirs: Recent Advances and their Applications Conference Abstract*.
- Harding, R., Huuse, M., 2015. Salt on the move: Multi stage evolution of salt diapirs in the Netherlands North Sea. *Marine and Petroleum Geology* 61, 39–55.
- Helland-Hansen, W., Hampson, G.J., 2009. Trajectory analysis: concepts and applications. *Basin Research* 21, 454–483.
- Henriksen, S., Helland-Hansen, W., Bullimore, S., 2011. Relationships between shelf-edge trajectories and sediment dispersal along depositional dip and strike: A different approach to sequence stratigraphy. *Basin Research* 23, 3–21.

- Huisman, D.J., Klaver, G.T., 2007. Heavy Minerals in the subsurface: Tracking sediment sources in three dimensions, *Developments in Sedimentology*, *Developments in Sedimentology* 58, 869-885.
- Hunt, D., Tucker, M.E., 1992. Stranded parasequences and the forced regressive wedge systems tract: deposition during base-level fall—reply. *Sedimentary Geology* 95, 147–160.
- Johannessen, E.P., Steel, R.J., 2005. Shelf-margin clinoforms and prediction of deepwater sands. *Basin Research* 17, 521–550.
- Jones, G.E.D., Hodgson, D.M., Flint, S.S., 2015. Lateral variability in clinoform trajectory, process regime, and sediment dispersal patterns beyond the shelf-edge rollover in exhumed basin margin-scale clinothems. *Basin Research* 27 (6), 1-24.
- Jones, G.E.D., Hodgson, D.M., Flint, S.S., 2013. Contrast in the process response of stacked clinothems to the shelf-slope rollover. *Geosphere* 9, 299–316.
- Khripounoff, A., Vangriesheim, A., Babonneau, N., Crassous, P., Dennielou, B., Savoye, B., 2003. Direct observation of intense turbidity current activity in the Zaire submarine valley at 4000 m water depth. *Marine Geology* 194, 151–158.
- Kolla, V., Perlmutter, M.A., 1993. Timing of turbidite sedimentation on the Mississippi Fan. *AAPG Bulletin* 77, 1129–1141.
- Kuhlmann, G., de Boer, P.L., Pedersen, R.B., Wong, T.E., 2004. Provenance of Pliocene sediments and paleoenvironmental changes in the southern North Sea region using Samarium–Neodymium (Sm/Nd) provenance ages and clay mineralogy. *Sedimentary Geology* 171, 205–226.
- Kuhlmann, G., Langereis, C., Munsterman, D., Jan van Leeuwen, R., Verreussel, R., Meulenkamp, J., Wong, T., 2006a. Chronostratigraphy of Late Neogene sediments in the southern North Sea Basin and paleoenvironmental interpretations. *Palaeogeography, Palaeoclimatology, Palaeoecology* 239, 426–455.
- Kuhlmann, G., Langereis, C., Munsterman, D., Jan van Leeuwen, R., Verreussel, R., Meulenkamp, J., Wong, T., 2006b. Chronostratigraphy of Late Neogene sediments in the southern North Sea Basin and paleoenvironmental interpretations. *Palaeogeography, Palaeoclimatology, Palaeoecology* 239, 426–455.
- Kuhlmann, G., Wong, T.E., 2008. Pliocene paleoenvironment evolution as interpreted from 3D-seismic data in the southern North Sea, Dutch offshore sector. *Marine and Petroleum Geology* 25, 173–189.
- Leeder, M.R., 2009. *Sedimentology and sedimentary basins: from turbulence to tectonics*. John Wiley & Sons.
- Lisiecki, L.E., Raymo, M.E., 2005. A Pliocene-Pleistocene stack of 57 globally distributed benthic δ 18O records. *Paleoceanography* 20, 1–17.

- Meijer, T., Cleveringa, P., Munsterman, D.K., Verreussel, R.M.C.H., 2006. The Early Pleistocene Praetigian and Ludhamian pollen stages in the North Sea Basin and their relationship to the marine isotope record. *Journal of Quaternary Science* 21, 307–310.
- Menier, D., Reynaud, J.Y., Proust, J.N., Guillocheau, F., Guennoc, P., Bonnet, S., Tessier, B., Goubert, E., 2006. Basement control on shaping and infilling of valleys incised at the southern coast of Brittany, France. *SEPM Special Publication* 85, 37–55.
- Miller, K., Mountain, G., Wright, J., Browning, J., 2011. A 180-Million-Year Record of Sea Level and Ice Volume Variations from Continental Margin and Deep-Sea Isotopic Records. *Oceanography* 24, 40-53.
- Miller, K.G., Kominz, M.A., Browning, J. V, Wright, J.D., Mountain, G.S., Katz, M.E., Sugarman, P.J., Cramer, B.S., Christie-Blick, N., Pekar, S.F., 2005. The Phanerozoic Record of Global Sea-Level Change. *Science* 310 , 1293–1298.
- Miller, K.G., Mountain, G.S., Browning, J. V., Katz, M.E., Monteverde, D., Sugarman, P.J., Ando, H., Bassetti, M. A., Bjerrum, C.J., Hodgson, D., Hesselbo, S., Karakaya, S., Proust, J.N., Rabineau, M., 2013. Testing sequence stratigraphic models by drilling Miocene foresets on the New Jersey shallow shelf. *Geosphere* 9, 1236–1256.
- Mitchum Jr., R.M., Vail, P.R., Sangree, J.B., 1977. Seismic stratigraphy and global changes of sea level, Part six: stratigraphic interpretation of seismic reflection patterns in depositional sequences. *Seismic Stratigraphy — applications to hydrocarbon exploration* 117–134.
- Muto, T., Steel, R.J., 2000. The accommodation concept in sequence stratigraphy: some dimensional problems and possible redefinition. *Sedimentary Geology* 130, 1–10.
- Nalpas, T., Le Douaran, S., Brun, J.-P., Unternehr, P., Richert, J.-P., 1995. Inversion of the Broad Fourteens Basin (offshore Netherlands), a small-scale model investigation. *Sedimentary Geology* 95, 237–250.
- Neal, J., Abreu, V., 2009. Sequence stratigraphy hierarchy and the accommodation succession method. *Geology* 37, 779–782.
- Noorbergen, L.J., Lourens, L.J., Munsterman, D.K., Verreussel, R.M.C.H., 2015. Stable isotope stratigraphy of the early Quaternary of borehole Noordwijk, southern North Sea. *Quaternary International* 386, 148-157.
- Overeem, I., Weltje, G.J., Bishop-Kay, C., Kroonenberg, S.B., 2001. The Late Cenozoic Eridanos delta system in the Southern North Sea Basin: a climate signal in sediment supply? *Basin Research* 13, 293–312.
- Patrino, S., Hampson, G.J., Jackson, C. A L, Whipp, P.S., 2014. Quantitative progradation dynamics and stratigraphic architecture of ancient shallow-marine clinoform sets: A new method and its application to the Upper Jurassic Sognefjord Formation, Troll Field, offshore Norway. *Basin Research* 27 (4), 412-452.

- Pekar, S.F., Kominz, M. A., 2001. Two-Dimensional Paleoslope Modeling: A New Method for Estimating Water Depths of Benthic Foraminiferal Biofacies and Paleoshelf Margins. *Journal of Sedimentary Research* 71, 608–620.
- Pharoh, T.C., Dusar, M., Geluk, M.C., Kockel, F., Krawczyk, P., Scheck-Wenderoth, M., Thybo, H., Vejbaek, O.V., Van Wees, J.D., 2010. Tectonic evolution. *In* Doornenbal, J.C and Stevenson, A.G. (editors): *Petroleum Geological Atlas of the Southern Permian Basin Area*. EAGE Publications b.v. (Houten): 25-57.
- Piper, D.J.W., Normark, W.R., 2009. Processes that initiate turbidity currents and their influence on turbidites: a marine geology perspective. *Journal of Sedimentary Research* 79, 347–362.
- Porebski, S.J., Steel, R.J., 2006. Deltas and Sea-Level Change. *Journal of Sedimentary Research* 76, 390–403.
- Porębski, S.J., Steel, R.J., 2003. Shelf-margin deltas: Their stratigraphic significance and relation to deepwater sands. *Earth-Science Reviews* 62, 283–326.
- Posamentier, H.W., 2004. Seismic Geomorphology: Imaging Elements of Depositional Systems from Shelf to Deep Basin Using 3D Seismic Data: Implications for Exploration and Development. *Geological Society, London, Memoirs* 29, 11–24.
- Posamentier, H.W., 2001. Lowstand alluvial bypass system : Incised vs. unincised. *American Association of Petroleum Geologists Bulletin* 10, 1771–1793.
- Posamentier, H.W., Allen, G.P., James, D.P., Tesson, M., 1992. Forced regressions in a sequence stratigraphic framework: concepts, examples, and exploration significance. *American Association of Petroleum Geologists Bulletin* 76 (11), 1687-1709.
- Posamentier, H.W., Kolla, V., 2003. Seismic Geomorphology and Stratigraphy of Depositional Elements in Deep-Water Settings. *Journal of Sedimentary Research* 73, 367–388.
- Posamentier, H.W., Vail, P.R., 1988. Eustatic controls on clastic deposition II — Sequence and systems tract models. *SEPM Special Publication* 42, 125-154.
- Prather, B.E., 2003. Controls on reservoir distribution, architecture and stratigraphic trapping in slope settings. *Marine and Petroleum Geology* 20, 529–545.
- Purves, S.J., Henderson, J., Leppard, C., 2007. Rgb Visualisation Based Delineation of Geological Elements from Volumetric Spectral Decomposition of 3d Seismic Data. Extended abstracts EAGE 69th Conference & Exhibition London, UK, 11 - 14 June.
- Remmelts, G., 1996. Salt tectonics in the southern North Sea, the Netherlands, in: *Geology of Gas and Oil under the Netherlands*. 143–158.

- Remmelts, G., 1995. Fault-Related Salt Tectonics in the Southern North Sea, The Netherlands. AAPG Memoir 65, 261–272.
- Ryan, M.C., Helland-Hansen, W., Johannessen, E.P., Steel, R.J., 2009. Erosional vs. accretionary shelf margins: The influence of margin type on deepwater sedimentation: An example from the Porcupine Basin, offshore western Ireland. *Basin Research* 21, 676–703.
- Sømme, T.O., Helland-Hansen, W., Granjeon, D., 2009. Impact of eustatic amplitude variations on shelf morphology, sediment dispersal, and sequence stratigraphic interpretation: Icehouse versus greenhouse systems. *Geology* 37, 587–590.
- Steckler, M.S., Mountain, G.S., Miller, K.G., Christie-Blick, N., 1999. Reconstruction of Tertiary progradation and clinoform development on the New Jersey passive margin by 2-D backstripping. *Marine Geology* 154, 399–420.
- Steel, R., Carvajal, C., Olariu, C., Petter, A., Plink-bjorklund, P., Sanchez, C., 2010. Shelf-Margin Trajectories : Significance for Sediment By-Pass. *Search and Discovery Article* 50297.
- Steel, R.J., Olsen, T., 2002. Clinoforms, clinoform trajectories and deepwater sands. *Sequence Stratigraphic Models for Exploration and Production: Evolving Methodology, Emerging Models and Application Histories* 367–381.
- Sylvester, Z., Deptuck, M.E., Prather, B.E., Pirmez, C., O'Byrne, C., 2012. Seismic stratigraphy of a shelf-edge delta and linked submarine channels in the northeastern Gulf of Mexico, *SEPM Special Publication* 99, 31-59.
- Ten Veen, J.H., van Gessel, S.F., den Dulk, M., 2012. Thin- and thick-skinned salt tectonics in the Netherlands; a quantitative approach. *Netherlands Journal of Geosciences* 91, 447–464.
- Trampe, A.F., Lutz, R., Franke, D., Thöle, H., Arfai, J., 2013. Shallow gas in Cenozoic sediments of the Southern North Sea, in: *EGU General Assembly Conference Abstracts*. p. 1835.
- Vail, I., Mitchum, R.M., Thompson, S., 1977. Seismic stratigraphy and global changes of sea level, Part IV: Global cycles of relative changes of sea level. In: *Stratigraphic interpretations of seismic data. American Association of Petroleum Geologists Bulletin* 26, 83–97.
- Van Wagoner, J.C., Mitchum, R.M., Campion, K.M., Rahmanian, V.D., 1990. Siliciclastic sequence stratigraphy in well logs, cores, and outcrops: concepts for high-resolution correlation of time and facies. *AAPG Methods in Exploration Series* 7, 3–55.
- Zagwijn, W.H., 1992. The beginning of the Ice Age in Europe and its major subdivisions. *Quaternary Science Reviews* 11 (5), 583-591.

Ziegler, P.A., 1992. North Sea rift system. *Tectonophysics* 208, 55–75.

CHAPTER 5

**CAN ENIGMATIC INTRA SLOPE CLINOFORMS
PROVIDE AN INDEPENDENT CALIBRATION OF
EARLY PLEISTOCENE EUSTATIC CHANGES?**

CHAPTER 5: CAN ENIGMATIC INTRA SLOPE CLINOFORMS PROVIDE AN INDEPENDENT CALIBRATION OF EARLY PLEISTOCENE EUSTATIC CHANGES?

Rachel Harding¹, Mads Huuse¹, Rob Gawthorpe²,

¹School of Earth, Environmental and Atmospheric Sciences, University of Manchester

²Department of Earth Sciences, University of Bergen, Norway

5.0 ABSTRACT

Sand prone wedges of high angle descending trajectory clinoforms are prevalent on the slope, basinwards of the shelf edge across the southern North Sea (SNS) during the Cenozoic period, most abundantly in the Early Quaternary of the Netherlands North Sea. Continuous MegaScale 3D seismic reflection data, borehole calibration and a high resolution chronostratigraphic framework allows, for the first time, over twenty of these enigmatic depositional features to be interpreted, dated and placed in context of a sequence stratigraphic framework and the global sea level curve. Within a sequence stratigraphic framework, the Intra Slope Clinoforms are representative of forced regressive wedges. They are deposited during rapid sea level fall, in cold climate marine conditions where relative sea level falls below the shelf edge. Via the chronostratigraphic framework, the forced regressions correspond to glacial stages of the oxygen isotope curve. The clinoform roll over points of the descending clinoforms of the forced regressive wedged are identified as representing fall in base level within the basin and therefore can be used to understand the relative sea level curve of the basin. Sand prone slope wedges have been overlooked in the past in terms of sequence stratigraphy, but they represent sand partitioning basinwards, which has implications for the exploration of reservoir quality sands.

5.1 INTRODUCTION

The Late Cenozoic southern North Sea (sNS) shelf-prism is a natural laboratory to study shelf to basin floor processes. Continuous basin-wide 3D seismic data allows source to sink coverage of depositional systems and the study of sand partitioning basinward of the shelf edge. Neogene and Quaternary age sediments locally exceed 1000 m in thickness (Cameron et al., 1987; Overeem et al., 2001) and therefore have recorded sedimentation through a crucial period of geological time: the descent into Icehouse conditions and their related glacial-interglacial cycles. A number of sandy clinoform wedges which consistently occur basinward and downward of the breakpoint of the preceding shelf-prism clinoform are the focus of the study. The clinoform wedges occur in several parts of the Cenozoic North Sea basin fill (Møller et al., 2009; Kuhlmann and Wong, 2008; Clausen et al., 2012), but are particularly abundant in the Late Pliocene-Earliest Pleistocene succession of the sNS, where chronostratigraphic control by basin-scale 3D seismic data and high-resolution magnetostratigraphy and biostratigraphy allows a detailed insight into their formation and relation with forcing factors.

In this study we document the architecture of the sub 100 m Intra Slope Clinoforms and their spatial and temporal distribution across the sNS. The cyclical nature of the Intra Slope Clinoforms are discussed and placed for the first time within sequence stratigraphic context to aid prediction of sand prone facies basinwards of the shelf break. We aim to understand how they can be used to provide independent calibrations of the eustatic curve during the Late Pliocene and earliest Pleistocene.

5.1.1 Geological Setting

The sNS is an intra-cratonic basin, dominated by the interaction of structural elements associated with the E-W-trending Southern Permian Basin and the NW-SE/NNE-SSW Mesozoic rift basins which were inverted during the Late Cretaceous to Early Paleogene (Ziegler, 1992; Remmelts, 1995). Salt structures are a key feature of the sNS. Halokinesis of halite from the Permian Zechstein supergroup occurred during both the

Mesozoic and Cenozoic (Remmelts, 1996), and continued to the Quaternary in some areas (ten Veen et al., 2012; Harding and Huuse, 2015).

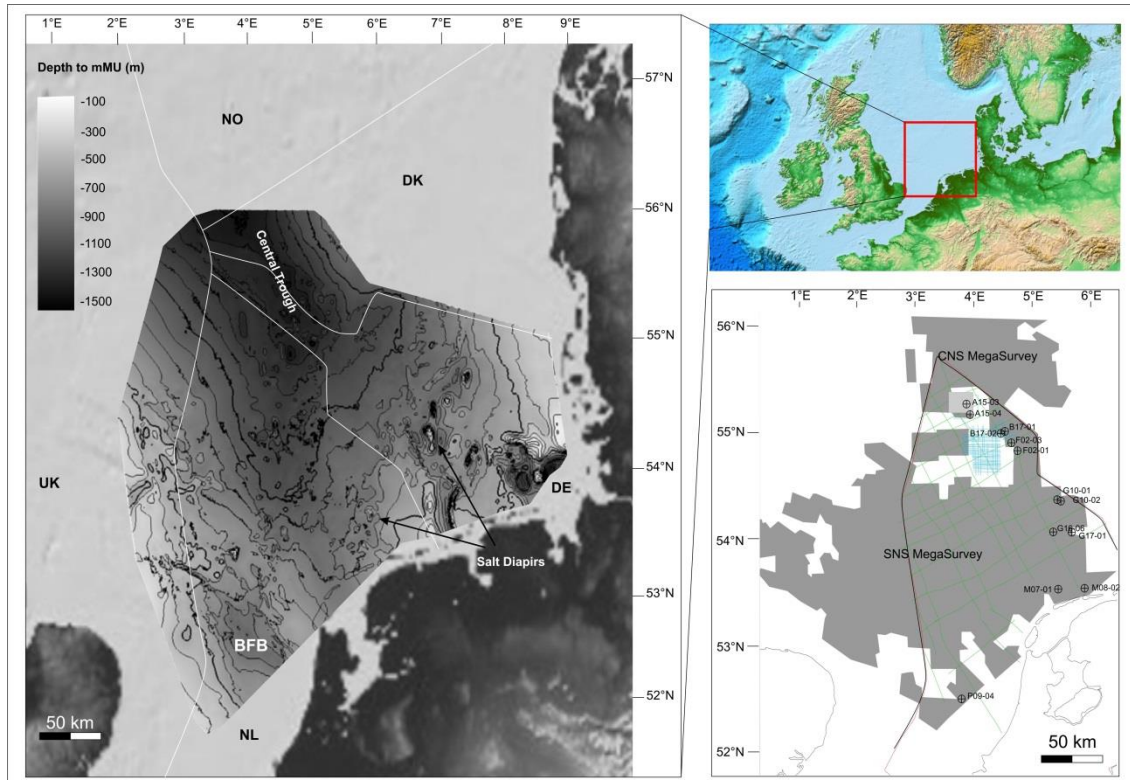


Figure 5.1 Regional setting and dataset map. Left: Mid Miocene Unconformity (mMU) depth structure map. Map is the result of seismic interpretation from this study, (UK, NL and DK sectors) combined with the German mMU structure map from Geopotenzial Deutch Nordsee project (www.gpnd.de). Key areas of accommodation creation marked, Central Trough and BFB (Broad Fourteens Basin). NL Netherlands; DE Germany; DK Denmark; NO Norway. Top Right: GEBCO bathymetry for North Sea showing location of dataset within the contemporary setting. Bottom right: Dataset map. Grey areas represent 3D seismic coverage. 2D seismic lines and key boreholes used the lithological determination also shown.

From the Late Miocene to Quaternary the SNS was the southern part of a north-south elongate basin with a strong tidal regime (Galloway, 2002) dominated by fine-grained marine to fluvio-deltaic sediments from the Baltic River system (Bijlsma, 1981; Cameron et al., 1987; Gibbard et al., 1991; Kuhlmann et al., 2006b). Additional contributions came from the proto-Rhine, Meuse, Scheldt, Weser and Elbe (Kuhlmann et al., 2006b; Huisman and Klaver, 2007).

The dominant seismic architecture of the Late Cenozoic SNS in the Plio-Pleistocene is of shelf-prism clinoforms 100-400 m high, prograding broadly east- west and downlapping on the mid Miocene Unconformity (mMU), a regional seismic reflection (Fig. 5.1). The mMU represents a significant hiatus that spans 5-12 Ma (Anell et al., 2012) which becomes younger towards the west of the North Sea basin (Huuse and Clausen, 2001). The mMU seismic reflector in the Netherlands North Sea is interpreted as a combined Middle Miocene transgressive and Mid-Late Miocene erosive surface (ten Veen, et al., 2013).

Eustacy during the Late Pliocene – Early Pleistocene (3.6 -1.78 Ma) is dominated by 41,000 year obliquity Milankovich cycles (Ruddiman et al., 1986). Regional Northern Hemisphere climate on both land and sea surface varies in tandem with local sea level in the SNS with a small lead of temperature over Northern Hemisphere ice sheet growth (Donders et al., in prep). The first glaciations to indicate widespread vegetation change are MIS 100, 98 and 96 in the earliest Gelasian (Fig. 5.2) (Zagwijn, 1992). Subsequent glacial stages exhibit 30-70 m scale global sea level falls (Miller et al., 2005, 2011).

5.1.2 Chronostratigraphic Framework

The stratigraphy of the Plio-Pleistocene Netherlands North Sea is constrained by high resolution chronostratigraphic, lithological, quantitative palynological and geochemical data from core and palaeomagnetic logs for wells *A15-03 and A15-04* in the north Netherlands North Sea (Kuhlmann et al., 2006ab; ten Veen et al, 2013). Biostratigraphy and benthic stable isotope analysis in the Noordwijk borehole, onshore Netherlands, has also been carried out (Meijer et al., 2006; Noorbergen et al., 2015) (Fig. 5.2).

Linking local climate and sea level change events from palynology and geochemical studies from the Netherlands North Sea and onshore Netherlands to the Marine Isotope Stages (MIS) of the global oxygen isotope curve (Lisiecki and Raymo, 2005) has allowed further dates to be identified and suggests a complex relationship between glacioeustacy and the sedimentary record in the SNS (Meijer et al., 2006; Kuhlmann et al., 2006ab; Noorbergen et al., 2015; Donders et al., in prep).

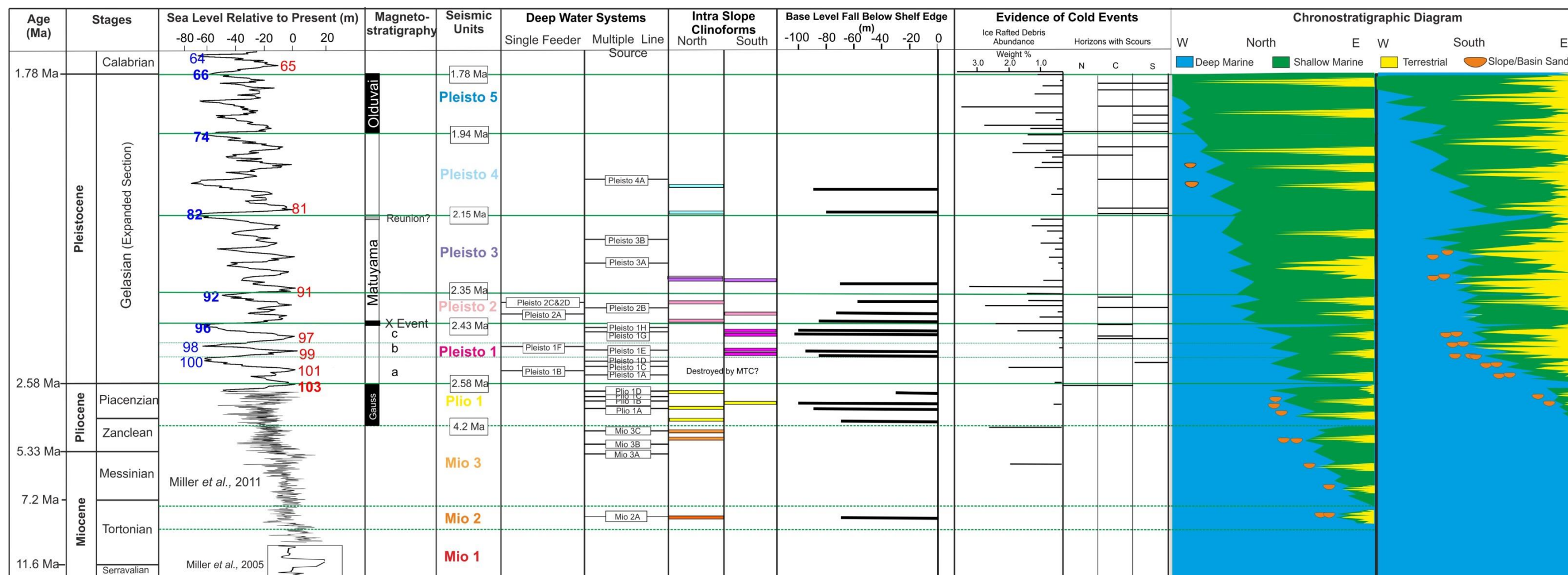


Figure 5.2. Chronostratigraphic framework. Eustatic sea level for the period 11.6–1.78 Ma. Sea level curves scaled from oxygen isotope values from 57 globally distributed benthic ^{18}O records from (Lisiecki and Raymo, 2005) using assumptions given in Miller et al. (2011, 2005). Sea level is relative to present day. Interglacial Marine Isotope Stages in red; Glacial in blue. Age scale is non-linear in order to visualise the study period in one figure. Magnetostratigraphy from Kuhlmann et al., 2006ab and ten Veen et al., 2013. Deep water depositional systems and Intra Slope Clinoform systems are placed in their relative position within a set of dated horizons. The base level falls below shelf edge (black lines) are the vertical distance in meters between the most basinward Intra Slope Clinoform roll over point and the previous shelf edge roll over point, after structural restoration. The grey lines are the measured amount of incision on the upper slope of the Single Feeder canyons, which feed basin floor fans (Chapter 4). This uses each Intra Slope Clinoform events to attempt to understand relative sea level fall in the basin. Cold event information is from Newton et al., in prep (Chapter 6) which shows the presence of iceberg scours on seismic surfaces from this study. N= north; C = central; S=south.

Terrestrial to marine palynology ratios indicate proximity of the coast in the Netherlands North Sea, which transits landwards and basinwards in accordance to early Gelasian glacial-interglacial cycles (MIS 103-92), suggesting relative minimum and maximum sea level in the SNS are as expected for icehouse conditions and governed by eustasy. The global oxygen isotope records (Lisiecki and Raymo, 2005) are strikingly similar to the benthic stable isotope record from onshore Netherlands (Noorbergen et al., 2015), well enough that they can be tuned to the global standard. This suggests the regional glacial-interglacial cycles match that of the global response and it is valid to attempt to understand relative sea level and basin infill in the North Sea in relation to the global sea level curve, at least for the early Gelasian time period. Sea level curves are scaled from oxygen isotope values from 57 globally distributed benthic ^{18}O records from (Lisiecki and Raymo, 2005) using assumptions given in (Miller et al., 2005) and (Miller et al., 2011) (Fig. 5.2).

A reverse coupling of sediment grain size and sea level in the basin is noted by Kuhlmann and Wong, (2008); Noorbergen et al. (2015) and Donders et al. (in prep). Finer grained sediment is associated with the glacial cold conditions and low sea level. The finest grained material, which is interpreted to enter the basin towards the glacial stage termination, is the product of weathering metamorphic rocks of Scandinavia and a long transport route (Kuhlmann et al., 2004; Noorbergen et al., 2015). The finest grained sediments (glacial terminations) are linked to the gamma ray log and seismic character in the north Netherlands North Sea (Kuhlmann and Wong, 2008; ten Veen et al., 2011; 2013) and identified as gamma ray peaks, and are correlated to strong amplitude, semi-regional continuous seismic reflections. Coarser material associated with low gamma ray values is related to warm interglacial conditions and higher relative sea level. Therefore, though regional base level reflects glacioeustasy during the earliest Gelasian (2.58-2.35 Ma), grain size is not directly controlled by it (ten Veen et al., 2013; Donders et al, in prep). Sediment supply, local subsidence and underlying geomorphology create variability in how eustasy is expressed within the sedimentary architecture of the SNS (Chapters 3 & 4).

In the Netherlands North Sea the majority of post mid Miocene Unconformity sedimentation consists of Gelasian sedimentation from 2.58 Ma (base Quaternary) and the Top Gelasian at 1.78 Ma. Several key chronostratigraphic surfaces are identified in the literature from the period studied here (Cande and Kent, 1995; Kuhlmann et al.,

2006ab; Noorbergen et al., 2015; Donders et al., in prep) (Fig. 5.2). The base Quaternary (2.58 Ma) corresponds to the Gauss-Matuyama magnetic reversal, an event in the pollen record which correlates to climatic degradation and the last occurrence of *Monspeliensina pseudotepida*, benthic foraminifera. In the Netherlands North Sea the surface is recognised as a regional flooding event and the top MIS 103 interglacial. The X event at 2.43 Ma is a regional strong amplitude shale layer and gamma ray peak and is correlated to the termination of glacial MIS 96. Two additional regional strong shale layers between the Gauss-Matuyama magnetic reversal and the X-event correspond to the termination of glacial period MIS 100 (~2.51 Ma) and 98 (~2.48 Ma). An additional shale layer corresponds to a change in palynology and is correlated to the termination of MIS 92 and therefore gives an additional date at 2.35 Ma.

The Reunion event dated at ~2.15 Ma may correspond to MIS 82 (Kuhlmann, et al., 2006ab). The top and base of the Olduvai event within the Matuyama epoch gives additional dates at 1.96 Ma and 1.78 Ma, corresponding with the Top Gelasian (Kuhlmann et al., 2006ab).

5.2. DATASET AND METHODOLOGY

The dataset comprises a continuous 3D seismic MegaSurvey, covering 55,000 km² of the Netherlands, UK, German and Danish sectors of the southern North Sea (Fig. 5.1). The MegaSurvey is composed of merged 3D seismic surveys and was interpreted at a bin spacing of 50 m by 50 m, sampling rate 4 ms TWT. The vertical resolution is 10-15 m in the top 1500 m.

The study utilizes released well data from the Netherlands North Sea. Petrophysical well logs, including gamma ray and sonic logs; cuttings descriptions, plus biostratigraphic picks are available for 172 boreholes. Key wells are identified in Fig. 5.1. High resolution chronostratigraphic, lithological, quantitative palynological and geochemical data from core and palaeomagnetic logs for wells *A15-03 and A15-04* in the north of the Netherlands sector are used to create a chronostratigraphic framework across the SNS using well and seismic correlation (Kuhlmann et al., 2006ab; ten Veen et al., 2013; Chapter 3). This has given several dated basin-wide horizons, linked to the

Marine Isotope Curve. Additional controls on the base Quaternary (2.58 Ma) and the Top Gelasian (1.78 Ma) across the basin are provided by Chris King (*pers comms* 2013, See Appendix).

Standard seismic stratigraphic techniques as developed by Mitchum et al. (1977) are used to establish the basin-wide chronostratigraphic framework. A combination of traditional horizon based seismic interpretation using Schlumberger Petrel v2013 and auto interpretation using Eliis PaleoScan software was used to map horizons and investigate the 3D seismic character of reflections between picked horizons. For 3D visualisation, seismic geomorphology techniques such as time slicing, stratal slicing and horizon slicing are combined with RMS amplitude extractions and RGB blending techniques using FFA Geoteric software (Davies and Posamentier, 2005; Posamentier and Kolla, 2003; Henderson et al., 2007; Purves, et al., 2007). To understand depositional trajectories of the clinoforms, flattening on overlying topsets in order to back rotate clinoforms is carried out where necessary. Calibrated TWT to Depth plotted from available industrial check shot data in the Netherlands North Sea from ten Veen et al. (2013) is utilised (Chapter 2).

5.3 SEISMIC STRATIGRAPHIC FRAMEWORK

The key bounding seismic surfaces, the link to well logs character and climate proxies within the time period between >11.6 Ma (Seravallian-Tortonian) and 1.78 Ma (Top Gelasian) SNS shelf-prism are described. Linking and enhancing the established chronostratigraphic framework (section 5.1.2) to the seismic stratigraphy across the dataset allows a correlation of seismic architecture to the global sea level curve.

The dominant seismic architecture of the SNS in the Late Cenozoic is of highly progradational sigmoidal and oblique shelf-prism clinoforms, 100-400 m high, downlapping on to the mMU. The depositional environment of the shelf-prism clinoform is determined in Chapter 3 as the topset, foreset and bottomset representing the shelf, slope and basin floor respectively and the shelf-prism clinoform roll over point represents the shelf edge (Fig. 5.3). Delta-scale clinoforms, defined as less than

100 m in height are also identified, superimposed on the larger shelf-prism clinoforms. They are divided into *Intra Slope* and *Intra Shelf Clinoforms*.

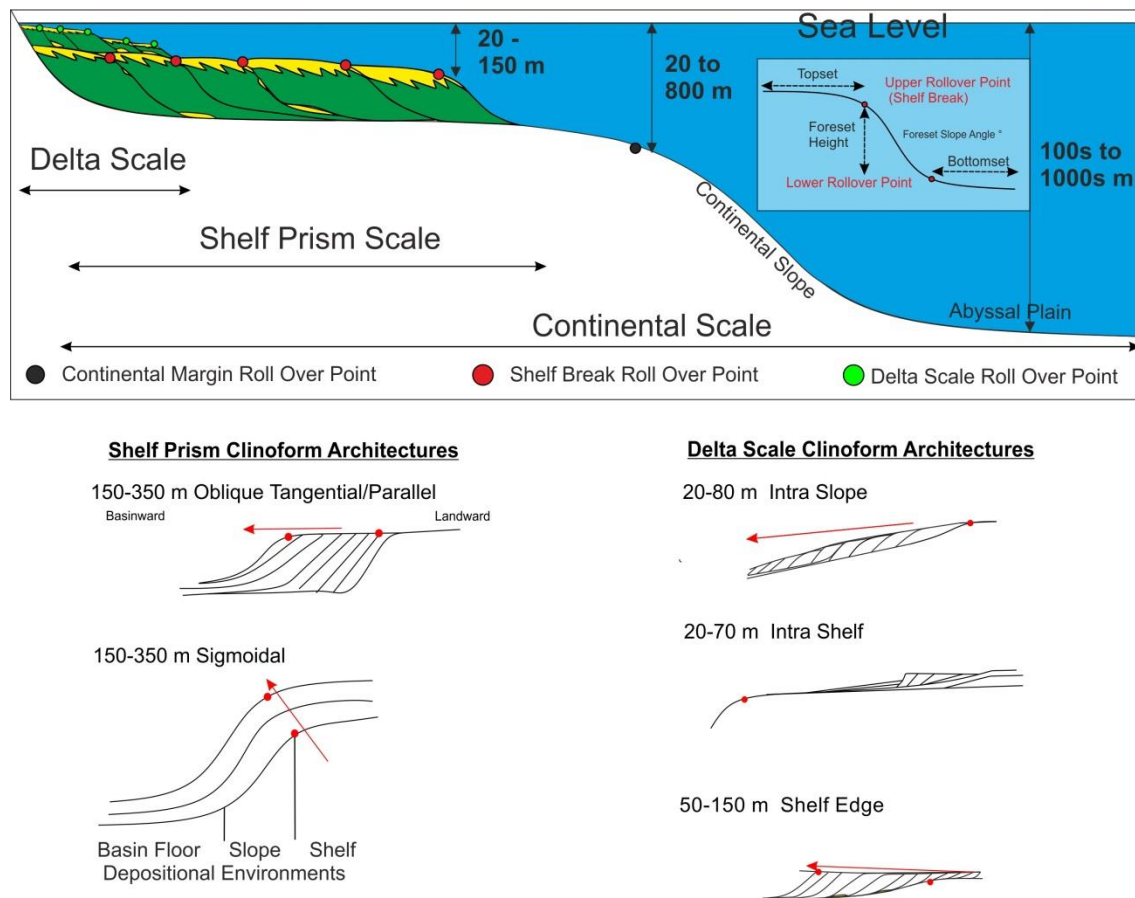


Figure 5.3. Clinoform terminology. Key definitions used in this paper. Adapted from Helland-Hansen and Hampson, 2009; Patruno et al., 2015). Measurements on the delta scale, shelf-prism scale and the continental scale clinoform are regarding the water depth. Clinoform nomenclature used in this paper is illustrated on the sigmoidal clinoform architecture.

Intra Slope Clinoforms are found on the upper to lower slope, generally have a sloping top and base surface with individual clinoforms reducing in height basinwards (Fig. 5.4a). They are distributed across the SNS basin throughout the Late Cenozoic (Fig. 5.5a). Intra Shelf Clinoforms are found on the mid shelf to upper slope, have a flatter top surface and clinoforms which are consistent in height or increase basinwards and have a lower dip angle than the Intra Slope Clinoforms (Fig. 5.4a).

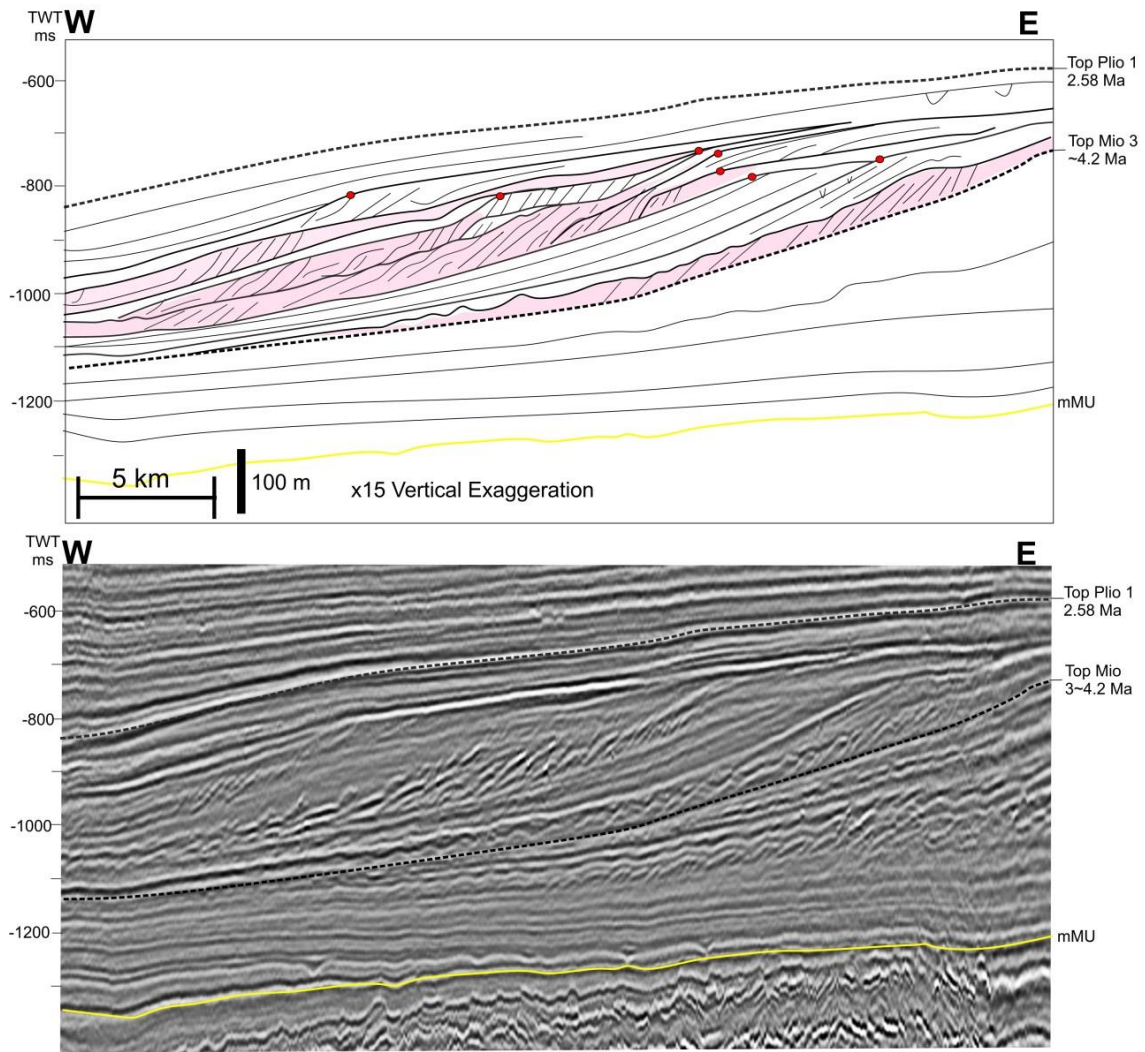


Figure 5.4 Intra Slope Clinoform seismic cross sections. a) East-west seismic cross section through the east of the Netherlands North Sea show an abundance of Intra Slope Clinoform and Intra Shelf Clinoform sets, of *Mio 3* and *Plio 1* seismic units. Intra Shelf Clinoforms are preserved in this example. Pink shaded areas represent the Intra Slope Clinoforms. Dotted lines represent a key seismic reflection. mMU= mid Miocene unconformity. Locations of seismic cross sections are shown in Fig. 5.5.

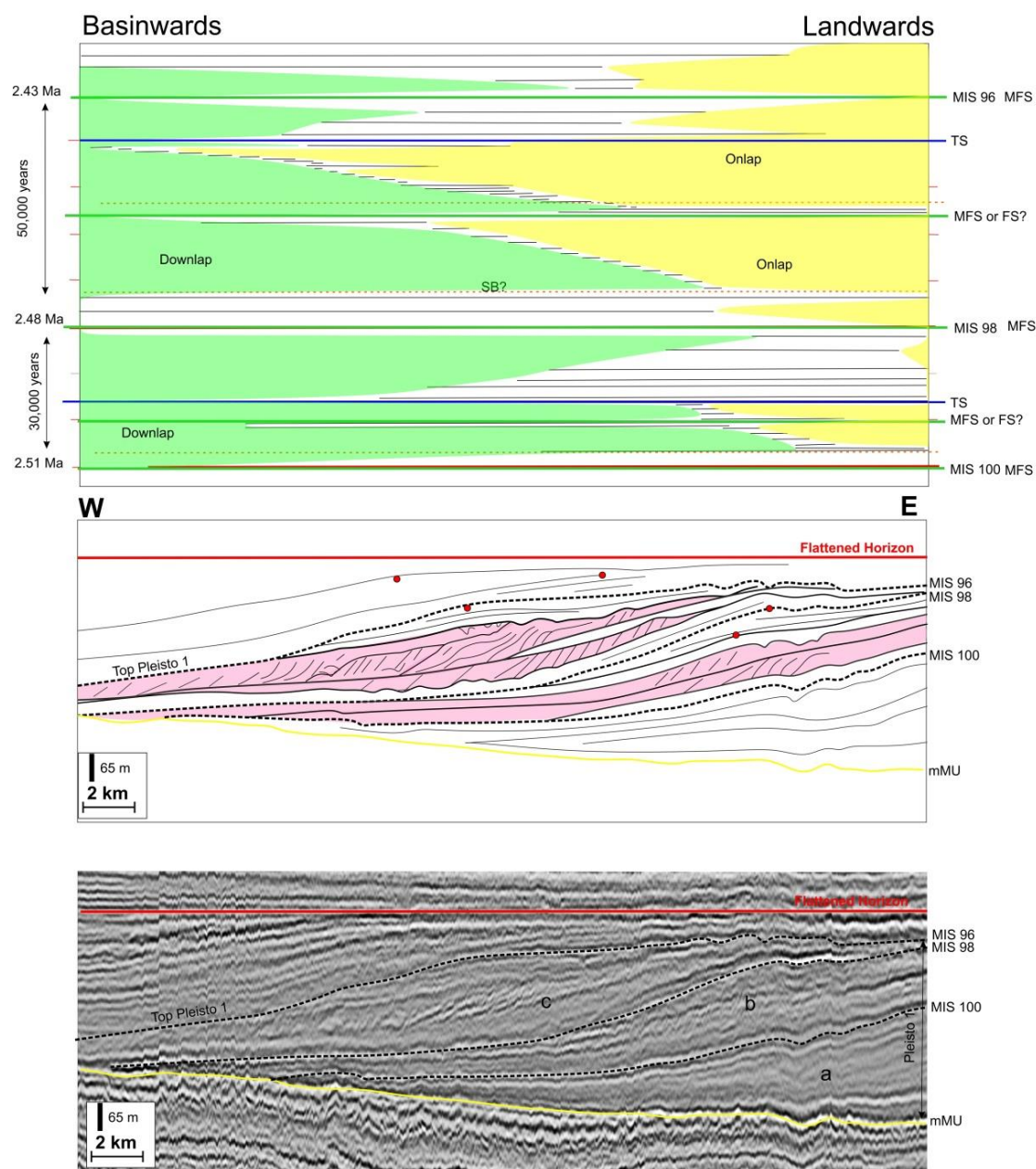


Figure 5.4 cont. b) NNE-SSW seismic cross section through *Pleisto 1* Intra Slope Clinoform examples in the south of the Netherlands North Sea. *Top* Wheeler Diagram representing patterns of sedimentation of the shelf-prism within the basin through the MIS 100-96 time period 2.51-2.43 Ma. The diagram assumes a constant sedimentation rate between the dated horizons. *Centre* and *Bottom*, seismic cross section interpreted and uninterpreted respectively. Basin floor deposition is associated with the first intra slope wedge after MIS 98.

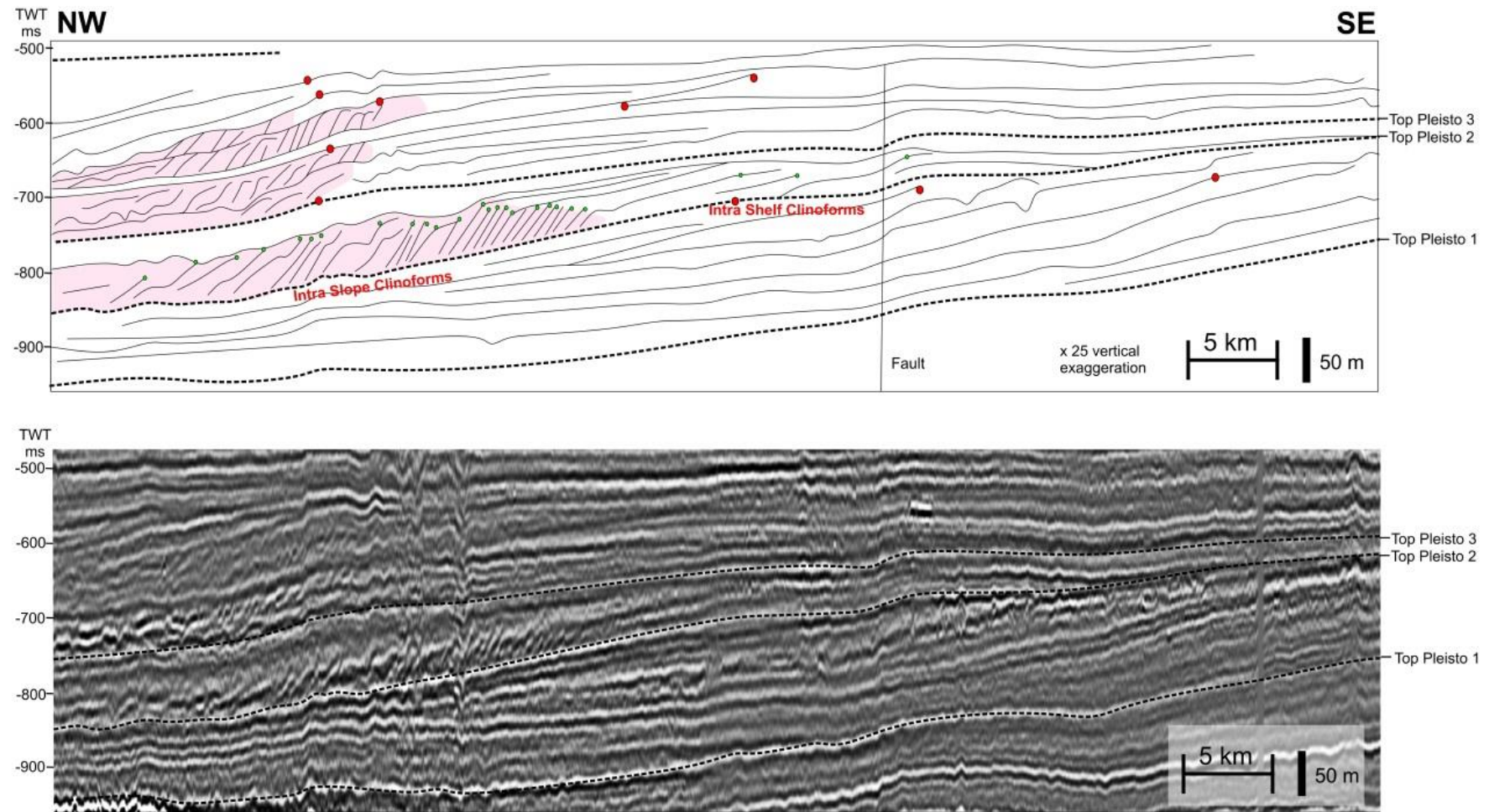


Figure 5.4 cont. c) SE-NW seismic cross section through examples from *Pleisto 2* and *Pleisto 3* seismic units. This example highlights the link between Intra Slope Clinoforms and Intra Shelf Clinoforms.

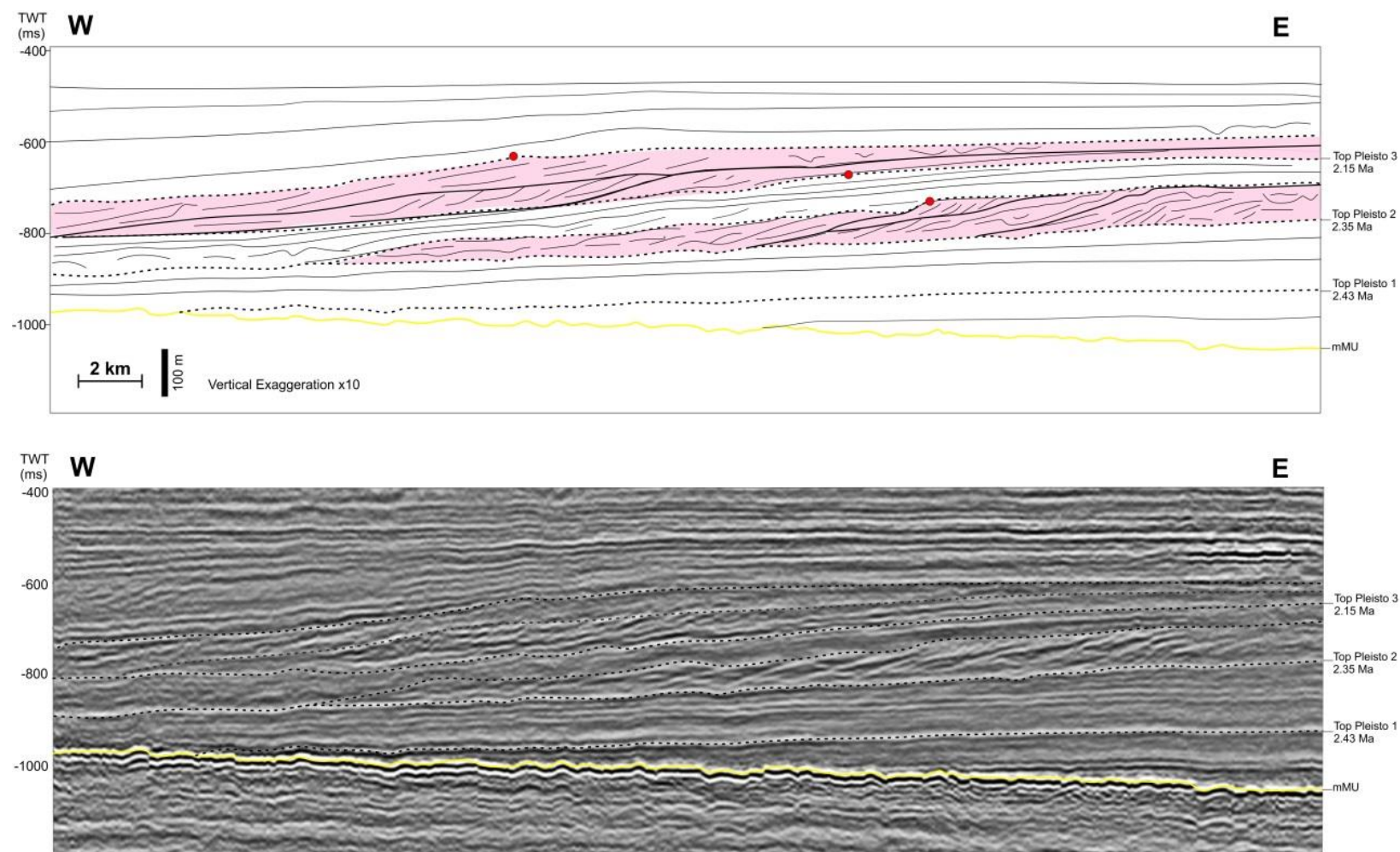


Figure 5.4 cont. d) East-west seismic cross section through two sets of Intra Slope Clinoform examples from seismic units *Pleisto 3* and *Pleisto 4* in the north east of the Netherlands North Sea.

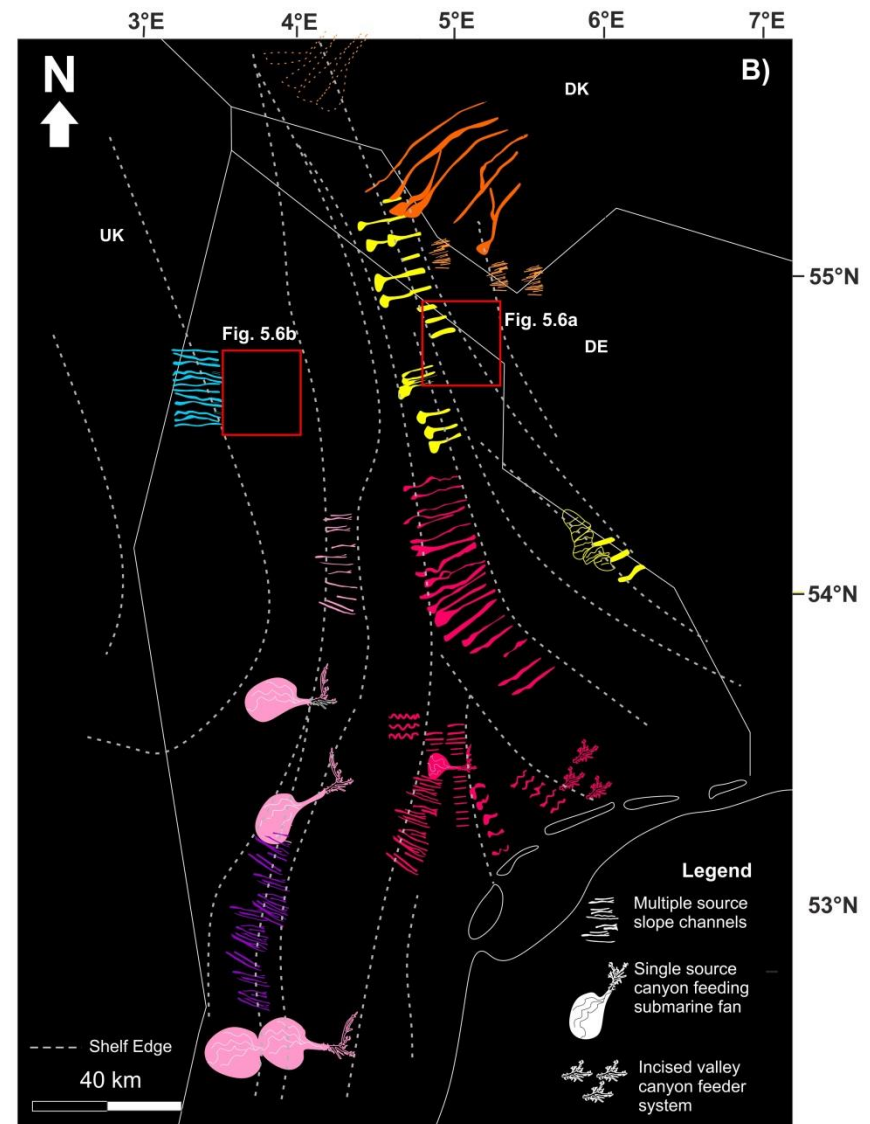
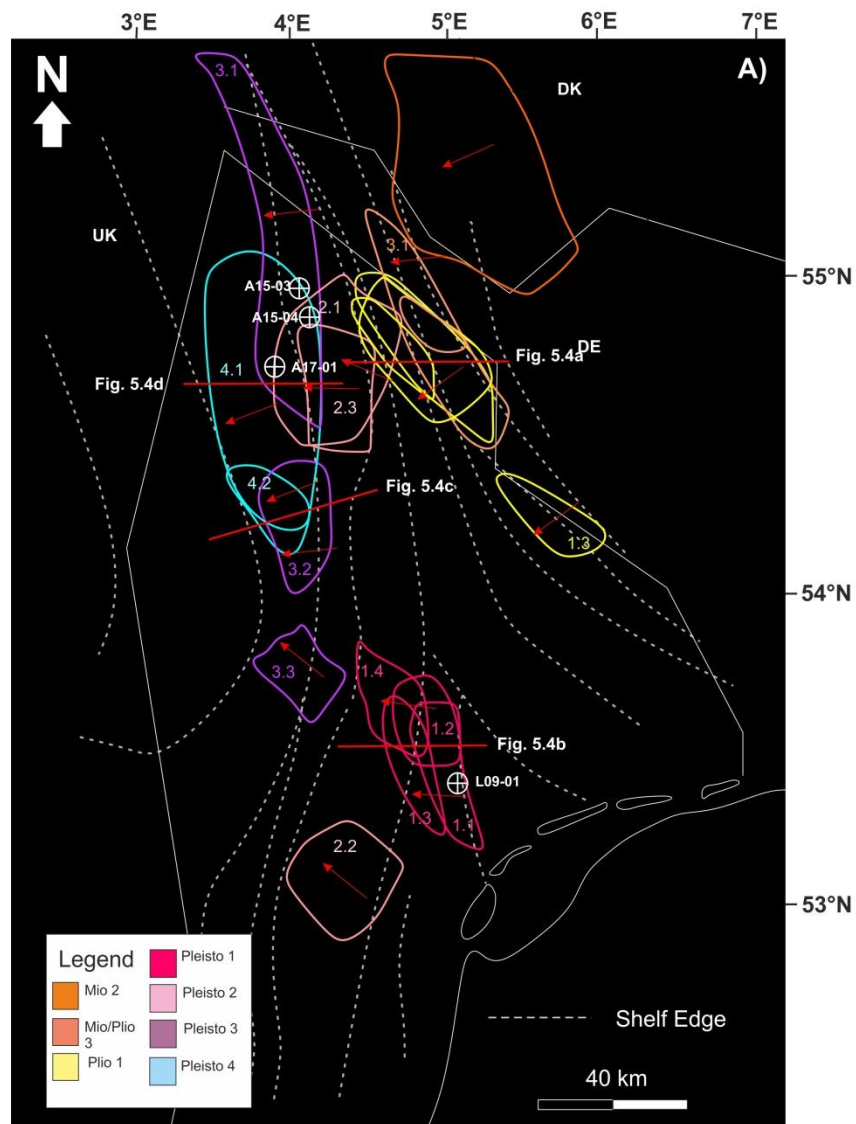


Figure 5.5 Distribution of Intra Slope Clinoforms (previous page). **Left** Map of the lateral distribution of the slope clinoforms through time and their aerial extent. Colour coded based on the seismic unit they occur in. **Right** Deep water sedimentation and feeder system distribution map from Chapter 4. North Sea sectors labelled NL= Netherlands, DE= German, DK= Denmark, UK= United Kingdom. Locations of seismic cross sections and well correlations of Figs. 5.4 & 5.7 are shown.

Many geomorphic features are identified on the shelf-prism clinoforms. Key seismic features identified in planform include elongate pockmarks, basin floor fans and feeder canyons; *Multiple Line Source* slope channels and attached lobes (Fig. 5.5b) and mass transport complexes on the slope and basin floor. Iceberg scours, incised valleys, channel features and lobes are identified on the shelf (Chapter 3 & 4). These key features occur cyclically throughout the Late Cenozoic basin fill (Fig. 5.5).

The post mMU section is divided into nine seismic units, dependent on the well log and seismic characteristics; and chronostratigraphic significance of normally laterally extensive downlap surfaces (Chapter 3; Fig. 5.2). Dates to constrain the *Mio 2* seismic unit are correlated from Danish sector studies (Rasmussen et al., 2005; Møller et al., 2009). The top *Mio 3* is correlated to a shift in depocentre southwards and biostratigraphy indicating an age of 4.2 Ma in wells B17-01; B17-02; F02-01 and F02-03; (Chris King *Pers. Comm 2013*, see appendix). Seismic units *Mio 1-3* depocentres are focused to the east of the dataset in the German and Danish sectors and represent a condensed section within dataset area, covering millions of years (Fig. 5.2). Deposition is predominantly >1° deep water low angle bottomsets. The following seismic units *Plio 1* to *Pleisto 5* are constrained by the existing chronostratigraphic framework outlined in section 5.1.2.

Plio 1 seismic unit (~4.2 Ma- 2.58 Ma) deposition is focused in an arcuate shape in the far east of the Netherlands North Sea along the boundary with the German sector and corresponds to an E-W sediment input direction compared to NE-SW previously (Fig. 5.5). Shelf-prism clinoform architectures are sigmoidal towards the north and oblique tangential to the centre and the south of the depocentre. Foreset angles of shelf-prism clinoforms are a maximum 4° and 300-400 m height in the southern part of the Netherlands North Sea. *Top Plio 1* is identified by a regional flooding surface at the top of a marked transgression.

Pleisto 1 seismic unit (2.58-2.43 Ma) represents the first 150,000 years of the Quaternary. The unit shows a greater than order of magnitude increase in sedimentation (from $\sim 3 \text{ km}^3$ per 1000 years to $\sim 55 \text{ km}^3$ per 1000 years) from the previous unit, progradation rates are high which suggests supply dominated river systems feeding the shelf-prism in the north and south of the dataset (Chapter 3). *Top Pleisto 1*, a regional strong amplitude reflection and downlap surface is correlated to the termination of glacial MIS 96. Two additional regional strong shale layers within *Pleisto 1* are correlated across the dataset and correspond to the termination of glacial period MIS 98 and 100. This allows the unit to be divided into three chronostratigraphically constrained sub units, a, b and c (Figs. 5.2 & 5.4b).

A change from an arcuate convex to a linear concave shelf edge (Fig. 5.5) suggests a change from river dominated to a wave/storm dominated system (Hampson et al., 2015) between MIS 100 and 98, sub unit a and b. Direct evidence of glaciation in the Northern Hemisphere is identified from *Pleisto 1b* onwards, as abundant iceberg scouring events are identified (Figs. 3.12 & 5.2; Chapter 6.1).

The bathymetry of the SNS changes significantly in the earliest Quaternary. Clinoform height reduces in the south of the dataset through the earliest Quaternary (Gelasian, 2.58-1.78 Ma). At the base Quaternary (2.58 Ma), backstripped clinoform heights exceed 300 m the south of the Netherlands North Sea in comparison to ~ 200 m in the Danish sector. The southern part of the SNS shallows significantly by *Top Pleisto 2* (2.35 Ma) with clinoforms reducing to 50-100 m in average foreset height (Chapters 3 & 6.2).

The *Pleisto 2* and *Pleisto 3* seismic units' shelf edges are linear and their depocentres trend north-south across the central Netherlands North Sea (Fig. 5.5). *Top Pleisto 2* is a strong amplitude downlap surface and is linked to the glacial termination of MIS 92 at 2.35 Ma. *Pleisto 3* corresponds to a downlap surface in the north Netherlands North Sea at ~ 2.15 Ma, and is possibly linked to the glacial termination of MIS 82.

By this time of *Pleisto 4* and *Pleisto 5* seismic units the south of the Netherlands North Sea has limited accommodation due to infill and the NW of the dataset becomes the main area of deposition with increased height of clinoforms (up to 300 m, $1-2^\circ$). The *Pleisto 5* main depocentre is to the NW of the Netherlands North Sea in the UK sector. Greater topset preservation across the entire basin is identified in these units

suggesting an overall increase in relative sea level at this time. *Top Pleisto 4* and *5* are associated with downlap surfaces which are constrained by the Olduvai magnetic event at 1.94 and 1.78 Ma, respectively.

5.4 DESCRIPTION OF INTRA SLOPE CLINOFORMS

In this section, the seismic character and lithology of the Intra Slope Clinoforms are described. The Intra Slope Clinoform systems are then put into context of the chronostratigraphic framework by their position relative to key dated surfaces (Fig. 5.2).

The Intra Slope Clinoforms are, in planform, identified as strong amplitude bands, offset several km from, and parallel, to the shelf edge (Fig. 5.6). The length of the unit along strike can be from 20 km to 90 km and the width of the system down dip is commonly 20-30 km, but can vary from 10 km to 50 km. The width of the system is dependent on the width of the slope, which in turn is associated to the angle of basal shelf-prism clinoform. The planform area of the unit is variable in aspect ratio from square low aspect ratio examples to elongate high aspect ratio systems present along a greater proportion of the slope (Fig. 5.5b). The maximum thickness is between 30 and 100 m.

5.4.1 Seismic Reflection Character

The base of an Intra Slope Clinoform unit is typically a laterally continuous strong amplitude reflection with a clinoform geometry of 150 m- 400 m height and foreset dips ranging from $<1-4^{\circ}$. It is consistently a downlap surface for the Intra Slope Clinoforms and becomes conformable to the underlying and overlying reflections up-dip on the upper slope and shelf. The base can be a composite downlap surface as several lower order downlap surfaces within the Intra Slope Clinoform units can merge at the base of the unit (Fig. 5.4).

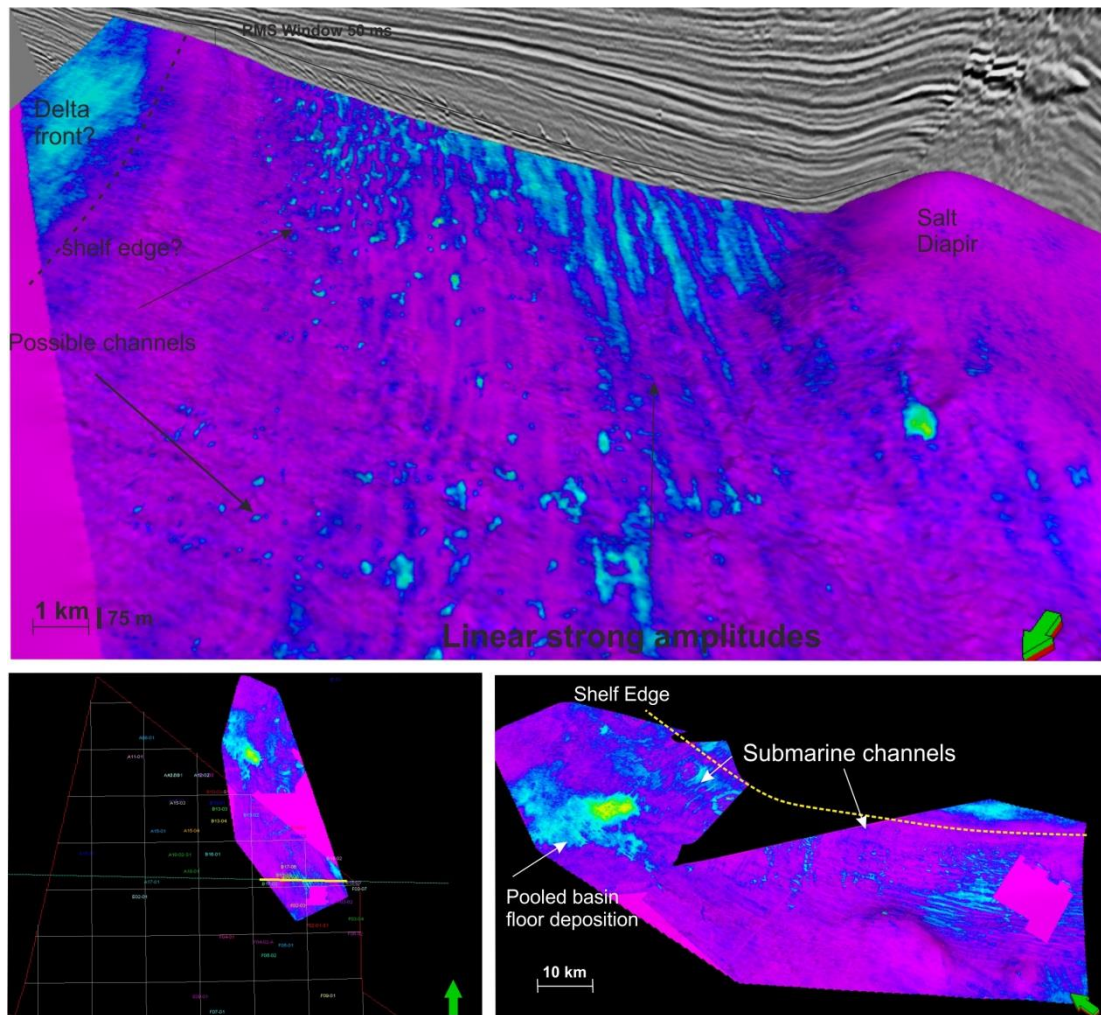


Figure 5.6. Planform examples of Intra Slope Clinoforms. Locations shown in Fig. 5.5. **a)** Base of an Intra Slope Clinoform set in the earliest *Plio 1* seismic unit. RMS amplitude extraction on a surface. RMS window 50 ms TWT above surface. Lighter colours correlate to coarser grained lithology. **Top** 3D View of *Plio 1b* Intra Slope Clinoform. Linear strong amplitude bands associated with the Intra Slope Clinoforms extend 50 km along strike. **Bottom left** Location of the system within the Netherlands north Sea. Red outline represent the Netherlands North Sea sector. **Bottom right** Extended example of the same RMS amplitude extraction extending into the Danish North Sea. This illustrates the lateral variation across the slope as to the north the Intra Slope Clinoforms are replaced with Multiple Line Source deep water conduits, described in Chapter 4.

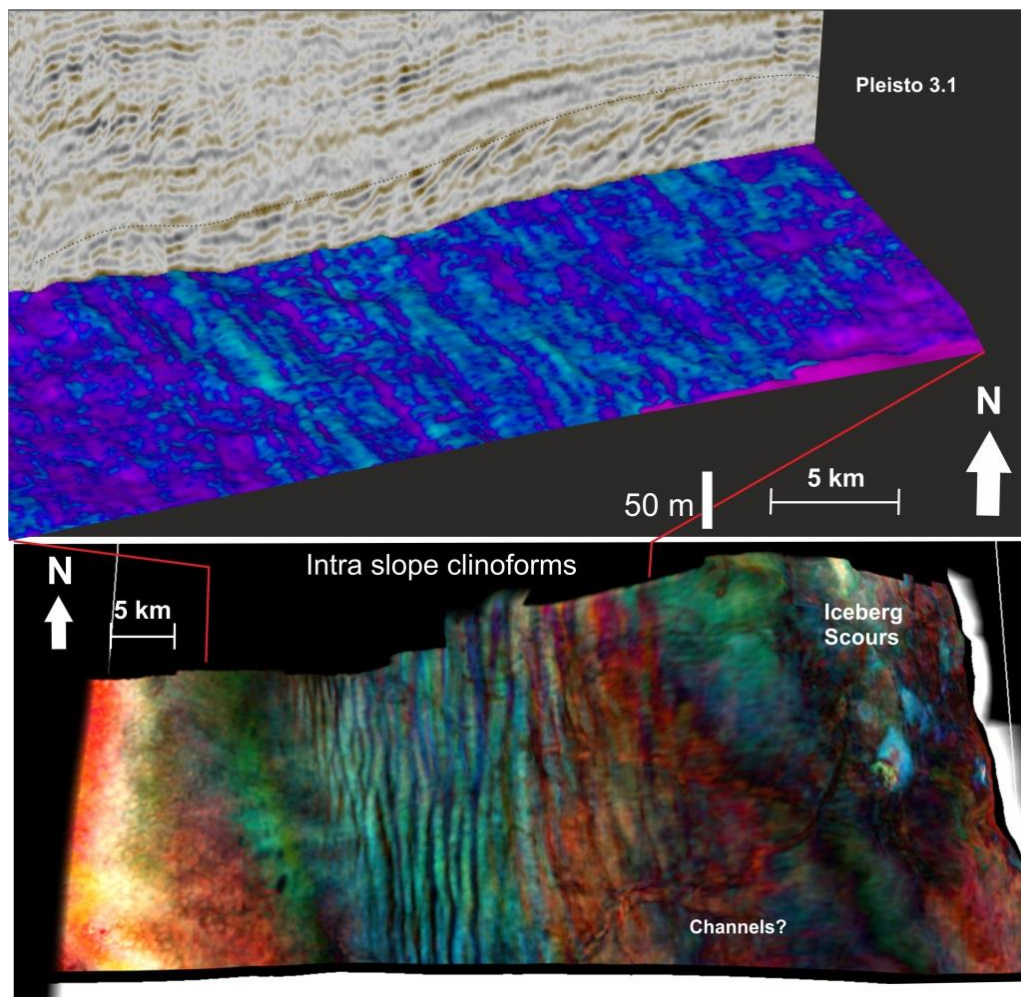


Figure 5.6 cont. b) *Pleisto 3* example from west Netherlands North Sea **Top** RMS Extraction 50 ms above *Top Pleisto 2* seismic reflection (2.35 Ma) which is the downlap surface for the *Pleisto 3* Intra Slope Clinoforms. Lighter colours represent coarser grained lithology. The same Intra Slope Clinoforms are shown in Fig. 5.4d. **Bottom** Frequency decomposition extracted on to *Top Pleisto 2* surface vertical exaggeration greater than in the above RMS figure. The 3D geometry of the linear bands of the Intra Slope Clinoforms is shown in greater detail. Indicates that there are possibly some feeder systems on the shelf or topset but this is not clear. Locations shown in Fig.5.5b.

The Intra Slope Clinoform top reflection is an irregular, undulating surface of similar height and angle as the base of the clinoforms. The relationship with the underlying reflections changes from toplap to conformable, depending on whether topsets of the Intra Slope Clinoforms are preserved (Fig. 5.4). Weaker amplitude reflections above the Intra Slope Clinoforms bidirectionally onlap between stronger amplitude Intra Slope Clinoforms, suggesting post depositional infill. Incisions are identified on the top surface in cross section in several cases, generally 20-30 m depth and 0.1-3 km wide. In planform, the top surface shows strong amplitude linear bands parallel to the shelf edge (Figs. 5.5a & b) which can be individually up to 60 km in length and are 1-2 km wide. The incisions identified in cross section are related in planform to ellipse shaped

incisions up to 3 km in length and elongate parallel to the shelf edge on the mid to lower slope (Fig. 5.6). Incisions are more commonly associated with multiple channel features perpendicular to the strike of the shelf edge, which span the length of the slope (Fig. 5.6a).

The internal character of the Intra Slope Clinoform units is highly variable (Figs. 5.3 & 5.5) and can comprise an individual downslope thinning wedge of clinoforms, as in the first marked wedge in Fig. 5.4a, or a complex set of sub-units, identified by a change in seismic character and the presence of internal downlap surfaces. They can comprise two aggradation downslope thinning wedges (Fig. 5.4c) separated by a thin < 40 m interval of weak amplitude continuous reflections or can be several progradational/aggradation subunits with complex trajectories, separated by internal downlap surfaces (Figs. 5.4 a-d).

The seismic reflection geometry of individual Intra Slope Clinoforms can be oblique parallel to convex upwards sigmoidal clinoforms, sometimes chaotic with little bottomset preservation. The clinoforms commonly exhibit a descending clinoform trajectory; each progressive clinoform overlapping the previous clinoform. Topset preservation is highly variable within and between Intra Slope Clinoform examples.

Individual clinoform widths are typically 0.5-1.5 km, increasing downslope. The height of the foreset is generally 30-60 m with a maximum of 100 m (in Pleisto 4, Fig. 5.6b). The foreset height overall reduces basinwards, but can increase within sub units on the upper slope (Fig. 5.4d). The smallest clinoforms identified are just above seismic resolution, 15-20 m (Figs. 5.4a & d). Intra Slope Clinoform dips are mostly between 2-3° on the upper to mid slope of the shelf-prism, though angles of up to 6° are identified. Towards the lower slope, the Intra Slope Clinoforms reduce in dip to match the underlying and overlying bounding reflections at 0.5-2°.

The seismic character is generally stronger than the surrounding reflections but is dependent on the lithological contrast. Reflection strength is variable within the Intra Slope Clinoform wedges, in some cases weakening basinwards, but in other cases stronger amplitudes are found at the base of the unit. Generally the upper foreset and topset of each Intra Slope Clinoform is stronger than the lower foreset and bottomset. Internal structure is mostly below seismic resolution but when visible, the internal

reflections are of weaker amplitude (Figs. 5.4a & d). The individual Intra Slope Clinoforms do not have seismic geomorphic features at the seismic resolution of this study.

5.4.2 Well Log Character

The seismic character of the Intra Slope Clinoforms is tied to gamma ray petrophysical log character and lithological descriptions. Two examples, from the *Pleisto 1* and *Pleisto 4* seismic units, wells L09-01 and A17-01 respectively, show strong amplitude continuous seismic reflections at the base of the Intra Slope Clinoform unit are correlated to high gamma ray values (Fig. 5.7). The gamma ray character on the mid to upper slope shows a sharp decrease with either a “blocky” or upwards coarsening well log motif (Fig. 5.7b). When the well penetrates the Intra Slope Clinoform unit down dip on the lower slope, the well log motif appears to be fining upwards (Fig. 5.7a A17-01). At the top of the Intra Slope Clinoforms the gamma ray value increases suggesting a fining upwards. The two examples show a decrease in gamma ray associated with the Intra Slope Clinoforms from 100 API to 30 API in the L09 well and from 80 to 38 API in the A17 well.

Lithological information from cuttings descriptions show the higher gamma ray correlates to grey mudstone grade lithology typical of deep water slope sedimentation. The lower gamma ray associated with the Intra Slope Clinoforms is composed of fine, rarely medium grained sand lithology. In the northern half of the Netherlands North Sea, such as the example of *Pleisto 4* (shown in Figs. 5.4d & 5.6b), the lithology of the Intra Slope Clinoforms (A17-01) is described as very fine to fine sand, traces of silt with abundant carbonaceous specs (organic material).

The Intra Shelf Clinoforms have a coarsening upwards gamma ray motif, and are associated with grain sizes from clay to medium/locally coarse sand with layers of brown coal and peat.

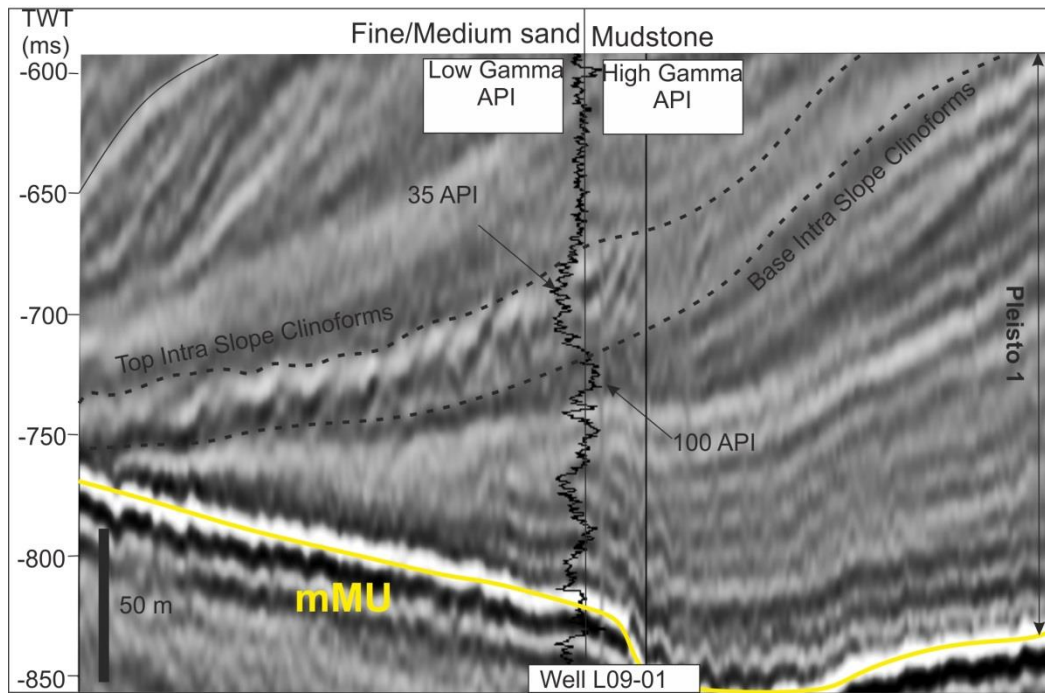
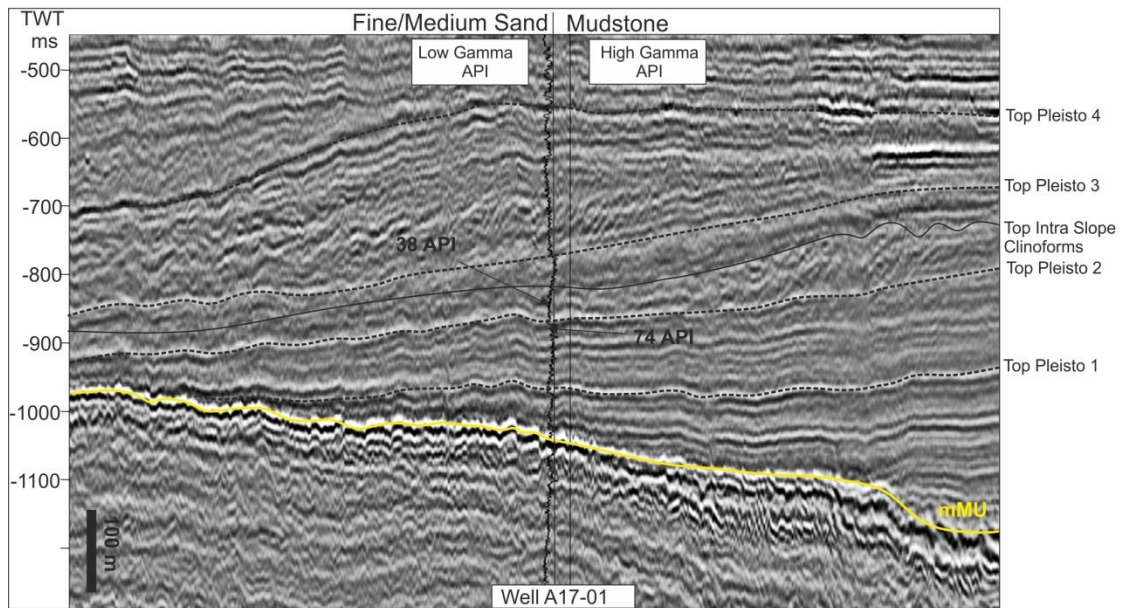


Figure 5.7. Well log correlations. *top* Well A17-01 gamma ray log tied to seismic section through *Pleisto 3* and *Pleisto 4* Intra Slope Clinoforms in the west of the Netherlands North Sea. Minimum and maximum gamma ray values associated with the Intra Slope Clinoforms are identified. *bottom* Well L09-01 through *Pleisto 1* between MIS 100 and 98. Minimum and maximum gamma ray values associated with the Intra Slope Clinoforms are identified. Locations shown in Fig. 5.5.

5.4.3 Relationship to the Shelf Edge

In planform the seismic character of the preceding shelf edge at the base of the Intra Slope Clinoforms is generally featureless and weak amplitude, though landward of the shelf edge can exhibit very strong amplitudes (Fig. 5.6a). The topsets can exhibit many geomorphic features such as channels and iceberg scour features (Figs. 5.4 & 5.5b). The relationship of the Intra Slope Clinoforms with the Intra Shelf Clinoforms is complex (Fig. 5.4). In examples from the *Plio 1* and *Pleisto 3* seismic unit, the two clinoform types appear contiguous with each other (Figs. 5.4a & c), and share a common downlap surface. However, in other cases the Intra Shelf Clinoforms downlap onto the upper foreset of the Intra Slope Clinoform top surface (*Pleisto 4*, Fig. 5.5d) or occur far landwards of the preceding shelf edge.

Evidence of the shelf depositional environment is not clear in certain units where there is little topset preservation at the time. *Pleisto 1* unit is an example of where oblique shelf-prism clinoforms with little topset preservation are dominant and a wheeler diagram of the unit indicates there is little deposition landwards of the shelf edge during the deposition of the Intra Slope Clinoforms (Fig. 5.4b). The *Plio 1* unit has greater topset preservation and therefore greater information about the conditions at the time and the presence of Intra Shelf Clinoforms is preserved (Fig. 5.4a).

The first clinoform within the Intra Slope Clinoform wedge appears consistently to downstep from the preceding shelf edge. This initial drop is observed to be between 17.6-70 m. This is calculated by back rotating seismic sections, where necessary, and measuring the distance from the shelf edge of the previous shelf-prism clinoform to the first Intra Slope Clinoform roll over point (Fig. 5.4a). The vertical distance from the previous shelf edge to the last clear clinoform roll over of the Intra Slope Clinoform wedge is also measured and found to be 50-100 m (Fig. 5.2).

5.4.4 Sequence Position

Shelf-prism scale sigmoidal clinoforms (150-400 m, <1-2°) with preserved bottomsets and foresets precede the Intra Slope Clinoforms. Intra Slope Clinoforms, in many cases

downlap onto a strong amplitude continuous reflection with shale lithology (Figs. 5.4a & 5.7). In some examples, Intra Shelf Clinoforms are identified prior to the Intra Slope Clinoform deposition.

The top of the Intra Slope Clinoforms is typically a toplap/truncation surface which can be traced along the entire length of the Intra Slope Clinoform wedge, with a downlap surface directly above. Channel features and iceberg scours incising into this top surface are common. The iceberg scours are typically in the same surface or one seismic cycle above in the later examples (*Pleisto 3 & 4*; Figs. 5.4c & d).

Progradational clinoforms with flat to slightly ascending trajectories (70-200 m, 2-3°) downlap above the Intra Slope Clinoforms and deposition is concentrated on outer topset and upper to mid foreset of the shelf-prism (example highlighted in Fig. 5.4a). The wheeler diagram of the *Pleisto 1* examples (Fig. 5.4b) illustrates the change in the focus of deposition. The progradational clinoforms have a higher angle slope compared to the underlying sigmoidal clinoforms (<1-2°). The progradational unit is generally followed by a set of aggradational to retrogradational reflections (<1-2°; Fig. 5.4), topped by another strong continuous amplitude reflection. This describes the fullest sequence, however in some cases the progradational wedge is not present and the aggradational unit lies directly above the Intra Slope Clinoforms (Fig. 5.4b, *Pleisto 1* examples). The sequence varies laterally and in *Pleisto 1b* seismic unit (Fig. 5.3b), a retrogradational package lies above the Intra Slope Clinoforms, but along strike the progradational oblique clinoforms occur above the Intra Slope Clinoforms associated with fan deposition at the base of slope (Fig. 5.5b).

5.5 DEPOSITIONAL ENVIRONMENT

A sharp increase in grain size is associated with the deposition of Intra Slope Clinoforms. The lithological interpretation of the Intra Slope Clinoforms is based on a decrease in gamma ray values, the increase in seismic reflection strength and increase in grain size from mudstone to very fine-medium sand in the cuttings descriptions. The sharp grain size changes at the top and base of the system suggests rapid changes in depositional environment. The increase in grain size could suggest a proximal sediment input system. The descending trajectory of the Intra Slope Clinoforms could be indicative of a

base level fall which would result in the progradation of the sediment system basinwards.

The locus of deposition on the slope during the Intra Slope Clinoforms and the thinning or lack of associated topsets preserved suggests that the coarser grained sediment is being delivered to the slope during these systems, basinwards of the shelf edge and is bypassing the shelf staging area. In *Pleisto 4.1* (Fig. 5.4d), the ~ 80 m thick wedge thins towards the shelf edge and is represented as a single seismic cycle (~15 m) on the shelf. This shows there is a little accommodation on the shelf at the time of deposition and the wheeler diagram representing the *Pleisto 1* examples illustrates the basinwards shift in deposition which occurs during the Intra Slope Clinoform deposition (Fig. 5.4b).

The depositional environment interpretation of the Intra Slope Clinoforms is aided by the seismic geomorphology of related seismic reflections. Ellipse shaped incisions identified on the slope, parallel to the shelf edge are identified as lower slope current incisions, which occur in a deep marine environment and can be evidence of strong currents (Seismic Facies 2, SF2 in Chapter 3). Linear channel features perpendicular to the shelf edge are consistent with the geometry of *Multiple Line Source* slope channels (Seismic Facies 3, SF3 in Chapter 3; Chapter 4). These are interpreted as submarine channels formed by and conveying sediment-gravity flows, not fluvial in origin (Janocko et al., 2013). The incisions are normally found on the top reflection of the Intra Slope Clinoform unit but are also present on the top of sub units in some cases including *Mio 2* (Fig. 5.5). *Plio 1b* (Fig. 5.6a) shows that *Multiple Line Source* channels can occur contiguously along strike of Intra Slope Clinoforms. Iceberg scours affecting the Intra Slope Clinoforms top surface on the shelf are indicative of marine flooding of the shelf and of glacial conditions (Fig. 5.2). Iceberg scours are identified in the *Pleisto 3* & *Pleisto 4* examples.

Therefore there is evidence that submarine, cold climate conditions prevailed at least just after the deposition of the Intra Slope Clinoforms but also possibly during the deposition. There is no direct evidence that the individual clinoform topsets are terrestrial and therefore that the clinoform roll over points of the Intra Slope Clinoforms represent the coastline. However, it is possible that evidence of terrestrial facies have been eroded by the transgressive reworking, ocean bottom currents or is below seismic

resolution. The elongate geometries could suggest that there is some reworking by ocean bottom currents. Either the Intra Slope Clinoforms are deltaic in origin but underwent periodic and rapid flooding back allowing the submarine associated facies to occur or they were deposited under submarine conditions.

This is in contrast to the evidence of the Intra Shelf Clinoforms, where the lithological information identifies coal and peat within the Intra Shelf Clinoforms and their position on the shelf suggests they are either terrestrial, or proximal to the sediment delivery system. In planform they are associated with very strong amplitudes, arcuate in geomorphology suggestive of a deltaic lobe (Fig. 5.6a). A direct connection between the Intra Shelf Clinoforms and the Intra Slope Clinoforms is observed in many examples (Figs. 5.4a - d), and is only preserved where there is topset preservation and accommodation on the shelf. The two types of “delta scale” clinoforms are different in character but are likely two components of the same system.

In summary it is not possible to confirm that the Intra Slope Clinoforms are deltaic in origin as evidence of terrestrial facies is limited in the Intra Slope Clinoforms. It is believed that even if the clinoforms are deposited under marine conditions, the trajectories represent base level rises and falls and could represent storm wave base of a falling stage sequence under cold climate/glacial conditions.

5.6 INTRA SLOPE CLINOFORM DISTRIBUTION

This section describes the Intra Slope Clinoform distribution across the study area through the Miocene to early Pleistocene. The distribution maps (Fig. 5.5a) show the area of each Intra Slope Clinoform system mapped with relation to the shelf edge. The distribution reflects the prograding nature of the shelf-prism from east to west during the study period. Submarine channel and fan systems, described in detail in Chapter 4, are also shown for comparison (Fig. 5.5b). The Intra Slope Clinoforms are found in almost all the seismic units identified in this study and are more prevalent in the north of the dataset. Many events are identified from *Mio 2* to *Plio 1* (>7.2 Ma to 4.2 Ma) and are indicative of the primary depocentres, confined to the east and NE of the dataset.

The *Mio 3-Plio 1* examples are limited in areal extent and reflect the aggradational nature of the system at the time (Fig. 5.4a). Four *Pleisto 1* (2.58 Ma to 2.43 Ma) Intra Slope Clinoform units are found in the south of the Netherlands North Sea, and appear to alternate between low aspect ratio and high aspect ratio areal extent. Three examples are identified during *Pleisto 2* (2.43-2.35 Ma) both in the north and the south of the dataset. *Pleisto 3* (2.35-2.15 Ma) seismic unit is linked to three individual Intra Slope Clinoform units all downlapping on the base of the seismic unit, striking north-south along the entire Netherlands North Sea, reflecting the linear and laterally extensive depocentres of the time. *Pleisto 4* (2.15-1.94 Ma) clinoforms are identified only in the north east of the Netherlands North Sea. The relationship to the deep water depositional systems (Fig. 5.5b) shows early Intra Slope Clinoforms (*Mio 2 –Plio 1* seismic units) and the elongate *Pleisto 1* examples are found in conjunction with *Multiple Line Source* depositional systems (Fig. 5.5). However, from *Pleisto 1-Pleisto 4* the north of the dataset is more dominated by Intra Slope Clinoforms, and there is no correlation between the deep water events, which are more dominant in the south of the dataset. Single Feeder deep water depositional systems, which feed large submarine fans, only occur in the south of the dataset, during the Pleistocene.

5.7 DISCUSSION

The formation of the Intra Slope Clinoforms is discussed below and the examples are placed within the chronostratigraphic framework of the sNS. This then allows a comparison of the Intra Slope Clinoforms place within the global sea level curves and within a sequence stratigraphic framework.

5.7.1 Intra Slope Clinoform Genesis

Several examples of Intra Slope Clinoforms within the Late Cenozoic North Sea are identified in previous studies. Møller et al. (2009) identified the *Mio 2* clinoforms as subaerial deltaic clinoforms and suggested the clinoform roll over points represent the coastline (Fig. 5.5a). Clausen et al. (2012) observed similar clinoforms in the Oligocene Danish North Sea and identified them as climate induced forced regressive wedges. The

seismic character was linked to the presence of Svalbardella, a high latitude dinocyst, indicating the Intra Slope Clinoforms were deposited during cold sea surface temperatures and marine conditions, linked to the Oi2 glacial maximum (Clausen et al., 2012). *Pleisto 3.1* and *Pleisto 4.1* (Fig. 5.5a), penetrated by borehole A15-03, are identified in Kuhlmann and Wong (2008) are linked to regression caused by cooling. Therefore, the literature reiterates the observations in this study that the Intra Slope Clinoforms are likely deposited under cold, marine conditions. The interpretation of *Mio 2* as representing the coastline was not sufficiently backed up by evidence of a terrestrial depositional environment in Møller et al. (2009).

The examples in this dataset share key features with forced regressive wedges or falling stage systems tracts. Many examples exhibit blocky well log character and have a sharp base in the gamma ray log. The seismic geometry shows progressive offlap and downstepping of progressive clinoforms downslope, becoming less vertically extensive downslope and are capped by a seaward dipping top surface (Hunt and Tucker, 1992; Posamentier et al., 1992; Michelsen and Danielsen, 1996; Posamentier and Morris, 2000; Plink-Björklund and Steel, 2002; Catuneanu et al., 2009).

The planform geometry of the Intra Slope Clinoforms share characteristics with sub-aqueous deltas in that they have a shore-parallel, laterally extensive, near linear plan view (Patruno et al., 2015). However, sub-aqueous deltas are present landwards of the shelf edge and not basinwards like the Intra Slope Clinoforms described in this study. These similarities suggest that the geometry is largely dominated by basinal processes, such as waves and currents which could provide insight into how these are formed compared to river dominated shelf deltas.

The most convincing analogue to the Intra Slope Clinoforms outside of the North Sea are the *sand-prone slope accumulations* identified in seismic scale outcrops of the Eocene Central Basin, Spitsbergen (Plink-Björklund et al., 2001; Plink-Björklund and Steel, 2005, 2002). The detailed outcrop analysis suggests that they occur when sea level falls below the shelf edge and sediment is partitioned to the slope rather than to the basin floor via an incising canyon system. Higher rates of sediment fallout at the shelf edge and upper slope during the falling stage can prevent deep channelling at the shelf margin and therefore requires a high sediment supply system (Plink-Björklund and

Steel, 2005). Observations of the distribution of basin floor fans fed by Single Point Source incised canyons are not present where Intra Slope Clinoforms systems are abundant (most notably in the *Mio 3-Pliesto 1* seismic units, Figs. 5.2 & 5.5). The lowest sea level is recorded by the most basinwards clinothem set within the sand prone slope accumulations and the sequence boundary can be identified with high density of erosive turbidite shoots at the upper surface (Plink-Björklund et al., 2001).

The non-uniqueness of seismic geometries at the seismic resolution scale has led to features of similar geometry having a broad range of interpretations. Similar geometries have been interpreted as landslides (Lee et al., 2002). The lateral continuity of the Intra Slope Clinoforms (Fig. 5.6) suggests that they are not landslides. Examples of landslides and mass transport complexes in the area have clear headwall scarps and are not laterally extensive across a slope (Seismic Facies 5, SF5, and Chapter 3). The clinoform geometry and the continuous link to the Intra Shelf Clinoforms (deltas) suggest this interpretation does not fit in this case.

Similar geometries from the Adriatic Shelf are commonly interpreted as sand waves (Cattaneo et al., 2007). The examples from the Adriatic Shelf have similar rugose top surfaces and strong amplitude basal downlap surface to the Intra Slope Clinoforms, however are much smaller in height (<10 m) and have a different internal character. Sandwaves also migrate up slope (Stow and Mayall, 2000; Wynn et al., 2000), but it is clear from the examples shown in Fig 5.4 that being able to link updip with reflections of deltaic origin and the progressive offlap of clinoforms downdip suggest this cannot be the case. Intra Slope Clinoforms are also not the correct orientation to be interpreted as turbidite associated sandwaves (Kane et al., 2010; Normark et al., 2002) and are too laterally extensive. It is possible that some of the less well imaged examples in our study of Intra Slope Clinoforms could be sandwaves. Higher resolution seismic data or collection of core borehole data would be required to better clarify this.

Even if the Intra Slope Clinoform roll overs do not represent the coastline, it is summarised that the descent of the clinoforms represents forced regressions. This is an indication of falling relative sea level and could reflect the magnitude of relative sea level changes. Therefore we suggest that, in conjunction with incision events of basin

floor fan forming canyons (Chapter 4), that Intra Slope Clinoforms can be used as an independent measure of base level fall and compared to the eustatic sea level curve.

5.7.2 Comparisons to Global Events

The evidence comparing base level falls to the global sea level curve is most reliable in the Gelasian period (2.58-1.78 Ma) as this period is best constrained by the high resolution chronostratigraphic framework and an expanded sedimentary section within the dataset (Fig. 5.2). The Intra Slope Clinoform systems are dated and placed within a glacial-interglacial context by understanding their position relative to dated seismic units and other seismic geomorphic features (such as deep water sedimentary systems and iceberg scours, Fig. 5.2).

The Gelasian is a period where 41,000 year obliquity Milankovich cycles are said to dominate the Northern Hemisphere climate (Ruddiman et al., 1986). The position of the coastline and regional sea level mirrors that of the global sea level curve during at least the earliest Gelasian (Noorbergen et al., 2015; Donders et al., in prep). A clear comparison can be made of the density of the Intra Slope Clinoform events and the evidence for cold periods from the North Sea Basin within seismic units *Pleisto 1-4* (Fig. 5.2). For instance, in *Pleisto 3*, there is little evidence for iceberg scours and much less evidence of ice rafted debris suggesting glacial periods of lower magnitude at this time, this coincides with a lack of downstepping events. Whilst in *Pleisto 1* to early *Pleisto 3* seismic units, Intra Slope Clinoform systems are more abundant during periods where cold events are evident.

Within the *Pleisto 1* seismic unit, many more base level fall events are identified than there are Marine Isotope Stages (Figs. 5.2 & 5.3b). The *Pleisto 1* sub units, b and c, represent one glacial-interglacial cycle each and yet contain at least two separate forced regressions and a Single Feeder canyon with feeding incised valley on the shelf (Pleisto 1F, Fig. 5.5). During this sub unit, sediment supply is very high, from $\sim 3 \text{ km}^3$ per 1000 years to $\sim 55 \text{ km}^3$ per 1000 years change from the *Plio 1* to the *Pleisto 1* unit, it could be possible that such a high sedimentation rate is preserving higher order

sedimentary cycles and the influence of precession cycles, linked to a periodicity of 23,000 years.

The most basinward clinoform roll over point of the Intra Slope Clinoforms is 40-100 m beneath that of the preceding shelf edge. The magnitudes of these drops show a correlation to the global sea level falls in relation to glacial periods (Fig. 2). There is a correlation with the relative magnitudes of the glacial eustatic falls but the exact amount of base level fall identified from this study does not always fit with the eustatic curve. This could be due to local changes in accommodation, created by active salt tectonics, local tectonics and subsidence. Furthermore, as the Intra Slope Clinoform roll over point was likely deposited in marine conditions they may not necessarily represent the absolute sea level but should still reflect changes in base level. Another key reason could be the global sea level curve used in this study itself, though the relative magnitudes are likely correct the exact values are to be expected to have some error (Ken Miller pers comms 2015). However, some correlation is seen and this corroborates the findings of Donders et al. (in prep) and Noorbergen et al. (2015) that eustasy is the main control of base level in the SNS.

The correlation between the Intra Slope Clinoform systems and cold events in the North Sea during *Pleisto 4* suggest there could be a chronostratigraphy issue with the base of the unit (dated at 2.15 Ma) or could be indicative of a delay between the global Marine Isotope Stages and cold periods in the North Sea. For instance, there appears to be a correlation of MIS stages 82 and 80 to two large sea level falls of 80-100 m calculated from the Intra Slope Clinoforms. The top of both of these Intra slope Clinoform events are iceberg scoured though there is little evidence of ice rafted debris, but the first one is slightly offset from the MIS stage 82. Therefore accurate timing of the *Top Pleisto 3* (~2.15 Ma) reflection needs to be investigated further.

5.7.3 Implications for Sequence Stratigraphy

Single Feeder systems and their attached basin floor fans and the Intra Slope Clinoforms occur within a similar position of a sequence and represent the degradational part of an APD stacking pattern (Aggradational-Progradational-Degradational, sensu Neal and Abreu, (2009), indicated by a decrease in shelf accommodation during deposition. This stacking pattern would traditionally be interpreted as a highstand systems tract (Fig.

5.8). However, we are inclined in this study to represent the degradational package as separate from the AP. The sequence boundary is identified by the lowest point of base level, or the point of maximum regression, prior to a switch to increasing base level. In the forced regressive scenario, this is represented by the clinoform roll over point of the last identifiable Intra Slope Clinoform. In the *Single Feeder* scenario it is recognised at the point of maximum incision on the upper slope and with maximum regression of incised valleys.

The sequence boundary in many cases coincides with the Maximum Flooding Surface as the “highstand” is absent or condensed on the slope and may only be present landwards of the shelf edge (Fig. 5.8b). Degradation is directly followed either by *Multiple Line Source* slope channels in some cases, or by a PA stacking pattern (Progradational–Aggradational) associated with increasing accommodation on the shelf and traditionally identified as a “lowstand” systems tract. Retrogradation is predicted to occur after the PA and before the next APD sequence set. Shale layers which are identified as the downlap surfaces for the Intra Slope Clinoforms and are correlated with glacial terminations in *Pleisto 1* & *Pleisto 2* seismic units occur at the top of the PA stacking pattern, therefore a maximum flooding surface coincides with the glacial termination shale layer where retrogradational packages are thin or below seismic resolution.

The SNS prograding shelf-prism appears to consist mainly of sedimentation that occurs during the lowering base level and the early rise of base level. Traditional “highstands” are rarer and typified by Intra Shelf Clinoforms on the shelf-prism topset (Fig. 5.8b). Previous studies of the SNS have suggested lowstands represent a limited part of the basin infill (ten Veen et al., 2011, 2013). These studies were based on the north Netherlands North Sea in the area of the Central Trough (Fig. 5.1) where accommodation creation is greater throughout the Gelasian and does not take into account that the most expanded section is within the south of the Netherlands North Sea. Transgressions throughout the Gelasian flooded the shelf back 100’s m south-eastwards (Fig. 3.16) and therefore it is expected that the highstands would be deposited where there is less accommodation and are less represented in the basin. The findings illustrate the importance of the regional scale study; combined with detailed 3D seismic interpretation, as the most expanded section for each time period can be interpreted to give the fullest representation of the stratigraphy as possible.

Cyclicity of key elements of the depositional sequence such as the Intra Slope Clinoforms, Intra Shelf Clinoforms and the *Multiple Line Source* slope channels (Fig. 5.5b), indicate that from the Oligocene onwards a depositional system was depositing in a cyclical manner and likely governed by similar controls. The high resolution chronostratigraphic framework within *Pleisto 1* indicates that a common sequence such as that described in Fig. 5.8, can take <20,000 years to deposit. Other units, such as *Plio 1*, which reflects a much larger time frame, still shows the same sequence development, but with fewer sequences within the 1.62 Ma timeframe. This suggests either that there are many periods of non-deposition within *Plio 1* and other units, or that cyclical sequences reflect different time scales and are dependent on sedimentation rate and the accommodation available.

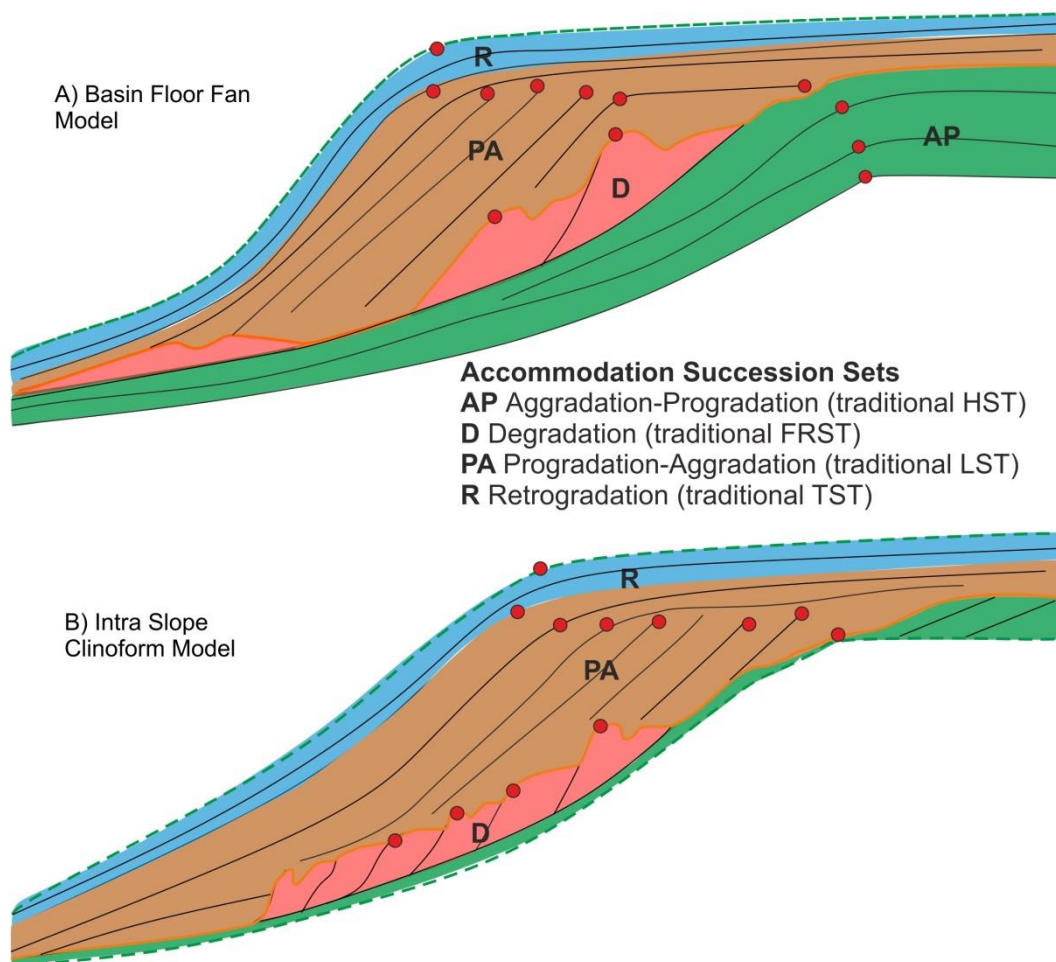


Figure 5.8 Sequence stratigraphic models (previous page) **a) Basin floor fan model** when base level falls below the shelf edge sediment is partitioned to the basin floor via incision and incised valleys on the shelf and slope **b) Intra Slope Clinoforms** when base level falls below the shelf edge sediment is stored on the shelf due to inhibited incision. Orange line = Sequence Boundary Green dashed line = Maximum Flooding Surface. Red circles represent clinoforms roll over points and the rise and fall of base level.

The Intra Slope Clinoforms, identified as forced regressive wedges are sand prone and generally capped by finer grained sediment at the top and base, and pinch out up dip onto finer grained shelf-prisms, creating a stratigraphic trap. Forced regressive wedges are good reservoirs (Plink-Björklund and Steel, 2002) and therefore could be an overlooked part of the sequence stratigraphic framework, and an overlooked hydrocarbon play.

5.8 CONCLUSIONS

- Sand prone Intra Slope Clinoform wedges <100 m in height are identified cyclically across the southern North during the Cenozoic.
- Intra Slope Clinoforms are associated with forced regressions and are likely deposited in cold marine conditions.
- The clinoforms roll over points likely represent storm wave base during early glacial periods when rapid sea level falls result in base level falls below the shelf edge but incision is inhibited by high sediment rate.
- Intra Slope Clinoforms are proposed to be used as indicators of the magnitudes of relative sea level fall along with canyon incision on the upper slope.
- The correlation between base level falls in the southern North Sea and eustatic falls related to glacial conditions in the Gelasian is positive suggesting that eustasy is a controlling factor of base level in the southern North Sea.
- More analysis using higher resolution data from shallow site surveys and direct geological information from core data would be ideal to understand the clinoforms relationship to paleo-bathymetry and further work would include identifying analogs in other basins with high resolution stratigraphic control in order to test the methodology further.

5.9 REFERENCES

- Anell, I., Thybo, H., Rasmussen, E., 2012. A synthesis of Cenozoic sedimentation in the North Sea. *Basin Research* 24, 154–179.
- Bijlsma, S., 1981. Fluvial sedimentation from the Fennoscandian area into the North-West European Basin during the Late Cenozoic. *Geologie en Mijnbouw/Netherlands Journal of Geosciences* 60, 337–345.
- Cameron, T.D.J., Stoker, M.S., Long, D., 1987. The history of Quaternary sedimentation in the UK sector of the North Sea Basin. *Journal of the Geological Society* 144, 43–58.
- Cattaneo, A., Trincardi, F., Asioli, A., Correggiari, A., 2007. The Western Adriatic shelf clinoform: energy-limited bottomset. *Continental Shelf Research* 27, 506–525.
- Catuneanu, O., Abreu, V., Bhattacharya, J.P., Blum, M.D., Dalrymple, R.W., Eriksson, P.G., Fielding, C.R., Fisher, W.L., Galloway, W.E., Gibling, M.R., Giles, K. A., Holbrook, J.M., Jordan, R., Kendall, C.G.S.C., Macurda, B., Martinsen, O.J., Miall, a. D., Neal, J.E., Nummedal, D., Pomar, L., Posamentier, H.W., Pratt, B.R., Sarg, J.F., Shanley, K.W., Steel, R.J., Strasser, A., Tucker, M.E., Winker, C., 2009. Towards the standardization of sequence stratigraphy. *Earth-Science Reviews* 92, 1–33.
- Clausen, O.R., Śliwińska, K.K., Gołędowski, B., 2012. Oligocene climate changes controlling forced regression in the eastern North Sea. *Marine and Petroleum Geology* 29, 1–14.
- Davies, R.J., Posamentier, H.W., 2005. Geologic processes in sedimentary basins inferred from three-dimensional seismic imaging. *GSA Today* 15, 4–9.
- Donders, T., Verreussel, R., van Helmond, N., Munsterman, D., Ten Veen, J., Speijer, R., Weijers, J., Sangiorgi, F., Reichart, G-J., Damsté, J-S., Lourens, L., Kuhlmann, G., Brinkhuis, H., n.d. Early Pleistocene glaciations exhibit predominant Northern Hemisphere forcing. In Prep.
- Galloway, W.E., 2002. Paleogeographic setting and depositional architecture of a sand-dominated shelf depositional system, Miocene Utsira Formation, North Sea basin. *Journal of Sedimentary Research* 72, 476–490.
- Gibbard, P.L., West, R.G., Zagwijn, W.H., Balson, P.S., Burger, A.W., Funnell, B.M., Jeffery, D.H., de Jong, J., van Kolfschoten, T., Lister, A.M., Meijer, T., Norton, P.E.P., Preece, R.C., Rose, J., Stuart, A.J., Whiteman, C.A., Zalasiewicz, J.A., 1991. Early and early Middle Pleistocene correlations in the southern North Sea basin. *Quaternary International* 10, 23–52.
- Hampson, G.J., Graham, G.H., Holgate, N.E., Morris, J.E., Patruno, S., Sech, R.P., Petersen, S.A., Jackson, C.-L., Jackson, M.D., Johnson, H., 2015. Sedimentological Characterisation, Impact and Modelling of Clinoforms in Shallow Marine

Reservoirs. Sedimentology of Paralic Reservoirs: Recent Advances and their Applications Conference Abstract.

- Harding, R., Huuse, M., 2015. Salt on the move: Multi stage evolution of salt diapirs in the Netherlands North Sea. *Marine and Petroleum Geology* 61, 39–55.
- Helland-Hansen, W., Hampson, G.J., 2009. Trajectory analysis: concepts and applications. *Basin Research* 21, 454–483.
- Henderson, J., Purves, S.J., Leppard, C., 2007. Automated delineation of geological elements from 3D seismic data through analysis of multi-channel, volumetric spectral decomposition data. *First Break* 25, 87–93.
- Huisman, D.J., Klaver, G.T., 2007. Heavy Minerals in the subsurface: Tracking sediment sources in three dimensions, *Developments in Sedimentology, Developments in Sedimentology* 58, 869–885.
- Hunt, D., Tucker, M.E., 1992. Stranded parasequences and the forced regressive wedge systems tract: deposition during base-level fall—reply. *Sedimentary Geology* 95, 147–160.
- Huuse, M., Clausen, O.R., 2001. Morphology and origin of major Cenozoic sequence boundaries in the eastern North Sea Basin: top Eocene, near-top Oligocene and the mid-Miocene unconformity. *Basin Research* 13, 17–41.
- Janocko, M., Nemec, W., Henriksen, S., Warchoř, M., 2013. The diversity of deep-water sinuous channel belts and slope valley-fill complexes. *Marine and Petroleum Geology* 41, 7–34.
- Kane, I. a., McCaffrey, W.D., Peakall, J., Kneller, B.C., 2010. Submarine channel levee shape and sediment waves from physical experiments. *Sedimentary Geology* 223, 75–85.
- Kuhlmann, G., de Boer, P.L., Pedersen, R.B., Wong, T.E., 2004. Provenance of Pliocene sediments and paleoenvironmental changes in the southern North Sea region using Samarium–Neodymium (Sm/Nd) provenance ages and clay mineralogy. *Sedimentary Geology* 171, 205–226.
- Kuhlmann, G., Langereis, C., Munsterman, D., Jan van Leeuwen, R., Verreussel, R., Meulenkamp, J., Wong, T., 2006. Chronostratigraphy of Late Neogene sediments in the southern North Sea Basin and paleoenvironmental interpretations. *Palaeogeography, Palaeoclimatology, Palaeoecology* 239, 426–455.
- Kuhlmann, G., Langereis, C.G., Munsterman, D., Leeuwen, R. Van, Verreussel, R., Meulenkamp, J.E., Wong, T.E., 2006. Integrated chronostratigraphy of the Pliocene–Pleistocene interval and its relation to the regional stratigraphical stages in the southern North Sea region.

- Kuhlmann, G., Wong, T.E., 2008. Pliocene paleoenvironment evolution as interpreted from 3D-seismic data in the southern North Sea, Dutch offshore sector. *Marine and Petroleum Geology* 25, 173–189.
- Lee, H.J., Syvitski, J.P., Parker, G., Orange, D., Locat, J., Hutton, E.W., Imran, J., 2002. Distinguishing sediment waves from slope failure deposits: field examples, including the “Humboldt slide”, and modelling results. *Marine Geology* 192, 79–104.
- Lisiecki, L.E., Raymo, M.E., 2005. A Pliocene-Pleistocene stack of 57 globally distributed benthic δ 180 records. *Paleoceanography* 20, 1–17.
- Meijer, T., Cleveringa, P., Munsterman, D.K., Verreussel, R.M.C.H., 2006. The Early Pleistocene Praetiglian and Ludhamian pollen stages in the North Sea Basin and their relationship to the marine isotope record. *Journal of Quaternary Science* 21, 307–310.
- Michelsen, O., Danielsen, M., 1996. Sequence and systems tract interpretation of the epicontinental Oligocene deposits in the Danish North Sea. Geological Society, London, Special Publications 117, 1–13.
- Miller, K., Mountain, G., Wright, J., Browning, J., 2011. A 180-Million-Year Record of Sea Level and Ice Volume Variations from Continental Margin and Deep-Sea Isotopic Records. *Oceanography* 24, 40–53.
- Miller, K.G., Kominz, M.A., Browning, J. V, Wright, J.D., Mountain, G.S., Katz, M.E., Sugarman, P.J., Cramer, B.S., Christie-Blick, N., Pekar, S.F., 2005. The Phanerozoic Record of Global Sea-Level Change. *Science* 310 , 1293–1298.
- Mitchum Jr., R.M., Vail, P.R., Sangree, J.B., 1977. Seismic stratigraphy and global changes of sea level, Part six: stratigraphic interpretation of seismic reflection patterns in depositional sequences. *Seismic Stratigraphy — applications to hydrocarbon exploration* 117–134.
- Møller, L.K., Rasmussen, E.S., Clausen, O.R., 2009. Clinoform migration patterns of a Late Miocene delta complex in the Danish Central Graben; implications for relative sea-level changes. *Basin Research* 21, 704–720.
- Neal, J., Abreu, V., 2009. Sequence stratigraphy hierarchy and the accommodation succession method. *Geology* 37, 779–782.
- Noorbergen, L.J., Lourens, L.J., Munsterman, D.K., Verreussel, R.M.C.H., 2015. Stable isotope stratigraphy of the early Quaternary of borehole Noordwijk, southern North Sea. *Quaternary International* 386, 148–157.
- Normark, W.R., Piper, D.J.W., Posamentier, H., Pirmez, C., Migeon, S., 2002. Variability in form and growth of sediment waves on turbidite channel levees, *Marine Geology* 192 (1–3), 23–58.

- Overeem, I., Weltje, G.J., Bishop-Kay, C., Kroonenberg, S.B., 2001. The Late Cenozoic Eridanos delta system in the Southern North Sea Basin: a climate signal in sediment supply? *Basin Research* 13, 293–312.
- Patrino, S., Hampson, G.J., Jackson, C.A.-L., 2015. Quantitative characterisation of deltaic and subaqueous clinoforms. *Earth-Science Reviews* 142, 79–119.
- Plink-Björklund, P., Mellere, D., Steel, R.J., 2001. Turbidite Variability and Architecture of Sand-Prone, Deep-Water Slopes: Eocene Clinoforms in the Central Basin, Spitsbergen. *Journal of Sedimentary Research* 71, 895–912.
- Plink-Björklund, P., Steel, R., 2005. Deltas on falling-stage and lowstand shelf margins, the Eocene Central Basin of Spitsbergen: importance of sediment supply. *SEPM Special Publication* 179–206.
- Plink-Björklund, P., Steel, R., 2002. Sea-level fall below the shelf edge, without basin-floor fans. *Geology* 30, 115–118.
- Posamentier, H.W., Allen, G.P., James, D.P., Tesson, M., 1992. Forced regressions in a sequence stratigraphic framework: concepts, examples, and exploration significance. *American Association of Petroleum Geologists Bulletin* 76 (11), 1687–1709.
- Posamentier, H.W., Kolla, V., 2003. Seismic Geomorphology and Stratigraphy of Depositional Elements in Deep-Water Settings. *Journal of Sedimentary Research* 73, 367–388.
- Posamentier, H.W., Morris, W.R., 2000. Aspects of the stratal architecture of forced regressive deposits. *Geological Society, London, Special Publications* 172, 19–46.
- Purves, S.J., Henderson, J., Leppard, C., 2007. Rgb Visualisation Based Delineation of Geological Elements from Volumetric Spectral Decomposition of 3d Seismic Data. Extended abstracts EAGE 69th Conference & Exhibition London, UK, 11 - 14 June.
- Rasmussen, E.S., Vejbaek, O. V, Bidstrup, T., Piasecki, S., Dybkjær, K., 2005. Late Cenozoic depositional history of the Danish North Sea Basin: implications for the petroleum systems in the Kraka, Halfdan, Siri and Nini fields. *Geological Society, London, Petroleum Geology Conference Series* 6, 1347–1358.
- Remmelts, G., 1996. Salt tectonics in the southern North Sea, the Netherlands, in: *Geology of Gas and Oil under the Netherlands*. pp. 143–158.
- Remmelts, G., 1995. Fault-Related Salt Tectonics in the Southern North Sea, The Netherlands. *AAPG Memoir* 65, 261–272.
- Ruddiman, W.F., Raymo, M., McIntyre, A., 1986. Matuyama 41,000-year cycles: North Atlantic Ocean and northern hemisphere ice sheets. *Earth and Planetary Science Letters* 80, 117–129.

- Stow, D.A., Mayall, M., 2000. Deep-water sedimentary systems: New models for the 21st century. *Marine and Petroleum Geology* 17, 125–135.
- Ten Veen, J.H., van Gessel, S.F., den Dulk, M., 2012. Thin- and thick-skinned salt tectonics in the Netherlands; a quantitative approach. *Netherlands Journal of Geosciences* 91, 447–464.
- Ten Veen, J.H., Verweij, H., Donders, T., Geel, K., de Bruin, G., Munsterman, D., Verreussel, R., Daza Cajigal, V., Harding, R., Cremer, H., 2013. Anatomy of the Cenozoic Eridanos Hydrocarbon System. TNO Report R10060.
- Wynn, R.B., Masson, D.G., Stow, D. A. V, Weaver, P.P.E., 2000. The Northwest African slope apron: A modern analogue for deep-water systems with complex seafloor topography. *Marine and Petroleum Geology* 17, 253–265.
- Zagwijn, W.H., 1992. The beginning of the Ice Age in Europe and its major subdivisions. *Quaternary Science Reviews* 11. 583-591.
- Ziegler, P.A., 1992. North Sea rift system. *Tectonophysics* 208, 55–75.

CHAPTER 6

SECOND AUTHOR PAPERS

CHAPTER 6: SECOND AUTHOR PAPERS

6.1 EVIDENCE FOR REPEATED LOW LATITUDE MARINE TERMINATING ICE SHEETS IN A 41 KYR EARLY QUATERNARY WORLD

Andrew M. W. Newton¹, Rachel Harding¹, Rachel M. Lamb¹, Mads Huuse¹, Simon H. Brocklehurst¹

¹ School of Earth, Atmospheric and Environmental Sciences, University of Manchester

References kept in the format it will be submitted in

6.1.1 First Paragraph

Iceberg scours are a common feature on high-latitude margins where glaciers have, or once had, a marine-terminating margin. Scours are formed when an iceberg's draft exceeds water depth and ploughs a furrow in the seabed as it is moved by winds¹ and ocean currents². Iceberg scours and ice-rafted detritus preserved in the stratigraphic record provide insight into ice sheet geometry^{3,4} and location⁵; how and when ice sheets previously grew and collapsed⁶, their freshwater input into the ocean⁷, and their influence on ocean circulation patterns⁸⁻¹⁰. However, the mapping of iceberg scours has only been performed on local¹¹⁻¹³, rather than basin-wide scales. Here, we show the results from the first basin-wide mapping of iceberg scours in the Early Quaternary record of the North Sea, based on 3D seismic reflection data. We find over 8000 iceberg scours across 25 stratigraphic horizons in the interval between 2.58 and 1.7 Ma. This period was dominated by low-amplitude 41 kyr climate cycles¹⁴ which were progressively replaced with high-amplitude 100 kyr cycles after ~1.2 Ma¹⁵. It was previously thought that ice was restricted to small ice caps over Fennoscandia prior to 1.1 Ma¹⁶, as a 41 kyr glacial cycle was not considered long enough for ice to advance to the continental shelf. Our results indicate frequent marine-terminating ice sheets in the Early Quaternary, and suggest that glaciations in southern Norway were capable of

reaching the coast within a 41 kyr glacial cycle. These data emphasise how little is known of the earliest Quaternary glaciations and raise important questions about the efficacy of a 41 kyr glacial cycle to form large ice masses.

6.1.2 Main Text

Understanding long-term changes in ice dynamics is critical for models of sea level change¹⁷, and ocean-climate evolution^{18,19}. Developing a clearer understanding of historical changes means that we can better evaluate climate models used for projecting future environmental changes^{20,21}. The North Sea sedimentary succession (Fig. 6.1.1) comprises an up to 1.5 km thick archive of glacial and interglacial fluctuations through the Quaternary. Sedimentation in the Early Quaternary consists of glaciomarine and marine-deltaic deposits²² that are strongly related to low-amplitude 41 kyr climate cycles. After ~1.2 Ma the 41 kyr cycles were progressively replaced with high-amplitude 100 kyr cycles¹⁵ during the mid-Pleistocene transition (MPT). A switch from marine-deltaic, to glacial settings during the MPT resulted in complete ice cover during glaciations over much of the North Sea from Marine Isotope Stage (MIS) 12 (478-424 kyr) onwards²². The sediments deposited during the Quaternary vary from glacial tills to deep marine contourites^{23,24} and provide a record of changing sediment delivery patterns from the UK, Norway and mainland Europe^{22,24,25}.

The record of $\delta^{18}\text{O}$ fluctuations¹⁴ (Fig. 6.1.2) is a proxy for changes in sea level²⁶ related to global glacial-interglacial cycles, but does not directly indicate the contribution from a Fennoscandian ice sheet. Ice-rafted detritus (IRD) helps to fill this gap and data collected from offshore cores can be used to infer the presence of marine-terminating ice margins. Low amounts of IRD from the Vøring Plateau²⁷ off the mid-Norwegian shelf suggest that northern Norway was first covered by ice ~2.8 Ma and that ice was restricted to high latitudes and altitudes during the Early Quaternary. Massive ice sheets formed after the MPT²⁸ show a marked IRD increase after ~1.1 Ma²⁹ that is attributed to the expansion of ice onto the continental shelf in the west, and into the North Sea to the south.

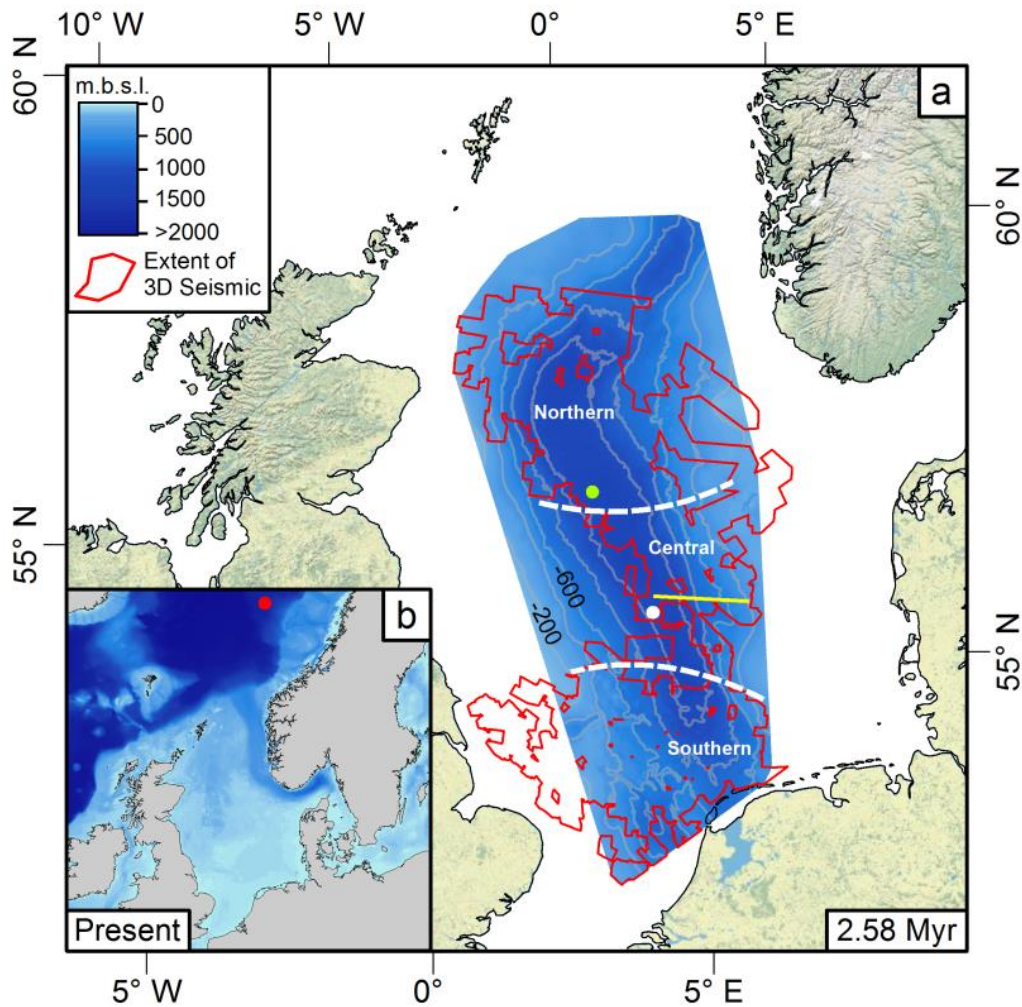


Figure 6.1.1 Map of the North Sea and data coverage. **a)** large red polygon indicates the area of 3D seismic coverage used for this study. Smaller polygons represent areas with no 3D data coverage inside the study area. Depths represent the distance between the contemporary sea floor and the base Quaternary reflector. Compaction of sediment has not been accounted for here, but the data nevertheless show the general, substantially narrower shape of the basin at 2.58 Ma. Backstripping of the base-Quaternary surface suggests maximum water depths of ~300 m (in prep. R.H.L., R.H., M.H., and S.H.B.). Drill sites used for dating and seismic correlation are also indicated. The white and green circles refer to the A15-03 and Josephine-1 core sites respectively. Contours are every 200 m. The north, central and southern regions referred to in Fig. 6.1.2 are shown. The location of the seismic line in Fig. 6.1.3 is displayed as the yellow line. **b)** inset map. GEBCO bathymetry for North Sea showing the contemporary environment, using the same colour scale as (a).

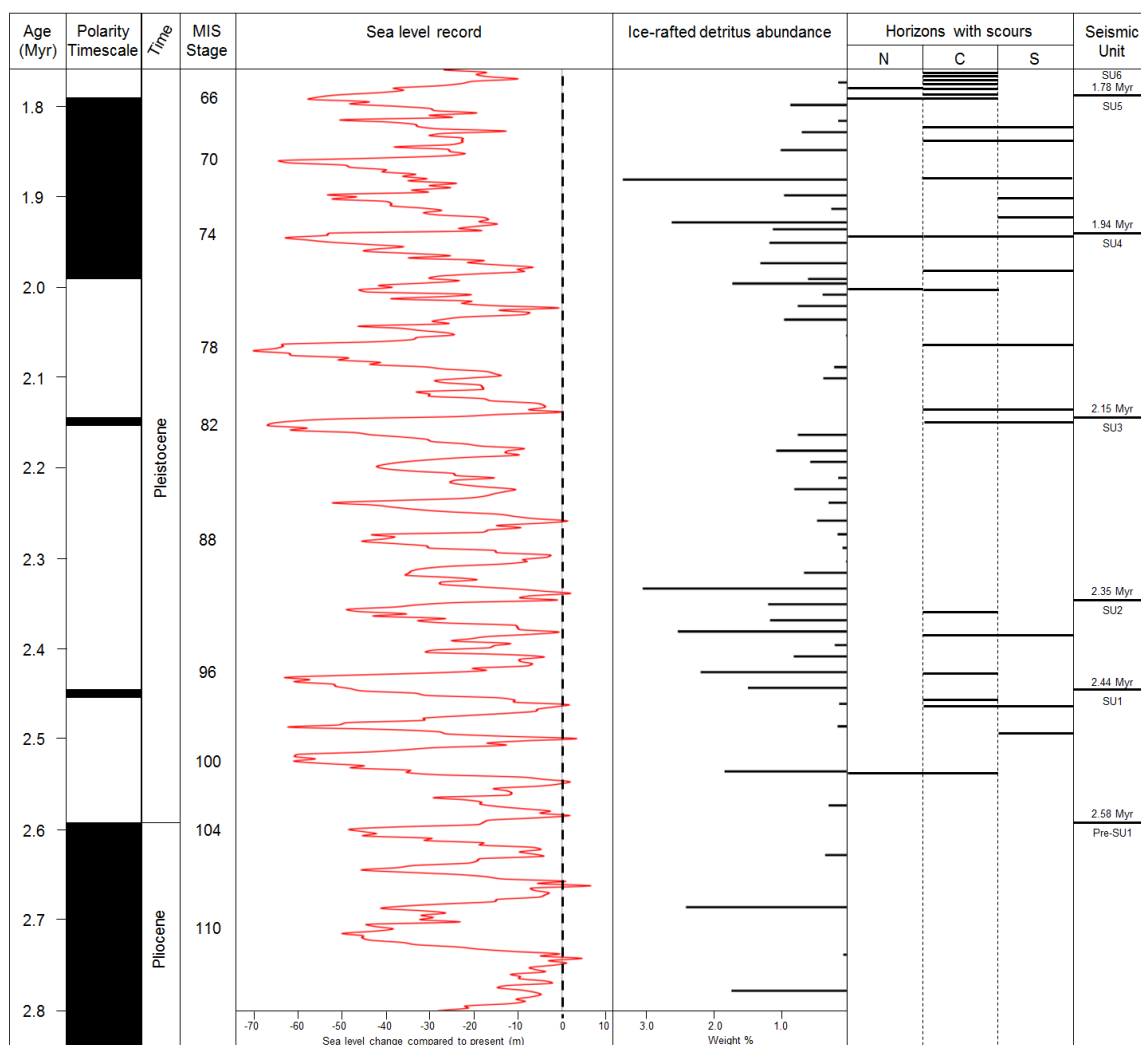


Figure 6.1.2 Late Cenozoic datasets. The sea level record²⁶ calculated from benthic $\delta^{18}\text{O}$ records¹⁴ and the ice-rafted detritus²⁶ record from ODP site 642 on the Vøring Plateau for the late Pliocene and Early Quaternary. IRD abundance is dated using a constant sedimentation rate between magnetically dated intervals²⁷. Using the six dated seismic units as a chronological constraint, the scoured horizons are dated by using their position within the seismic unit and by a speculative correlation with the sea level record. See Fig. 6.1.1 for the location of the north (N), central (C) and southern (S) areas used to describe iceberg scour locations.

Most work investigating the glacial geomorphology of the North Sea²² has concentrated on ice sheets younger than MIS 12. Limited work has investigated older glaciations and has shown iceberg scouring is present for the last 2 Myr⁸ in the central North Sea.

Previous work has imaged scouring events using time slices. Seismic reflections are generally accepted as representing time lines and in an area like the North Sea, where the sedimentology is dominated by prograding clinoforms, time slices cut across these time periods. This, therefore, does not accurately reflect the number of iceberg-scoured horizons present in the offshore record. We account for this by systematically creating surfaces for every prominent reflection in basin-wide 3D seismic data from the North Sea (Fig. 6.1.3a), and use this to define six seismic units across the Pliocene-Quaternary boundary (Fig. 6.1.2). Dating from nearby drilling sites are tied to the seismic data²³ (in prep, R. H. and M.H.) and using seismic volume attributes (Fig. 6.1.3b) we map over 8000 linear and curvilinear iceberg scours between 2.58 and 1.7 Ma. This record of seismic geomorphology shows that Quaternary glaciations and their areal extent were more complex than hitherto believed.

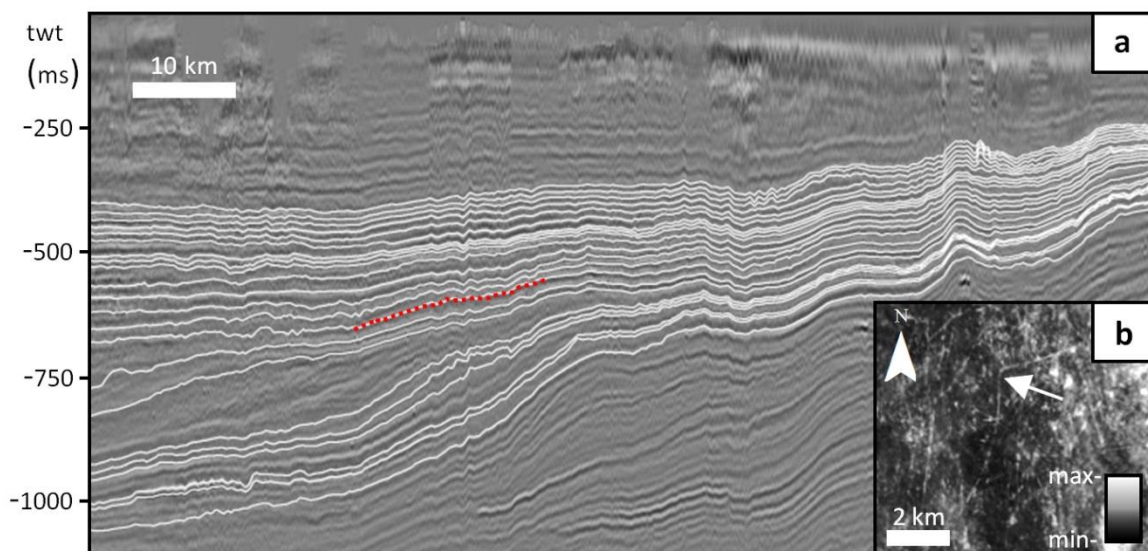
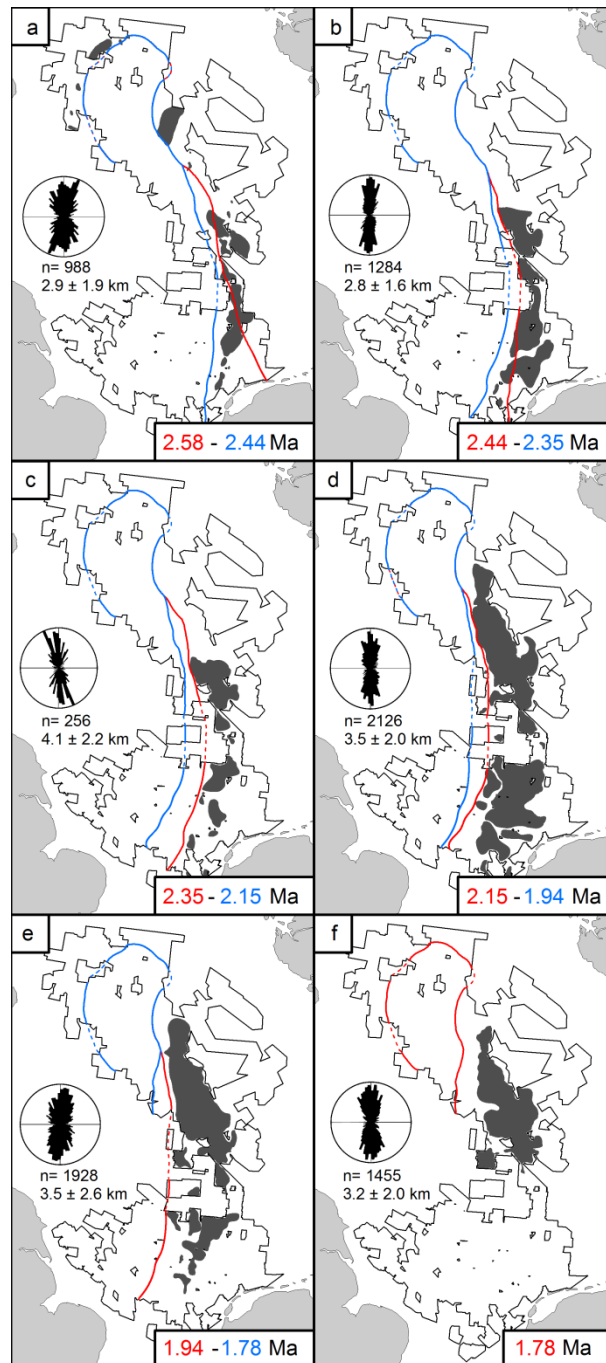


Figure 6.1.3 Clinoform geometry. **a)** White lines show the semi-automatically picked reflections from the seismic data. These reflections were then used with different seismic volume attributes to investigate the resultant 3D surface for glacial geomorphological features. The red stippled line shows the stratigraphic location of the surface displayed in (b). Seismic line location is shown in Fig. 6.1.1a. The clinoform geometry highlights how time slices cut across different time periods. **b)** root-mean squared amplitude attribute draped over the surface created from the 3D seismic. White arrow shows an example of an iceberg scour that was visible on the surface and digitised.

Fig. 6.1.1a shows the shape of the North Sea basin at the beginning of the Quaternary (in prep, R.M.L., R.H., M.H., and S.H.B.) compared to the present (Fig. 6.1.1b). This evolution of the basin shape has been an important factor in the distribution of iceberg scours and their formation in shallower water (Fig. 6.1.4). There is very limited evidence for scours beyond the shelf break; the majority of the scours mapped are at the shelf edge or on the adjacent shelf, where they appear to be either more common in shallower depths, or better preserved in the slightly coarser-grained sediments found here. In the oldest seismic unit (SU1), 2.58 – 2.43 Ma (Fig.6.1.4a), we find four iceberg-scoured horizons (Fig. 6.1.2). The first scoured horizon shows iceberg scours in the north and central parts of the survey area. These scours are very close to the base of the unit, and indicate a glacial influence in the North Sea almost immediately in the Quaternary, much earlier than previously shown⁸. Scours in this earliest horizon are also distributed either side of the central trough in the basin. The eastern scours show trajectories away from the Norwegian coast and to the southwest whilst the scours in the west indicate that they are moving away from the British coast to the southeast. If these icebergs were calved from a British ice sheet it would present additional geomorphological evidence to the IRD data offshore Ireland that suggests a British-Irish ice sheet since the earliest Pleistocene³⁰.

Figure 6.1.4 Iceberg scour distribution (following page). Distribution of iceberg scours during deposition of each seismic unit. Location of the shelf edge in each figure is indicated for the start (red line) and the end (blue line) of each time period. This shows how the basin shape changed with migration of the shelf edge to the west and reduction in the size of the central trough. Note that in the north the blue line covers the red line. This is due to the minimal change across the full time period for the northernmost part of the study area. The southwestern basin shape is not displayed because there is no depositional system from which to pick a shelf edge and seismic resolution and post-depositional movement make interpretation difficult. Rose diagrams are plotted for iceberg scour trajectory for all the scours in each time period, showing a predominantly north to south trajectory. Stippled lines show the shelf edge position outside the 3D coverage from 2D seismic profiles. **a.** deposition of the SU1 unit from 2.58 – 2.44 Ma. **b.** SU2 unit from 2.44 – 2.35 Ma. **c.** SU3 unit from 2.35 – 2.15 Ma. **d.** SU4 unit from 2.15 – 1.94 Ma. **e.** SU5 unit from 1.94 – 1.78 Ma. **f.** SU6 unit after 1.78 Ma



The remaining horizons in the SU1 package and the three scoured horizons in the SU2 (2.43 – 2.35 Ma) package (Fig. 6.1.4b) appear to correlate with the number of deglacial sea-level transgressions between MIS 98 and 92 (Fig. 6.1.2). With the exception of the earliest scouring event, which is correlated to MIS 104, the scours are preserved in the central and southern parts of the study area. Basin shape and ice sheet size are likely the main reasons for this, as the central trough of the North Sea at this time (Fig. 6.1.1a) was too deep for icebergs to scour, and the icebergs themselves, having been calved from what was probably a thin ice sheet, were not of sufficient draft to interact with a

comparatively deep seafloor. The scours would have only formed as a result of icebergs moving south and becoming grounded in shallower waters.

The SU3, (2.35–2.15 Ma), package (Fig. 6.1.4c) shows what appears to be a hiatus in iceberg scouring in the North Sea. The amplitude of sea level change in this period is muted; the sea level during the glacial lowstand is 10-25 m higher than those before and after. The lack of scours may reflect greater water depths during this period, such that any scouring would have taken place in shallower waters outside of the study area. The seismic data also shows minimal/or less topset preservation during this time period. Therefore, any icebergs scours that were formed may not have been preserved due to sediment bypass and reworking of the shelf during transgressions. Alternatively, the higher sea level may simply reflect a smaller Fennoscandian ice sheet. Concomitant with this would be a reduction of its marine-terminating margins, reduced calving fluxes and smaller icebergs. Despite the lack of geomorphological evidence for iceberg presence, IRD data on the Vøring Plateau remain steady during this time period²⁷. An important constraint on these IRD data²⁷ is the assumption of constant sedimentation rates between magnetically dated intervals. This assumption is necessitated by the lack of datable material in the succession but would, nonetheless, be highly unlikely as the region experiences transitions between glacial, interglacial and deglacial stages. It is also possible that the IRD data represent a marine-terminating margin over Fennoscandia, but at higher latitudes. Therefore, IRD found on the Vøring Plateau may not be a suitable proxy for predicting major iceberg calving events further south in our study area. However, given the lack of more proximal data a comparison is, nonetheless, informative. Another caveat for the use of IRD to infer marine ice margins is that the absence of IRD does not necessarily mean the absence of icebergs. IRD deposition in an environment as distal to the ice sheet as the Vøring Plateau, even if it is centred over Fennoscandia, requires that any sub- or englacial material not be melted out before it gets there. There is also plenty of evidence in contemporary environments of very clean, sediment-poor icebergs being calved. Thus, IRD data from the Vøring Plateau requires careful consideration when compared to sea level change and seismic geomorphology of the North Sea.

The SU4 (2.15– 1.94 Ma) (Fig. 6.1.4d) package contains the two largest glacial lowstands of the study period. The 2.15 Ma reflection is not as well-constrained but two reflections

appear to coincide with the deglaciation of MIS 82. Scours are present in the central and southern parts of the study area and could represent two separate stages of a periodic disintegration of the Fennoscandian ice sheet, when both calving and sedimentation fluxes varied during deglaciation. A further seismic reflection is correlated to the deglacial phase of MIS 78 but is again restricted to the central and southern parts of the survey coverage. Starting with the MIS 76 and 74 glaciations in the upper part of the SU4 package, scours become more common in the northern area of the data coverage. This is due to the progradation and infill of the central basin (Fig. 6.1.4) allowing scouring to take place across more widely-spread shallow bathymetry.

In the SU5 (1.94 – 1.78 Ma) package (Fig. 6.1.4e) and above (SU6) (Fig. 6.1.4f) there are numerous scouring events across the central and southern areas of the survey. In the top part of this package, scours are again present in the northern area at around ~1.78 Ma. Over 2000 scours are present across seven surfaces during the deglaciation of MIS 66. No scours are present in the south as the basin has infilled, and subsequently the area has become partially terrestrial during glacial lowstands²³. The frequency of scouring events during the deglaciation suggests that sedimentation rates were sufficiently high as to allow different scouring events to plough younger sediments and not destroy evidence of older scouring events from the same deglaciation. The different scouring events represent different phases of the deglaciation and indicate that it probably happened in a sustained manner rather than as a dramatic collapse.

We find no evidence for Late Pliocene iceberg scouring in the North Sea but numerous events through the Early Quaternary. The frequency with which icebergs have scoured palaeo-seafloors in the Early Quaternary has a number of implications. The most obvious implication is that these scours represent several different events where icebergs drifted into the basin from the north, which all occurred shortly after the onset of the Quaternary. Early Quaternary margin progradation shows a dominant sediment source from Fennoscandia and northern Europe²⁴ rather than from Great Britain. Sediments in the northern area were of glaciogenic origin²⁴ and suggests that the parent ice sheet of the icebergs was likely over Fennoscandia. Such a system would require that there is at least seasonally open water access to the North Sea and that ice extended beyond the coastline onto the shelf in order to calve sufficiently large icebergs. It was previously suggested that ice coverage was restricted to the more mountainous regions

of Norway in the Early Quaternary²⁹. There has been great uncertainty as to whether ice masses could grow sufficiently large during a 41 kyr glacial cycle to reach the coast. However, the evidence presented here suggests that ice was much more extensive than previously thought and marine-terminating margins were common through several different glaciations. Pre-existing regolith may have allowed ice sheets to thin and stretch towards the coast on a 41 kyr cycle²⁸, but an alternative mechanism allowing such frequent expansion of ice onto the shelf may be the presence of permanent ice cover over Norway. A positive mass balance over a full glacial-interglacial cycle means that less snow accumulation would be required during the next in order to increase the areal extent and move beyond the coast. This would give rise to an early expansion of a Late Pliocene mountainous ice sheet in Norway which grew with successive glaciations before it reached the coast at the onset of the Quaternary. Regardless of the mechanism, the data presented in this letter provide compelling evidence for high-frequency oscillations of Early Quaternary marine-terminating ice sheets in Europe, which had not been thought possible. There remains great uncertainty as to the full chronology and dynamics of the earliest glaciations in northwest Europe.

6.1.3 Methods

Using Eliis Paleoscan auto horizon-track software, reflection surfaces were generated semi-automatically for all 3D seismic volumes. The 3D seismic volumes include the PGS Southern North Sea MegaSurvey and the Central North Sea MegaSurvey. Surfaces were imported into the Petrel seismic interpretation software for analysis. Amplitude, root-mean squared amplitude and amplitude variance volumes were extracted onto the auto-interpreted reflection surfaces to identify all occurrences of iceberg scours in the data. Additional surfaces were picked so that all reflections with iceberg scours were represented. Volume attribute extractions were exported as georeferenced images, and added to a GIS. Using ArcMap software all of the scours from each surface were digitised for subsequent analysis. Dates from nearby drill sites were tied to the seismic²³ (in prep, R.H., and M.H.) and scoured surfaces were dated by using their position between six absolutely dated seismic horizons. These surfaces were then compared to the global sea level curve and IRD data, as described above.

6.1.4 References

- 1 Carlson, P. R., Hooge, P. N. & Cochrane, G. R. Discovery of 100–160-Year-Old Iceberg Gouges and Their Relation to Halibut Habitat in Glacier Bay, Alaska. *American Fisheries Society Symposium* **41**, 235-243 (2005).
- 2 Woodworth-Lynas, C. M. T. in *Past Glacial Environments: Sediments, Forms and Techniques* (ed J. Menzies) (Butterworth-Heinemann, 1996).
- 3 Dowdeswell, J. A. & Bamber, J. L. Keel depths of modern Antarctic icebergs and implications for sea-floor scouring in the geological record. *Marine Geology* **243**, 120-131 (2007).
- 4 Arndt, J. E., Niessen, F., Jokat, W. & Dorschel, B. Deep water paleo-iceberg scouring on top of Hovgaard Ridge–Arctic Ocean. *Geophysical Research Letters* **41**, 5068-5074, doi:doi:10.1002/2014GL060267 (2014).
- 5 De Schepper, S., Gibbard, P. L., Salzmann, U. & Ehlers, J. A global synthesis of the marine and terrestrial evidence for glaciation during the Pliocene Epoch. *Earth-Science Reviews* **135**, 83-102 (2014).
- 6 Jansen, E. & Sjøholm, J. Reconstruction of glaciations over the past 6 Myr from ice born deposits in the Norwegian Sea. *Nature* **349**, 600-603 (1991).
- 7 Bigg, G. R. *et al.* Sensitivity of the North Atlantic circulation to break-up of the marine sectors of the NW European ice sheets during the last Glacial: A synthesis of modelling and palaeoceanography. *Global and Planetary Change* **98-99**, 153-165 (2012).
- 8 Dowdeswell, J. A. & Ottesen, D. Buried iceberg ploughmarks in the early Quaternary sediments of the central North Sea: A two-million year record of glacial influence from 3D seismic data. *Marine Geology* **344**, 1-9 (2013).
- 9 Hill, J. C., Gayes, P. T., Driscoll, N. W., Johnston, E. A. & Sedberry, G. R. Iceberg scours along the southern U.S. Atlantic margin. *Geology* **36**, 447-450 (2008).
- 10 Kleiven, H. F., Jansen, E., Fronval, T. & Smith, T. M. Intensification of Northern Hemisphere glaciations in the circum Atlantic region (3.5–2.4 Ma) – ice-rafted detritus evidence. *Palaeogeography, Palaeoclimatology, Palaeoecology* **184**, 213-223 (2002).
- 11 Todd, B. J., Lewis, C. F. M. & Ryall, P. J. C. Comparison of trends of iceberg scour marks with iceberg trajectories and evidence of paleocurrent trends on Saglek

- Bank, northern Labrador Shelf. *Canadian Journal of Earth Science* **25**, 1374-1383 (1988).
- 12 Sacchetti, F., Benetti, S., Ó Cofaigh, C. & Georgiopoulou, A. Geophysical evidence of deep-keeled icebergs on the Rockall Bank, Northeast Atlantic Ocean. *Geomorphology* **159-160**, 63-72 (2012).
 - 13 Syvitski, J. P. M., Stein, A. B., Andrews, J. T. & Milliman, J. D. Icebergs and the Sea Floor of the East Greenland (Kangerlussuaq) Continental Margin. *Arctic, Antarctic, and Alpine Research* **33**, 52-61 (2001).
 - 14 Lisiecki, L. E. & Raymo, M. E. A Pliocene-Pleistocene stack of 57 globally distributed benthic $\delta^{18}\text{O}$ records. *Palaeoceanography* **20** (2005).
 - 15 Head, M. J. & Gibbard, P. L. in *Early-Middle Pleistocene Transitions: The Land-Ocean Evidence Special Publications* (eds M. J. Head & P. L. Gibbard) 1-18 (Geological Society, 2005).
 - 16 Henrich, R. & Baumann, K. H. Evolution of the Norwegian current and the Scandinavian ice sheet during the past 2.6 my: evidence from ODP Leg 104 biogenic carbonate and terrigenous records. *Palaeoceanography, Palaeoclimatology, Palaeoecology* **108**, 75-94 (1994).
 - 17 Miller, K. G. *et al.* The Phanerozoic Record of Global Sea-Level Change. *Science* **310**, 1293-1298 (2005).
 - 18 Rahmstorf, S. Ocean circulation and climate during the past 120,000 years. *Nature* **419**, 207-214 (2002).
 - 19 Lambeck, K., Esat, T. M. & Potter, E.-K. Links between climate and sea levels for the past three million years. *Nature* **419**, 199-206 (2002).
 - 20 Braconnot, P. *et al.* Evaluation of climate models using palaeoclimatic data. *Nature Climate Change* **2**, 417-424 (2012).
 - 21 Martinez-Boti, M. A. *et al.* Plio-Pleistocene climate sensitivity evaluated using high-resolution CO_2 records. *Nature* **518**, 49-54 (2015).
 - 22 Graham, A. G. C., Stoker, M. S., Lonergan, L., Bradwell, T. & Stewart, M. A. in *Quaternary Glaciations - Extent and Chronology* (eds J. Ehlers & P. L. Gibbard) 261-278 (2011).
 - 23 Kuhlmann, G. *et al.* Chronostratigraphy of Late Neogene sediments in the southern North Sea Basin and paleoenvironmental interpretations. *Palaeogeography, Palaeoclimatology, Palaeoecology* **239**, 426-455 (2006).

- 24 Ottesen, D., Dowdeswell, J. A. & Bugge, T. Morphology, sedimentary infill and depositional environments of the Early Quaternary North Sea Basin (56° 62° N). *Marine and Petroleum Geology* **56**, 123-146 (2014).
- 25 Bradwell, T. *et al.* The northern sector of the last British Ice Sheet: maximum extent and demise. *Earth-Science Reviews* **88**, 207-226 (2008).
- 26 Miller, K. G., Mountain, G. S., Wright, J. D. & Browning, J. V. A 180-million-year record of sea level and ice volume variations from continental margin and deep-sea isotopic records. *Oceanography* **24**, 40-53, doi:10.5670/oceanog.2011.26 (2011).
- 27 Krissek, L. A. in *Proceedings of the Ocean Drilling Program, Scientific Results Vol. 104* (eds O. Eldholm, J. Thiede, & E. Taylor) 61-74 (1989).
- 28 Clark, P. U. & Pollard, D. Origin of the middle Pleistocene transition by ice sheet erosion of regolith *Palaeoceanography* **13**, 1-9 (1998).
- 29 Jansen, E., Fronval, T., Rack, F. & Channell, J. E. T. Pliocene-Pleistocene ice rafting history and cyclicity in the Nordic Seas during the last 3.5 Myr. *Palaeoceanography* **15**, 709-721 (2000).
- 30 Thierens, M. *et al.* Ice-rafting from the British-Irish ice sheet since the earliest Pleistocene (2.6 million years ago): implications for long-term mid-latitudinal ice-sheet growth in the North Atlantic region. *Quaternary Science Reviews* **44**, 229-240 (2012).

6.2 THE EARLY QUATERNARY OF THE NORTH SEA BASIN

Rachel M. Lamb¹, Rachel Harding¹; Mads Huuse¹, Margaret Stewart², Simon. H. Brocklehurst¹

¹School of Earth, Atmospheric and Environmental Sciences, University of Manchester, Oxford Road, Manchester, UK.

² British Geological Survey, Murchison House, West Mains Road, Edinburgh, UK.

*Submitted to **Quaternary Science Reviews** in **October 2015** in review (references kept in format the paper submitted in)*

6.2.0 Abstract

The base Quaternary (2.58 Ma) surface has been mapped in detail across the entire central and southern North Sea Basin for the first time, adding > 0.5 km thickness to the Quaternary stratigraphy of the North Sea with respect to previous maps of the central North Sea. The newly identified depocentre is of importance to the study of palaeoclimate at the onset of Northern Hemisphere glaciation and improve our understanding of the dynamic palaeo-environment of the early Quaternary.

The new base Quaternary map is based on a modern database including MegaSurvey 3D seismic datasets and regional 2D seismic data covering the entire basin and calibrated by chrono-stratigraphic studies from the Dutch and UK North Sea. The new map defines a deep, elongate marine basin over 600 km in length and 100 km wide orientated NNW-SSE. A shallow water connection to the northeast Atlantic is located at the northern end of the basin while early Pleistocene palaeo-water depths in the main basin are estimated at about 300 m. Extremely rapid sedimentation rates (2.6 ± 0.5 mm yr⁻¹) in the earliest Pleistocene resulted in an expanded palaeoclimate archive for the early Pleistocene. This archive preserves the record of a critical period of global climatic cooling in an important mid-high latitude epicontinental basin fed by continental scale drainage systems and connected to the global ocean. The revised early Quaternary

framework has important implications for understanding basin infill, subsidence and for shallow reservoirs and hazards to hydrocarbon exploration and development.

6.2.1 Introduction

The onset of cooling at the Plio-Pleistocene transition and the onset of widespread Northern Hemisphere glaciation is an important marker for palaeo-climate and palaeo-environmental studies worldwide (Raymo 1994; Lisiecki & Raymo 2007). Climate records often vary strongly with latitude and cooling trends such as the Plio-Pleistocene transition are often best preserved in mid-to-high latitude basins. In the North Sea Basin, a mid-latitude epicontinental sea, understanding the nature and extent of the consequences of the early Pleistocene cooling has previously been difficult due to the poor definition and identification of the base Quaternary boundary. It has long been known that there is a considerable thickness of Quaternary deposits in the central North Sea (CNS) (Holmes 1977; Cameron et al. 1987; Gatliff et al. 1994), but the discrepancies among lithostratigraphic and chronostratigraphic studies in the five bordering countries, combined with spatio-temporal changes in climate and sediment supply (Huuse 2002) and a strong glacial overprint, has impeded the accurate definition of the basal Quaternary across the basin (Cameron et al. 1987). Additionally, in 2010 the global definition of the base Quaternary was changed from 1.81 (Marine Isotope Stage 65) to 2.58 Ma (MIS 103), adding 0.77 Ma of stratigraphy to the Pleistocene (Gibbard et al. 2010).

Regional 3D seismic data acquired for deeper petroleum exploration has been used previously for glacial geomorphological studies on local to sub-regional scales, highlighting the step change in horizontal resolution provided by these data and allowing previously hidden insights into the structure and stratigraphy of the Late Cenozoic succession (e.g. Praeg 1996, 2003; Stewart & Lonergan 2011; Kristensen & Huuse 2012; Stewart et al. 2012, 2013; Moreau & Huuse, 2014). This study documents the shape and evolution of the earliest Quaternary North Sea basin through integration of regional basin-scale 3D seismic data with recent biostratigraphic studies from the southern North Sea to accurately map the Plio-Pleistocene boundary across the entire central and southern North Sea (CNS, SNS) for the first time. The newly defined base Quaternary has direct and important implications for palaeo-climatological studies of

the onset and history of glaciation in the Northern Hemisphere and for site investigations carried out for the hydrocarbon industry.

6.2.2 Regional Setting

The present day North Sea basin is an epicontinental sea reaching average water depths of 100 m (outside the Norwegian Channel) and bordered by the Northwest European, Scandinavian and British landmasses. The North Sea originated during episodic extensional rifting related to the unzipping of the Atlantic from the Palaeozoic until the Early Cretaceous (Ziegler 1992). This was followed by continuous subsidence throughout the Late Cretaceous and Cenozoic punctuated by basin inversion episodes during the Paleogene (Ziegler 1992; White & Lovell 1997; Stoker et al. 2005). The role of regional and local tectonic activity into the late Cenozoic is still debated although most evidence favours a model of passive thermal subsidence enhanced by sediment loading in the CNS and marginal uplift due to denudation and unloading of the Norwegian landmass (Huuse 2002; Nielsen et al. 2009; Anell et al. 2010; Goledowski et al. 2012).

In previous studies the early Quaternary stratigraphy in the North Sea has been mapped as one unit, the Aberdeen Ground Formation, of pro-deltaic to marine sediments (Gatliff et al. 1994; Stoker et al. 2011), mostly sourced from the Rhine-Meuse and Baltic river systems of northern Europe and Scandinavia (Bijlsma 1981; Overeem et al. 2001; Busschers et al. 2007; Moreau & Huuse 2014). The timing of onset of glaciation(s) in the Quaternary remains unclear, although there is growing evidence for several ice sheet advances during the Middle-Late Pleistocene, sourced from the UK and Scandinavian landmasses (Graham et al. 2011) and evidence for iceberg scouring even in the SNS Basin since the onset of the Quaternary (Kuhlmann et al. 2006; Stuart & Huuse, 2012; Dowdeswell & Ottesen 2013).

6.2.3 Data and Methods

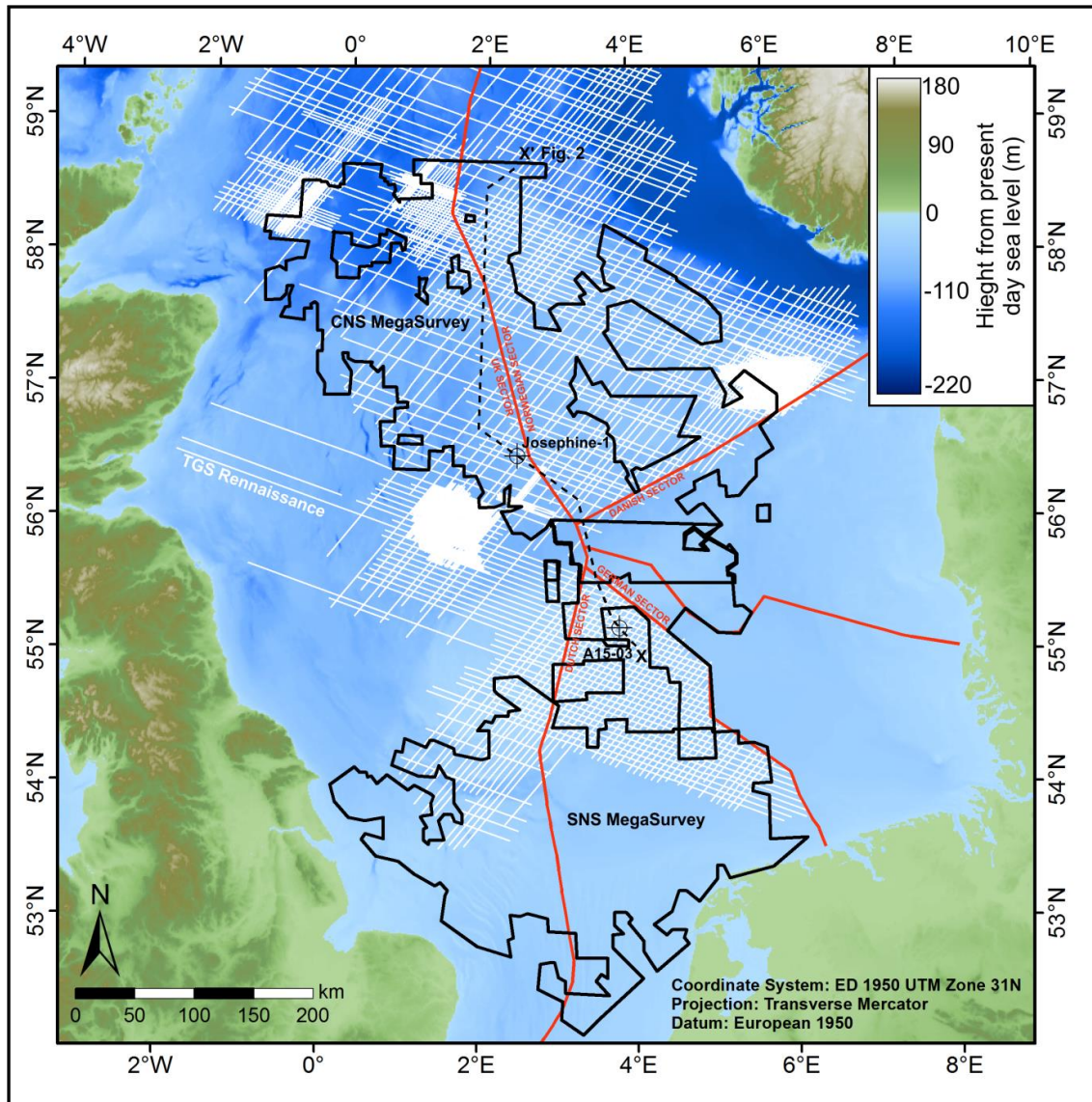


Figure 6.2.1. Location map and datasets. Data shown are the PGS Central North Sea and Southern North Sea 3D seismic MegaSurveys, the TGS North Sea Renaissance 2D lines and the locations of the Josephine-1 and A15-03 wells used for dating of the basal Pleistocene. Bathymetry and topography data from Ryan et al (2009). Location of Figure 6.2.2 seismic section indicated.

This study uses seismic stratigraphical and seismic geomorphological techniques (Mitchum et al. 1977a, b; Posamentier et al 2007) to analyse a basin scale 3D seismic dataset covering 128,000 km² of the CNS and SNS. The study uses the continuous PGS CNS and SNS 3D seismic MegaSurveys with a sub-sampled bin size of 50 m and sampling rate of 4 ms TWT to map the deepest part of the Quaternary North Sea basin (Figure 6.2.1). In areas not covered by the MegaSurvey, regional 2D seismic lines were used to resolve the basin shape. In the top 1.5 s TWT, the vertical resolution of the MegaSurveys is 8-16 m while the resolution of the 2D lines is between 10 and 18 m with variable line spacing between 1 and 15 km. The base Quaternary stratigraphic surface was correlated to a well-defined and continuous seismic reflection using the Dutch North Sea well A15-03 for which very detailed bio- and magneto-stratigraphic dating has been performed (Kuhlmann et al. 2006; see discussion in the next section). The horizon was mapped down the depositional dip of the clinoforms into the basin, which minimised correlation errors to about half the dominant wavelength (20-35 m), and the correlation compared to the biostratigraphic record of the Josephine-1 well (Knudsen & Abjórnsdóttir 1991) which is commonly used as a reference point for studies of the UKCS Quaternary (Figure 6.2.2). Calibrated TWT – depth data from 1122 wells from the UK and Norwegian North Sea were plotted to find a simple but robust depth conversion equation (Equation 1) with defined error margins (Figure 6.2.3).

$$Depth (m) = -81.0 \times TWT(s)^2 + 878 \times TWT(s) - 1.094(\pm 100 m) \quad [1]$$

Several transects representing the overall structure of the basin were identified for calculating approximate palaeo-water depths from the heights of clinoforms infilling the Quaternary basin. In order to provide realistic water depth estimates from buried clinoforms, they need to be back-rotated so their topsets are approximately horizontal and their height de-compacted (Pekar et al. 2000; Patruno et al. 2014).

In this study the infill of the basin was first split into four seismic stratigraphic packages bounded by dated surfaces, the youngest/shallowest package was decompacted first along the chosen transects, using Allen & Allen's (1990) decompaction equation:

$$y'_2 - y'_1 = y_2 - y_1 - \frac{\Phi_0}{c} \times \{e^{(-cy_1)} - e^{(-cy_2)}\} + \frac{\Phi_0}{c} \{e^{(-cy'_1)} - e^{(-cy'_2)}\} \quad [2]$$

Where y_1 is the depth to the top of the sediment layer; y_2 is the depth to the bottom of the sediment layer; y'_1 is the depth to the top of the decompacted sediment layer, y'_2 is the depth to the bottom of the decompacted sediment layer; ϕ_0 is the porosity of the sediment at the surface and c is a constant that defines the curve representing the change of porosity with depth.

The decompacted package was then back-stripped using a simple Airy isostasy model and the strata below were unloaded accordingly. The process was repeated with each of the successive packages, in turn restoring the early Quaternary surfaces and finally the base Quaternary surface to its approximate structure at 2.58 Ma. This back-stripping methodology is a simplified model based on Allen & Allen (1990) and does not account for complexities such as eustatic changes, flexural responses of the sediment, or heterogeneity of sediment within the packages and should be taken as an estimate only.

The strata immediately below the base Quaternary surface were interpreted with regards to the age of the sub-crop in order to identify features influencing the evolution of the earliest Quaternary basin. The mapping of the sub-crop followed a standard geological mapping process in which geological contacts between units 'exposed' on the base Quaternary surface were mapped on the regional 2D lines and then interpreted across the study area to form a complete map. Geological units were identified according to Evans et al. (2004).

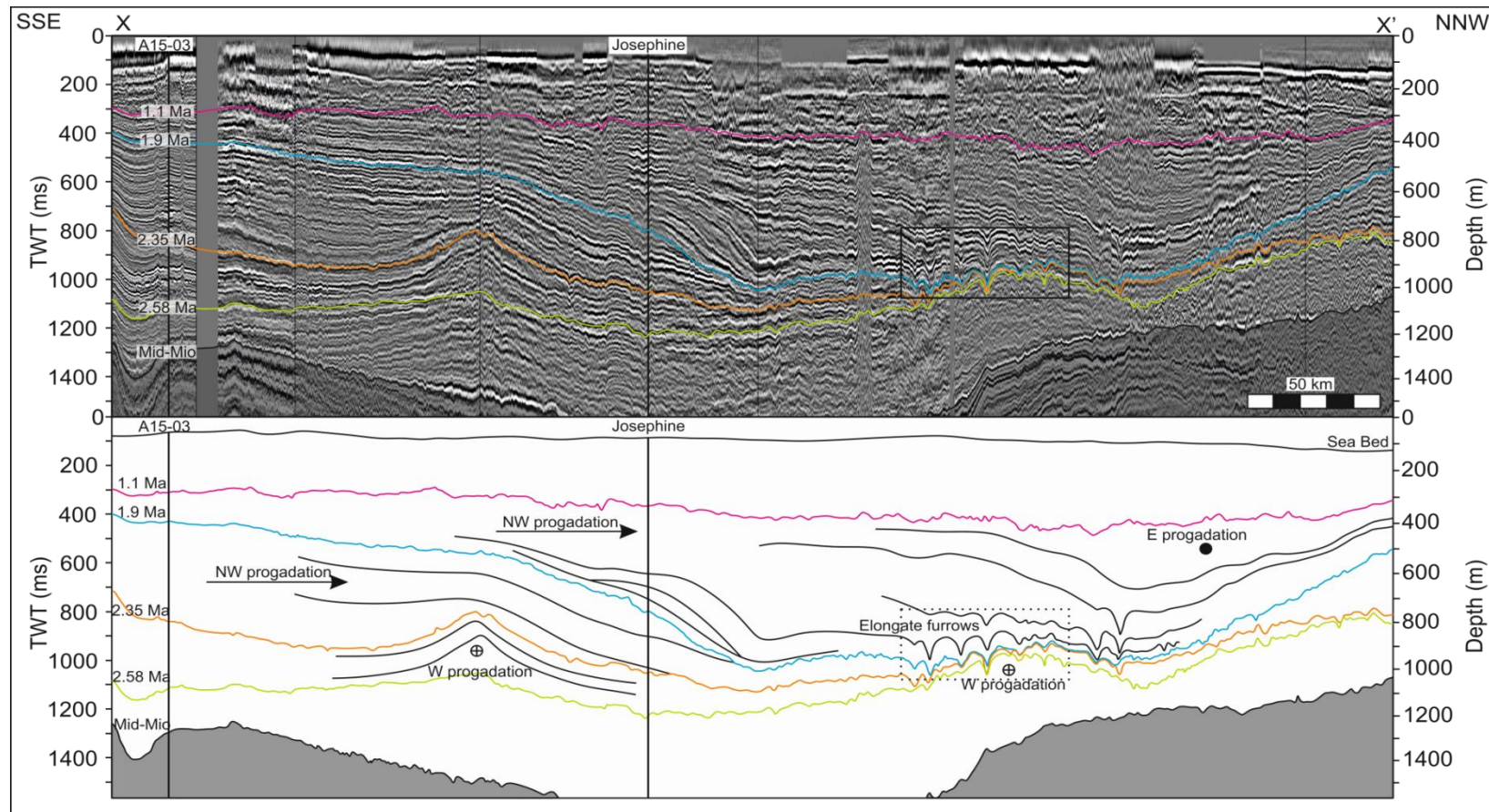


Figure 6.2.2. Seismic section and line interpretation, at 75x vertical exaggeration, showing the location of Josephine-1 and A15-03 wells plus surfaces for the mid-Miocene (c. 17 - 14 Ma), 2.58 Ma (base Quaternary), 2.35 Ma, 1.9 Ma and 1.1 Ma (base-Jaramillo palaeo-magnetic event). Location in Figure 6.2.1. Data courtesy of PGS.

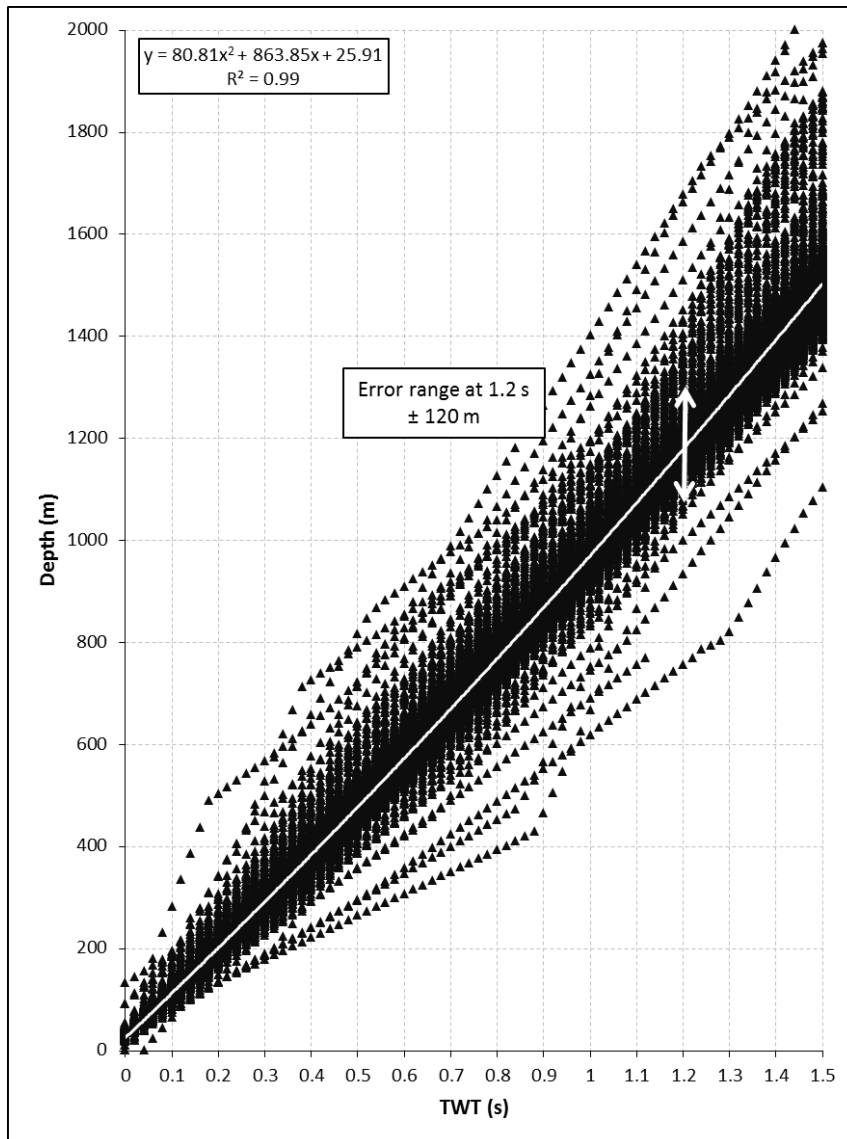


Figure 6.2.3. Calibrated depth plotted against TWT for top 1.5 seconds TWT in 1122 wells across the UK and Norwegian sectors of the CNS MegaSurvey with regression line and R^2 value for depth conversion as well as maximum error margins. Data courtesy of TGS.

6.2.4 Chronostratigraphic Calibration of the Base Quaternary

In seismic reflection data from the UK sector of the CNS, the base Quaternary is usually identified through correlation to one of two markers, the ‘crenulated reflector’ (Holmes 1977; Gatliff et al. 1994; Stoker et al., 2011), which is not regionally extensive, or the SNS regional unconformity, which transitions into a correlative conformity along the Plio-Pleistocene clinoform slope. Cameron et al. (1987, p.46) state ‘*The base of the Quaternary is less easily identified in the centre of the North Sea Basin... The seismic boundary which we have used to define the base of the Quaternary offshore is almost certainly diachronous*’.

Attempts at mapping into the UK sector from the Norwegian sector by Ottesen et al. (2014) identified the base Quaternary as equivalent to the base-NAUST at 2.7 Ma. This method correlated the two through the locally extensive unconformity at the top of the Middle-Upper Miocene Utsira formation, but this relationship assumes that post-Utsira pre-Pleistocene deposits are absent. Towards the southern half of the basin the relationship between the base Quaternary, base-NAUST and Utsira unconformity breaks down as the Pliocene sediments from the SNS deposited over the top of the Miocene strata. In order to identify and constrain mapping of the base Quaternary a new marker was identified through integrated bio- and magnetostratigraphic studies on shallow gas exploration wells in the SNS by Kuhlmann et al. (2006). The authors identified an event in the pollen record which correlates with the climatic degradation at the Plio-Pleistocene transition, the palaeo-magnetic Gauss-Matuyama transition, and the last occurrence of the benthic foraminifera species *Monspeliensina pseudotepida* (Table 6.2.1).

Chronostratigraphic Marker	Age (Ma)	Josephine-1 (Knudsen and Abjornsdottir 1991)	A15-03 (Kuhlmann et al 2006)
<i>Cibicides Grossus</i>	1.9	771 m b.s.l	770 m b.s.l
MIS 92	2.35	980 m b.s.l	816 m b.s.l
<i>Monspeliensina pseudotepida</i>	2.58	1096 m b.s.l	1071 m b.s.l

Table 6.2.1. Chronostratigraphic correlation adapted from Kuhlmann et al. (2006) and Knudsen & Abjornsdottir (1991) indicating three primary surfaces mapped at 2.58 Ma, 2.35 Ma and 1.9 Ma.

The new base Quaternary horizon was mapped northward in the direction of progradation into the basin and compared to the biostratigraphic record of the Josephine-1 well (56°36.11'N, 2°27.09'E; Figure 6.2.1) to ensure that the *M. pseudotepidia* event was preserved before being extended across the rest of the basin (Figure 6.2.2). For comparison a correlation was made using the base Quaternary as identified in Knudsen & Abjórnsdóttir (1991) and Buckley (2012) at the Josephine-1 well using the benthic foraminifera species *Cibicides grossus* which Buckley (2012) correlated to the 'crenulate reflector'. *C. grossus* is a deep water species and the biostratigraphic event it defines is diachronous across the North Sea due to the clinoform infill representing a range of water depths in the early Pleistocene (Chris King. *Pers. Comm.* 2013). In the southern part of the Quaternary basin, where basin infill occurred earlier than in the central areas, shallow-water conditions resulted in the *C. grossus* event corresponding approximately to 2.35 Ma, whereas in the central part of the Quaternary basin, it corresponds to an age of about 1.9 Ma (MIS 75) (Chris King. *Pers. Comm.* 2013). Therefore the *C. grossus* biostratigraphic event cannot be correlated to a single chronostratigraphic horizon and for this reason two surfaces were mapped for the assessment of the earliest Quaternary basin infill corresponding to the 1.9 Ma *C. grossus* event in the Josephine-1 well and to MIS 92 at 2.35 Ma in the Netherlands North Sea well A15-03 respectively (55°18'N, 3°48'E; Figure 6.2.1) based on the biostratigraphic information and comparison of the well log data from Kuhlmann et al. (2006) (Table 6.2.1, Figure 6.2.2).

6.2.5 The Quaternary North Sea Basin

The base Quaternary event defined in the SNS has been mapped across the southern and central North Sea basin and depth converted according to the borehole-derived velocity function provided above (Figures 4 & 5). The base Quaternary follows the structural form of the underlying Mesozoic Central Graben elongated NW-SE, until 57°30'N where the northern portion of the basin switches to a NE-SW trend. The maximum depth of the base Quaternary is 1248 ms TWT (1158 m). The minimum depth along the basin axis is 812 ms (792 m), found in the northernmost part of the basin where a relatively shallow connection exists into the northern North Sea and eventually the North Atlantic. The maximum width of the basin is 130 km and the axial length about 600 km, amounting to some $6 \times 10^4 \text{ km}^3$ of Quaternary sediment.

The mapped base Quaternary surface was progressively back-stripped, using the dated 2.35 and 1.9 Ma reference horizons as well as the sea floor and the horizon corresponding to the base of the Jaramillo palaeo-magnetic event at 1.1 Ma, to produce transects of the changing basin geometry and architecture through time (Figure 6). The calculations indicate clinoformal heights in the region of 250 m to 300 m in the southernmost part of the basin, and 200 m to 250 m in the central parts, indicating a shallowing of the basin towards the north and maximum palaeo-water depths of the order of $300 \text{ m} \pm 50 \text{ m}$.

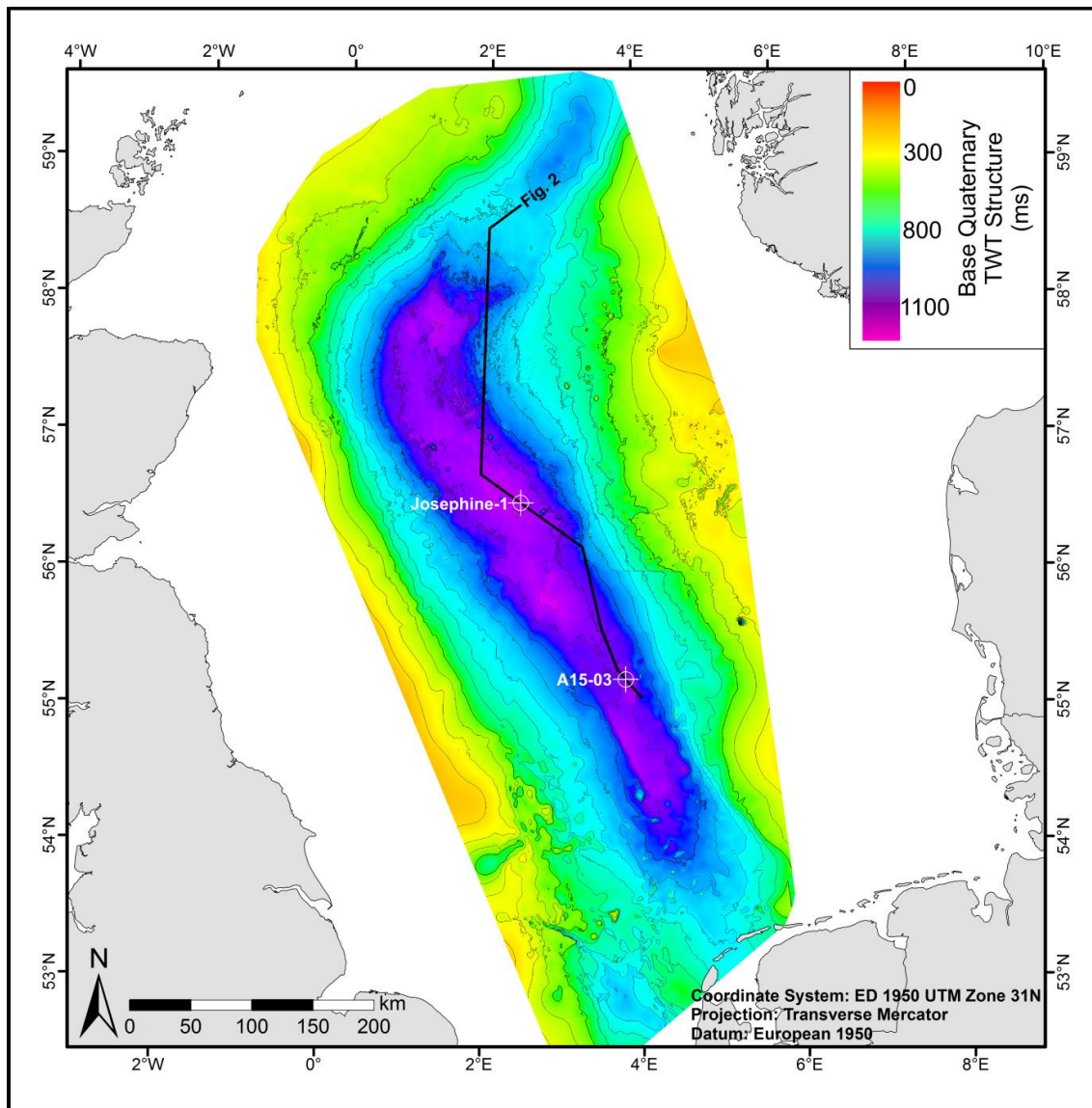


Figure 6.2.4. TWT structure map of the 2.58 Ma surface. Contours are every 100 ms TWT. Identifies locations of Josephine-1 and A15-03 wells and seismic section in Figure 6.2.2.

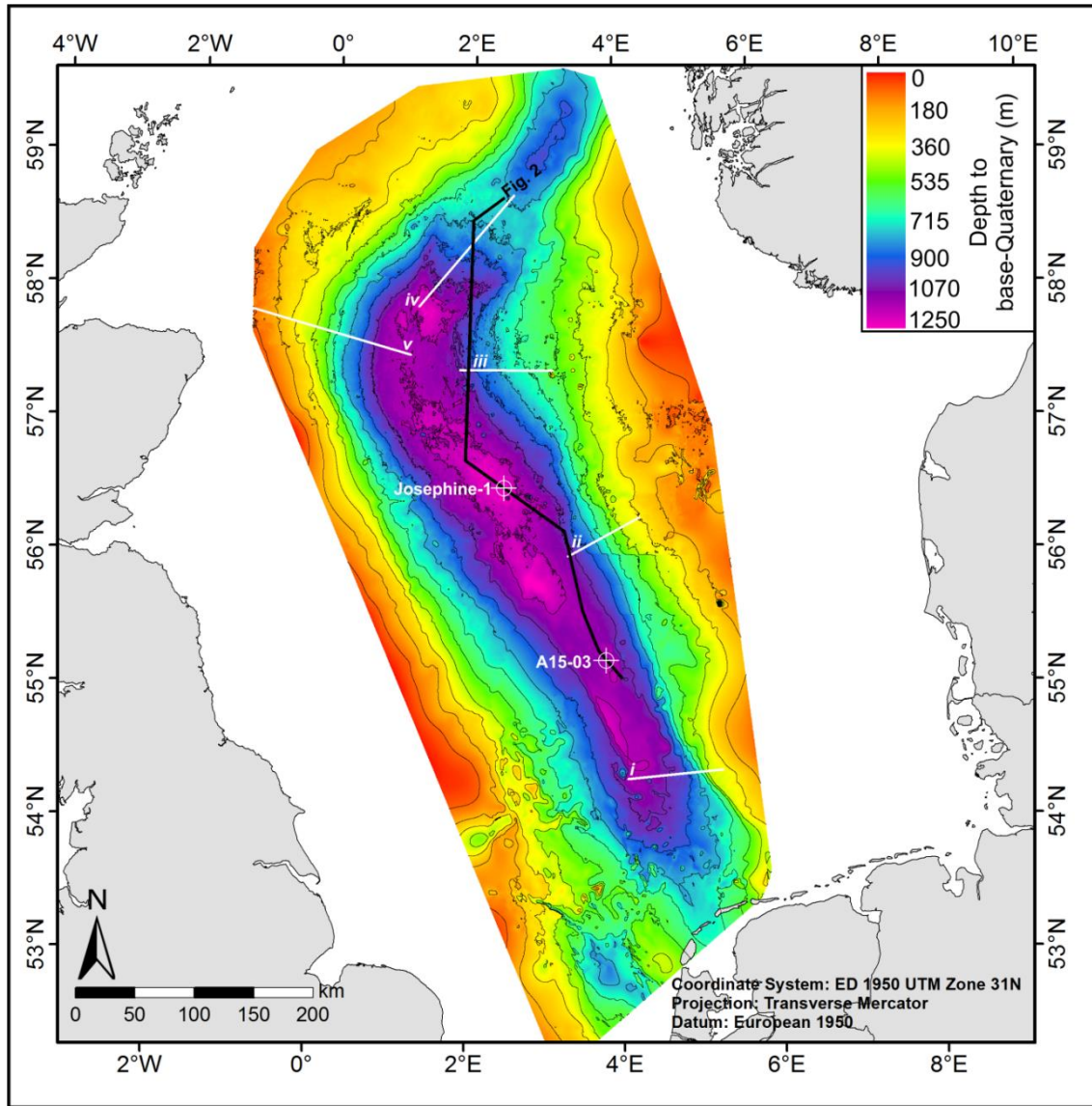


Figure 6.2.5. Depth converted 2.58 Ma surface using velocity function derived in Fig. 4. Contours are every 100 m. Identifies locations of Josephine-1 and A15-03 wells, the seismic section in Figure 6.2.2 and transects *i* to *v* used in the back-stripping process.

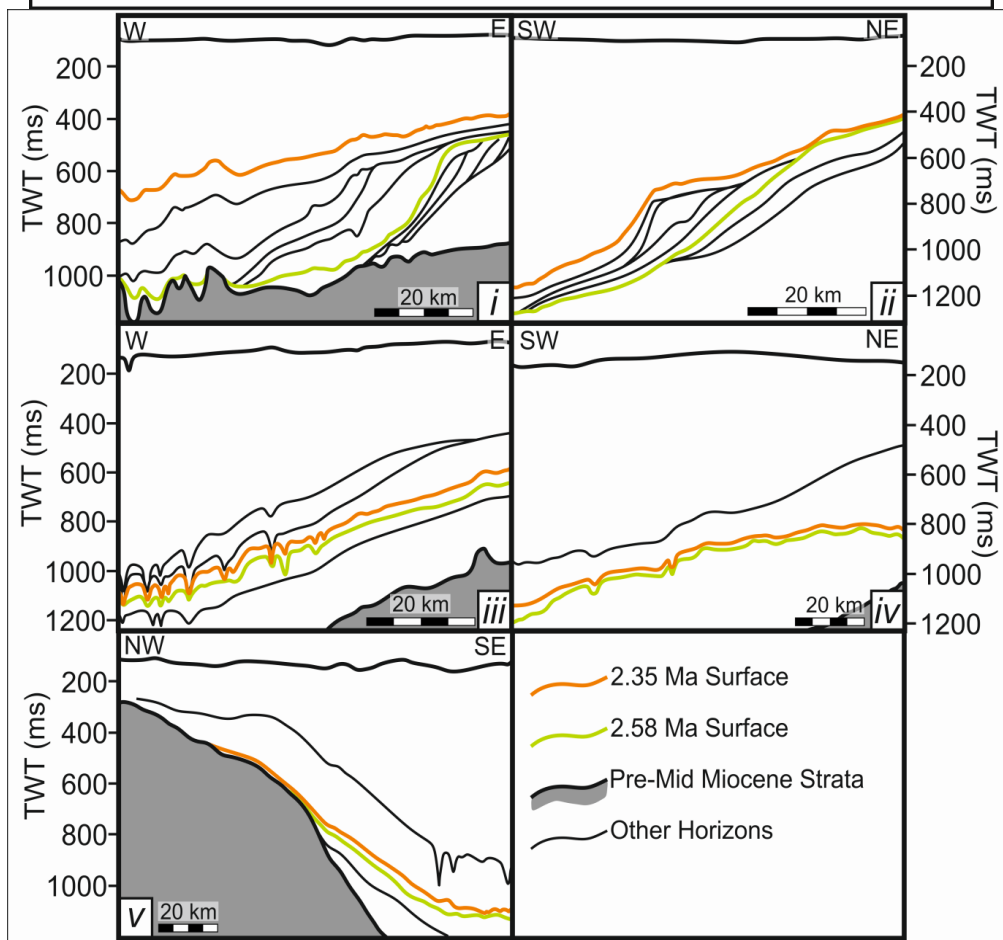
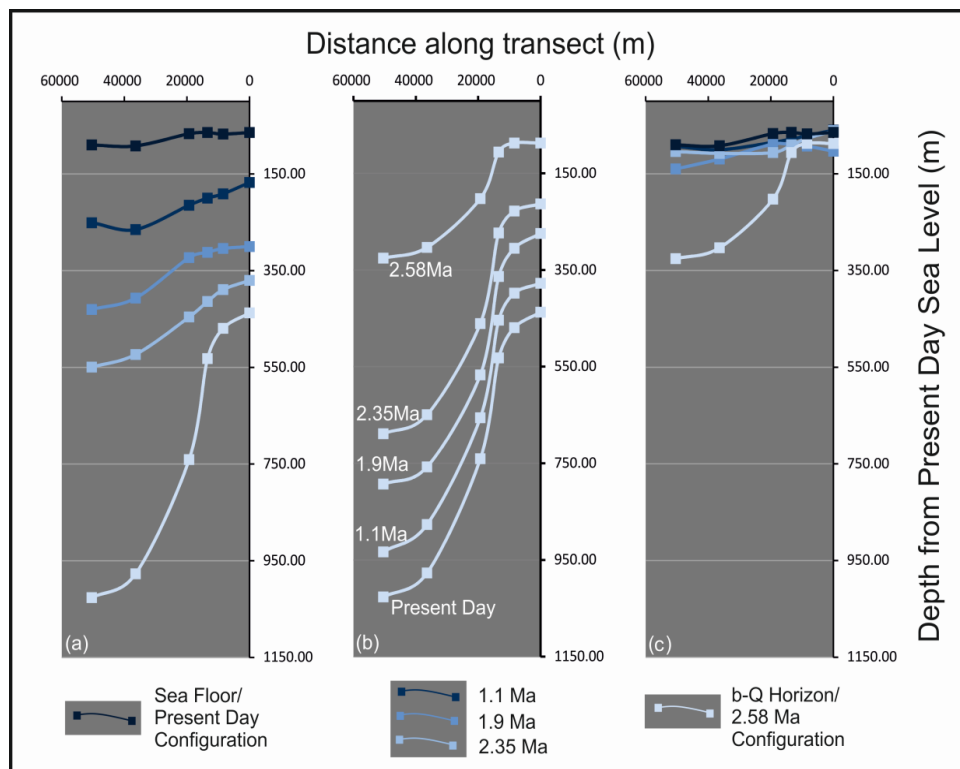


Figure 6.2.6. (previous page) Simplified sections from transect *i* (location Figure 6.2.3) used in the backstripping process, each point along the transect was used in the calculations and positioned according to distance along the transect. (a) Current configuration of dated horizons. (b) Burial history of the base Quaternary horizon. (c) The changing back-stripped basin configuration through time, note the infill of the basin in this area was virtually completed within the first 230,000 years of the Quaternary.

Figure 6.2.7 (previous page): Series of simplified line transects used in back-stripping process showing structure of the margins of the earliest Quaternary basin and progradation of clinoform packages.

The eastern margin of the base Quaternary basin comprises at least three major clinoform packages (Figure 6.2.7), which also incorporate the northern and southern margins, while the western margin represents the distal toesets of the NW- and westward progradational clinoforms, which on-lap Miocene strata (Figures 6.2.8 & 6.2.9). The base Quaternary is identified as a flooding surface in A15-03 (Kuhlmann et al 2006), with few preserved features on it. However, in the CNS, pockmarks are scattered across the top- and foreset of one of the eastern clinoforms. These features were previously identified by Kilhams et al. (2011) who tentatively suggested a Miocene age based on very limited chronostratigraphic data. Our revised chronology clearly demonstrates a base Quaternary age for these features.

The earliest Pleistocene sediments within the basin have a clinoformal geometry, which varies between high angle (4-5°) sigmoidal or oblique reflections with well-defined break points to very low angle (<0.5°), comparatively flat reflections (Figure 6.2.7). The palaeo-environments along the clinoforms most likely range from floodplain and shallow shelf along the topsets through outer littoral and upper to middle bathyal environments along the slope and toeset, with each clinoform thus representing a suite of palaeo-environmental conditions with associated variations in sediment grain size distribution (Posamentier & Allen 1993; Stuart & Huuse 2012; Patruno et al 2014, 2015).

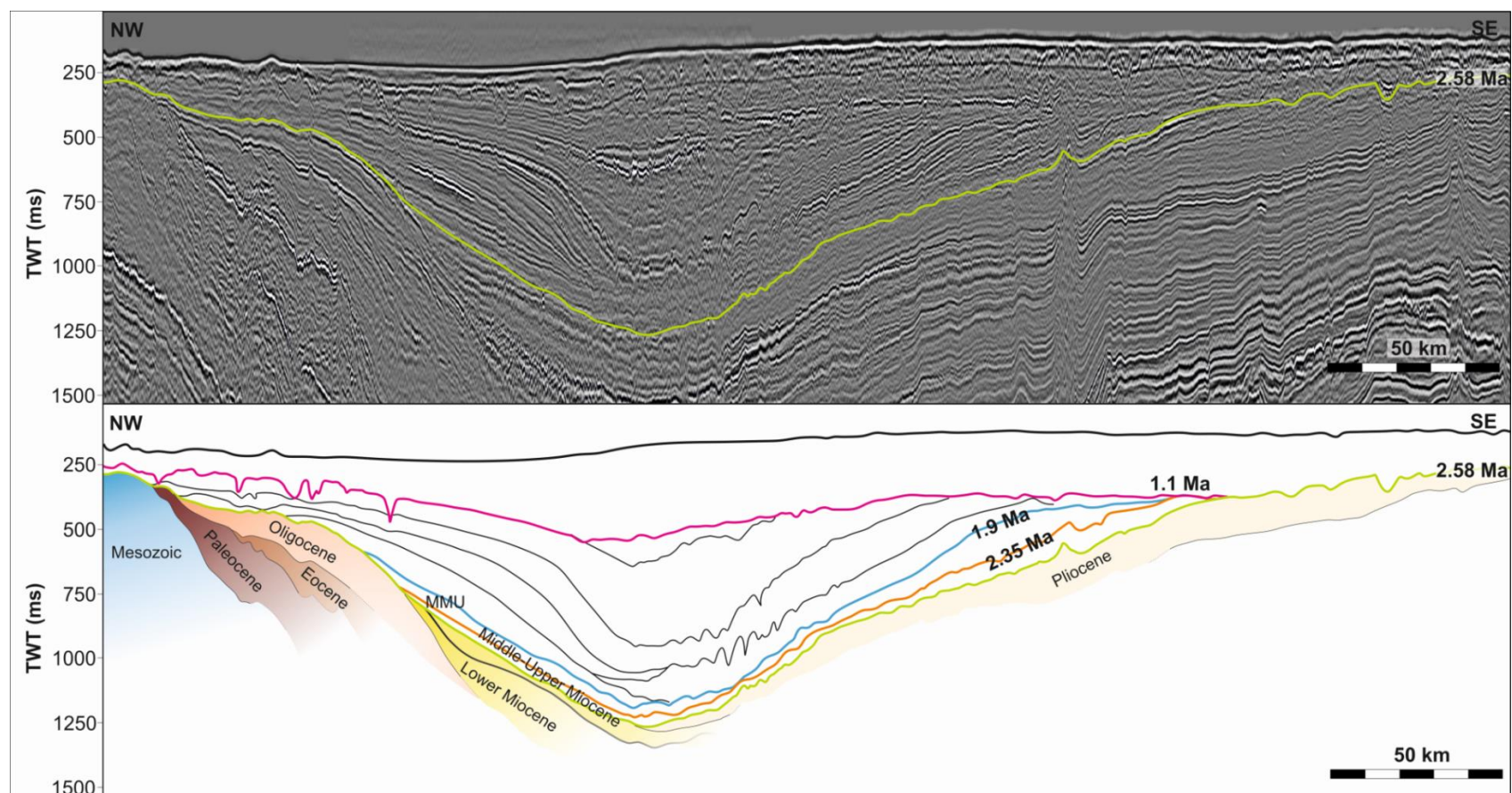


Figure 6.2.8: Seismic section showing interpretation of sub-crop beneath the 2.58 Ma surface used to produce sub-crop map (Figure 6.2.9). Packages separated by age after Evans et al 2003. See Figure 6.2.9 for location. Data courtesy of TGS.

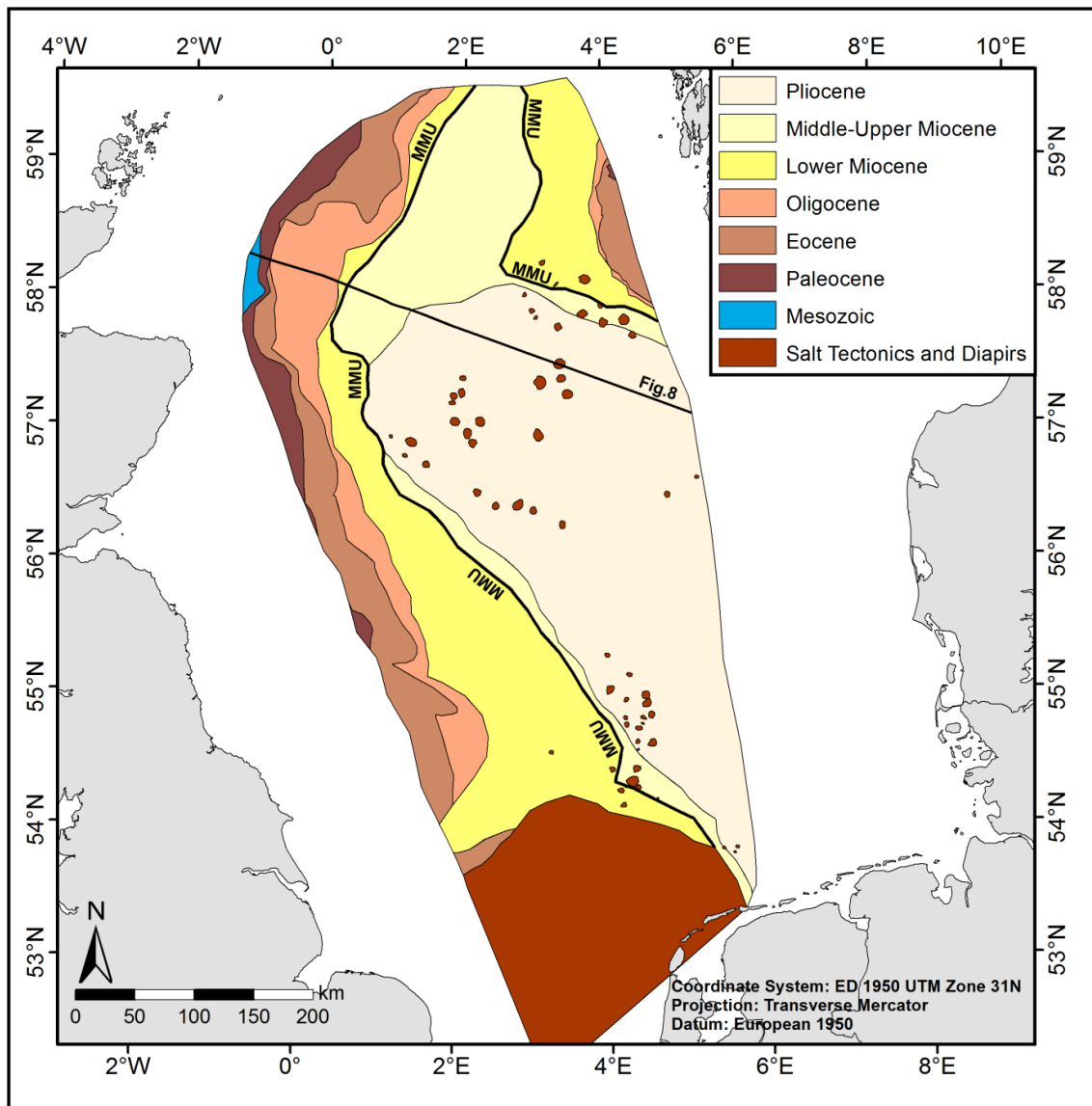


Figure 6.2.9: Simplified map of the base Quaternary subcrop indicating areas of sediment hiatus particularly on the western side of the basin. In the SNS the subcrop becomes extremely complex due to the presence of large scale salt tectonic features which heavily disturb the seismic reflection correlated to the base Quaternary.

The majority of Quaternary strata in the centre of the basin can be seen to overlie Pliocene sediments (Figures 6.2.8 & 6.2.9) and represent a continuation of the Pliocene clinoforms (Sørensen et al. 1997; Overeem et al 2001). This is particularly the case for the southernmost clinoform package (Figure 6.2.7, transect i). The southern clinoform package prograded towards the south-west during the earliest Quaternary and has an arcuate planform with sigmoidal slopes between 2° and 4° with a maximum back-stripped clinoform height of 240 ± 50 m (Figure 6.2.4) although this reaches 300 ± 50 m

away from the main transect. Between 2.58 Ma and 2.35 Ma the southern clinoform set deposited 590 ± 50 m of mud to fine sand as the clinoforms prograded 110 km westwards (Figure 6.2.10). This equates to an average sedimentation rate of 2.6 ± 0.2 mm yr⁻¹ for the 230,000 year period, with the southern part of the basin nearly filled by 2.35 Ma with remaining accommodation illustrated by back-stripped clinoform heights at this time of approximately 40 m. The eastern clinoform set has an initial back-stripped clinoform height of 180 m (Figure 6.2.7, transect ii). Between 2.58 and 2.35 Ma 60 m of sediment was deposited (Figure 6.2.10) at an average rate of 0.26 mm yr⁻¹ producing a sigmoidal geometry with a back-stripped clinoform height of 216 m. The northern clinoform set is comparatively flat, and with an initial clinoform height of 150 m dropping to 108 m by 2.35 Ma. The northern clinoforms do not appear to actively prograde during the first 230,000 years; the minor deposition (30 m at 0.13 mm yr⁻¹) is more aggradational in nature and primarily on the topsets rather than the foresets (Figure 6.2.7, transect iv).

In the SNS, downslope channels and mass transport deposits are preserved on the slopes and toesets in the 2.58 to 2.35 Ma package (Figure 6.2.11a). Further north into the CNS these features are replaced by a series of elongated, near-linear features with 'u' shaped cross sections (Figures 6.2.2 & 6.2.11b), previously described by Cartwright (1995), Knutz (2010), Kilhams et al. (2011) and Buckley (2012).

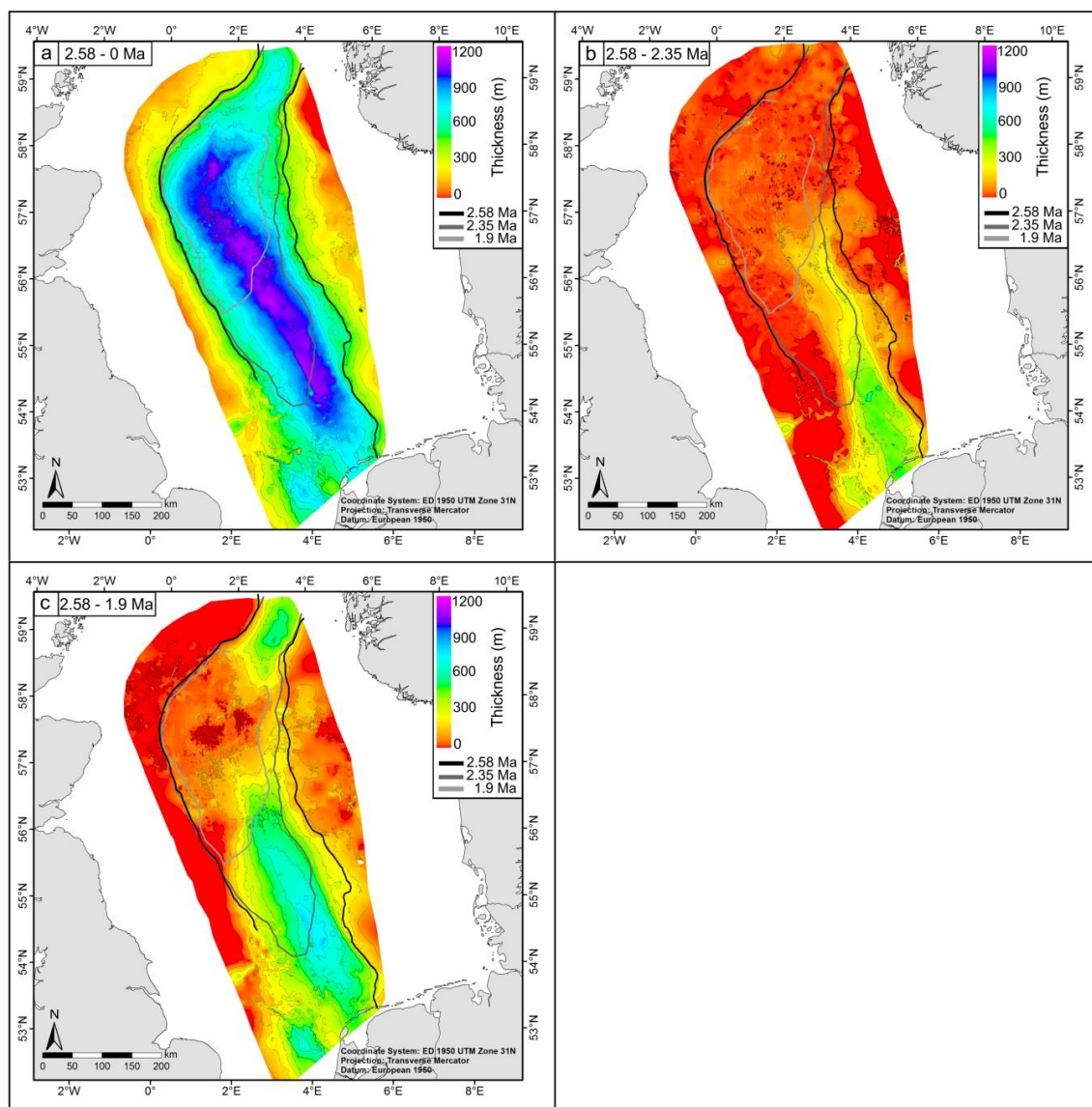


Figure 6.2.10: Thickness maps of Quaternary strata used to estimate sedimentation rates a) 2.58Ma to present day sea bed b) 2.58 to 2.35 Ma c) 2.58 Ma to 1.9 Ma. c) arepresents the difference between traditional base Quaternary maps such as Holmes (1977) and the new base Quaternary. Contours are every 100 m thickness. Indicates location of clinoform breakpoints at 2.58 and 2.35 Ma.

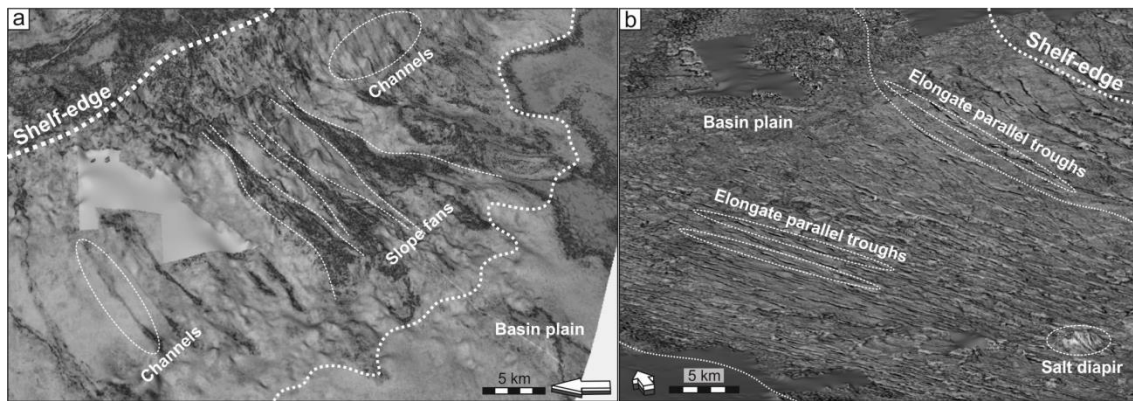


Figure 6.2.11: a) RMS amplitude extraction of horizon within the earliest (2.58 Ma to 2.35 Ma) Quaternary package in the southern North Sea showing downslope channels and fan deposits on the clinoform slopes and toesets. b) Seismic amplitude extraction across base Quaternary (2.58 Ma) surface in the central North Sea showing elongate, semi-parallel furrows linked to deep-water processes.

6.2.6 Discussion

Mapping of the current geometry of the basal Quaternary reflection coupled with back-stripping of the clinoforms indicates a basin with water depths in the region of 300 m, in agreement with the biostratigraphy from Kuhlmann et al (2006), enclosed by the NW European landmasses, with a narrow marine connection to the north (Figure 6.2.12). Analysis of the sedimentation rates and distribution patterns suggests the primary source of basin infill was from the south. The infill of the basin appears to correlate to the Baltic (Biljsma 1981; Sørensen et al. 1997; Overeem et al. 2001) and Rhine-Meuse (Busschers et al. 2007) river systems resulting in the dominant clinoform progradation from south to north. The two river systems drained large areas of northern Europe during this time, including the Fennoscandian shield, the Baltic platform and large areas of NW Europe from the Alps to the present day mouth of the Rhine (Overeem et al. 2001; Busschers et al. 2007). The rapid northward progradation has been linked with climatic cooling and increased sediment supply due to glacial activity in the sediment source areas (Overeem et al. 2001; Huuse 2002). Strontium isotope ratios indicate a high freshwater input in this section (Kuhlmann et al. 2006) suggesting the expanded stratigraphic section between 2.58 Ma and 2.35 Ma may provide key information for the northern European climate record of the earliest Quaternary.

The northern end of the basin saw relatively low sedimentation rates in the earliest Quaternary, with the primary sedimentation type being aggradation rather than progradation. One possible cause of this is the paleo-topographic sill north of 58°N (Figures 6.2.5, 6.2.12) which, while allowing a connection to the North Atlantic, could have restricted the accommodation space available in this area. The shallowing of the basin on either side of the sill would restrict flow of sediment-laden water over it particularly that sourced from the western margin of Norway. Another cause may be the drainage pattern of the Fennoscandian shield proposed by Overeem et al (2001), where drainage is directed southwards into the Baltic river systems; ultimately draining into the North Sea basin to feed the more southerly clinoform sets. Further work on the provenance of the sediments from the depocentres is required to confirm the palaeo-drainage patterns.

In either case, the low sedimentation rates during the earliest Quaternary mean any correlation between the Norwegian and North Sea depositional systems, such as that presented by Ottesen et al (2014), is very difficult to test using the present-day distribution of high-quality chronostratigraphic calibrations. The restriction of sedimentation could indicate completely separate depositional systems, one preserving solely the Scandinavian climate signal, and the other the Northern European signal, or a mixed signal routed through the southern clinoform set.

Back-stripping of the clinoforms indicates that the geometry of the basin changed dramatically through the earliest Pleistocene, with the deepest parts of the basin, in the SNS, being almost filled, while the clinoforms further north increase in height. In the SNS, the sedimentation rate can therefore be presumed to far outstrip the rate of subsidence due to sediment loading, while sedimentation rates further north into the CNS initially were lower than subsidence rates. However, caveats to this suggested fill pattern include the relatively simplistic calculations for the de-compaction and back-stripping used in this study. The calculations do not account for eustasy, variations in sediment composition, or flexural effects from the narrow, elongate basin being loaded principally at one end. The calculations produce a first order estimate of clinoform heights, within a 50 m error margin, but for accurate models of subsidence history much more detailed is needed.

The size and geometry of the southern clinoforms coupled with the presence of mass transport deposits and downslope channels suggests a shelf system onto which multiple small deltas prograded rather than a single large delta. Correlation of gamma-ray logs from Kuhlmann et al. (2006) indicates that the base Quaternary surface is a flooding surface associated with a rise and high stand of sea level, in agreement with the global sea level curve from Miller et al. (2005) which indicates a sea-level rise at 2.58 Ma. This would suggest that large parts of the shelf would have been flooded at the base Quaternary leading to a an extensive shallow marine environment on the top set part of the clinoforms – possibly as shallow as 20 m water depth -dropping sharply at the clinoform breakpoint of the shelf prism into the elongate deep water basin with depths in the region of 300 m (Figure 6.2.12). This agrees with interpretations of onshore stratigraphy from south-eastern Britain which suggests that the basal Quaternary was deposited in a shallow-marine environment (McMillan et al 2005; Rose 2009).

The elongate ‘u’ shaped features seen on the basal Quaternary in the central part of the basin have been interpreted as troughs formed by a strong downslope currents or contourite systems (Cartwright 1995; Knutz 2010; Kilhams et al 2011) or as part of a glacial imprint (Buckley 2012). Given the water depths proposed for the basal Quaternary and lack of other glacial geomorphic features we suggest that a current system is a more likely scenario. The source and nature of these troughs remain unclear (Lamb et al. submitted) although it would not be unreasonable to suggest that the high influx of sediment-laden water during this period had some influence on the formation of a large-scale significant current systems.

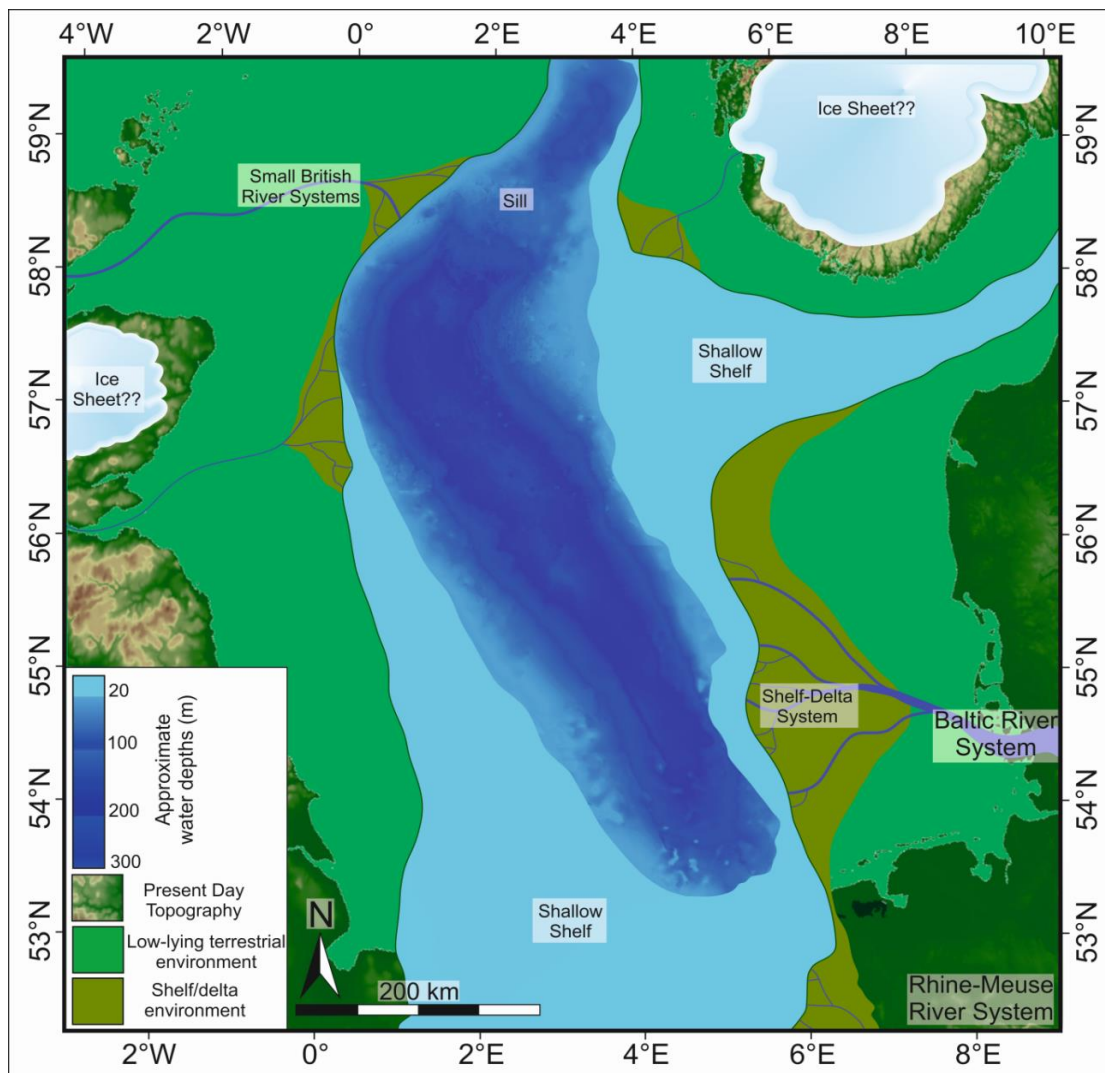


Figure 6.2.12: (previous page) Reconstructed palaeo-environmental map of 2.58 Ma North Sea based on results of this study, Overeem et al 2001, McMillan et al 2005, Busschers et al 2007, Rose 2009 and Noorbergen et al. 2015. Large parts of the present-day North Sea would have been flooded under the high-stand conditions at the onset of the Quaternary creating a very shallow shelf but were otherwise terrestrial.

6.2.7 Implications

The newly identified depocentre of >0.5 km thick MIS 103-75 strata is of great importance for the study of palaeo climate, particularly surrounding the onset of Northern Hemisphere glaciation. Analysis of the seismic geomorphology is now well established for the late Quaternary of the North Sea (Praeg 1996, 2003; Stewart & Lonergan 2011; Graham et al 2011; Buckley 2012; Kristensen & Huuse, 2012; Stewart et

al 2012, 2013; Moreau & Huuse, 2014) and, if applied to this newly defined early Quaternary succession, could fill in large gaps in our understanding of how ice sheets grew and behaved during the 41 kyr glacial-interglacial cycles of the early Quaternary (Raymo & Nisancioglu, 2003). The structural map of the earliest Quaternary basin can be combined with the back-stripping calculations to create a proxy that represents the pre-glacial palaeo-bathymetry of the North Sea, which is one of the more poorly defined boundary conditions in ice sheet modelling (Peltier 1994). The thickness map define areas of anomalously high sedimentation rates producing an expanded section which, if drilled, could be used to produce one of the strongest chronostratigraphic calibrations for the Quaternary . If combined with drilling of the marine tosets, also identified from the thickness maps, it would provide one of the most complete and detailed mid-latitude palaeo-climate records of the earliest Quaternary anywhere in the world. The shift of the base Quaternary > 500 m deeper into the basin fill will influence estimates of burial history, stress fields, and thermal history of the sedimentary substrate (Guidish et al 1985; Ehrenberg et al 2009). All of these estimates as well as the palaeo-water depths and palaeo-surface temperatures are used in the modelling of hydrocarbon migration, trapping and leakage (Goff 1983; Duncan et al 1998) which is of interest to petroleum exploration, carbon capture and storage (Chadwick et al 2004; Eiken et al 2011; EU 2011) and the analysis of geohazards (Haskell et al 1999).

6.2.8 Conclusions

The base Quaternary (2.58 Ma) surface in the central North Sea has been mapped in detail for the first time, revealing an elongated semi-enclosed deep marine basin with palaeowater depths throughout the early Quaternary of up to 300 m +/- 50 m. Evidence from seismic geomorphological analysis suggests this marine basin was influenced by high sediment input from Northern Europe, resulting in a palaeo-environment dominated by turbidities, channels and fans as well as shelf-margin deltas. The presence of contourites suggests strong deep water currents in the earliest Quaternary prior to 2.3 Ma. Estimates of an average sedimentation rate of 2.6 ± 0.5 mm yr⁻¹ from clinoform progradation suggest that a significant expanded record of climate change in the earliest Quaternary could be preserved in the southern part of the CNS and SNS. The map of the base Quaternary and the early Pleistocene depocentre have powerful implications,

academically and applied, for the evolution of the North Sea basin and the palaeoclimate evolution at of the Plio-Pleistocene transition.

ACKNOWLEDGMENTS

The authors would like to acknowledge NERC and BUFI in conjunction with Forewind for supporting this work through RL's NERC CASE studentship at the University of Manchester and the British Geological Survey (No. A87604X). We would like to thank PGS for providing the CNS and SNS MegaSurveys, TGS for providing 2D North Sea renaissance seismic lines and well data through their Facies Map Browser, IHS for Kingdom software, and Schlumberger for the donation of *Petrel* software. Thanks to Stefano Patruno for his invaluable advice on the back-stripping process and Chris King for sharing his insights on the biostratigraphy of the North Sea.

6.2.9 References

Allen, P., Allen, J., 1990 'Basin Analysis: Principles and Applications' *Blackwell Science*

Anell, I., Thybo, H., Stratford, W., 2010 'Relating Cenozoic North Sea sediments to topography in southern Norway: The interplay between tectonics and climate' *Earth and Planetary Science Letters*, **300**, 19-32

Buckley, F.A., 2012 'An Early Pleistocene grounded ice sheet in the Central North Sea' From: Huuse, M., Redfern, J., Le Heron, D.P., Dixon, R.J., Moscariello, A., Craig, J. (eds) 'Glaciogenic reservoirs and Hydrocarbon Systems' *Geological Society, London, Special Publications*, **368**

Busschers, F.S., Kasse, C., van Balen, R.T., Vandenberghe, J., Cohen, K.M., Weerts, H.J.T., Wallinga, J., Johns, C., Cleveringa, P., Bunnik, F.P.M., 2007 'Late Pleistocene evolution of the Rhine-Meuse system in the southern North Sea basin: imprints of climate change, sea-level oscillation and glacio-isostasy' *Quaternary Science Reviews* **26**, 3216-3248

Cameron, T.D.J., Stoker, M.S., Long, D., 1987 'The history of Quaternary sedimentation in the UK sector of the North Sea Basin' *Journal of the Geological Society* **144**, 43-58

- Cartwright, J., 1995 'Seismic-stratigraphical analysis of large-scale ridge-trough sedimentary structures in the Late Miocene to Early Pliocene of the central North Sea' *Spec. Publs int. Ass. Sediment.* **22**, 285 - 303
- Chadwick, R.A., Zweigel, P., Gregersen, U., Kirby, G.A., Holloway, S., Johannessen, P.N., 2004 'Geological reservoir characterization of a CO₂ storage site: the Utsira Sand, Sleipner, northern North Sea' *Energy*, **29**, 1371-1381
- Doornenbal, H., Stevenson, A., (eds) 2010 'Petroleum Geological Atlas of the Southern Permian Basin Area' *EAGE publications* b.v. (Houten)
- Dowdeswell, J.A., Ottesen, D., 2013 'Buried iceberg ploughmarks in the early Quaternary sediments of the central North Sea: A two-million year record of glacial influence from 3D seismic data' *Marine Geology*, **344**, 1-9
- Duncan, W.I., Green, P.F., Duddy, I.R., 1998 'Source rock burial history and seal effectiveness: Key facets to understanding hydrocarbon exploration potential in the east and central Irish Sea basins' *American Association of Petroleum Geologists Bulletin*, **82** (7), 1401-1415
- Ehrenberg, S.N., Nadeau, P.H., Steen, O., 2009 'Petroleum reservoir porosity versus depth: Influence of geological age' *The American Association of Petroeulm Geologists Bulletin*, **93** (10), 1281-1296
- Eiken, O., Ringrose, P., Hermanrud, C., Nazarian, B., Torp, T.A., Høier, L., 2011 'Lessons learned from 14 years of CCS operations: Sleipner, In Salah and Snøhvit' *Energy Procedia*, **4**, 5541-5548
- EU, 2011 'Implementation of Directive 2009/31/EC on the geological storage of carbon dioxide Guidance Document 2: Characterisation of the Storage Complex, CO₂ stream composition, monitoring and corrective measures' http://ec.europa.eu/clima/policies/lowcarbon/ccs/implementation/docs/gd2_en.pdf
- Evans, D., Graham, C., Armour, A., Bathurst, P., (eds) 2003 'The Millennium Atlas: Petroleum geology of the central and northern North Sea' *The Geological Society of London*.

Gatliff, R.W., Richards, P.C., Smith, K, Graham, C.C., McCormac, M, Smith, N.J.P., Long, D, Cameron, T.D., Evans, D, Stevenson, A.G., Bulat, J, Ritchie, J.D. 1994 'United Kingdom offshore regional report: the geology of the central North Sea.' (London: HMSO for the British Geological Survey)

Gibbard, P.L., Head, M.J., Walker, M.J.C., 2010 'Formal ratification of the Quaternary System/Period and the Pleistocene Series/Epoch with a base at 2.58 Ma' *Journal of Quaternary Science* **25**(2), 96-102

Goff, J.C., 1983 'Hydrocarbon generation and migration from Jurassic source rocks in the E Shetland Basin and Viking Graben of the northern North Sea' *Journal of the Geological Society of London*, **140**, 445-474

Golodowski, B., Nielsen, S.B., Clausen, O.R., 2012 'Patterns of Cenozoic sediment flux from western Scandinavia' *Basin Research* **24**, 377-400

Graham, A.G.C., Stoker, M.S., Lonergan, L., Bradwell, T., Stewart, M.A., 2011 'The Pleistocene Glaciations of the North Sea basin' in *Developments in Quaternary Science*, edited, Elsevier B.V.

Huuse, M, 2002 'Cenozoic uplift and denudation of southern Norway: insights from the North Sea Basin' from: Dore, A.G., Cartwright, J.A., Stoker, M.S., Turner, J.P. White, N, 2002 'Exhumation of the North Atlantic margin: Timing, Mechanisms and Implications for Petroleum Exploration' *Geological Society, London, Special Publications*, **196**, 209-233

Guidish T.M., Kendall, C.G.St.C., Lerche, I., Toth, D.J., Yarzab, R.F., 1985 'Basin evaluation using burial history calculations; an overview' *The American Association of Petroleum Geologists Bulletin*, **69** (1), 92-105

Haskell, N., Nissen, S., Hughes, M., Grindhaug, J., Dhanani, S., Heath, R., Kantorowicz, J., Antrim, L., Cubanski, M., Nataraj, R., Schilly, M., Wigger, S., 1999 'Delineation of geological drilling hazards using 3D seismic attributes' *The Leading Edge*, **18** (3), 373-382

- Holmes, R., 1977 'Quaternary deposits of the central North Sea 5. The Quaternary geology of the UK sector of the North Sea between 56° and 58°N' *Report of Institute of Geological Sciences* **77/14** 50 pp
- Kilhams, B., McArthur, A., Huuse, M., Ita, E., Hartley, A., 2011 'Enigmatic large-scale furrows of Miocene to Pliocene age from the central North Sea: current-scoured pockmarks?' *Geo-Marine Letters* **31**, 437-449
- Knudsen, K.L., Asbjörnsdóttir, L., 1991 'Plio-Pleistocene foraminiferal stratigraphy and correlation in the central North Sea' *Marine Geology* **101**, 113-124
- Knutz, P.C., 2010 'Channel structures formed by contour currents and fluid expulsion: significance for Late Neogene development of the central North Sea basin' *Petroleum Geology Conference series* **7**, 77-94
- Kristensen, T.B., Huuse, M., 2012 'Multistage erosion and infill of buried Pleistocene tunnel valleys and associated seismic velocity effects' From: Huuse, M., Redfern, J., Le Heron, D.P., Dixon, R.J., Moscariello, A., Craig, J. (eds) 'Glaciogenic reservoirs and Hydrocarbon Systems' *Geological Society, London, Special Publications*, **368**
- Kuhlmann, G., Langereis, C.G., Munsterman, D., van Leeuwen, R.-J., Verreussel, R., Meulenkamp, J.E., Wong, T.E., (2006) 'Integrated chronostratigraphy of the Pliocene-Pleistocene interval and its relation to the regional stratigraphical stages in the southern North Sea region' *Netherlands Journal of Geoscience*, **85**(1), 29-45
- Lamb, R.M, Huuse, M., Stewart, M., Submitted 'Central North Sea contourites and scours: Evidence for deep water processes in the earliest Quaternary' *Journal of Quaternary Sciences Special Publication*
- Lisiecki, L.E., Raymo, M.E., 2007 'Plio-Pleistocene climate evolution: trends and transitions in glacial cycle dynamics' *Quaternary Science Reviews*, **26**, 56-69
- McMillan, A.A., Hamblin, R.J.O., Merritt, J.W., 2005 'An overview of the lithostratigraphical framework for the Quaternary and Neogene deposits of Great Britain (onshore)' *British Geological Survey Research Report* RR/04/04 38 p.

Miller, K.G., Kominz, M.A., Browning, J.V., Wright, J.D., Mountain, G.S., Katz, M.E., Sugarman, P.J., Cramer, B.S., Christie-Blick, N., Pekar, S.F., 2005 'The Phanerozoic Record of Global Sea-Level Change' *Science*, **310**, 1293-1298

Mitchum Jr, R.M., Vail, P.R., Thompson III, S., 1977a 'Seismic stratigraphy and Global Changes of Sea Level, Part 2: The Depositional Sequence as a Basic Unit for Stratigraphic Analysis' From: Payton, C.E. (ed) 'Seismic stratigraphy – applications to hydrocarbon exploration' American Association of Petroleum Geologists Memoir 26, p. 53-62

Mitchum Jr, R.M., Vail, P.R., Thompson III, S., 1977b 'Seismic stratigraphy and Global Changes of Sea Level, Part 6: Stratigraphic Interpretation of Seismic Reflection Patterns in Depositional Sequences' From: Payton, C.E. (ed) 'Seismic stratigraphy – applications to hydrocarbon exploration' American Association of Petroleum Geologists Memoir 26, p. 117-133

Moreau, J., Huuse, M., 2014 'Infill of tunnel valleys associated with landward-flowing ice sheets: The missing Middle Pleistocene record of the NW European rivers?' *Geochemistry Geophysics Geosystems* **15**, 1-9

Nielsen, T., Mathiesen, A., Bryde-Auken, M., 2008 'Base Quaternary in the Danish parts of the North Sea and Skagerrak' *Geological Survey of Denmark and Greenland Bulletin* **15**, 37-40

Ottesen, D., Dowdeswell, J.A., Bugge, T., 2014 'Morphology, sedimentary infill and depositional environments of the Early Quaternary North Sea Basin (56° - 62°N)' *Marine and Petroleum Geology* **56**, 123-146

Noorbergen, L.J., Lourens, L.J., Munsterman, D.K., Verreussel, R.M.C.H., 2015 'Stable isotope stratigraphy of the early Quaternary of borehole Noordwijk, southern North Sea' *Quaternary International*

Overeem, I., Weltje, G.J., Bishop-Kay, C., Kroonenberg, S.B., 2001 'The Late Cenozoic Eridanos delta system in the Southern North Sea Basin: a climate signal in sediment supply?' *Basin Research* **13**, 293-312

Patrino, S., Hampson, G.J., Jackson, C.A.-L., Whipp, P.S., 2014 'Quantitative progradation dynamics and stratigraphic architecture of ancient shallow-marine clinoform sets: a

new method and its application to the Upper Jurassic Sognefjord Formation, Troll Field, offshore Norway' *Basin Research* 1-41, doi:10.1111/bre.12081

Patrino, S., Hampson, G.J., Jackson, C.A-L., 2015 'Quantitative characterisation of deltaic and subaqueous clinoforms' *Earth-Science Reviews*, **142**, 79-119

Pekar, S.F., Miller, K.G., Kominz, M.A., 2000 'Reconstructing the stratal geometry of latest Eocene to Oligocene sequence in New Jersey; resolving a patchwork distribution into a clear pattern of progradation' *Sedimentary Geology* **134**, 93-109

Peltier, W.R., 1994 'Ice Age Paleotopography' *Science*, **265** (5169), 195-201

Posamentier, H.W., Davies, R.J., Cartwright, J.A., Wood, L. 2007 'Seismic geomorphology – an overview' From: Davies, R.J, Posamentier, H.W., Wood, L.J., Cartwright, J.A. (eds) 'Seismic Geomorphology: Applications to Hydrocarbon Exploration and Production' *Geological Society Special Publications*, **277**, 1-14

Posamentier, H.W., Allen, G.P., 1993 'Variability of the sequence stratigraphic model: effects of local basin factors' *Sedimentary Geology*, **86**, 91-109

Praeg, D, 1996 'Morphology, stratigraphy and genesis of buried mid-Pleistocene tunnel-valleys in the southern North Sea basin' [Ph.D. thesis]: University of Edinburgh 207 p.

Praeg, D., 2003 'Seismic imaging of mid-Pleistocene tunnel-valleys in the North Sea Basin – high resolution from low frequencies' *Journal of Applied Geophysics* **53**, 273-298

Raymo, M.E., 1994 'The Initiation of Northern Hemisphere Glaciation' *Annual Review of Earth and Planetary Sciences*, **22**, 353-383

Raymo, M.E., Nisancioglu, K., 2003 'The 41 kyr world: Milankovitch's other unsolved mystery' *Paleoceanography*, **18** (1)

Rose, J., 2009 'Early and Middle Pleistocene landscapes of eastern England' *Proceedings of the Geologists Association*, **120**, 3-33

Ryan, W.B.F., S.M. Carbotte, J.O. Coplan, S. O'Hara, A. Melkonian, R. Arko, R.A. Weissel, V. Ferrini, A. Goodwillie, F. Nitsche, J. Bonczkowski, and R. Zemsky (2009), Global Multi-Resolution Topography synthesis, *Geochem. Geophys. Geosyst.*, 10, Q03014, from: http://www.marine-geo.org/tools/maps_grids.php

Stewart, M.A., Lonergan, L., 2011 'Seven glacial cycles in the middle-late Pleistocene of northwest Europe: Geomorphic evidence from buried tunnel valleys' *Geology* **39**, 283-286

Stewart, M., Lonergan, L., Hampson, G., 2012 '3D seismic analysis of buried tunnel valleys in the Central North Sea: tunnel valley fill sedimentary architecture' From: Huuse, M., Redfern, J., Le Heron, D.P., Dixon, R.J., Moscariello, A., Craig, J. (eds) 'Glaciogenic reservoirs and Hydrocarbon Systems' *Geological Society, London, Special Publications*, **368**

Stewart, M.A., Lonergan, L., Hampson, G., 2013 '3D seismic analysis of buried tunnel valleys in the central North Sea: morphology, corss-cutting generations and glacial history' *Quaternary Science Reviews*, **72**, 1-17

Stoker, M.S., Praeg, D., Shannon, P.M., Hjelstuen, B.O., Laberg, J.S., Nielsen, T., van Weering, T.C.E., Sejrup, H.P., Evans, D., 2005 'Neogene evolution of the Atlantic continental margin of NW Europe (Lofoten Islands to SW Ireland); anything but passive. From: Dore, A.G., Vining, B., (eds) 'Petroleum Geology: North West Europe and Global Perspectives' *Proceedings of the 6th Petroleum Geology Conference*, 1057-1076

Stoker M.S., Balson, P.S., Long, D, Tappin, D.R., 2011 'An overview of the lithostratigraphical framework for the Quaternary deposits on the United Kingdom continental shelf.' *British Geological Survey Research Report*, RR/11/03. 48 p.

White, N., Lovell, B., 1997 'Measuring the pulse of a plume with the sedimentary record' *Nature* **387**, 888-891

Ziegler P.A., 1992 'North Sea rift system' *Tectonophysics* **208**, 55-75

CHAPTER 7

SYNTHESIS AND CONCLUSIONS

CHAPTER 7: SYNTHESIS AND CONCLUSIONS

The purpose of this chapter is to document the main findings of the thesis and how the chapters have addressed the aims of the project. Key themes that have become apparent throughout the project are also discussed. The contribution of the key findings from this thesis to geological knowledge is assessed and future work which could be carried out is identified.

To recap, the broad aims of this study were to:

- 1) Develop a regional chronostratigraphic framework for the Late Cenozoic section of the southern North Sea using seismic data and well correlation.
- 2) Utilise “MegaScale” continuous 3D seismic data to investigate the geomorphology and depositional environment model of the SNS basin for an important period of time in climate history, the descent into icehouse conditions.
- 3) Use the chronostratigraphic framework to link the southern North Sea stratigraphy to the Marine Isotope Curve in order to assess the control of eustacy on the formation of stratigraphic architectures and investigate other controlling forces on stratigraphic architecture and sequence development.
- 4) Investigate the utility of sequence stratigraphic concepts and methodologies in full spatial-temporal detail.

7.1. SUMMARY OF RESULTS AND CONCLUSIONS

7.1.1 Regional Evolution of a Shelf-Prism in the Late Cenozoic: Eustacy, Sediment Supply and Subsidence in the Southern North Sea

Chapter 3 focused on the regional interpretation and the seismic stratigraphy of the case study, the Late Cenozoic shelf-prism in the southern North Sea, aimed at unravelling the controlling factors on the evolution of a large shelf-prism and to take a step towards better visualisation of the lateral variation of sequences within a basin. The chronostratigraphic control enabled a correlation of sequences, seismic

architectures, geomorphology and seismic facies with full 3D control, to eustatic change, subsidence and sediment supply.

This chapter addressed all four major aims of the study to some degree and the key conclusions from the chapter were:

- The high resolution chronostratigraphic framework for the north Netherlands North Sea based on biostratigraphy and magnetostratigraphy was extended across the area of the SNS MegaSurvey in the Netherlands North Sea and into Danish North Sea. Nine seismic units were identified and correlated across the basin.
- The importance of correlating well logs along strike when correlating across clinoformal geometry and the importance of integrating the seismic geometries to guide the interpretation were identified. The gamma ray signal of glacial terminations of MIS 100, 98, 96 and 92 can be traced over 500 km along strike of the depositional trend from the A15-03 well in the Netherlands North Sea to the Noordwijk borehole onshore Netherlands. This is because along strike settings inhabit a similar depositional environment on the basal Quaternary shelf-prism. However the gamma ray character is hard to trace even 50 km landwards or basinwards (updip or downdip).
- The lateral variation of basin infill within the study period was highlighted by the identification of a range of clinoform architectures and seismic facies in planform using seismic geomorphology and mapping them for each seismic unit against the respective thickness map.
- Seismic geomorphology was utilized to identify depositional environments in the absence of direct geological observation and along with the seismic architectures; an idea of the position of the coastline was interpreted. A novel way of measuring the extent of transgressions of the shelf during base level highs was developed using the mapping of iceberg scours across the shelf during the Gelasian. As iceberg scours can only form in subaqueous conditions, these were taken as a key indicator that the shelf was flooded.
- Eustasy is the main control on regional sea level and climate in the early Gelasian (2.58 Ma – 2.15 Ma) with accelerated subsidence in the late Gelasian overriding the eustatic signal (2.15-1.78 Ma).

- Sediment supply (amount and proximity to the source), local subsidence and underlying geomorphology of the shelf create variability in how eustasy is expressed within the sedimentary architecture of the SNS.
- The variation in the expression of a glacial-interglacial cycle within the seismic stratigraphy of the southern North Sea highlights the need for 3D large scale seismic interpretation to understand the regional over local base level trends and their link to global sea level.

One of the key positive outcomes of this chapter is that it provided the groundwork not only for the following original research in Chapters 4 & 5 but the mapping provided the possibility to expand the chronostratigraphic framework through to the northern North Sea, carried out by Rachel Lamb (Chapter 6.2) and to collaborate on North Sea wide papers which have great implications for the scientific knowledge of early Quaternary glaciation in the North Sea (Chapter 6.1).

A major limitation of the chapter is that the study aimed to understand a very large, regional study area in high resolution detail which showed that seismic architectures and facies varied greatly across the region. The 3D variability of clinoform types and seismic facies was distilled into 2D distribution maps however there is still a lot of work to do in order to fully represent the variability of stacking patterns and interpretations of base level across the region in a coherent and more novel manner for publication.

7.1.2 Deep Water Sedimentary Systems Linked to Shelf Edge Trajectory and Global Sea Level

Chapter 4 utilised the mapping, detailed seismic geomorphological investigation and chronostratigraphic framework of Chapter 3 to investigate deep water channel systems and their associated basin floor deposition in greater detail. The rationale of the paper was to provide a link up dip to the shelf edge trajectory and the conditions on the shelf at the time of deposition for each system and understand where in the relative sea level curve the deposition occurs. This was then used to establish where the depositional systems fit within the sequence stratigraphic framework and whether existing sequence stratigraphic methodology predicts the existence of basin/slope deposition events sufficiently. This chapter addressed aims three and four of the project.

The key conclusions from the chapter were:

- For the first time, Plio-Pleistocene submarine channels were identified and imaged in 3D in the Netherlands North Sea and dated using a high resolution chronostratigraphic framework.
- Each system was described in relation to the conditions at the shelf edge; the seismic architectures and trajectory of the associated shelf edge. The most common shelf edge trajectory conditions for bypass of the shelf into the basin is flat lying to descending shelf edge trajectories of oblique tangential clinoforms with strong amplitudes on the outer shelf. However, many instances of basinwards deposition are associated with sigmoidal clinoforms and an ascending shelf edge trajectory.
- The high resolution dating and correlation of key seismic reflections events mean that the deep water depositional systems could be linked to the Marine Isotope Curve between MIS 103 and MIS 82 (2.58 Ma-~2.15 Ma). This is the first time that so many depositional systems have been linked to the global sea level curve. It has highlighted that the amount of glacial-interglacial cycles and deep water depositional systems do not coincide. For instance between 2.58 Ma and 2.43 Ma at least eight distinct submarine depositional systems occurred within three glacial-interglacial cycles.
- *Single Feeder* systems association with the traditional “LST” Lowstand Systems Tract, appears valid in relation to the seismic architecture, however when related to the global sea level curve it is clear that a basin floor fan is not present during every global sea level low, and in fact several can occur within one glacial-interglacial cycle. This makes clear that many other factors affect the basinwards deposition of sediment and that sequence boundaries should not be based on the position of basin floor fans. Sequence boundaries should be identified from clinoform architectures rather than the position of deep water sedimentation and their related incision events.
- Previous palynological and geochemical analysis of the SNS showed that the regional sea level is governed by glacial –interglacial cycles. By the identification of regional shale layers and clinoform architectures this is reflected to some extent in the seismic stratigraphy of the basin. However, it is clear from this

study that the relationship between predicated base level falls and sediment being delivered to the basin floor is not straight forward.

- This chapter supports that sediment can be transported to the deep water when relative sea level is rising and sediment supply is high. The deposition of reservoir quality sediments basinwards of the shelf edge can be moderately predictable by investigating stacking patterns of clinoform architectures but knowledge of the regional lateral variability of the basin, seismic geomorphology of the shelf area, sediment supply and knowledge of the basins relationship to the global sea level curve is imperative.

The key contributions of this paper to scientific knowledge is that the presence of either basin floor fans (*Single Feeder*) or slope channels (*Multiple Line Source*) is not reliably linked to eustatic lows and therefore are not reliable indicators of the positions of sequence boundaries. Also, coarser grained sediment deposition basinwards of the shelf edge can occur during most scenarios of the southern North Sea relative sea level curve. This strongly implies that prediction of reservoir quality sands using current sequence stratigraphic models is flawed.

The key limitations of the study include the seismic resolution, as it is possible that not all of the deep water systems have been identified during the study period. Studying clinoform trajectories in seismic data is not without its issues. The clinoforms imaged in this study do not necessarily represent the original depositional architecture. Due to the role of loading on palaeotopography, topsets are largely less loaded than the bottomsets (Steckler et al., 1999) and therefore vertical differences between the topset and bottomset are exaggerated in TWT compared to the original depositional architecture (Miller et al., 2013b). Also the effects of differing velocities of sediment above the clinoforms could distort the original depositional architecture of the clinoforms. New research based on computer modelling investigated the non-uniqueness of seismic architectures, arguing that during rapid sea level fall topsets can still be deposited (Burgess and Prince, 2014). Also the toplap/truncation and lack of topset preservation used to identify oblique clinoforms and the bypass of the shelf, can in fact be “apparent toplap” which is due to tuning and resolution effects of the seismic data (Catuneanu et al., 2009). It is important to recognise the limitations of the resolution of seismic data in comparison to core and outcrop studies.

7.1.3 Can Enigmatic Intra Slope Clinoforms Provide an Independent Calibration of Early Pleistocene Eustatic Changes?

In this study we documented the architecture of the sub 100 m Intra Slope Clinoforms and their spatial and temporal distribution across the SNS. The cyclical nature of the Intra Slope Clinoforms were discussed and placed for the first time within sequence stratigraphic context to aid prediction of sand prone facies basinwards of the shelf break. We aimed to understand how they can be used to provide independent calibrations of the eustatic curve during the Late Pliocene and earliest Pleistocene. This chapter addressed aims three and four of the project.

The key conclusions from the chapter were:

- Sand prone Intra Slope Clinoform wedges <100 m in height are identified cyclically across the southern North during the Cenozoic.
- Intra Slope Clinoforms are associated with forced regressions and were likely deposited in cold marine conditions.
- The clinoform roll over points likely represent storm wave base during early glacial when rapid global sea level fall results in base level fall below the shelf edge in the SNS but incision is inhibited by high sediment rate.
- Intra Slope Clinoforms are proposed to be used as indicators of the magnitudes of relative sea level fall along with canyon incision on the upper slope.
- The Plio-Pleistocene section of the southern North Sea largely represents sediments deposited during falling base level associated with the descent to glacial conditions.
- The correlation between base level falls in the southern North Sea and eustatic falls related to glacial conditions in the Gelasian are positive suggesting that eustasy is a controlling factor of base level in the southern North Sea.
- This corroborates the findings of Chapter 4 that seismic architectures are a more reliable indicator of base level changes linked to eustasy than incision events and deep water deposition.

The same limitations in discerning original clinoform architectures and non-uniqueness are the same as in Chapter 4 (Section 7.1.3). The issue of non-uniqueness is much greater in this chapter due to similar features at the seismic resolution being interpreted as several different depositional features, with differing meanings for the sequence stratigraphic framework.

7.2 FUTURE WORK

Several possible areas of further work are identified. Future work could build on the chronostratigraphic framework and seismic geomorphic analysis of the Late Cenozoic. This dataset could be a huge asset for both the study of sequence stratigraphy but also as a key dataset for understanding the earliest Quaternary. With over 70 km of progradation of clinoforms up to 200 m high in the southern Netherlands North Sea during the time period from 2.58 Ma to 2.43 Ma, covering the first major glaciations of the Quaternary to affect the North Sea (Zagwijn, 1992), this expanded section could be utilised in a much greater way to unravel the depositional environments of this incredibly important, little known time period.

At the present moment the chronostratigraphic framework and direct geological information comes mainly from two wells A15-03 and A15-04 (Kuhlmann et al., 2006). Collection of additional borehole data and core from the most expanded section of the earliest Quaternary, with biostratigraphy/magnetostratigraphy and geochemical analysis would increase the power of the dataset and give a more robust record of the early Quaternary paleoclimate and palaeoenvironment. Access to higher resolution data such as site surveys would also add accuracy to the depositional environment interpretations made in this thesis.

The author sees this dataset as the start of many years work, in a similar vein to the New Jersey Cenozoic continental shelf (Fulthorpe and Austin, 1998; Miller et al., 2013b; Steckler et al., 1999); the Permian Karoo basin, (Hodgson, 2006; Flint et al., 2011; Brunt et al., 2013; Jones et al., 2014) and the Eocene Spitsbergen basin, Svalbard (Plink-Björklund et al., 2001; Steel and Olsen, 2002; Johannessen and Steel, 2005); to which comparisons of the depositional systems can be made. An IODP proposal in the Central

North Sea and a ICDP proposal CONOSC (Coring **N**Orth **S**ea **C**enozoic) targeting the Late Cenozoic marine section, to the north and south of this project study area could increase the knowledge of the chronostratigraphic framework and depositional environments in the next few years.

Due to the large dataset a lot of the project has been qualitative in nature in order to document the general trends and seismic facies and architectures of the basin for the Late Cenozoic. There is great potential to take aspects of this project and create more detailed quantitative projects. This could include quantitatively assessing the clinoform architectures in greater detail sensu Anell and Midtkandal, (2015) and Patruno et al. (2015) or detailing individual Single Feeder or Multiple Line Source systems in the vein of Sylvester et al. (2012). The progradation rates and characteristics of the shelf-prism and its sediment supply system could be placed into context of global examples using the literature to understand the depositional system further (Burgess and Hovius, 1998; Muto and Steel, 2000; Patruno et al., 2014).

Creating a more sophisticated structural restoration in order to better understand the original depositional architectures of the shelf-prism is essential further work for this study. This would include using 2D flexural decomposition backstripping techniques (Steckler et al., 1999; Pekar and Kominz, 2001). This would increase the accuracy of the results displayed in this thesis.

Several other lines of analysis were carried out during the PhD, which are still in progress:

- A study just on the seismic geomorphology of seismic unit *Pleisto 1*, (2.58 Ma- 2.43 Ma). The link to individual glacial-interglacial cycles is highly constrained by palynological and geochemical data and this study focuses on understanding the evolution of depocentres on a high resolution scale in relation to the global sea level curve and the knowledge of the earliest Quaternary and is in conjunction with TNO and University of Utrecht, Dr. Johan ten Veen and Dr. Timme Donders.
- Investigating seismic unit *Plesito 1* understand the nature of lateral variation and continuity of key surfaces. The main aim is to understand the attributes of key sequence stratigraphic surfaces, whether they are time transgressive and if they represent chronostratigraphic significant surfaces (Cartwright et al., 1993;

Christie-Blick et al., 2007; Miller et al., 2013a). This paper also goes into more detail about the time locked up in the preserved strata (time verses sequence stratigraphy) and whether cyclicity of key seismic architectures and seismic facies occur within similar timescales across the basin (this is briefly mentioned in Chapter 5).

7.3 REFERENCES

- Anell, I., Midtkandal, I., 2015. The quantifiable clinothem – types, shapes and geometric relationships in the Plio-Pleistocene Giant Foresets Formation, Taranaki Basin, New Zealand. *Basin Research*.
- Brunt, R.L., Di Celma, C.N., Hodgson, D.M., Flint, S.S., Kavanagh, J.P., Van der Merwe, W.C., 2013. Driving a channel through a levee when the levee is high: An outcrop example of submarine down-dip entrenchment. *Marine and Petroleum Geology* 41, 134–145.
- Burgess, P.M., Hovius, N., 1998. Rates of delta progradation during highstands: consequences for timing of deposition in deep-marine systems. *Journal of the Geological Society* 155, 217–222.
- Burgess, P.M., Prince, G.D., 2014. Non-unique stratal geometries: Implications for sequence stratigraphic interpretations. *Basin Research* 351–365.
- Cartwright, J. A., Haddock, R.C., Pinheiro, L.M., 1993. The lateral extent of sequence boundaries. *Geological Society, London, Special Publications* 71, 15–34.
- Catuneanu, O., Abreu, V., Bhattacharya, J.P., Blum, M.D., Dalrymple, R.W., Eriksson, P.G., Fielding, C.R., Fisher, W.L., Galloway, W.E., Gibling, M.R., Giles, K. A., Holbrook, J.M., Jordan, R., Kendall, C.G.S.C., Macurda, B., Martinsen, O.J., Miall, A. D., Neal, J.E., Nummedal, D., Pomar, L., Posamentier, H.W., Pratt, B.R., Sarg, J.F., Shanley, K.W., Steel, R.J., Strasser, A., Tucker, M.E., Winker, C., 2009. Towards the standardization of sequence stratigraphy. *Earth-Science Reviews* 92, 1–33.
- Christie-Blick, N., Pekar, S.F., Madof, A.S., 2007. Is there a role for sequence stratigraphy in chronostratigraphy? *Stratigraphy* 4, 217–230.
- Flint, S.S., Hodgson, D.M., Sprague, A. R., Brunt, R.L., Van der Merwe, W.C., Figueiredo, J., Pr  lat, a., Box, D., Di Celma, C., Kavanagh, J.P., 2011. Depositional architecture and sequence stratigraphy of the Karoo basin floor to shelf edge succession, Laingsburg depocentre, South Africa. *Marine and Petroleum Geology* 28, 658–674.
- Fulthorpe, C.S., Austin, J. A., 1998. Anatomy of rapid margin progradation: Three-dimensional geometries of miocene clinoforms, New Jersey margin. *AAPG Bulletin* 82, 251–273.
- Hodgson, D.M., 2006. Stratigraphic Evolution of Fine-Grained Submarine Fan Systems, Tanqua Depocenter, Karoo Basin, South Africa. *Journal of Sedimentary Research* 76, 20–40.
- Johannessen, E.P., Steel, R.J., 2005. Shelf-margin clinoforms and prediction of deepwater sands. *Basin Research* 17, 521–550.

- Jones, G.E.D., Hodgson, D.M., Flint, S.S., 2014. Lateral variability in clinoform trajectory, process regime, and sediment dispersal patterns beyond the shelf-edge rollover in exhumed basin margin-scale clinoforms. *Basin Research* 27 (6), 1-24.
- Kuhlmann, G., Langereis, C., Munsterman, D., Jan van Leeuwen, R., Verreussel, R., Meulenkamp, J., Wong, T., 2006. Chronostratigraphy of Late Neogene sediments in the southern North Sea Basin and paleoenvironmental interpretations. *Palaeogeography, Palaeoclimatology, Palaeoecology* 239, 426-455.
- Miller, K.G., Browning, J. V., Mountain, G.S., Bassetti, M. A., Monteverde, D., Katz, M.E., Inwood, J., Lofi, J., Proust, J.N., 2013a. Sequence boundaries are impedance contrasts: Core-seismic-log integration of Oligocene-Miocene sequences, New Jersey shallow shelf. *Geosphere* 9, 1257-1285.
- Miller, K.G., Mountain, G.S., Browning, J. V., Katz, M.E., Monteverde, D., Sugarman, P.J., Ando, H., Bassetti, M. A., Bjerrum, C.J., Hodgson, D., Hesselbo, S., Karakaya, S., Proust, J.N., Rabineau, M., 2013b. Testing sequence stratigraphic models by drilling Miocene foresets on the New Jersey shallow shelf. *Geosphere* 9, 1236-1256.
- Muto, T., Steel, R.J., 2000. The accommodation concept in sequence stratigraphy: some dimensional problems and possible redefinition. *Sedimentary Geology* 130, 1-10.
- Patruno, S., Hampson, G.J., Jackson, C. A L., Whipp, P.S., 2014. Quantitative progradation dynamics and stratigraphic architecture of ancient shallow-marine clinoform sets: A new method and its application to the Upper Jurassic Sognefjord Formation, Troll Field, offshore Norway. *Basin Research* 27 (4), 412-452.
- Patruno, S., Hampson, G.J., Jackson, C.A.-L., 2015. Quantitative characterisation of deltaic and subaqueous clinoforms. *Earth-Science Reviews* 142, 79-119.
- Pekar, S.F., Kominz, M. A., 2001. Two-Dimensional Paleoslope Modeling: A New Method for Estimating Water Depths of Benthic Foraminiferal Biofacies and Paleoshelf Margins. *Journal of Sedimentary Research* 71, 608-620.
- Plink-Björklund, P., Mellere, D., Steel, R.J., 2001. Turbidite Variability and Architecture of Sand-Prone, Deep-Water Slopes: Eocene Clinoforms in the Central Basin, Spitsbergen. *Journal of Sedimentary Research* 71, 895-912.
- Steckler, M.S., Mountain, G.S., Miller, K.G., Christie-Blick, N., 1999. Reconstruction of Tertiary progradation and clinoform development on the New Jersey passive margin by 2-D backstripping. *Marine Geology* 154, 399-420.
- Steel, R.J., Olsen, T., 2002. Clinoforms, clinoform trajectories and deepwater sands. *Sequence Stratigraphic Models for Exploration and Production: Evolving Methodology, Emerging Models and Application Histories* 367-381.
- Sylvester, Z., Deptuck, M.E., Prather, B.E., Pirmez, C., O'Byrne, C., 2012. Seismic stratigraphy of a shelf-edge delta and linked submarine channels in the northeastern Gulf of Mexico, *SEPM Special Publication* 99, 31-59.

Zagwijn, W.H., 1992. The beginning of the Ice Age in Europe and its major subdivisions. Quaternary Science Reviews 11. 583-591.

APPENDIX A
ADDITIONAL BIOSTRATIGRAPHY DATA
FROM CHRIS KING

top	source	notes			NS35		NS36a	NS36b	NS36	NS37	NS38	NS39		NS40	NS41			
REVISED																NS42		NS42a
					mid Langhian		late Langhian	early Serravallian		near top Serravallian		early Tortonian			REVISED mid Tortonian			near top Messinian
					c. 14.7 Ma					11.6 Ma	10.5 Ma				8.8 Ma	7.1 Ma	c. 5.3 Ma	c. 5.3 Ma
Symbol					TEN		SPH					US			M			LAN
					tenui		subdeh		sapro	clod	subfrag	US	E. docapenti	B. laevis	metzm	atl S/D	acosta	lang
NETHERLANDS																		
A/12-1		K			1240m						spir1210	1186m		(1174 gl)				
A/15-2	RRI X25m				1280m						spir 1220							
A/18-1	Laursen	X 40m			1240m					1210m	spir1190	1190m			?			
B/10-2	RRI rep old			1330 gl	sta 1270m													
B/10-3	Kuhlmann									acul1335	spir1245	1245m				(1121.5)		
B/13-1	RRI				1230m										1200m ?			
B/13-3	Kuhlmann				1220/1240							1220m						
B/17-1				1080m gl on mio				(spics)							1040 gl			
B/17-2	VLR			1290m gl	1280m					c. 1260m		1222m						
B/17-5	Kihlmann									pr								
D/12-1	CK			560m on E OL														
E/2-1	NETH				980sta													
E/12-1	NETH				948m													
E/16-1	NETH			640m on EO														
E/17-1	RRI old			610m on ?EO	gl													
F/2-1	ADK				1310m					1280m		1250m						
F/2-3	CK				1216m				1204m	c. 1192m					1162m	(1130 coral)	c. 1130m	
F/4-3	halli				3660 sta					pres					(3560gl)			
F/5-1	SSI	X100m		(1300) on OL ?														
F/5-5		KRONUS			1140m					??					??			
F/6-3	RRIwellsite			1135m on Ea Mio?														
F/7-1	VLR			977m on Mio														
F/14-3	PS			3430ft on Mio														
F/14-6	CK	X 30m			1090m													
G/17-1	RRI 1973				A.sta. 2720 ft		2640gl	2600 rads										
G/17c-3		X 50 ft			2700 ft													
K/3-2	RRI rep				2400 ft	spics	(2130 ft unco. ?)											
K/5-1	RRI old	X 50m			650m lag on OL													
K/9-1	CK				690m (sta)	630m gl												
K/16-1	ADK old				(560m EO)	560m gl												
L/1-1	CK	X 10m			980m	spics+aggs	(950 unco)											
L/1-2	BP summary				950m	rads	(925 or 940m gl)											
L/9-1	CK				864m	spics	(856 gl)											
L/10-1	VLR				(610m on OL)													
L/12-1	CK/VLR				(760m on OL)													
M/4-2	PS			gl	820m													
M/8-2	PS		(660m on OL)	gl														
P/2-1	VLR			gl	2800 ft ??	2760 gl spics rads												
P/4-1	old				c. 490m on OLEO													
P/7-1	RRI old		c. 345m EO															
P/9-2					610m													
P/9-4	PS	X 10m	(610m EO)		590m prob													
P/15-2	RRI		(530m OL)	gl														
P/15-3	ADK	?this well		gl	470m on OL													
P/15-4	CK			gl	470m on E OL													
Q/10-4																		
Q/13-1			(450m E OL)	gl														
Q/13-2	ADK				500m on E OL													
Q/13-3	PS		(520m on OL)	gl														
Q/14-2	PS	X 10m	(480m on MIO)	gl														
Q/16-1	Neth		(481m on PAL)	gl														
S/2-1	Neth																	
Noordwijk					443	434 gl												
Den Haag																		
Zaandam																		
Ameland N1					340													
Ameland 1				(522 on EoL)														

NS42				NS43				NS44				NS45				NS46a				NS46				NS47																																																																																																																																																																																																																																																																																																																																																																																																																																																																																																																																																																																																																																																																																																																																																																																																																																																																																																																																																																																																																																																																			
NS43				NS44a																usually diffuse																																																																																																																																																																																																																																																																																																																																																																																																																																																																																																																																																																																																																																																																																																																																																																																																																																																																																																																																																																																																																																																																							
intra-Zanclean				near top Zanclean				top Piacenzian												top Gelasian																																																																																																																																																																																																																																																																																																																																																																																																																																																																																																																																																																																																																																																																																																																																																																																																																																																																																																																																																																																																																																																																							
4.2 Ma								2.6 Ma				2.5 Ma				c. 2.2 Ma				1.85 Ma																																																																																																																																																																																																																																																																																																																																																																																																																																																																																																																																																																																																																																																																																																																																																																																																																																																																																																																																																																																																																																																																							
V								PST				PAC				O								H																																																																																																																																																																																																																																																																																																																																																																																																																																																																																																																																																																																																																																																																																																																																																																																																																																																																																																																																																																																																																																																																			
ven				Fo pst				Ang. angulosa				Valv compl				limb				lamm etc				Briz. catan				pst				FO hannai				pachy				oregon				groenl				grossus				Bulimina				FO Ammonia				C. laevigata				hannai																																																																																																																																																																																																																																																																																																																																																																																																																																																																																																																																																																																																																																																																																																																																																																																																																																																																																																																																																																																																																											
				1093m				1160m (r)				1130m RRI				980m				990m (no spl above)				930m				(865)r				648m				765ch				425m																																																																																																																																																																																																																																																																																																																																																																																																																																																																																																																																																																																																																																																																																																																																																																																																																																																																																																																																																																																																																																																			
								1070m				1040m																								460m																																																																																																																																																																																																																																																																																																																																																																																																																																																																																																																																																																																																																																																																																																																																																																																																																																																																																																																																																																																																																																																							
												1100m				1030m				(1070m) r																350m																																																																																																																																																																																																																																																																																																																																																																																																																																																																																																																																																																																																																																																																																																																																																																																																																																																																																																																																																																																																																																																							
								980m				990m (no spl above)				930m								820m												<560m																																																																																																																																																																																																																																																																																																																																																																																																																																																																																																																																																																																																																																																																																																																																																																																																																																																																																																																																																																																																																																																							
				1122/1162				1022m				965m				943.2m (943.5)																				<275m																																																																																																																																																																																																																																																																																																																																																																																																																																																																																																																																																																																																																																																																																																																																																																																																																																																																																																																																																																																																																																																							
				1050m ?				964/1010				910/865m				602m				912m				762m				600m/690m				360m																																																																																																																																																																																																																																																																																																																																																																																																																																																																																																																																																																																																																																																																																																																																																																																																																																																																																																																																																																																																																																																											
																																441/426				ust 426.5																																																																																																																																																																																																																																																																																																																																																																																																																																																																																																																																																																																																																																																																																																																																																																																																																																																																																																																																																																																																																																																							
980m								c. 920m								700m												580m								c. 330m																																																																																																																																																																																																																																																																																																																																																																																																																																																																																																																																																																																																																																																																																																																																																																																																																																																																																																																																																																																																																																																							
1137m								1080m				900m				880m								747m ?				747m c								350m																																																																																																																																																																																																																																																																																																																																																																																																																																																																																																																																																																																																																																																																																																																																																																																																																																																																																																																																																																																																																																																							
				988/1010				714/729m								620.3m (580.8m)																540.7 (+Virg)				<300m																																																																																																																																																																																																																																																																																																																																																																																																																																																																																																																																																																																																																																																																																																																																																																																																																																																																																																																																																																																																																																																							